

**SYNTHESIS AND ENZYMATIC EVALUATION OF ACTIVATED  
FLUOROSUGARS AS INACTIVATORS OF LYSOSOMAL ENZYMES**

by

BRIAN PATRICK REMPEL

B.Sc., The University of Alberta, 2003

A THESIS SUBMITTED IN PARTIAL FULFILLMENT OF  
THE REQUIREMENTS FOR THE DEGREE OF  
DOCTOR OF PHILOSOPHY

in

THE FACULTY OF GRADUATE STUDIES  
(Chemistry)

**THE UNIVERSITY OF BRITISH COLUMBIA**

(Vancouver)

July 2009

## **Abstract**

Activated fluorosugars are covalent inactivators for a number of glycosidases, functioning through accumulation of stable glycosyl-enzyme intermediates. Two approaches were taken in designing new inactivators: more highly fluorinated sugars that could form more stable intermediates, and fluorosugars bearing novel aglycones that could be manipulated to improve selectivity and efficiency.

Six novel difluorosugar fluorides were synthesized and evaluated as covalent inactivators. Four of the compounds were tested as time-dependent inactivators of the  $\beta$ -glucosidase from *Agrobacterium* sp. (Abg) and, while they were shown to behave as reversible competitive inhibitors, the only time-dependent inactivation was traced to the presence of an extremely small amount ( $<0.1\%$ ) of a contaminating impurity. The other two compounds were evaluated as inactivators of human lysosomal  $\alpha$ -iduronidase (Idua) the enzyme deficient in Mucopolysaccharidosis I. No time-dependent inactivation was observed, and only one functioned as a reversible competitive inhibitor for Idua.

Ten novel fluorosugars bearing dialkyl phosphate, phosphonate or phosphinate aglycones were also synthesized and evaluated as covalent inactivators for appropriate model retaining  $\alpha$ - and  $\beta$ -glycosidases, but as expected only inactivated retaining  $\beta$ -glycosidases. Some of these compounds were also tested as inactivators of human glucocerebrosidase (GCase), the enzyme that is deficient in Gauchers disease. Activated fluorosugars bearing phosphorus-based aglycones were found to be efficient inactivators of GCase with the best compound, dioctyl (2-deoxy-2-fluoro- $\beta$ -D-glucopyranosyl)phosphate, being  $\sim 4300$ -fold more efficient as an inactivator of GCase than the previously most efficient inactivator, 2-deoxy-2-fluoro- $\beta$ -D-glucopyranosyl fluoride.

Two compounds, 2-deoxy-2-fluoro- $\beta$ -D-glucopyranosyl fluoride and benzyl benzyl-(2-deoxy-2-fluoro- $\beta$ -D-glucopyranosyl)phosphonate, were evaluated as potential pharmacological chaperones for GCase. Both compounds raised the melting temperature of the enzyme *in vitro*, and cell-based assays showed an increase of GCase levels in the presence of both compounds, although no increase in enzyme activity was observed.

Finally, a radiosynthetic route was developed starting from 2-deoxy-2- $^{18}\text{F}$ -fluoro-D-glucose to produce 2,4-dinitrophenyl 2-deoxy-2- $^{18}\text{F}$ - $\beta$ -D-fluoroglucopyranoside, which behaved as an active-site directed inactivator of both Abg and GCase *in vitro*. The radiolabelled complex formed with GCase was purified, injected into mice, and imaged using positron emission tomography (PET). This represents a potentially useful technology for non-invasive studies on enzyme replacement therapy (ERT), which is used clinically to treat Gauchers disease.

## Table of Contents

<b>Abstract .....</b>	<b>ii</b>
<b>Table of Contents.....</b>	<b>iv</b>
<b>List of Tables.....</b>	<b>xiv</b>
<b>List of Figures .....</b>	<b>xv</b>
<b>List of Schemes.....</b>	<b>xix</b>
<b>List of Abbreviations .....</b>	<b>xxii</b>
<b>List of Amino Acid Abbreviations .....</b>	<b>xxvii</b>
<b>Acknowledgements .....</b>	<b>xxviii</b>
<b>Chapter 1: Introduction.....</b>	<b>1</b>
<b>1.1 Glycosidases.....</b>	<b>2</b>
<b>1.2 Glycosidase mechanisms .....</b>	<b>4</b>
<i>1.2.1 Inverting glycosidases .....</i>	<i>4</i>
<i>1.2.2 Retaining glycosidases.....</i>	<i>5</i>
<b>1.3 Small molecule inhibitors of glycosidases.....</b>	<b>8</b>
<i>1.3.1 The significance of glycosidase inhibitors.....</i>	<i>8</i>
<i>1.3.2 Noncovalent glycosidase inhibitors.....</i>	<i>9</i>
<i>1.3.3 Covalent inactivators.....</i>	<i>11</i>
<b>1.4 Lysosomal storage diseases .....</b>	<b>15</b>
<i>1.4.1 General introduction .....</i>	<i>15</i>
<i>1.4.2 Enzyme replacement therapy (ERT).....</i>	<i>16</i>
<i>1.4.3 Substrate reduction therapy (SRT) .....</i>	<i>17</i>
<i>1.4.4 Protein misfolding .....</i>	<i>17</i>
<i>1.4.5 Pharmacological chaperones .....</i>	<i>18</i>

1.4.6 Gauchers disease .....	19
1.4.7 Mucopolysaccharidosis I (MPS I) .....	23
<b>1.5 Positron emission tomography (PET) imaging .....</b>	<b>27</b>
1.5.1 Imaging techniques used in modern diagnostic medicine .....	27
1.5.2 A molecular description of the process underlying PET imaging .....	29
1.5.3 Advantages and disadvantages of PET imaging .....	30
1.5.4 Examples of three commonly employed PET imaging agents .....	31
1.5.4.1 Fluorodeoxyglucose (FDG) for imaging glucose metabolism .....	31
1.5.4.2 [ <sup>11</sup> C]clorgyline and [ <sup>11</sup> C]L-deprenyl for imaging monoamine oxidase (MAO) .....	33
1.5.5 Challenges surrounding radiochemistry .....	34
<b>1.6 Specific aims of this thesis .....</b>	<b>35</b>
<b>Chapter 2: Development of Fluorinated Carbohydrates as Covalent Inactivators of Glycosidases .....</b>	<b>37</b>
<b>2.1 Model glycosidases: introduction .....</b>	<b>38</b>
2.1.1 <i>Agrobacterium</i> sp. $\beta$ -glucosidase (Abg) .....	38
2.1.2 Yeast $\alpha$ -glucosidase (Yag) .....	38
2.1.3 $\beta$ -Mannosidase from <i>Cellulomonas fimi</i> (Man2A) .....	39
2.1.4 Jack bean $\alpha$ -mannosidase (JBAM) .....	39
2.1.5 <i>E. coli</i> $\beta$ -galactosidase ( <i>E. coli</i> $\beta$ -gal) .....	40
<b>2.2 An introduction to fluorosugars as glycosidase inactivators .....</b>	<b>40</b>
2.2.1 Properties of fluorinated organic compounds .....	40
2.2.2 Activated fluorosugars as glycosidase inactivators .....	41
2.2.2.1 2-Deoxy-2-fluoro glycosides .....	42
2.2.2.2 5-Fluoro glycosides .....	44

2.2.2.3 2-Deoxy-2,2-difluoro glycosides .....	45
2.2.2.4 1-Fluoro-glycosyl fluorides .....	45
2.2.3 <i>General synthetic approaches to activated fluorosugars</i> .....	46
2.2.3.1 5-Fluoro and 1-fluoro glycosides.....	46
2.2.3.2 2-Deoxy-2-fluoro glycosides .....	48
<b>2.3: Chemical synthesis of difluorosugar fluorides.....</b>	<b>49</b>
2.3.1 <i>Target compounds</i> .....	49
2.3.2 <i>Chemical synthesis</i> .....	51
2.3.2.1 2-Deoxy-2-fluoro- $\beta$ -D-glucopyranosyl fluoride ( <b>2.1</b> ).....	51
2.3.2.2 5-Fluoro- $\beta$ -D-glucopyranosyl fluoride ( <b>2.2</b> ) and 5-fluoro- $\alpha$ -L-idopyranosyl fluoride ( <b>2.3</b> ) .....	52
2.3.2.3. 2-Deoxy-2,5-difluoro- $\alpha$ -L-idopyranosyl fluoride ( <b>2.4</b> ).....	53
2.3.2.4 1-Fluoro-D-glucopyranosyl fluoride ( <b>2.5</b> ), 1,5-difluoro-D-glucopyranosyl fluoride ( <b>2.7</b> ) and 1,5-difluoro-L-idopyranosyl fluoride ( <b>2.8</b> ).....	54
2.3.2.5 2-Deoxy-1,2-difluoro-D-glucopyranosyl fluoride ( <b>2.6</b> ) .....	55
<b>2.4: Enzymatic testing of difluorosugar fluorides.....</b>	<b>57</b>
2.4.1 <i>Kinetic analysis of the inactivation of Abg by 2.1 and 2.4-2.8</i> .....	57
2.4.1.1 2-Deoxy-2-fluoro- $\beta$ -D-glucopyranosyl fluoride ( <b>2.1</b> ).....	57
2.4.1.2 2-Deoxy-2,5-difluoro- $\alpha$ -L-idopyranosyl fluoride ( <b>2.4</b> ).....	58
2.4.1.3 Testing a sample of <b>2.4</b> for the presence of a highly reactive inhibitory impurity .....	61
2.4.1.4. 2-Deoxy-1,2-difluoro-D-glucopyranosyl fluoride ( <b>2.6</b> ), 1,5-difluoro-D- glucopyranosyl fluoride ( <b>2.7</b> ) and 1,5-difluoro-L-idopyranosyl fluoride ( <b>2.8</b> ) .....	65
2.4.1.5 Enzymatic evaluation of <b>2.4</b> , <b>2.6</b> , <b>2.7</b> and <b>2.8</b> as reversible inhibitors of Abg65	
2.4.1.6 1-Fluoro-D-glucopyranosyl fluoride ( <b>2.5</b> ).....	68
2.4.2 <i>Kinetic analysis of the inactivation of Yag by 2.6, 2.7 and 2.8</i> .....	71

2.4.3 General conclusions for the difluorosugar fluorides .....	72
<b>2.5 Previous studies on the role of aglycones in activated fluorosugars .....</b>	<b>73</b>
2.5.1 General aglycone considerations .....	73
2.5.2 Fluoride aglycones .....	74
2.5.3 2,4-Dinitrophenol aglycones .....	74
2.5.4 2,4,6-Trinitrophenol aglycones .....	75
2.5.5 Chloride aglycones .....	75
2.5.6 Natural aglycones.....	76
<b>2.6: Chemical synthesis of activated fluorosugars bearing novel aglycones .....</b>	<b>77</b>
2.6.1 Target compounds .....	77
2.6.2 Synthesis .....	79
2.6.2.1 Attempted synthesis of 2-deoxy-2-fluoro- $\beta$ -D-glucopyranosyl chloride ( <b>2.32</b> ) and 2-deoxy-2,5-difluoro- $\alpha$ -L-idopyranosyl chloride ( <b>2.33</b> ) .....	79
2.6.2.2 Attempted synthesis of methyl-(2-deoxy-2-fluoro- $\beta$ -D-glucopyranosyl)- sulfonate ( <b>2.34</b> ), para-toluene-(2-deoxy-2-fluoro- $\beta$ -D-glucopyranosyl)-sulfonate ( <b>2.35</b> ), para-toluene-(2-deoxy-2-fluoro- $\beta$ -D-glucopyranosyl)-sulfinic acid ( <b>2.36</b> ).....	80
2.6.2.3 Synthesis of dimethyl (2-deoxy-2-fluoro- $\beta$ -D-glucopyranosyl) phosphate ( <b>2.37</b> ), and attempted syntheses of methyl methyl-(2-deoxy-2-fluoro- $\beta$ -D- glucopyranosyl) phosphonate ( <b>2.38</b> ), and dimethyl (2-deoxy-2-fluoro- $\beta$ -D- glucopyranosyl) phosphinate ( <b>2.39</b> ) .....	82
2.6.2.4 Proposed mechanism for decomposition of methyl methyl-(3,4,6-tri-O-acetyl- 2-deoxy-2-fluoro- $\beta$ -D-glucopyranosyl) phosphonate ( <b>2.51</b> ), and dimethyl (3,4,6-tri- O-acetyl-2-deoxy-2-fluoro- $\beta$ -D-glucopyranosyl) phosphinate ( <b>2.53</b> ) under acidic or basic conditions .....	84
2.6.2.5 Synthesis of dibenzyl (2-deoxy-2-fluoro- $\beta$ -D-glucopyranosyl) phosphate ( <b>2.62</b> ), benzyl benzyl-(2-deoxy-2-fluoro- $\beta$ -D-glucopyranosyl) phosphonate ( <b>2.67</b> ), and dibenzyl (2-deoxy-2-fluoro- $\beta$ -D-glucopyranosyl) phosphinate ( <b>2.70</b> ).....	87

<b>2.7 Enzymatic testing of fluorosugars bearing phosphorus-based aglycones .....</b>	<b>90</b>
2.7.1 <i>Kinetic analysis of the inactivation of Abg by 2.37, 2.55, 2.60 and 2.63 .....</i>	90
2.7.1.1 Dimethyl (2-deoxy-2-fluoro- $\beta$ -D-glucopyranosyl) phosphate ( <b>2.37</b> ) .....	90
2.7.1.2 Dibenzyl (2-deoxy-2-fluoro- $\beta$ -D-glucopyranosyl) phosphate ( <b>2.62</b> ).....	93
2.7.1.3 Benzyl benzyl-(2-deoxy-2-fluoro- $\beta$ -D-glucopyranosyl) phosphonate ( <b>2.67</b> )	95
2.7.1.4 Dibenzyl (2-deoxy-2-fluoro- $\beta$ -D-glucopyranosyl) phosphinate ( <b>2.70</b> ).....	96
2.7.3 <i>Tests for the stability of glucosides bearing phosphorus-based aglycones towards spontaneous hydrolysis.....</i>	98
2.7.4 <i>General conclusions for aglycone variants .....</i>	100
2.7.4.1 Considerations of aglycone properties.....	100
2.7.4.2 Summary of kinetic parameters for inactivation of Abg using the fluorosugar variants with novel aglycones.....	101
2.7.4.3 Stability considerations.....	104
<b>2.8 Expanding the scope of fluorosugars bearing phosphorus-based aglycones as inactivators of other enzymes .....</b>	<b>105</b>
2.8.1 <i>Target compounds .....</i>	105
2.8.1 <i>Chemical synthesis.....</i>	107
2.8.1.1 Synthesis of benzyl benzyl-(2-deoxy-2-fluoro- $\beta$ -D-mannopyranosyl) phosphonate ( <b>2.71</b> ) .....	107
2.8.1.2 Synthesis of benzyl benzyl-(2-deoxy-2-fluoro- $\beta$ -D-galactopyranosyl) phosphonate ( <b>2.72</b> ) .....	107
2.8.1.3 Synthesis of dibenzyl (2-deoxy-2-fluoro- $\alpha$ -D-glucopyranosyl) phosphate ( <b>2.73</b> ).....	108
2.8.1.4 Synthesis of dibenzyl (2-deoxy-2-fluoro- $\alpha$ -D-mannopyranosyl) phosphate ( <b>2.74</b> ) and benzyl benzyl-(2-deoxy-2-fluoro- $\alpha$ -D-mannopyranosyl) phosphonate ( <b>2.75</b> ).....	110



<b>2.9 Enzymatic testing of fluorosugars bearing phosphorus-based aglycones as inactivators of other enzymes .....</b>	<b>111</b>
2.9.1 <i>Kinetic analysis of the inactivation of Abg by 2.64 and 2.65 .....</i>	111
2.9.1.1 Benzyl benzyl-(2-deoxy-2-fluoro- $\beta$ -D-mannopyranosyl) phosphonate ( <b>2.71</b> ) .....	111
2.9.1.2 Benzyl benzyl-(2-deoxy-2-fluoro- $\beta$ -D-galactopyranosyl) phosphonate ( <b>2.72</b> ) .....	112
2.9.2 <i>Kinetic analysis of the inactivation of Man2A by 2.64.....</i>	115
2.9.3 <i>Kinetic analysis of the inactivation of E. coli <math>\beta</math>-Gal by 2.65.....</i>	116
2.9.4 <i>Kinetic evaluation of 2.66 as a covalent inactivator of Yag.....</i>	118
2.9.5 <i>Kinetic evaluation of 2.67 as a covalent inactivator of JBAM.....</i>	119
<b>2.10: General conclusions regarding scope and usefulness of various aglycones in fluorosugars as inactivators of glycosidases .....</b>	<b>122</b>
<b>Chapter 3: Development of More Efficient Covalent Inactivators for Two Lysosomal Enzymes.....</b>	<b>123</b>
<b>3.1 Glucocerebrosidase (GCase).....</b>	<b>124</b>
3.1.1 <i>General introduction .....</i>	124
3.1.2 <i>Known inactivators of GCase.....</i>	125
3.1.1.1 Conduritol B-epoxide .....	125
3.1.1.2 2-Deoxy-2-fluoro- $\beta$ -D-glucosyl fluoride.....	126
3.1.3 <i>General considerations for GCase inactivators.....</i>	127
3.1.4 <i>Target compounds .....</i>	128
3.1.5 <i>Chemical synthesis.....</i>	129
3.1.4.1 Synthesis of 2,4-dinitrophenyl 2-deoxy-2-fluoro- $\beta$ -D-glucopyranoside ( <b>3.3</b> ) and 5-amidooctyl-2,4-dinitrophenyl 2-deoxy-2-fluoro- $\beta$ -D-glucopyranoside ( <b>3.4</b> )	129

3.1.4.2 Synthesis of diisooctyl (2-deoxy-2-fluoro- $\beta$ -D-glucopyranosyl) phosphinate ( <b>3.5</b> ), synthesis of dioctyl (2-deoxy-2-fluoro- $\beta$ -D-glucopyranosyl) phosphate ( <b>3.6</b> ), attempted synthesis of octyl octyl-(2-deoxy-2-fluoro- $\beta$ -D-glucopyranosyl) phosphonate ( <b>3.7</b> ), and attempted synthesis of dioctyl (2-deoxy-2-fluoro- $\beta$ -D-glucopyranosyl) phosphinate ( <b>3.8</b> ). .....	131
<i>3.1.6 Kinetic analysis of the inactivation of Abg by 3.4, 3.5 and 3.6</i> .....	134
3.1.5.1 5-Amidooctyl-2,4-dinitrophenyl 2-deoxy-2-fluoro- $\beta$ -D-glucopyranoside ( <b>3.4</b> ) .....	134
3.1.5.2 Diisooctyl (2-deoxy-2-fluoro- $\beta$ -D-glucopyranosyl) phosphinate ( <b>3.5</b> ).....	136
3.1.5.3 Dioctyl (2-deoxy-2-fluoro- $\beta$ -D-glucopyranosyl) phosphate ( <b>3.6</b> ) .....	136
<i>3.1.6 Kinetic analysis of the inactivation of GCase by 2.2, 2.3, 2.37, 2.55, 2.60, 2.63, 2.64, 3.3, 3.4, 3.5 and 3.6.</i> .....	138
3.1.6.1 2,4-Dinitrophenyl 2-deoxy-2-fluoro- $\beta$ -D-glucopyranoside ( <b>3.3</b> ).....	139
3.1.6.2 5-Amidooctyl-2,4-dinitrophenyl 2-deoxy-2-fluoro- $\beta$ -D-glucopyranoside ( <b>3.4</b> ) .....	140
3.1.6.3 5-Fluoro- $\beta$ -D-glucopyranosyl fluoride ( <b>2.2</b> ) and 5-fluoro- $\alpha$ -L-idopyranosyl fluoride ( <b>2.3</b> ).....	141
3.1.6.4 Dimethyl (2-deoxy-2-fluoro- $\beta$ -D-glucopyranosyl) phosphate ( <b>2.37</b> ) .....	142
3.1.6.5 Dibenzyl (2-deoxy-2-fluoro- $\beta$ -D-glucopyranosyl) phosphate ( <b>2.62</b> ), benzyl benzyl-(2-deoxy-2-fluoro- $\beta$ -D-glucopyranosyl) phosphonate ( <b>2.67</b> ) and dibenzyl (2-deoxy-2-fluoro- $\beta$ -D-glucopyranosyl) phosphinate ( <b>2.70</b> ) .....	143
3.1.6.6 Dioctyl (2-deoxy-2-fluoro- $\beta$ -D-glucopyranosyl) phosphate ( <b>3.6</b> ) .....	146
3.1.6.7 Benzyl benzyl-(2-deoxy-2-fluoro- $\beta$ -D-mannopyranosyl) phosphonate ( <b>2.71</b> ) .....	147
3.1.6.8 Diisooctyl (2-deoxy-2-fluoro- $\beta$ -D-glucopyranosyl) phosphinate ( <b>3.5</b> ).....	148
<i>3.1.8 Conclusions and future considerations</i> .....	149

<b>3.2 <math>\alpha</math>-L-Iduronidase (Idua) .....</b>	<b>151</b>
3.2.1 <i>General introduction .....</i>	151
3.2.2 <i>History of activated fluorosugars as Idua inactivators .....</i>	152
3.2.3 <i>Chemical synthesis of difluorosugar fluorides as potential inactivators of Idua .....</i>	153
3.2.2.1 Target compounds .....	153
3.2.2.2 Synthesis of 2-deoxy-2,5-difluoro- $\alpha$ -L-idopyranosyl uronic acid fluoride (3.18).....	154
3.2.2.3 Synthesis of 1,5-difluoro-L-idopyranosyl uronic acid fluoride (3.19) .....	156
3.2.4 <i>Enzymatic evaluation of 3.18 and 3.19 as inhibitors of Idua .....</i>	158
3.2.5 <i>Conclusions and future considerations .....</i>	160
<b>Chapter 4: Testing of Fluorinated Carbohydrates as Potential Therapeutic and Diagnostic Tools for Gauchers Disease .....</b>	<b>161</b>
<b>4.1: Investigating pharmacological chaperones for GCase .....</b>	<b>162</b>
4.1.1 <i>Current therapeutic strategies in the treatment of Gauchers disease .....</i>	162
4.1.1.1 Enzyme replacement therapy (ERT) .....	162
4.1.1.2 Substrate reduction therapy (SRT) .....	163
4.1.1.3 Other potential treatments .....	164
4.1.1.4 Enzyme enhancement therapy (EET) through the use of pharmacological chaperones (PC).....	164
4.1.2 <i>An introduction to activated fluorosugars as potential PCs .....</i>	166
4.1.3 <i>Testing of 2.1 and 2.60 as PC for GCase in a cell-based system.....</i>	168
4.1.3.1 Testing the ability of <b>2.1</b> and <b>2.67</b> to raise the melting temperature of GCase <i>in vitro</i> .....	168
4.1.3.2 Preliminary testing of <b>2.1</b> as a PC for GCase .....	171
4.1.3.3 Preliminary testing of <b>2.67</b> as a PC for GCase .....	172

4.1.3.4 Conclusions and future directions for the use of <b>2.1</b> and <b>2.67</b> as PC of GCase .....	174
<b>4.2 Development of activated fluorosugars as PET imaging agents for monitoring ERT in Gauchers disease .....</b>	<b>175</b>
4.2.1 <i>Objectives in development of a PET imaging agent</i> .....	175
4.2.2 <i>Previous attempts to radiolabel GCase</i> .....	176
4.2.2.1 2,6-Dideoxy-2-fluoro-6-[ <sup>18</sup> F]-fluoro-β-D-glucosyl fluoride ( <b>4.13</b> ) .....	177
4.2.2.2 2-Deoxy-2-[ <sup>18</sup> F]fluoro-β-D-mannopyranosyl [ <sup>18</sup> F]-fluoride ( <b>4.16</b> ) .....	178
4.2.3 <i>Radiolabelling of GCase with 2,4-dinitrophenyl 2-deoxy-2-[<sup>18</sup>F]-fluoro-β-D-glucopyranoside (4.19) and PET imaging results</i> .....	179
4.2.3.1 Radiosynthesis of 2,4-dinitrophenyl 2-deoxy-2-[ <sup>18</sup> F]-fluoro-β-D-glucopyranoside ( <b>4.19</b> ) .....	179
4.2.3.2 Radiolabelling of Abg with <b>4.19</b> .....	182
4.2.3.3 Radiolabelling of GCase with <b>4.19</b> .....	184
4.2.3.4 PET imaging experiments using GCase radiolabelled by <b>4.19</b> .....	187
4.2.4 <i>Conclusions and future directions</i> .....	189
<b>Chapter 5: Materials and Methods.....</b>	<b>191</b>
<b>5.1 Synthetic chemistry .....</b>	<b>192</b>
5.1.1 <i>General procedures for chemical synthesis</i> .....	192
5.1.1.1 General procedure A for bromination.....	193
5.1.1.2 General procedure B for deprotection of esters.....	193
5.1.1.3 General procedure C for free radical bromination.....	193
5.1.1.4 General procedure D for deprotection of esters.....	194
5.1.2 <i>Synthesis and compound characterization</i> .....	194
<b>5.2 Enzymology .....</b>	<b>252</b>
5.2.1 <i>Generous gifts</i> .....	252

5.2.2 General enzymatic materials and methods.....	252
5.2.3 Continuous enzymatic assays .....	255
5.2.4 Stopped enzymatic assays .....	255
5.2.5 Enzyme inactivation assays .....	255
5.2.6 Enzyme reactivation assays .....	256
5.2.7 Test for a highly active contaminant .....	257
5.2.8 Determination of apparent $K_i'$ values .....	257
5.2.9 Determination of $K_i$ values .....	257
<b>5.3 Radiochemistry .....</b>	<b>258</b>
5.3.1 Radiosynthesis of 2,4-dinitrophenyl 2-deoxy-2- $[^{18}\text{F}]$ -fluoro- $\beta$ -D-glucopyranoside (4.19).....	258
5.3.2 Radiochemical labelling of Abg with purified 4.19.....	259
5.3.3 Radiochemical labelling of GCase with purified 4.19.....	259
<b>References.....</b>	<b>261</b>
<b>Appendix I .....</b>	<b>274</b>
<b>Equations Representing Enzyme Kinetics .....</b>	<b>274</b>
Michaelis-Menten kinetics .....	275
Enzyme kinetics with a mechanism-based inactivator.....	278
<b>Appendix II: List of Publications .....</b>	<b>280</b>

## **List of Tables**

<b>Table 2.1.</b> Kinetic parameters for selected inactivators of Abg.....	60
<b>Table 2.2.</b> Kinetic parameters for selected fluorosugars as inactivators of Abg. ....	102
<b>Table 2.3.</b> Kinetic parameters for selected fluorosugars as inactivators of Abg. ....	114
<b>Table 2.4.</b> Kinetic parameters for selected fluorosugars as inactivators of <i>E. coli</i> $\beta$ -Gal....	117
<b>Table 3.1.</b> Kinetic parameters for known activated fluorosugar inactivators of GCase. ....	138
<b>Table 3.2.</b> Kinetic parameters for selected activated fluorosugars as inactivators of GCase. .....	150

## List of Figures

<b>Figure 1.1.</b> General glycosidase-catalyzed hydrolysis reaction.....	2
<b>Figure 1.2.</b> Cleavage of a glycoside catalyzed by either a retaining (upper pathway) or inverting (lower pathway) glycosidase.....	3
<b>Figure 1.3.</b> Ion-pair intermediate proposed by Phillips as an intermediate during hydrolysis of a glycoside catalyzed by a retaining glycosidase, shown here for a retaining $\beta$ -glucosidase. ....	6
<b>Figure 1.4.</b> Chemical structures of the glycosidase inhibitors deoxynojirimycin ( <b>1.1</b> ) and isofagomine ( <b>1.2</b> ). ....	9
<b>Figure 1.5.</b> Chemical structures of the $\beta$ -glucosidase inhibitors gluconolactone ( <b>1.3</b> ), <i>gluco</i> -hydroximolactam ( <b>1.4</b> ), and glucotetrazole ( <b>1.5</b> ). ....	11
<b>Figure 1.6.</b> Structures of some representative covalent glycosidase inactivators. X = F or dinitrophenolate. ....	14
<b>Figure 1.7.</b> Structures of three commonly employed PET imaging agents, FDG ( <b>1.12</b> ), [ $^{11}\text{C}$ ]clorgyline ( <b>1.13</b> ) and [ $^{11}\text{C}$ ]L-deprenyl ( <b>1.14</b> ). ....	32
<b>Scheme 1.9.</b> Schemes depicting a) cellular metabolism of FDG, and b) first two steps of cellular metabolism of glucose. HK = Hexokinase, PGI = Phosphoglucose isomerise. Adapted from Voet and Voet.....	33
<b>Figure 2.1.</b> Structures of activated fluorosugar glycosidase inactivators, represented as glucosides. ....	42
<b>Figure 2.2.</b> Mechanism of inactivation of a retaining $\beta$ -glucosidase using 2-deoxy-2-fluoro- $\beta$ -D-glucosyl fluoride through accumulation of the stable covalent glycosyl-enzyme intermediate. ....	42
<b>Figure 2.3.</b> Turnover of covalent glycosyl-enzyme intermediate by a) hydrolysis and b) transglycosylation. ....	43
<b>Figure 2.4.</b> Fluorosugar variants chosen as synthetic targets. ....	50
<b>Figure 2.5.</b> Inactivation of Abg with <b>2.1</b> .....	57
<b>Figure 2.6.</b> Residual enzymatic activity versus time curve for the reactivation of covalent 2-deoxy-2-fluoro-glucosyl-Abg intermediate following incubation with 20 mM thiophenyl $\beta$ -D-glucopyranoside.....	58
<b>Figure 2.7.</b> Apparent inactivation of Abg with <b>2.4</b> .....	59
<b>Figure 2.7.</b> Residual activity versus time for Abg treated with 20 mM $\beta$ -Glc-SPh, following treatment of Abg with <b>2.4</b> .....	61

<b>Figure 2.8.</b> Test for the presence of a contaminating impurity in the preparation of <b>2.4</b> using different concentrations of Abg.....	62
<b>Figure 2.9.</b> ESI-MS analysis of a) Abg, b) Abg inactivated with <b>2.1</b> , and c) Abg inactivated with <b>2.4</b> .....	64
<b>Figure 2.10.</b> Dixon plot representation of compounds a) <b>2.4</b> , b) <b>2.6</b> , c) <b>2.7</b> and d) <b>2.8</b> tested as reversible inhibitors of Abg.....	67
<b>Figure 2.12.</b> Dixon plot representation of the testing of <b>2.5</b> as a competitive inhibitor of Abg. ....	69
<b>Figure 2.13.</b> Observed absorbance vs. time data for the hydrolysis of pNP- $\beta$ -Glc by Abg in the presence and absence of <b>2.5</b> .....	70
<b>Figure 2.14.</b> Mechanism of production of gluconolactone by sequential enzymatic and non-enzymatic reactions. ....	70
<b>Figure 2.15.</b> Residual activity versus time of Yag, following treatment of with a) <b>2.7</b> and b) <b>2.8</b> . ....	71
<b>Figure 2.16.</b> Structures of the fluorosugar inactivators incorporating natural aglycones. a) 2-deoxy-2-fluoro-glucosyl tropaeolin and b) 2'-deoxy-2'-fluoro-cellobiose. ....	76
<b>Figure 2.17.</b> Structures of the target compounds bearing an equatorial anomeric chloride as the aglycone.....	77
<b>Figure 2.18.</b> Structures of the target aglycone variants incorporating sulfur- and phosphorus-based aglycones. ....	78
<b>Figure 2.19.</b> Decomposition of both <b>2.27</b> and <b>2.30</b> when treated with NH <sub>3</sub> in MeOH. ....	79
<b>Figure 2.20.</b> Schematic depiction of the mechanism of decomposition 1 for <b>2.51</b> and <b>2.53</b> . 85	
<b>Figure 2.21.</b> Schematic depiction of the mechanism of decomposition 2 for <b>2.51</b> and <b>2.53</b> . 85	
<b>Figure 2.22.</b> Mechanism of decomposition for DNP-glycosides under basic conditions.....	86
<b>Figure 2.23.</b> General structure for the proposed impurity in the preparation of <b>2.70</b> .....	90
<b>Figure 2.24.</b> Inactivation of Abg with <b>2.37</b> .....	91
<b>Figure 2.25.</b> Inactivation of Abg and <b>2.37</b> in the presence and absence of 2.5 $\mu$ M gluconolactone.....	92
<b>Figure 2.26.</b> Residual activity versus time for Abg incubated with 20 mM Glc-SPh, following treatment of Abg with <b>2.37</b> . ....	93
<b>Figure 2.27.</b> Inactivation of Abg with <b>2.62</b> .....	94
<b>Figure 2.28.</b> Inactivation of Abg with <b>2.67</b> .....	95
<b>Figure 2.29.</b> Inactivation of Abg with the impure solution of <b>2.70</b> . ....	97



<b>Figure 2.30.</b> Monitoring stability of a) <b>2.62</b> , b) <b>2.67</b> and c) <b>2.70</b> by measuring residual enzyme activity as a function of inactivator incubation time. ....	99
<b>Figure 2.31.</b> Structures of target compounds chosen as inactivators of other glycosidases. ....	106
<b>Figure 2.32.</b> Inactivation of Abg with <b>2.71</b> .....	112
<b>Figure 2.33.</b> Inactivation of Abg with <b>2.72</b> .....	113
<b>Figure 2.34.</b> Inactivation of Man2A by <b>2.71</b> . ....	115
<b>Figure 2.35.</b> Inactivation of <i>E. coli</i> $\beta$ -Gal with <b>2.72</b> .....	116
<b>Figure 2.36.</b> TLC analysis of hydrolysis of <b>2.73</b> by Yag, 18 minutes incubation at 37 °C. Lane 1 = positive control (2-deoxy-2-fluoro-glucose). Lane 2 = <b>2.73</b> + Yag. Lane 3 = negative control, <b>2.73</b> only. ....	118
<b>Figure 2.37.</b> Testing of <b>2.73</b> as a competitive substrate for Yag by plotting 1/rate of pNP- $\alpha$ -Glc hydrolysis catalyzed by Yag vs. concentration of <b>2.73</b> . ....	119
<b>Figure 2.38.</b> TLC plate showing <b>2.74</b> incubated in the presence and absence of JBAM. ...	120
<b>Figure 2.39.</b> Testing of <b>2.74</b> as a competitive substrate for JBAM. ....	121
<b>Figure 3.1.</b> Structures of two known covalent inactivators of GCCase. ....	125
<b>Figure 3.2.</b> Structures of the known GCCase inactivator 2-deoxy-2-fluoro- $\beta$ -D-glucosyl fluoride ( <b>2.1</b> ) and the natural substrate of GCCase, glucosyl ceramide ( <b>3.2</b> ). ....	128
<b>Figure 3.3.</b> Structures of the GCCase-targeted aglycone variants.....	128
<b>Figure 3.4.</b> Fischer diagrams depicting potential stereoisomers of a) diisooctyl phosphinic acid, R=CH <sub>2</sub> C(CH <sub>3</sub> ) <sub>3</sub> , R'=H and b) <b>3.15</b> , R=CH <sub>2</sub> C(CH <sub>3</sub> ) <sub>3</sub> , R'=tetra-O-acetyl-2-deoxy-2-fluoro- $\beta$ -D-glucopyranoside. ....	132
<b>Figure 3.5.</b> Inactivation of Abg with <b>3.4</b> .....	135
<b>Figure 3.6.</b> Inactivation of Abg with <b>3.6</b> .....	137
<b>Figure 3.7.</b> Inactivation of GCCase with <b>3.3</b> .....	139
<b>Figure 3.8.</b> Inactivation of GCCase with <b>2.37</b> .....	142
<b>Figure 3.9.</b> Inactivation of GCCase with <b>2.62</b> .....	143
<b>Figure 3.10.</b> Inactivation of GCCase with <b>2.67</b> .....	145
<b>Figure 3.11.</b> Inactivation of GCCase with <b>2.70</b> .....	145
<b>Figure 3.12.</b> Inactivation of GCCase with <b>3.6</b> .....	147
<b>Figure 3.13.</b> Inactivation of GCCase with <b>2.71</b> .....	148
<b>Figure 3.14.</b> Structures of activated fluorosugars previously tested as covalent inactivators of Idua. ....	152

<b>Figure 3.15.</b> Structures of difluorosugar fluoride targets chosen as potential Idua inactivators.....	153
<b>Figure 3.16.</b> Dixon plot representation of inhibition of Idua by <b>3.18</b> .....	159
<b>Figure 4.1.</b> Structure of <i>N</i> -butyldeoxynojirimycin ( <b>4.1</b> ).....	163
<b>Figure 4.2.</b> Representative structures of some compounds shown to act as PCs for GCCase. .....	165
<b>Figure 4.3.</b> Structures of activated fluorosugars tested as PCs for GCCase.....	168
<b>Figure 4.4.</b> Relative fluorescence versus temperature curves for GCCase incubated for 30 minutes in the presence of a) <b>2.67</b> , b) isofagomine, and c) <b>2.1</b> . ....	169
<b>Figure 4.5.</b> Western blot analysis of GCCase from fibroblast cells bearing an Asn370Ser point mutation. ....	171
<b>Figure 4.6.</b> Western blot analysis of GCCase from patient fibroblast cells bearing an Asn370Ser point mutation. Cells treated with.....	173
<b>Figure 4.7.</b> Radio-TLC analysis of the crude reaction mixture following treatment of <b>1.12</b> with DNFB, using a 4 : 1 EtOAc : MeOH eluent.....	181
<b>Figure 4.8.</b> Radio-TLC analysis of <b>4.19</b> following HPLC purification using a 4:1 EtOAc : MeOH eluent. ....	182
<b>Figure 4.9.</b> Radio-TLC analysis of <b>4.19</b> treated with Abg for 10 minutes using a 4:1 EtOAc : MeOH eluent. ....	183
<b>Figure 4.10.</b> Radio-TLC analysis of <b>4.19</b> treated with Abg, followed by incubation with 20 mM thiophenyl $\beta$ -D-glucopyranoside using a 4:1 EtOAc : MeOH eluent, sampled at a) 10 minutes, and b) 2 hours.....	184
<b>Figure 4.11.</b> Radio-TLC analysis of the reaction of <b>4.19</b> with GCCase using a 4:1 EtOAc : MeOH eluent. ....	185
<b>Figure 4.12.</b> Radio-TLC analysis of purified radiolabelled GCCase using a 4:1 EtOAc : MeOH eluent. ....	186
<b>Figure 4.13.</b> Micro-PET images generated by injection of radiolabelled GCCase into a mouse. .....	187
<b>Figure 4.13.</b> Comparison of PET images obtained for mice treated and untreated with mannan prior to injection by GCCase radiolabelled by <b>4.19</b> . ....	188

## List of Schemes

<b>Scheme 1.1.</b> Mechanism of an inverting $\beta$ -glucosidase.....	4
<b>Scheme 1.2.</b> Mechanism of a retaining $\beta$ -glucosidase.....	6
<b>Scheme 1.3.</b> Mechanism of generation of reactive aglycone from <b>1.9</b> .....	14
<b>Scheme 1.4.</b> The hydrolytic cleavage reaction of glucosylceramide to glucose and ceramide that is catalyzed by GCase.....	20
<b>Scheme 1.5.</b> The enzymatic degradation of gangliosides in the lysosome.....	21
<b>Scheme 1.6.</b> The hydrolytic reaction catalyzed by Idua.....	24
<b>Scheme 1.7.</b> The enzymatic degradation of dermatan sulfate in the lysosome.....	25
<b>Scheme 1.8.</b> The enzymatic degradation of heparan sulfate in the lysosome.....	26
<b>Scheme 1.10.</b> Mechanism of a) MAO oxidation of a primary amine, and b) covalent inactivation of MAO with [ $^{11}\text{C}$ ]clorgyline ( $\text{R}' = (\text{CH}_2)_3\text{-2,4-dichlorophenol}$ ) or [ $^{11}\text{C}$ ]L-deprenyl ( $\text{R}' = \text{CH}(\text{CH}_3)\text{CH}_2\text{Ph}$ ).....	34
<b>Scheme 2.1.</b> Light catalyzed free-radical generation of a C5 bromide by <i>N</i> -bromosuccinimide (NBS). $\text{R} = \text{OAc}$ , $\text{OPh}$ , $\text{OMe}$ .....	47
<b>Scheme 2.2.</b> The synthesis of 2-deoxy-2-fluoro-glucosyl fluoride ( <b>2.1</b> ).....	51
<b>Scheme 2.3.</b> Synthesis of 5-fluoro- $\beta$ -D-glucosyl fluoride ( <b>2.2</b> ) and 5-fluoro- $\alpha$ -L-idosyl fluoride ( <b>2.3</b> ).....	52
<b>Scheme 2.4.</b> Synthesis of 2-deoxy-2,5-difluoro- $\alpha$ -L-idopyranosyl fluoride ( <b>2.4</b> ).....	53
<b>Scheme 2.5.</b> Synthesis of 1-fluoro-D-glucopyranosyl fluoride ( <b>2.5</b> ), 1,5-difluoro-D-glucopyranosyl fluoride ( <b>2.7</b> ) and 1,5-difluoro-L-idopyranosyl fluoride ( <b>2.8</b> ).....	54
<b>Scheme 2.6.</b> Synthesis of 2-deoxy-1,2-difluoro-D-glucopyranosyl fluoride ( <b>2.6</b> ).....	56
<b>Scheme 2.7.</b> Attempted synthesis of methyl-(2-deoxy-2-fluoro- $\beta$ -D-glucopyranosyl)-sulfonate ( <b>2.34</b> ).....	80
<b>Scheme 2.8.</b> Attempted synthesis of <i>para</i> -toluene-(2-deoxy-2-fluoro- $\beta$ -D-glucopyranosyl)-sulfonate ( <b>2.35</b> ).....	81
<b>Scheme 2.9.</b> Attempted synthesis of <i>para</i> -toluene-(2-deoxy-2-fluoro- $\beta$ -D-glucopyranosyl)-sulfinate ( <b>2.36</b> ).....	81
<b>Scheme 2.10.</b> Synthesis of dimethyl (2-deoxy-2-fluoro- $\beta$ -D-glucopyranosyl) phosphate ( <b>2.37</b> ).....	82
<b>Scheme 2.11.</b> Attempted synthesis of methyl methyl-(2-deoxy-2-fluoro- $\beta$ -D-glucopyranosyl) phosphonate ( <b>2.38</b> ).....	83

<b>Scheme 2.12.</b> Attempted synthesis of dimethyl (2-deoxy-2-fluoro- $\beta$ -D-glucopyranosyl) phosphinate ( <b>2.39</b> ). .....	84
<b>Scheme 2.13.</b> Synthesis of dibenzyl (2-deoxy-2-fluoro- $\beta$ -D-glucopyranosyl) phosphate ( <b>2.62</b> ).....	88
<b>Scheme 2.14.</b> Synthesis of benzyl benzyl-(2-deoxy-2-fluoro- $\beta$ -D-glucopyranosyl) phosphonate ( <b>2.67</b> ). .....	88
<b>Scheme 2.15.</b> Synthesis of dibenzyl-(2-deoxy-2-fluoro- $\beta$ -D-glucopyranosyl) phosphinate ( <b>2.70</b> ).....	89
<b>Scheme 2.16.</b> Synthesis of benzyl benzyl-(2-deoxy-2-fluoro- $\beta$ -D-mannopyranosyl) phosphonate ( <b>2.71</b> ). .....	107
<b>Scheme 2.17.</b> Synthesis of benzyl benzyl-(2-deoxy-2-fluoro- $\beta$ -D-galactopyranosyl) phosphonate ( <b>2.72</b> ). .....	108
<b>Scheme 2.18.</b> Synthesis of dibenzyl (2-deoxy-2-fluoro- $\alpha$ -D-glucopyranosyl) phosphate ( <b>2.73</b> ).....	109
<b>Scheme 2.19.</b> Synthesis of dibenzyl (2-deoxy-2-fluoro- $\alpha$ -D-mannopyranosyl) phosphate ( <b>2.74</b> ) and benzyl benzyl-(2-deoxy-2-fluoro- $\alpha$ -D-mannopyranosyl) phosphonate ( <b>2.75</b> ). ..	110
<b>Scheme 3.1.</b> Mechanism of inactivation of GCase by <b>3.1</b> through covalent bond formation to the a) catalytic nucleophile and b) catalytic acid/base residue. ....	125
<b>Scheme 3.2.</b> Synthesis of 2,4-dinitrophenyl 2-deoxy-2-fluoro- $\beta$ -D-glucopyranoside ( <b>3.3</b> ). ..	130
<b>Scheme 3.3.</b> Synthesis of 5-amidooctyl-2,4-dinitrophenyl 2-deoxy-2-fluoro- $\beta$ -D-glucopyranoside ( <b>3.4</b> ). .....	130
<b>Scheme 3.5.</b> Synthesis of diisooctyl (2-deoxy-2-fluoro- $\beta$ -D-glucopyranosyl) phosphinate ( <b>3.5</b> ).....	131
<b>Scheme 3.4.</b> Synthesis of dioctyl (2-deoxy-2-fluoro- $\beta$ -D-glucopyranosyl) phosphate ( <b>3.6</b> ). .....	133
<b>Scheme 3.6.</b> Synthesis of 2-deoxy-2,5-difluoro- $\alpha$ -L-idopyranosyl uronic acid fluoride ( <b>3.18</b> ). .....	155
<b>Scheme 3.7.</b> Synthesis of 1,5-difluoro-L-idopyranosyl uronic acid fluoride ( <b>3.19</b> ). .....	157
<b>Scheme 4.1.</b> Radiosynthesis of 2,6-dideoxy-2-fluoro-6-[ $^{18}\text{F}$ ]-fluoro- $\beta$ -D-glucosyl fluoride ( <b>4.13</b> ).....	177
<b>Scheme 4.2.</b> Radiosynthesis of 2-deoxy-2-[ $^{18}\text{F}$ ]-fluoro- $\beta$ -D-mannopyranosyl [ $^{18}\text{F}$ ]fluoride ( <b>4.16</b> ).....	178
<b>Scheme 4.3.</b> Radiosynthesis of 2,4-dinitrophenyl 2-deoxy-2-[ $^{18}\text{F}$ ]-fluoro- $\beta$ -D-glucopyranoside ( <b>4.19</b> ). .....	180

<b>Scheme 4.4.</b> Proposed mechanism for recovery of Abg activity following incubation with 20 mM thiophenyl $\beta$ -D-glucopyranoside through transglycosylation of the radiolabelled glycosyl-enzyme intermediate. ....	184
---	-----

## **List of Abbreviations**

[2.2.2]-Kryptofix-		4,7,13,16,21,24-Hexaoxa-1,10-diazabicyclo[8.8.8]-hexacosane
2,4-DNP- $\beta$ -D-Glc-		2,4-dinitrophenyl $\beta$ -D-glucopyranoside
Abg	-	<i>Agrobacterium</i> sp. $\beta$ -glucosidase
AcCl	-	acetyl chloride
AcOH	-	acetic acid
AIDS	-	acquired immunodeficiency syndrome
BMT	-	bone marrow transplantation
Bn	-	benzyl
CNS	-	central nervous system
CT	-	computed tomography
DABCO	-	1,4-diazobicyclo[2.2.2]octane
DMF	-	dimethyl formamide
DMSO	-	dimethyl sulfoxide
DNFB	-	2,4-dinitrofluorobenzene
DNP	-	2,4-dinitrophenyl
<i>E. coli</i> $\beta$ -Gal	-	<i>Escherichia coli</i> $\beta$ -galactosidase
EET	-	enzyme enhancement therapy
ER	-	endoplasmic reticulum
ERAD	-	endoplasmic reticulum associated degradation
ERQC	-	endoplasmic reticulum quality control

ERT	-	enzyme replacement therapy
ESI MS	-	electrospray ionization mass spectrometry
EtOH	-	ethanol
FAD <sup>+</sup>	-	oxidized flavin adenine dinucleotide
FADH <sub>2</sub>	-	reduced flavin adenine dinucleotide
FDG	-	2-deoxy-2-[ <sup>18</sup> F]-fluoro-D-glucose, or fluorodeoxyglucose
fMRI	-	functional magnetic resonance imaging
GAG	-	glycosaminoglycans
GCase	-	human glucocerebrosidase
HIV	-	human immunodeficiency virus
HK	-	hexokinase
HPLC	-	high performance liquid chromatography
IC <sub>50</sub>	-	half maximal inhibitory concentration
IdoA	-	4-methylumbelliferyl $\alpha$ -L-iduronic acid
Idua	-	human $\alpha$ -L-iduronidase
JBAM	-	jack bean $\alpha$ -mannosidase
K <sub>m</sub>	-	Michaelis constant of an enzymatic substrate
k <sub>cat</sub>	-	catalytic rate constant (turnover number)
k <sub>H</sub> /k <sub>D</sub>	-	ratio of catalytic rate constants for protio and deuterio substrates
k <sub>hyd</sub>	-	observed rate constant of hydrolysis
K <sub>i</sub>	-	dissociation constant for an enzyme-inhibitor complex

$k_{\text{obs}}$	-	observed pseudo-first order rate constant
$k_{\text{uncat}}$	-	uncatalyzed reaction rate constant
LSD	-	lysosomal storage disease
Man2A	-	$\beta$ -Mannosidase from <i>Cellulomonas fimi</i>
MAO-A	-	human monoamine oxidase A
MAO-B	-	human monoamine oxidase B
MeCN	-	acetonitrile
MeOH	-	methanol
MPS	-	Mucopolysaccharidosis
MRI	-	magnetic resonance imaging
MS	-	mass spectrometry
Ms	-	methane sulfonyl (mesyl)
MUI	-	4-methylumbelliferyl $\alpha$ -L-iduronide
$\text{NAD}^+$	-	$\beta$ -nicotinamide adenine dinucleotide
NaOMe	-	sodium methoxide
NBS	-	<i>N</i> -bromosuccinimide
NMR	-	nuclear magnetic resonance
PC	-	pharmacological chaperone
PET	-	positron emission tomography
PGI	-	phosphoglucosomerase
pNP	-	<i>para</i> -nitrophenol



pNP- $\beta$ -D-Gal	-	<i>para</i> -nitrophenyl $\beta$ -D-galactopyranoside
pNP- $\alpha$ -D-Glc	-	<i>para</i> -nitrophenyl $\alpha$ -D-glucopyranoside
pNP- $\beta$ -D-Glc	-	<i>para</i> -nitrophenyl $\beta$ -D-glucopyranoside
pNP- $\alpha$ -D-Man	-	<i>para</i> -nitrophenyl $\alpha$ -D-mannopyranoside
pNP- $\beta$ -D-Man	-	<i>para</i> -nitrophenyl $\beta$ -D-mannopyranoside
ppm	-	parts per million
R <sub>f</sub>	-	retention factor
SDS	-	sodium dodecyl sulfate
Selectfluor™	-	1-chloromethyl-4-fluoro-1,4-diazonia-bicyclo[2.2.2]octane bis(tetrafluoroborate)
SPECT	-	single photon emission computed tomography
SRT	-	substrate reduction therapy
t <sub>1/2</sub>	-	half-life
TEMPO	-	2,2,6,6-tetramethylpiperidine-1-oxy radical
TLC	-	thin layer chromatography
TMSCl	-	trimethylsilyl chloride
TNP	-	2,4,6-trinitrophenyl
Ts	-	<i>para</i> -toluene sulfonyl (tosyl)
USD	-	United States dollars
UV	-	ultraviolet light
Vis	-	visible light

$V_{\max}$	-	maximum velocity of an enzyme-catalyzed reaction
X-Gal	-	5-bromo-4-chloro-3-indoyl- $\beta$ -D-galactopyranoside
Yag	-	Yeast $\alpha$ -glucosidase

## **List of Amino Acid Abbreviations**

Ala	A	Alanine
Cys	C	Cysteine
Asp	D	Aspartic acid
Glu	E	Glutamic acid
Phe	F	Phenylalanine
Gly	G	Glycine
His	H	Histidine
Ile	I	Isoleucine
Lys	K	Lysine
Leu	L	Leucine
Met	M	Methionine
Asn	N	Asparagine
Pro	P	Proline
Gln	Q	Glutamine
Arg	R	Arginine
Ser	S	Serine
Thr	T	Threonine
Val	V	Valine
Trp	W	Tryptophan
Tyr	Y	Tyrosine

## **Acknowledgements**

First and foremost, I am deeply grateful to my supervisor, Dr. Stephen Withers, for his mentorship and encouragement throughout the course of my degree. It goes without saying that without his hard work, encouragement, dedication, inspiration, and patience, this work would have been impossible. He has been more than a supervisor, he has been the scientific mentor that all students should be so lucky to have.

I am also grateful to my numerous excellent collaborators: Drs. Don Mahuran and Michael Tropak at the Hospital for Sick Children at the University of Toronto for cell-based testing of compounds and helpful discussions; Dr. Lorne Clarke and Ms. Karin Yip for providing mice and expertise for the MicroPET studies, and for providing the GCase enzyme; Biomarin for providing the Idua enzyme; Dr. Mike Adam for providing me the opportunity to learn radiochemistry; Mr. Milan Vukovic and Ms. Yulia Rozen of the B.C. Cancer Agency for providing FDG, Ms. Siobhan McCormick for animal handling and operation of the MicroPET scanner; and Dr. Doris Doudet for help and guidance in the planning of MicroPET experiments.

Many co-workers in the Withers lab have made my time here to be much more pleasurable and productive than it would otherwise have been, and deserve thanks: Dr. Neil Lim for work on the radiochemistry; Dr. Chris Phenix for working so diligently to make the PET imaging experiments a reality and for being a great friend; Dr. Hongming Chen for providing both compounds and useful advice; Dr. Ethan Goddard-Borger for conversations and assistance in reading thesis chapters; Dr. James MacDonald for helping a new graduate student to learn; Ms. Miranda Joyce for bringing order into chaos; and Dr. Thomas Morley for innumerable useful discussions (and countless more useless ones), immense patience in reading thesis chapters, and for being a great friend.

I am eternally grateful for all of the support from friends and family. To my friends in chemistry here at UBC and back in Edmonton, my family in Edmonton (Don, Madelon, Andy and Jan) and the single most important person in my life, my wife Daria: I could not have made it this far without the constant love and support, so thanks to you all.

For Daria

## **Chapter 1: Introduction**

## 1.1 Glycosidases

Glycoside hydrolases, or glycosidases, are widespread enzymes in nature that are responsible for the hydrolytic cleavage of the acetal bond (glycosidic bond) between a sugar (glycone) and a leaving group (aglycone). Glycosidic bond cleavage is accomplished by nucleophilic attack at the anomeric center by water to yield a reducing sugar and the free aglycone (Figure 1.1). Different glycosidases have different glycone and aglycone specificities; some are very promiscuous, whilst others are highly specific for the glycone, aglycone, or both. In addition, many glycosidases are known to accept a wide variety of unnatural aglycones and some are capable of cleaving C-OAryl, C-OAlkyl, C-F, C-S and C-N bonds.

Glycosidases are important enzymes in nature; their function and dysfunction have been implicated in a number of diseases, including HIV/AIDS, influenza, diabetes, and cancer, to name but a few. They are also industrially useful enzymes, with applications in the production of pulp and paper, various foods and food additives. They are also potentially useful in the generation of renewable energy sources and chemical feedstocks based on biomass conversion.

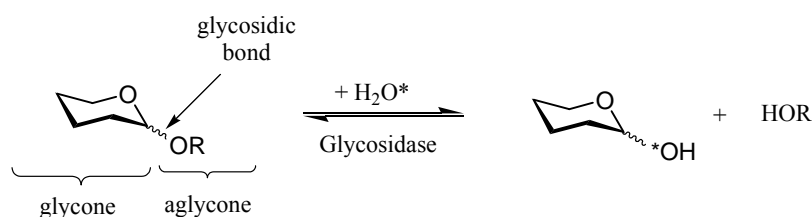


**Figure 1.1.** General glycosidase-catalyzed hydrolysis reaction.

The nature of the reaction catalyzed by a glycosidase allows for its classification according to the following criteria:

- 1) *Glycone specificity.* A given glycosidase usually has a sugar residue for which it has maximal hydrolytic activity. For example, a glucosidase has highest activity with glucoside substrates.

- 2) *Anomeric specificity*. A glycosidase usually catalyzes the cleavage of only  $\alpha$ - or  $\beta$ -linked glycosides. For example, an  $\alpha$ -glucosidase usually only catalyzes the hydrolysis of  $\alpha$ -glucosides, and generally is not capable of catalyzing the hydrolysis of a  $\beta$ -linked glucoside.
- 3) *Inverting or retaining*. A given glycosidase usually catalyzes the cleavage of the glycosidic linkage with either retention or inversion of stereochemistry at the anomeric center. For example, a retaining  $\alpha$ -glucosidase usually only catalyzes the hydrolysis of an  $\alpha$ -glucoside to yield an  $\alpha$ -configured sugar as the first formed product (Figure 1.2).

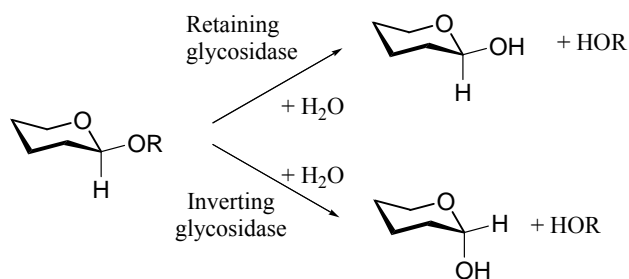


**Figure 1.2.** Cleavage of a glycoside catalyzed by either a retaining (upper pathway) or inverting (lower pathway) glycosidase.

In addition to the classification described on the basis of substrate specificity, glycosidases have been classified on the basis of their sequence similarity.<sup>1-3</sup> A searchable online database that groups sequence-related glycosidases into families can be found on the internet at <http://www.cazy.org>. In virtually all cases, enzymes within the same sequence-related family catalyze the cleavage of the glycosidic bond using the same mechanism, thus with the same stereochemical outcome (ie. either inverting or retaining), whilst sharing similar tertiary structures. Thus, the Carbohydrate Active enZYme (CAZY) database enables both the structure and function of a novel glycosidase to be predicted based solely on bioinformatics.

Glycosidases are among the most proficient enzymes known, showing rate enhancements ( $k_{\text{cat}}/k_{\text{uncat}}$ ) of up to  $10^{16}$ - $10^{17}$ -fold. To put this in context, while the half-life for

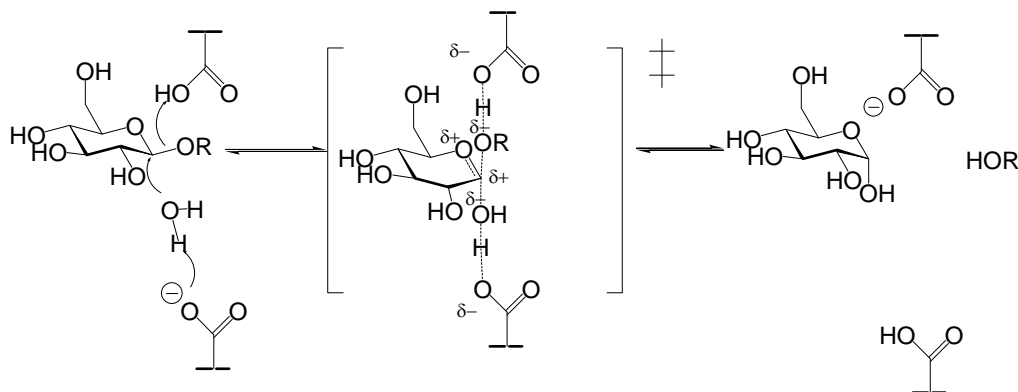


hydrolysis of cellulose at neutral pH and 25 °C has been estimated at 4.7 million years,<sup>4</sup> the glycosidase-catalyzed reaction can have a half-life of as little as 0.69 ms.<sup>5</sup>

## 1.2 Glycosidase mechanisms

### 1.2.1 Inverting glycosidases

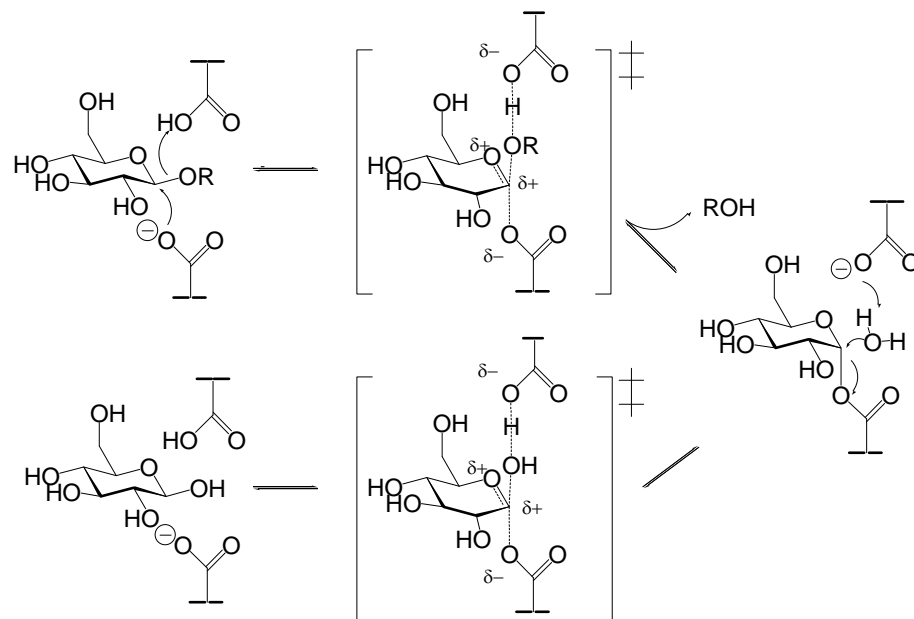
Inverting glycosidases effect bond cleavage through the action of two residues, usually carboxylic acids (Asp or Glu), located at least 6 Å apart on opposite faces of the active site.<sup>5</sup> Of the two carboxylic acids, only one is deprotonated in the enzyme's resting state and acts as a general base, removing a proton from the incoming nucleophile (typically water under normal conditions) as it attacks the anomeric carbon. The other carboxylic acid acts as an acid catalyst, protonating the departing aglycone oxygen atom and assisting in its departure from the anomeric center. The bond-making and bond-breaking steps proceed through a single, concerted oxocarbenium ion-like transition state in which the developing positive charge at the anomeric carbon is partially stabilized by electron donation from the endocyclic oxygen. The truncated sugar product is a hemi-acetal that initially has the opposite configuration at the anomeric center to that of the starting material; hence the enzyme is an “inverting” glycosidase. This mechanism, first suggested in a very insightful paper by Koshland in 1953,<sup>6</sup> is illustrated for an inverting β-glucosidase in Scheme 1.1.



**Scheme 1.1.** Mechanism of an inverting β-glucosidase.

### 1.2.2 Retaining glycosidases

Most retaining glycosidases, as with the inverting glycosidases, also have a pair of essential carboxylic acid residues (Asp or Glu) located on opposite faces of the enzyme's active site, but they are normally closer together at  $\sim 5.5$  Å apart.<sup>5</sup> The mechanism of these retaining  $\beta$ -glycosidases was first proposed in 1953 by Koshland<sup>6</sup> and, while some of the details have subsequently been revised, the essential ideas put forth by Koshland remain generally accepted. One of the residues functions as an acid catalyst in the first mechanistic step by donating a proton to the aglycone during its departure. At the same time, the other, deprotonated carboxylate acts as a nucleophile, attacking the anomeric carbon in a reaction that also proceeds through an oxocarbenium ion-like transition state. This step, referred to as the glycosylation step, leads to the formation of a covalently linked glycosyl-enzyme intermediate, which has an anomeric configuration opposite to that of the starting material. The second step of this reaction, the deglycosylation step, involves the hydrolysis of the glycosyl-enzyme intermediate. The carboxylate that first acted as an acid catalyst now acts as a base by abstracting a proton from the incoming nucleophile, normally a water molecule. The water molecule attacks the anomeric center of the sugar, and the carboxylate residue departs via a second oxocarbenium ion-like transition state. The product thus obtained is a hemi-acetal with the same anomeric configuration as the starting material. This mechanism is drawn for a retaining  $\beta$ -glucosidase in Scheme 1.2.



**Scheme 1.2.** Mechanism of a retaining  $\beta$ -glucosidase. Note that the proton delivered during general acid catalysis may be delivered in either a syn- or anti-fashion,<sup>7</sup> depending on the specific enzyme.

The double-displacement mechanism has not always been widely accepted; an alternate mechanism made on the basis of structural studies was first proposed by Phillips<sup>8</sup> and invokes an intermediate oxocarbenium ion/carboxylate pair (Figure 1.3) rather than a covalent glycosyl-enzyme intermediate.

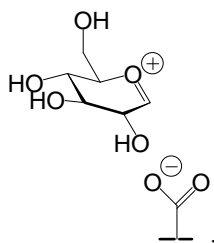


**Figure 1.3.** Ion-pair intermediate proposed by Phillips<sup>8</sup> as an intermediate during hydrolysis of a glycoside catalyzed by a retaining glycosidase, shown here for a retaining  $\beta$ -glucosidase.

Early evidence for the presence of a covalent glycosyl-enzyme intermediate in a retaining glycosidase came from the observation of kinetic isotope effects using modified

substrates.<sup>9</sup> In this study, substrates for which the second step of the enzyme-catalyzed reaction was rate-limiting showed a secondary deuterium kinetic isotope effect of  $(k_H/k_D) > 1$ , indicating that this step involved the anomeric center undergoing a  $sp^3 \rightarrow sp^2$ -like hybridization change between the intermediate and the transition state. If the ion pair mechanism was operating, then an inverse kinetic isotope effect  $(k_H/k_D) < 1$  would be expected, since the transition state would have an increased degree of  $sp^3$ -like character as it is more similar to the  $sp^3$ -hybridized product.

Further support for the double-displacement mechanism came from X-ray crystallographic studies of the three-dimensional structures of a large number of retaining glycosidases. These structures revealed the presence of two carboxylic acid residues approximately 5.5 Å apart,<sup>5,10</sup> which was consistent with the proposed mechanism involving a glycosyl-enzyme intermediate. Labelling studies with covalent inactivators of retaining glycosidases accompanied by mutagenesis studies confirmed that both of these carboxylic acid residues are important for catalysis. Kinetic analyses of mutants generated at both of these positions are consistent with one of the two residues playing the role of a nucleophilic catalyst, and the other playing the role of an acid-base catalyst.<sup>10-13</sup> A study of the behaviour of a series of artificial substrates containing aglycones with different leaving group abilities with the retaining  $\beta$ -glucosidase from *Agrobacterium sp.* (Abg) also supported the double-displacement mechanism. The kinetic data on these substrates were used to construct a Brønsted plot ( $\log k_{cat}$  vs.  $pK_a$ ) for these compounds, which showed a biphasic and concave-downwards relationship, indicating that the rate-limiting step for more chemically activated substrates is the deglycosylation step, while the glycosylation step is rate-limiting for less chemically activated substrates.<sup>14</sup> In this study, normal ( $k_H/k_D > 1$ ) secondary kinetic isotope effects were measured for both the glycosylation and deglycosylation steps,<sup>14</sup> in agreement with earlier investigations. Therefore, on the basis of these studies among others, the double-displacement mechanism has been widely accepted as the mechanism by which the majority of retaining glycosidases function.

However, it has recently been demonstrated that some glycosidase families utilize different mechanisms to effect hydrolysis of the glycosidic bond in a retaining fashion. Glycosidase families GH20<sup>15-17</sup> and GH84,<sup>18</sup> among others,<sup>10</sup> have been shown to operate

using the oxygen atom of the acetamido substituent next to the anomeric center in the substrate as the nucleophile, rather than an enzymatic nucleophilic residue. Glycoside hydrolase families GH4 and GH109 utilize a unique NAD<sup>+</sup>-dependent elimination/addition sequence.<sup>19</sup> Family GH33, GH34 and GH83 sialidases utilize a tyrosine residue as the nucleophile rather than a negatively charged carboxylate,<sup>10,20</sup> possibly to avoid unfavourable electrostatic interactions between the incoming nucleophile and the negatively-charged substrate. Finally, there are other examples of glycosidases which appear to hydrolyze the glycosidic bond utilizing other unique mechanisms, and these have been reviewed in an excellent article by Vocadlo and Davies.<sup>10</sup> However, as the enzymes studied in this body of work utilize the “classic” double-displacement mechanism, enzymes utilizing other mechanisms will not be discussed further.

## **1.3 Small molecule inhibitors of glycosidases**

### **1.3.1 The significance of glycosidase inhibitors**

Small molecule inhibitors of glycosidases have proven to be very useful reagents for a wide variety of purposes. Since glycosidases have been implicated in a number of disease states, inhibitors of these enzymes represent attractive potential therapeutic targets. For example, glycosidase inhibitors have been explored as potential therapeutics for cancer, Type II (non-insulin dependent) diabetes, HIV/AIDS and viral infections such as influenza.<sup>21-28</sup> In addition to having potential therapeutic applications, glycosidase inhibitors have also proven to be useful compounds for investigating the three-dimensional structures and catalytic mechanisms of glycosidases.<sup>5,10,12,13,23,29</sup> Inhibitors have also been used to perturb biological and biochemical pathways through the ablation of a particular glycosidase activity. The resulting effects on the animal or cell-based system help us to learn about the role played by this enzyme activity in the organism or biological pathway. For example, treatment of healthy mice with an inhibitor of the retaining  $\beta$ -glucosidase glucocerebrosidase (GCase) was shown to create a phenotype resembling a disease characterized by a deficiency in that enzyme, known as Gauchers disease (discussed below).<sup>30</sup>

Small molecules that reduce glycosidase activity can be divided into two general categories: compounds that noncovalently bind to the enzyme through the formation of specific interactions with the protein, or compounds that function through the formation of a covalent bond to the enzyme. In both cases, the usual mechanism of inhibition of enzyme activity is that the inhibitor can: bind to and block the active site, physically preventing the substrate from entering the active site; bind to and force the enzyme to adopt a catalytically inactive conformation; inhibit through a combination of both of these mechanisms.

### 1.3.2 Noncovalent glycosidase inhibitors

The most commonly studied class of glycosidase inhibitors are those that associate with the enzyme noncovalently. This class of inhibitor often behaves kinetically as a competitive inhibitor, as a result of binding, at least in part, to the enzyme active site. Thus, many noncovalent glycosidase inhibitors are molecules that chemically resemble the sugar substrates or transition states of the enzyme-catalyzed hydrolysis reaction,<sup>21,23-25,28</sup> although there are also examples of glycosidase inhibitors that do not fit this classification.<sup>31-33</sup>

Among the most potent glycosidase inhibitors are polyhydroxylated nitrogen-containing heterocycles in which the nitrogen atom can be protonated at physiological pH. This class of inhibitor is therefore positively charged, which can lead to very strong Coloumbic interactions between the inhibitor and the negatively charged carboxylate residues found in the glycosidase active site. Two groups of inhibitors bearing an endocyclic nitrogen that have proven to be potent glycosidase inhibitors are inhibitors based on the compound deoxynojirimycin (**1.1**, Figure 1.4) and inhibitors based on the compound isofagomine (**1.2**).

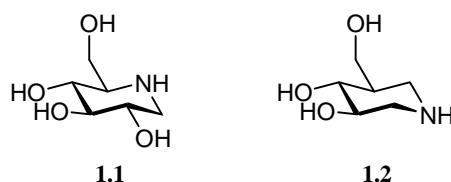


**Figure 1.4.** Chemical structures of the glycosidase inhibitors deoxynojirimycin (**1.1**) and isofagomine (**1.2**).

Deoxynojirimycin (**1.1**) has a nitrogen atom, and thus presumably a positive charge at physiological pH, in place of the endocyclic oxygen of a normal glycoside. By contrast, isofagomine (**1.2**) has this nitrogen atom at a location on the ring that would overlay with the anomeric center in a normal glycoside. This is an important feature, since in the transition state of glycoside hydrolysis by a retaining glycosidase, there is a build-up of partial positive charge at both the ring oxygen atom and at the anomeric center. This suggests that the enzyme active site has evolved to accommodate positive charge at both locations, although whether these two compounds represent true transition state mimics or compounds that fortuitously interact favourably with the enzyme active site is not entirely clear.<sup>34</sup> However, it is interesting to note that deoxynojirimycin is usually a more potent inhibitor of  $\alpha$ -glycosidases than  $\beta$ -glycosidases (for example,  $K_i = 12.6 \mu\text{M}^{23}$  and  $47 \mu\text{M}^{23}$  vs. the  $\alpha$ -glucosidase from baker's yeast, Yag, and the  $\beta$ -glucosidase from sweet almonds, respectively), while isofagomine usually shows the opposite selectivity ( $K_i = 86 \mu\text{M}^{35}$  and  $0.11 \mu\text{M}^{35}$  vs. Yag, and the  $\beta$ -glucosidase from sweet almonds, respectively). The origins of this inhibitor specificity are not entirely clear, although the preference of  $\alpha$ -glycosidases for deoxynojirimycins and  $\beta$ -glycosidases for isofagomines may arise from differences in partial positive charge build-up between their ground states and the respective transition states for enzyme-catalyzed glycoside cleavage. It has been suggested that  $\alpha$ -glycosidases show a larger difference in partial positive charge between the ground state and the transition state at the ring oxygen, while  $\beta$ -glycosidases show a larger difference in partial positive charge between the ground state and the transition state at the anomeric center.<sup>5</sup>

In addition to inhibitors that may function through mimicry of the charge distribution in the transition state of enzyme-catalyzed glycoside cleavage, other inhibitors may function by mimicking the conformation of the sugar ring in the transition state. Different sequence-related families of glycosidases proceed through transition states with different conformations about the sugar ring, with these transition states having the sugar ring adopting a geometry in which C5, O5, C1 and C2 are co-planar, such as in  $^4H_3$  or  $^3H_4$  half-chair conformations, or  $^{2,5}B$  or  $_{2,5}B$  boat conformations.<sup>36,37</sup> This means that inhibitors that adopt similar conformations may be powerful glycosidase inhibitors by harnessing the

enzyme's strong affinity for sugar-like molecules adopting these conformations. Examples of  $\beta$ -glucosidase inhibitors which may act through geometric mimicry of the transition state are shown in Figure 1.5.

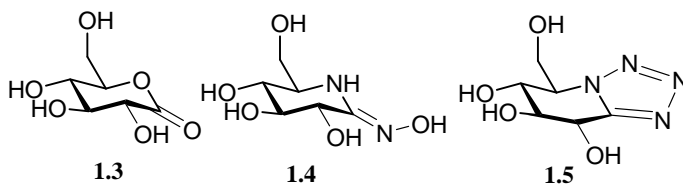


**Figure 1.5.** Chemical structures of the  $\beta$ -glucosidase inhibitors gluconolactone (**1.3**), *gluco*-hydroximolactam (**1.4**), and glucoimidazole (**1.5**).

Compound **1.3** does not bear a nitrogen that can be protonated, meaning that much of the inhibitory potency in that case ( $K_i = 1.4 \mu\text{M}$  vs. Abg,<sup>14</sup> for example) presumably derives from geometric mimicry of the flattened transition state. The other two inhibitors, *gluco*-hydroximolactam (**1.4**) and glucoimidazole (**1.5**) have nitrogen atoms that may be protonated at physiological pH, which may account for some of their inhibitory potency, but also adopt conformations that, when overlaid with a sugar ring, are more like a half-chair than the  ${}^4C_1$  conformation adopted by many sugars in solution. Thus, some of the potency of these inhibitors ( $K_i$  vs. Abg =  $30 \mu\text{M}$ <sup>14</sup> and  $1.4 \mu\text{M}$ <sup>38</sup> for **1.4** and **1.5** respectively) may be ascribed to the charge on the inhibitors, and some of the potency to the conformation adopted by the pyranose ring.

### 1.3.3 Covalent inactivators

Covalent inactivators of glycosidases are a class of molecules that ablate enzyme activity through the formation of a covalent bond between the enzyme and the inactivator.<sup>39,40</sup> The bond is typically formed by the attack of an enzyme-based nucleophile onto an electrophilic portion of the inactivator, leading to covalent attachment of the inactivator. This attachment leads to a loss of activity, most often because it either physically blocks access to the enzyme active site or because it modifies an active site residue that is critical for catalysis.



These irreversible glycosidase inhibitors can be used for many different purposes. One of the earliest and still most prevalent uses is in the identification of active site residues. Mutation of the identified residues followed by subsequent kinetic analysis of mutants modified at that position can confirm their function in either catalytic or structural roles. Covalent inactivators have also seen use in studying the catalytic mechanism(s) by which glycosidases function, both through kinetic and structural examination. Highly specific probes have been used to selectively inactivate a target enzyme or enzyme activity in complex biological systems while observing the effect of this ‘deletion’ on the organism. This has been further extended to the design of specific probes for the discovery and characterization of novel enzymes.

Covalent glycosidase inactivators can be shown to be active site-directed, even in the absence of any structural knowledge of the enzyme, by incubation of the inactivator in the presence and absence of a known active site-binding noncovalent inhibitor. Under these conditions, a reduction or ablation of irreversible inhibition should be observed if inactivation is indeed active site-directed, as both inhibitors are competing for the same region of the enzyme. The kinetic behaviour or extent of inactivation can usually be studied by incubating a solution of inactivator plus enzyme, and removal of enzyme aliquots at various time points. Residual enzymatic activity in these aliquots can be assayed to reveal the degree of inactivation as a function of time. Analysis of the data can reveal a time-dependent irreversible loss of enzyme activity, and the kinetic parameters of inactivation can be calculated by straightforward mathematical manipulations of the data.<sup>12,13,41</sup> No general statements can be made about the rapidity of inactivation with any class of compounds, as the rate constant for inactivation is highly dependent on both the inactivator and the specific enzyme being investigated. The time necessary to completely ablate activity for a given enzyme and inactivator pair can range from milliseconds to weeks.

Irreversible inhibitors can be divided into two general categories: affinity labels and mechanism-based inhibitors. An affinity label is any molecule that contains a region designed to impart specificity for a given protein, and a reactive functionality that will irreversibly covalently modify a neighbouring region of the protein.<sup>42</sup> These affinity labels can be further subdivided into two classes: labels that are inherently reactive as a

consequence of their chemical structure,<sup>42</sup> and labels that require external activation, such as photo-affinity labels.<sup>43</sup> By contrast, a mechanism-based inhibitor is a substrate analogue that is stable towards spontaneous decomposition, but, upon activation by the enzymatic catalytic machinery, produces a species that reacts to form a covalent bond to the enzyme.<sup>39,40</sup>

The structures of some sample covalent inactivators are shown in Figure 1.6. Compound **1.6** is one of the earliest examples of a photoaffinity probe applied to glycosidase labelling. This compound was found to be a modest inhibitor of the *lacZ*  $\beta$ -galactosidase from *Escherichia coli* (E. coli  $\beta$ -Gal). Upon irradiation, a reactive carbene electrophile was generated which covalently modified the enzyme, although only modest levels of inactivation were observed.<sup>44,45</sup> Compounds **1.7** and **1.8** are both examples of covalent glycosidase affinity probes that bear reactive electrophiles appended to a specificity tag, in the form of a pyranose ring. Compound **1.7** has been shown to act as a covalent glycosidase inactivator for some retaining  $\beta$ -glucosidases through proton donation to the aromatic amine, which results in decomposition, with expulsion of nitrogen gas and formation of a glycosyl-methyl carbocation. Nucleophilic attack of an enzymatic nucleophile on the carbocation results in covalent modification.<sup>46</sup> Similarly, compound **1.8** and related derivatives have been shown to act as covalent inactivators for a variety of retaining  $\beta$ -glycosidases.<sup>47-50</sup> These *N*-bromoacetyl glycosylamines have been found in many cases to covalently bond to the catalytic acid/base residue, making them useful reagents in identifying candidate residues, although this assignment is best confirmed by a detailed kinetic analysis of both wild-type and mutant enzymes that have been modified at the identified residue.<sup>50</sup> Compound **1.9** is an example of a mechanism-based inactivator that functions through the generation of a highly reactive quinone methide species following enzyme-catalyzed glycosidic cleavage (Scheme 1.3). While this class of covalent glycosidase inactivator has been extensively studied for possible proteomics applications, the resulting reactive aglycone species generated has no affinity for the glycosidase, and is capable of diffusing throughout the reaction mixture to react with any available nucleophile. Hence, this class of glycosidase inactivator has seen only limited use.<sup>51-56</sup> Compound **1.10** is one example of a broad class of glycosidase inactivator known as the conduritol epoxides.<sup>39</sup> Compound **1.10** functions through the attack of an enzymatic nucleophile on a carbon atom of the epoxide,

accompanied by departure of the epoxide oxygen through acid-catalyzed assistance. The mechanism of this class of inactivator is discussed in more detail in Section 3.1.1.1. Finally, compound **1.11** (X = F or dinitrophenolate) is a representative of a class of compound known as the activated fluorosugars that function as glycosidase inactivators through the generation of a very stable covalent glycosyl-enzyme intermediate. This class of compound has been developed and extensively studied in the Withers group,<sup>12,13,57,58</sup> and is one of the focuses of the work described in this thesis. This class of compound is therefore discussed in greater detail in Section 2.2.

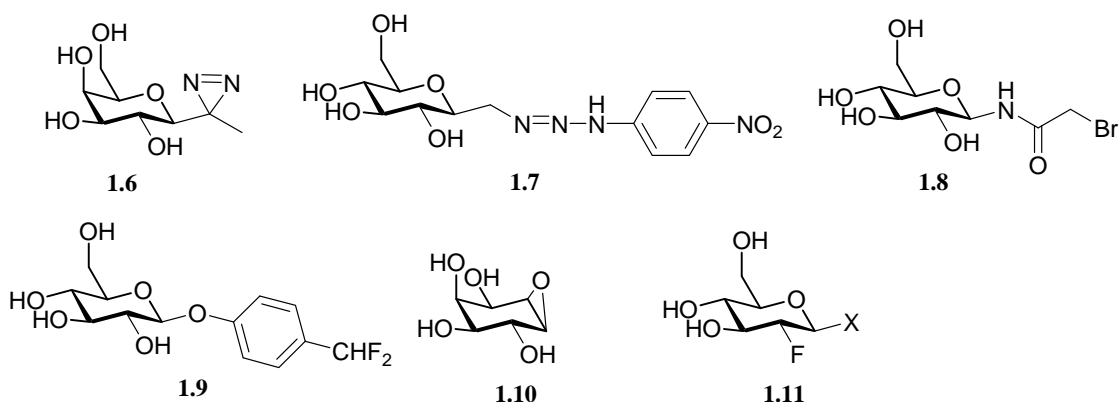
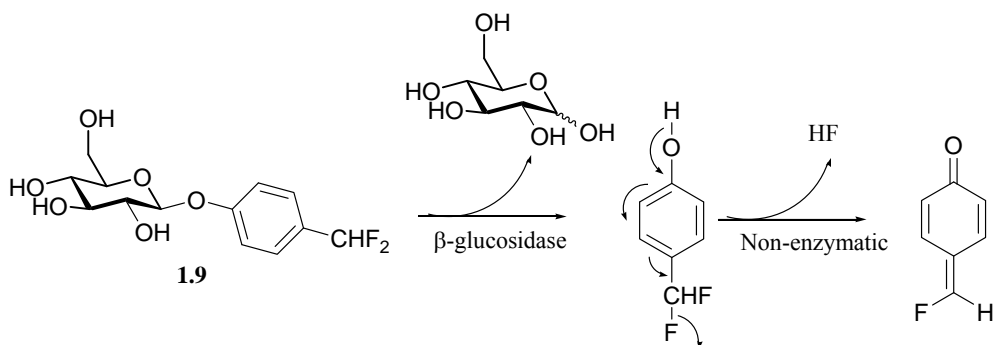


**Figure 1.6.** Structures of some representative covalent glycosidase inactivators. X = F or dinitrophenolate.



**Scheme 1.3.** Mechanism of generation of reactive aglycone from **1.9**.

## 1.4 Lysosomal storage diseases

### 1.4.1 General introduction

The lysosomal storage diseases (LSDs) are a group of genetic diseases caused by mutations in given lysosomal hydrolases that result in deficiencies in enzyme activity. The lysosome acts as a cellular recycling center, to which macromolecules are trafficked and degraded by a series of hydrolytic enzymes that operate most efficiently at low pH. Following hydrolysis, the macromolecular components such as lipids, sugars, or amino acids can be re-used by the organism.<sup>59</sup> There are over 40 LSDs described to date,<sup>60-62</sup> and they are caused by mutations that directly affect a given enzyme, one of the cofactors needed for enzymatic functionality, or one of the integral membrane proteins in the lysosome. This deficiency in enzyme activity compromises the entire catabolic pathway for a given macromolecule, and leads to a build-up of the unprocessed substrate. This accumulation is thought to be the major cause of the pathophysiology of these diseases, and leads to a wide variety of symptoms depending on the specific substrate that accumulates.<sup>61,62</sup>

These diseases can be broadly grouped into four categories that encompass most of the LSDs: the Sphingolipidoses, which result from the accumulation of sphingolipids or gangliosides; the Mucopolysaccharidoses, which result from the accumulation of the mucopolysaccharides heparan sulfate, dermatan sulfate, chondroitin sulfate or keratan sulfate; the Oligosaccharidoses and Glycoproteinoses, which result from the accumulation of oligosaccharides or glycoproteins; and diseases arising from defects in integral membrane proteins which lead to the accumulation of a variety of substances. There are other LSDs that do not fall into these sub-groups, but they are less common, and do not result from the accumulation of a common class of biomolecule.<sup>61</sup>

The incidence of an individual LSD is low in the general population; given the rarity of some of the diseases, it is difficult to obtain estimates for their prevalence.<sup>62,63</sup> The most common LSD is Gauchers disease, which arises from a deficiency in the enzyme glucocerebrosidase (GCase), and has an estimated frequency of 1 in 40,000 live births in the general population although it can occur in up to 1 in 800 live births in select

populations.<sup>63,64</sup> Gauchers disease is the most prevalent LSD, so it is the disease that is often regarded as the model for many other LSDs and has been studied the most. Therapeutic strategies that have been successfully adopted in the treatment of Gauchers disease have thus been explored in the context of other LSDs, since all these diseases share the common feature of an underlying defect in metabolism.<sup>65-68</sup>

In many, but not all of the LSDs, there remains a low level of residual enzyme activity. This residual enzyme activity arises from the low levels of mutant protein that are still present in the diseased tissues. In Gauchers disease, animal studies have suggested that the level of residual enzyme activity can be as low as 12-16% for a patient to remain asymptomatic.<sup>30</sup> This low level of residual enzyme activity plays a critical role in two of the therapeutic options that are being explored for the treatment of LSDs, substrate reduction therapy (SRT) and enzyme enhancement therapy (EET) using pharmacological chaperones (PC).

#### **1.4.2 Enzyme replacement therapy (ERT)**

Enzyme replacement therapy (ERT) is the most common treatment for managing patients with LSDs. In ERT, a recombinant form of the enzyme that is deficient is intravenously administered to the patient. The enzyme is then transported to the affected tissues, and is taken up into the lysosomes of cells in a receptor-mediated fashion. This results in an increase in the enzyme activity in the lysosome, and therefore leads to an increase in degradation of the accumulated substrate through the catalytic action of the enzyme. One limitation of ERT is that it is incapable of treating diseases in which there is neurological involvement, as the recombinant enzyme is unable to penetrate the blood-brain barrier.<sup>64,69-72</sup> While there have been some experiments examining new systems for direct delivery of recombinant enzyme to the central nervous system,<sup>73-75</sup> there is currently no consensus on the use of this strategy to alleviate neurological symptoms arising from a given LSD.<sup>76,77</sup>

### **1.4.3 Substrate reduction therapy (SRT)**

Substrate reduction therapy (SRT) is a treatment that has currently only been applied to Gauchers disease (Section 1.4.6). Whereas ERT relies on increasing the rate of degradation of accumulated substrate in the lysosome to relieve disease symptoms through the addition of an exogenous source of the deficient enzyme, SRT relies on reducing the amount of substrate that is synthesized, through the introduction of a competitive inhibitor of the biosynthetic enzyme(s) responsible for the synthesis of the substrate. This therapy therefore relies on the low amount of residual enzyme activity present in many LSDs to process the reduced amount of substrate that is then introduced into the lysosome.<sup>22,65,78-80</sup>

### **1.4.4 Protein misfolding**

In many of the LSDs, the mutation that leads to a deficiency in enzyme activity is a point mutation that results in a single-amino acid change. This mutant protein often retains some catalytic activity, and is responsible for the low level of residual activity observed in many patients diagnosed with a lysosomal storage disease. In the vast majority of cases, this mutation does not impact an essential amino acid residue in the active site of the enzyme, but instead alters a residue distant from the active site. However, if a residue that forms part of the tightly packed hydrophobic core of the protein is altered to a residue that is not well accommodated in the core, or if the altered residue is part of a secondary structural motif, then this will partially disrupt the folded conformation of the protein. In the LSDs, these partially misfolded proteins may retain some degree of catalytic activity, but they are thermodynamically much less stable than the native protein, and are recognized by the organism as being misfolded. Protein misfolding diseases, a group to which some LSDs belong, are a large class of disorders that include diseases such as Alzheimer's disease, Huntington's disease, the Spongiform encephalopathies ("Mad cow disease"), Parkinson's disease, and amyotrophic lateral sclerosis ("Lou Gherig's disease"), among many others.<sup>81-</sup>

85

A native protein that is synthesized in the endoplasmic reticulum (ER) is normally assisted during and after protein synthesis in reaching the properly folded conformation by a

series of enzymes, lectins and chaperone proteins. Once the proper conformation has been achieved, the protein passes by the Endoplasmic Reticulum Quality Control (ERQC) and is trafficked to its destination. A variant protein with a mutation that partially disrupts the folded conformation of the protein will not finish folding, and will remain in a molten globule-like conformation that resembles one of the normal intermediates along the folding pathway. Alternatively it folds, but the folded conformation is not very stable. Either this molten globule-like conformation or the hydrophobic patches of the protein that are exposed as a result of the partial folding are recognized by the ERQC and targeted for degradation through a pathway known as Endoplasmic Reticulum Associated Degradation (ERAD).<sup>86</sup>

In the context of the LSD, the majority of mutant enzyme molecules are targeted for ERAD, and therefore do not arrive in the lysosome where the unprocessed substrate accumulates. In diseases where there is residual enzyme activity, some small proportion of mutant enzyme molecules do properly traffic to the lysosome and are responsible for the low level of enzyme activity observed. However, the vast majority of the enzyme molecules that are synthesized are recognized by the ERQC and targeted for ERAD. This ER-stress can trigger the unfolded protein response,<sup>87</sup> which may be partially responsible for the pathology of the LSD. However, given that the symptoms of the individual LSDs are not uniform, this suggests that the nature of the misfolded protein and the nature of the stored substrate also play a role in determining the disease pathology.<sup>61</sup>

#### **1.4.5 Pharmacological chaperones**

The process of the mutant protein in the LSD being targeted for ERAD suggests that if the mutant protein can be stabilized or assisted in achieving its properly folded conformation, then the disease symptoms may be alleviated. There are a few different potential ways of achieving this goal: through the up-regulation of the expression of endogenous protein chaperones (such as the heat-shock proteins),<sup>88</sup> lowering the temperature of the ER,<sup>89</sup> using small-molecule osmolytes that thermodynamically increase the global stability of all folded proteins,<sup>90,91</sup> or using a specific small-molecule ligand for a protein to selectively increase the stability of a chosen protein.<sup>66,70,90</sup>

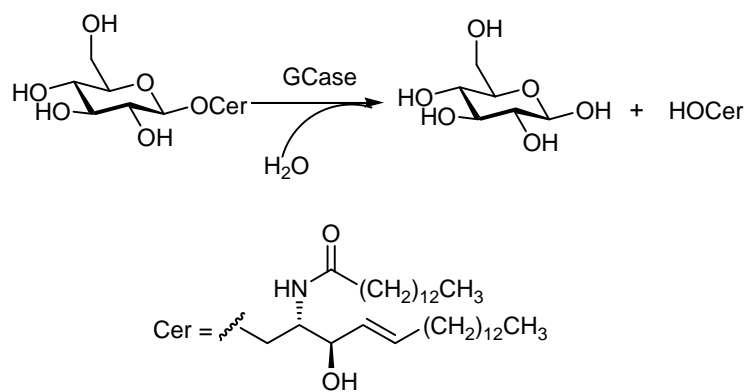
A pharmacological chaperone (PC) is a small molecule that is designed to selectively bind to the folded conformation of a given protein. This binding serves to stabilize the folded conformation of the protein, and should therefore help the protein pass by ERQC and avoid ERAD. In the context of the LSD, this means that the chosen enzyme will be trafficked to the lysosome in great quantities, and therefore decrease both the effects of the Unfolded Protein Response and also the levels of stored substrate, which will in turn lead to an alleviation of disease symptoms.

A PC may bind to any region of the protein, so long as it acts to stabilize the folded conformation. To date, the vast majority of PC studies have focused on compounds that bind to the active site of the enzyme, since lead compounds can be initially identified by their inhibition of enzyme activity. This leads to the apparent paradox that the addition of an inhibitor for a particular enzyme to a living cell leads to an increase in the respective enzyme activity. Therefore, the concentration of inhibitor that is administered is a key factor in this approach; the inhibitor must be added at a high enough level to show chaperoning activity, but not at such a high concentration that it inhibits the enzyme in the lysosome. Recent advances in high-throughput screening for PC activities using lysosomal enzymes may soon result in the discovery of new chaperones that are not active-site directed by screening of large libraries of compounds.<sup>32,33</sup>

#### **1.4.6 Gauchers disease**

Gauchers disease is the most prevalent of the LSD, and arises from a deficiency in the activity of the enzyme glucocerebrosidase (GCase), which is responsible for the cleavage of the  $\beta$ -linked glucosyl residue from glucosylceramide (Scheme 1.4) in the final step of lysosomal ganglioside degradation, which is represented schematically in Scheme 1.5.





**Scheme 1.4.** The hydrolytic cleavage reaction of glucosylceramide to glucose and ceramide that is catalyzed by GCcase.



The disease can be further divided into three sub-types, depending on the presence or absence of neuronopathic symptoms. Involvement of the central nervous system (CNS) is absent in Type I Gauchers disease, yet is present in Types II and III Gauchers disease. Types II and III Gauchers disease are differentiated by the age of onset of the neuronopathic symptoms; they appear very early (within days or weeks of birth) in Type II (acute) patients, with severe CNS involvement, and much later in Type III patients, usually in early adulthood. Of the three subtypes, Type I Gauchers disease is the most prevalent.<sup>62,64</sup> While some genotype-phenotype correlations can be drawn, it is not always possible to make predictive diagnoses on the basis of a patient's genotype owing to a wide variability in disease severity between individuals sharing identical genotypes.<sup>62,64</sup>

In all three Gauchers subtypes, some residual enzyme activity is observed.<sup>62,64</sup> This means that the mutations in the gene encoding for GCase are all point mutations, and no nonsense mutations have been observed (which would result in a non-functional protein product). It seems exceedingly unlikely that any Gauchers patients will be found with no residual enzyme activity, given that mouse knock-out studies indicate that some residual GCase activity is necessary for the animals to survive any significant time (>48 hours) after birth.<sup>93-96</sup> It has been estimated that 12-16% of control GCase activity is needed for a patient to remain asymptomatic, on the basis of animal and cell-based studies.<sup>30,97</sup>

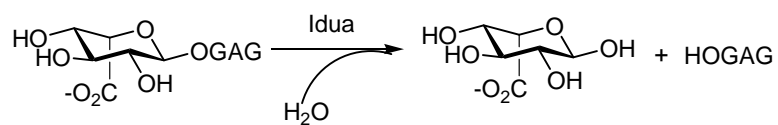
The two currently approved therapeutic options for the treatment of Gauchers disease are ERT and SRT. In ERT, a recombinant form of GCase expressed from Chinese Hamster Ovary cells (Cerezyme<sup>TM</sup>) is intravenously administered to the patient, although it is only approved for treatment of patients suffering from Type I Gauchers disease, since the intravenously injected enzyme is not capable of crossing the blood-brain barrier to alleviate neurological symptoms.<sup>64,69,70,78,98</sup> In SRT, a small molecule inhibitor (*N*-butyl deoxynojirimycin, Zavesca<sup>TM</sup>) of the glucosyltransferase enzyme which is responsible for the synthesis of the substrate, glucosyl ceramide, is orally administered to the patient. This therapy relies on reducing the influx of glucosyl ceramide into the lysosome to a level that can be degraded by the low level of residual GCase enzyme activity present, thus alleviating patient symptoms.<sup>22,65,78,79</sup> Currently, SRT has been approved for the treatment of patients

suffering from Type I Gauchers disease, and those who are either unable or unwilling to undergo ERT.<sup>64</sup>

#### **1.4.7 Mucopolysaccharidosis I (MPS I)**

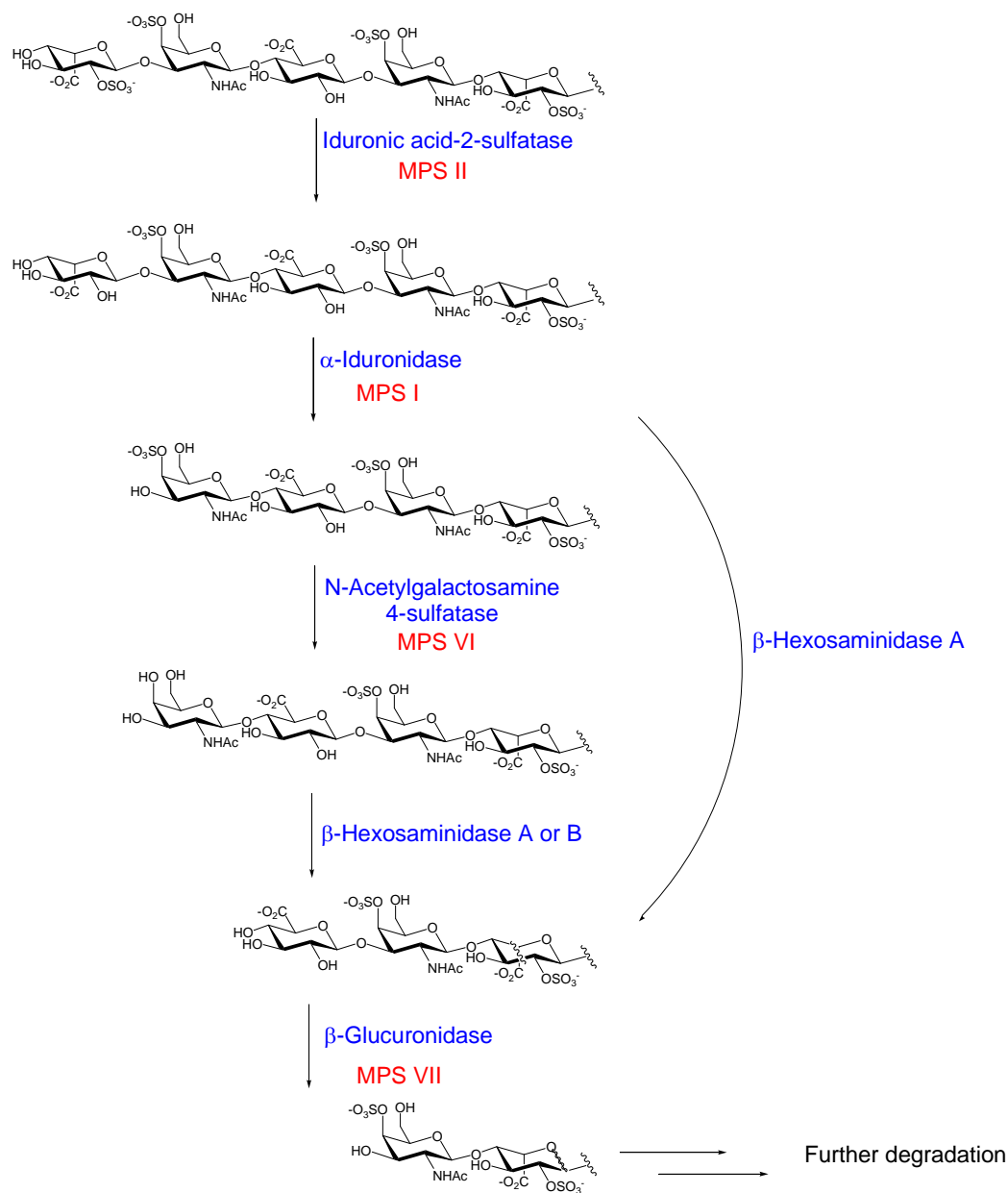
Mucopolysaccharidosis I (MPS I) arises from a deficiency in activity in  $\alpha$ -L-iduronidase (Idua). MPS I is also known as Hurler-Scheie syndrome. The more severe clinical phenotype, originally known as Hurler syndrome, presents with early onset of disease, with symptoms including mental retardation, enlarged liver and spleen, skeletal deformities, corneal clouding, and shortened lifespan, with those afflicted often not living past 10 years of age. The more attenuated form of the disease, originally known as Scheie syndrome, typically presents in early adulthood and displays symptoms such as enlarged liver and spleen, heart valve problems, skeletal defects and corneal clouding. MPS I is estimated to have a frequency in the general population of approximately 1 in 100,000 live births.<sup>63</sup>

In MPS I, there is an accumulation of dermatan sulfate and heparan sulfate arising from the lack of Idua enzyme activity. Idua is responsible for cleaving an  $\alpha$ -linked terminal L-iduronic acid residue from the non-reducing ends of both dermatan sulfate and heparan sulfate (Scheme 1.6) in the lysosomal degradation of both mucopolysaccharides (see Scheme 1.7 and Scheme 1.8 for the degradation pathways of dermatan sulfate and heparan sulfate, respectively). Note that because the substrate for this enzyme has the L-configuration at C5 that the  $\alpha$ - and  $\beta$ -stereochemical designations for the anomeric center are reversed from those more commonly seen for the D-series of sugars, even though they describe a stereocenter having the same relative configuration. This means that an L-iduronic acid residue bearing an axial substituent at the anomeric center when drawn in a  ${}^4C_1$  conformation is designated as  $\beta$ , rather than  $\alpha$  as would be the case for the equivalent D-glycoside. This is a consequence of the rules concerning the nomenclature of carbohydrates and glycosidic linkages.<sup>99</sup>

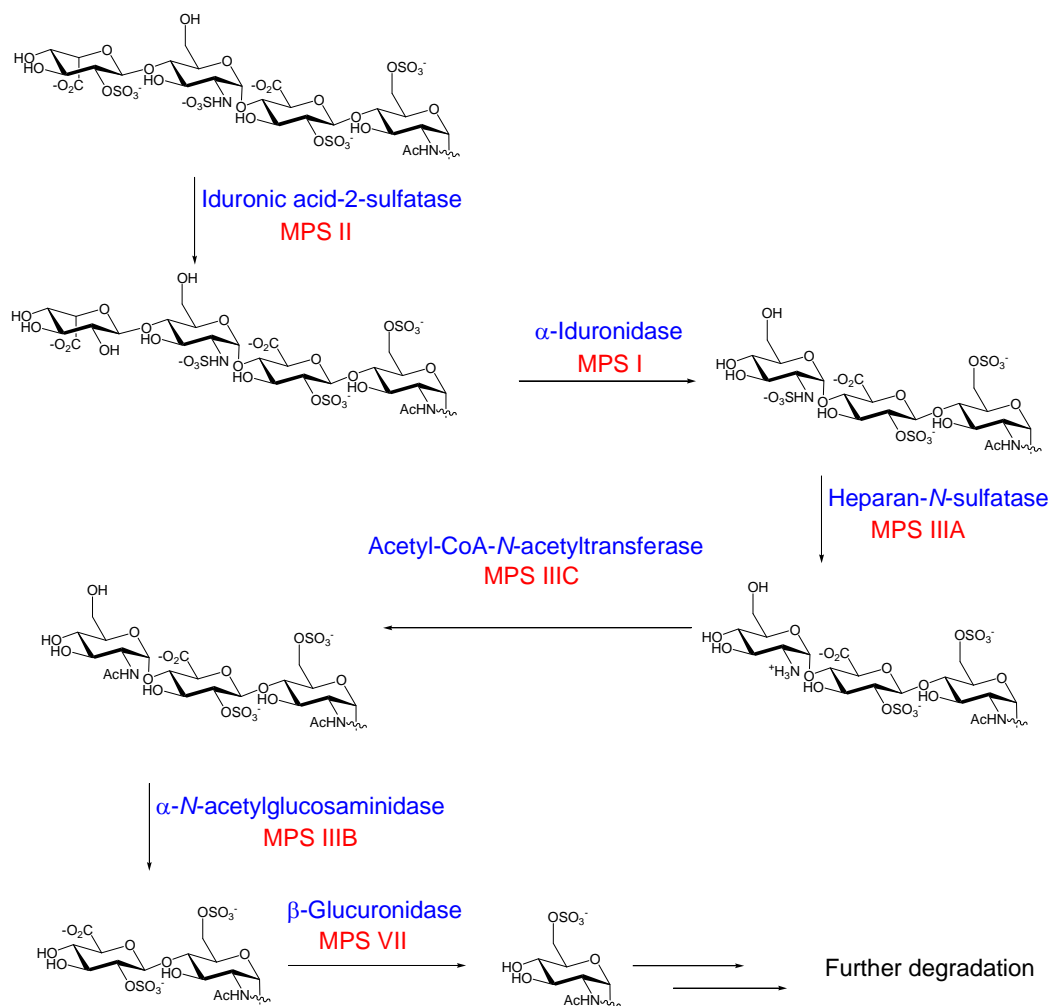


GAG = Glycosaminoglycans: heparan sulfate  
or dermatan sulfate

**Scheme 1.6.** The hydrolytic reaction catalyzed by Idua. Note that the iduronic acid residue is drawn in a  ${}^4C_1$  conformation for clarity.



**Scheme 1.7.** The enzymatic degradation of dermatan sulfate in the lysosome. Enzymes are shown in blue, and the respective diseases arising from their absence are shown in red. Note that iduronic acid residues are drawn in a  ${}^4C_1$  conformation for clarity. Adapted from Varki, et al.<sup>100</sup>



**Scheme 1.8.** The enzymatic degradation of heparan sulfate in the lysosome. Enzymes are shown in blue, and the respective diseases arising from their absence are shown in red. Note that iduronic acid residues are drawn in a  ${}^4C_1$  conformation for clarity. Adapted from Varki, et al.<sup>100</sup>

Unlike in the case of Gauchers disease, patients suffering from the severe form of MPS I do not have any detectable residual enzyme activity.<sup>76,101</sup> This is because some mutations in the gene encoding *Idua* are insertion or nonsense mutations,<sup>102</sup> which lead to a protein product unable to function catalytically. Therefore correlations between genotype and disease phenotype have remained challenging.<sup>102</sup> It has been shown on the basis of residual enzyme activity in patient fibroblasts, that residual *Idua* activity in patients afflicted with the severe form of MPS I, Hurler syndrome, can be as low as 0.17%,<sup>101</sup> which likely arises from extremely low levels of iduronidase activity arising from other lysosomal enzymes. Patients

afflicted with the attenuated form of the disease, Scheie syndrome, show as high as 7% residual enzyme activity, suggesting that the minimum activity threshold to be asymptomatic lies somewhere above this value.<sup>101</sup>

The currently approved therapeutic options for the treatment of MPS I are bone marrow transplantation (BMT) and ERT. BMT is a treatment option for patients suffering from the severe form of MPS I, in this treatment the patient's bone marrow cells are destroyed and replaced with marrow cells from a healthy, compatible donor. Iduronic acid is then synthesized by these newly introduced cells and is introduced into the circulatory system, where it presumably is taken up by affected cells. BMT requires early diagnosis before developmental deterioration has begun (< 2 years of age). It needs a compatible donor and carries significant risks of morbidity and mortality.<sup>76,103</sup> In ERT, a recombinant form of the iduronidase enzyme is intravenously administered, and the enzyme is taken up in a receptor-mediated process into the affected tissues. Once the enzyme has been trafficked to the lysosome, it hydrolyzes the accumulated substrate.<sup>67,69,76,104-107</sup>

## **1.5 Positron emission tomography (PET) imaging**

### **1.5.1 Imaging techniques used in modern diagnostic medicine**

Many forms of imaging used in modern diagnostic medicine rely on the external detection of electromagnetic radiation that interacts differentially with different tissues to generate an image. One way of classifying imaging technologies is to divide them on the basis of the source of the electromagnetic radiation that is detected: generated from an external source that is transmitted through the patient, or from an internal source that is first injected into the patient.

The most common imaging techniques employing electromagnetic radiation rely upon the detection of externally produced radiation that differentially interacts with different tissues. The first imaging technique to be introduced was X-ray radiography in 1895 by Röntgen. X-ray radiography relies on the generation of X-rays from a radiation source,



passage of this radiation through the patient, and collection of the transmitted X-rays on a photographic film. Different tissues have different transmission coefficients for X-rays, which allows a two-dimensional image that reflects different types of tissues to be generated. A series of two-dimensional X-ray scans can be taken around a single axis of rotation to create a Computed Tomography, or CT, image. This type of image is generated by the three-dimensional reconstruction of a series of two-dimensional X-ray radiographical images. The final type of medical imaging relying on an external radiation source that is commonly employed is Magnetic Resonance Imaging, or MRI. In MRI, an external radio frequency pulse aligns the nuclear magnetization of the hydrogen atoms in (usually) water with the external field. As the nuclear magnetization relaxes, the emitted photons are collected by the scanner and used to reconstruct a three-dimensional image of the tissues. The physical process underlying MRI is the same as that used in Nuclear Magnetic Resonance (NMR) spectroscopy for the characterization of small molecules. Most forms of imaging through the generation of external radiation provide structural data on the organism, rather than functional data, although there is a branch of MRI imaging called functional MRI (fMRI) that uses MRI to probe blood flow in the brain in response to neural activity.

The second class of imaging techniques that use radiation rely on a source of photons that are generated inside the patient, through the introduction into the patient of a radioisotope that decays to produce photons of sufficient energy to escape the patient tissues and be detected. This method of imaging generally provides functional rather than structural data, as the radiation emission is dependent on the biodistribution of the radiotracer. Two of the common imaging techniques using this strategy are Single Photon Emission Computed Tomography, or SPECT, and Positron Emission Tomography, or PET. Both rely on the injection of a small molecule that has been radiolabelled with a radioactive nucleus which will decay to produce the photons that are collected to generate the image. In SPECT, the radioactive nucleus (typically  $^{99}\text{Tc}$  or  $^{123}\text{I}$ ) decays to directly produce a gamma ray which is observed by the SPECT camera. In PET, the radioactive nucleus (most often  $^{18}\text{F}$  or  $^{11}\text{C}$ ) decays to produce a positron (an antimatter particle with the properties of an electron except that it bears a positive charge, also known as a  $\beta^+$  particle), which combines with a nearby electron (often from water) in an annihilation event to produce a pair of anti-parallel gamma rays that are detected by the PET scanner. In both instances, a series of two-dimensional

snapshots are reconstructed to generate a three-dimensional image representing the distribution of the radioisotope throughout the patient's tissues.

### **1.5.2 A molecular description of the process underlying PET imaging**

PET imaging relies on the detection of two 511 keV gamma rays that are simultaneously produced at 180° to each other following the collision of a positron emitted by a radioisotope in the imaging agent, and a nearby electron. Since these gamma rays are produced simultaneously, they will be simultaneously detected, and because they are generated at 180° to each other, a straight line can be constructed to their point of origin. Many molecules of the imaging agent decaying in the same location will generate many pairs of such gamma rays, which can be traced back in three-dimensional space to provide the point of origin in all three spatial coordinates. These line therefore gives the location of the positron annihilation event, yielding both spatial and temporal information on the annihilation event.<sup>108</sup>

The generation of the positron arises from a nuclear decay process involving an unstable nucleus, such as  $^{11}\text{C}$ ,  $^{13}\text{N}$ ,  $^{15}\text{O}$  or  $^{18}\text{F}$ . The energy imparted on the positron during the decay event will propel the positron a distance, depending on its energy before it encounters an electron and yields the gamma rays from the annihilation event. Therefore, the lower the energy of the positron emitted, the shorter the distance travelled on average, and therefore the higher the spatial resolution. This means that there is a slight distance of usually a few millimetres between the decay event and the annihilation event that represents a lower limit on the spatial resolution achievable by PET imaging. However, for most animal and human studies, this resolution is sufficient for the desired applications. Also, it is important that the decay process proceeds through positron emission with high efficiency, as opposed to decay through other processes.<sup>109</sup>

Out of the commonly used radioisotopes usually used in PET imaging,  $^{18}\text{F}$  is usually the isotope of choice. Chemically, fluorine is a small atom, meaning that it can be incorporated into a molecule with a relatively small structural perturbation. Other chemical properties of fluorine that make it useful in design of radiotracers are that fluorine is a weak

hydrogen-bond acceptor and that the carbon-fluorine bond is relatively strong. From a physical standpoint,  $^{18}\text{F}$  is also an ideal nucleus for PET imaging because of its high decay efficiency to produce positrons (97%), the low energy of the emitted positrons (0.635 MeV) and the relatively long half-life of decay (110 minutes), which means that  $^{18}\text{F}$ -labelled imaging agents can be shipped from their point of production to their point of use.  $^{18}\text{F}$  is available in both electrophilic ( $^{18}\text{F}^{+}$ ) and nucleophilic ( $^{18}\text{F}^{-}$ ) chemical forms. Electrophilic fluorine is produced by bombarding a  $^{20}\text{Ne}$  atom in  $[^{19}\text{F}]\text{F}_2$  carrier gas with a deuteron beam. Following ejection of an  $\alpha$ -particle ( $^4\text{He}$  nucleus), a mixture of  $[^{18}\text{F}]\text{F}_2$  and  $[^{19}\text{F}]\text{F}_2$  is produced that can be subsequently used in the fluorination reaction. Because of the presence of a large concentration of  $[^{19}\text{F}]\text{F}_2$  carrier gas, the specific activity, or amount of radioactivity present per unit mass or molar quantity, is not particularly high for  $[^{18}\text{F}]\text{F}_2$ . By contrast, nucleophilic  $^{18}\text{F}$  ( $^{18}\text{F}^{-}$ ) is produced by irradiation of  $\text{H}_2^{18}\text{O}$  with a proton beam, and  $^{18}\text{O}$  ejects a neutron to generate  $^{18}\text{F}^{-}$ . Because there is no carrier  $^{19}\text{F}^{-}$  added during the irradiation, the specific activity of  $^{18}\text{F}^{-}$  is usually quite high, and radiosyntheses utilizing  $^{18}\text{F}^{-}$  almost always have higher specific activities than syntheses employing  $[^{18}\text{F}]\text{F}_2$ .<sup>109,110</sup>

### 1.5.3 Advantages and disadvantages of PET imaging

PET imaging has many features that make it a useful imaging technique for diagnostic medicine and research. Because PET imaging is a functional imaging technique, the image that is generated is reflective of the biological process(es) that are relevant to the radiolabelled molecule injected. As a consequence of this, different labelled molecules will generate different types of images based on the interaction of that molecule with the biological system. Thus, the image generated from the injection of a labelled neurotransmitter, for example, will be very different from the image generated by injection of fluorodeoxyglucose (FDG, discussed below), which reports on local levels of glucose utilization. So the interaction of any molecule with a biological system can be studied using PET imaging, as long as an appropriately radiolabelled version of the molecule can be produced.

Additionally, as discussed above, PET imaging is a non-invasive imaging technique with very little risk for the subject. The extreme sensitivity of the detection of the gamma

rays arising from radioactive decay means that the actual radiation dose the patient is presented with is very low, and the concentration of the labelled molecule in the patient is also correspondingly low, leading to little toxicity associated with the injection of the tracer. PET imaging is capable of generating a series of images that vary in both space and time, meaning that PET imaging can be used to monitor not only the spatial distribution of the radiotracer, but also how the distribution in a particular spatial region or organ changes as a function of time.

Currently, the application of PET imaging in diagnostic medicine and in research is limited by the high cost associated with production of the radiotracer and the expensive equipment needed for collection of the PET image. Generation of the commonly used PET imaging nuclei generally requires the use of a cyclotron, which is a large and very expensive piece of equipment to build and operate. This means that the equipment necessary for PET imaging is usually only available in large population centers that have well-funded health care systems, since most of the nuclei used in PET imaging have half-lives that are short enough to preclude long-distance transport. PET imaging is a functional imaging modality, so a molecular probe for a process must exist before the process can be imaged using PET. This means that not every process can be studied with equal efficiency or even at all; it will depend on the specificity and strength of the interaction of the chosen radiolabelled molecule with its relevant biological target. Finally, a radiosynthetic route must be developed that is unique for each radiotracer employed in PET imaging; this can be a time and labour-intensive process.

#### **1.5.4 Examples of three commonly employed PET imaging agents**

##### **1.5.4.1 Fluorodeoxyglucose (FDG) for imaging glucose metabolism**

2-Deoxy-2- $^{18}\text{F}$ fluoro-D-glucopyranose (Fluorodeoxyglucose, or FDG, **1.12** in Figure 1.7), is the most commonly employed radiopharmaceutical for PET imaging in the world.

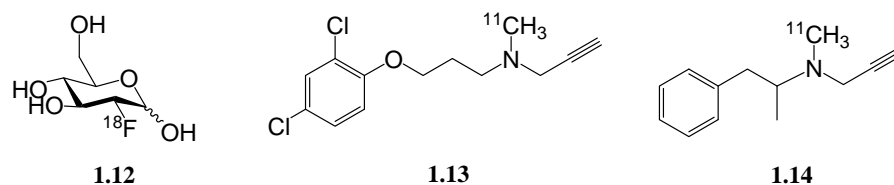
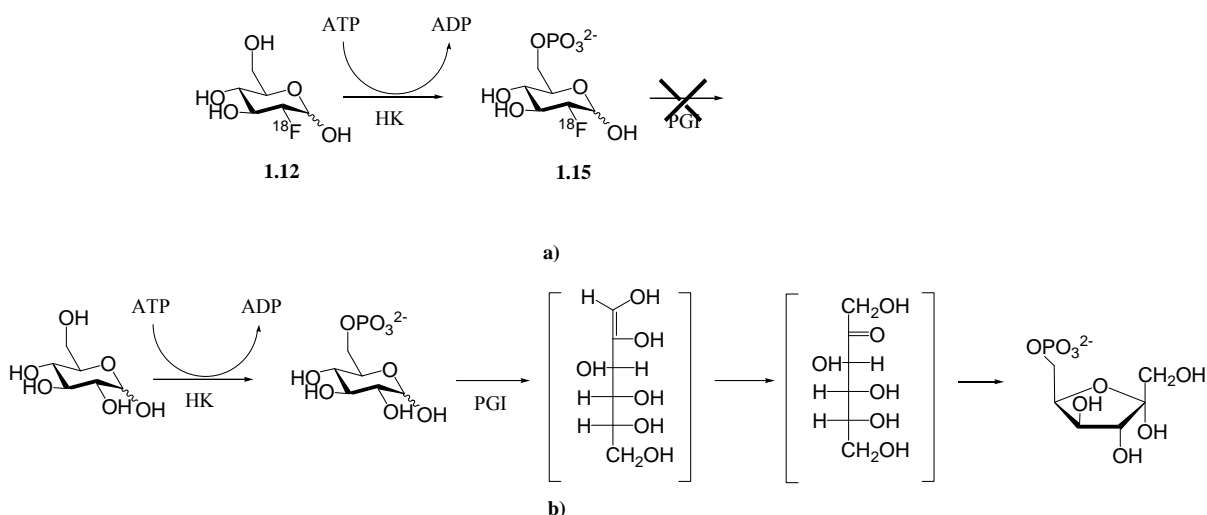


**Figure 1.7.** Structures of three commonly employed PET imaging agents, FDG (**1.12**), [ $^{11}\text{C}$ ]clorgyline (**1.13**) and [ $^{11}\text{C}$ ]L-deprenyl (**1.14**).

FDG acts as a glucose mimic, so is actively transported into cells in the same manner as glucose. Once in the cell, FDG undergoes the first committed step in the catabolism of glucose, phosphorylation at O6 catalyzed by hexokinase to form 6-phospho-FDG [**1.15** in Scheme 1.9, (a)].<sup>111</sup> However, the second step of glycolysis [Scheme 1.9, (b)] normally involves an isomerisation from glucose-6-phosphate to fructose-6-phosphate catalyzed by phosphoglucose isomerase. Its mechanism involves an ene-diol intermediate between C1 and C2. Because of the replacement of the fluorine atom for O2 in FDG, the phosphorylated FDG is not a substrate for this step in glycolysis, and therefore **1.15** accumulates. The presence of the phosphate group at C6 on **1.15** imparts a charge on the radiotracer, meaning that the compound no longer crosses the cell membrane and is trapped in the cell. As a result of these reactions, FDG accumulates in cells that have a high glucose uptake, and is most often used to image the rapidly-growing cells that are characteristic of cancers. FDG is an example of a PET imaging agent that accumulates in a cell as a consequence of being trapped by the action of an endogenous enzyme, so an amplification of the tracer signal occurs as many tracer molecules accumulate. This property makes FDG an extremely sensitive probe of cellular glucose utilization, and it has seen wide application as an imaging agent in oncology for visualising tumours.<sup>109,110,112</sup>



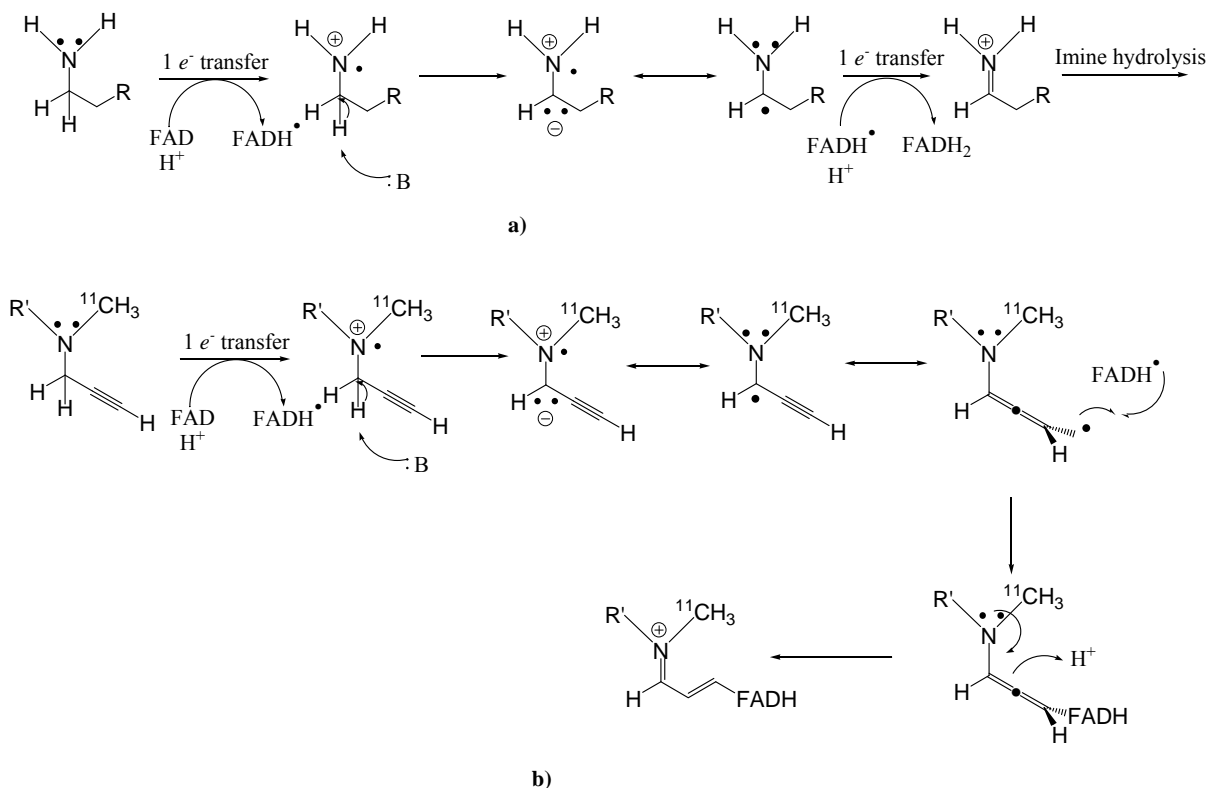
**Scheme 1.9.** Schemes depicting a) cellular metabolism of FDG, and b) first two steps of cellular metabolism of glucose. HK = Hexokinase, PGI = Phosphoglucose isomerase. Adapted from Voet and Voet.<sup>111</sup>

#### 1.5.4.2 [ $^{11}\text{C}$ ]clorgyline and [ $^{11}\text{C}$ ]L-deprenyl for imaging monoamine oxidase (MAO)

[ $^{11}\text{C}$ ]Clorgyline (**1.13** in Figure 1.7) and [ $^{11}\text{C}$ ]L-deprenyl (**1.14**) can be used to image human monoamine oxidase-A and -B (MAO-A or MAO-B) respectively. Monoamine oxidase is an enzyme responsible for the oxidative deamination of a number of endogenous and exogenous amines<sup>113</sup> through a radical flavin-mediated mechanism.<sup>114</sup> There are two isoforms of MAO (MAO-A and MAO-B) that have different substrate and inhibitor or inactivator specificities; MAO-A preferentially oxidizes norepinephrine, dopamine and serotonin, whereas MAO-B preferentially oxidizes benzylamine and phenylethylamine. These two isoforms react preferentially with the covalent inactivators clorgyline and L-deprenyl, respectively. The activities of these enzymes have been implicated in mood disorders such as depression, as well as in neurological diseases such as Parkinson's disease.<sup>113</sup>

Both [ $^{11}\text{C}$ ]clorgyline and [ $^{11}\text{C}$ ]L-deprenyl function as mechanism-based inactivators of their respective enzymes through the generation of a reactive alkenyl radical intermediate that reacts with the flavin-based radical to form a covalent adduct (Scheme 1.10). This means that [ $^{11}\text{C}$ ]clorgyline and [ $^{11}\text{C}$ ]L-deprenyl label their respective enzymes in a 1:1

stoichiometric ratio, and the resulting PET image directly reflects the activity of the relevant enzyme. So in contrast to the accumulation of a radiotracer metabolite that arises from using FDG as a PET imaging agent and the resulting signal amplification, the MAO imaging agents directly report on the number of molecules of MAO in different tissues.



**Scheme 1.10.** Mechanism of a) MAO oxidation of a primary amine, adapted from Bugg,<sup>115</sup> and b) covalent inactivation of MAO with [<sup>11</sup>C]clorgyline (R' = (CH<sub>2</sub>)<sub>3</sub>-2,4-dichlorophenol) or [<sup>11</sup>C]L-deprenyl (R' = CH(CH<sub>3</sub>)CH<sub>2</sub>Ph).

### 1.5.5 Challenges surrounding radiochemistry

The incorporation of a short-lived radionuclide into a compound to generate a radiotracer for use as a PET imaging probe presents some unique synthetic challenges. Owing to the short half-lives of the commonly employed nuclei used in PET imaging, the synthetic route must be designed with that restriction in mind. Additionally, the possibilities of radioactive contamination of the equipment, personnel, and/or surroundings are also major considerations. These two concerns lead to the following general considerations. The

incorporation of the radioactive nucleus is performed in one of the final steps of a synthesis, to minimize the handling and the number of decay half-lives that pass during subsequent chemical steps. The chemical reactions employed must usually be rapid, high-yielding, and readily purified, to minimize the time between radionuclide generation and injection of the imaging agent into the subject. Many techniques that are often used in synthetic organic chemistry are incompatible with the need for speed inherent in a radiosynthesis, or generate an unacceptably high risk of radioactive contamination. For example, techniques such as two-phase liquid extractions are avoided whenever possible in radiochemistry because of the possibility of creating radioactive aerosols that may contaminate nearby equipment or personnel, in addition to requiring a time-intensive rotary evaporation step. To reduce the risk of contamination and radiation dose, remote handling and automation are employed whenever possible. Another challenge often encountered is in the characterization of the species produced; since the radiotracer is often present in approximately nanomolar concentrations, most of the standard analytical techniques used in synthetic organic chemistry are insufficiently sensitive to characterize the products in addition to requiring longer analysis times, or risks for contamination that are unacceptable. One advantage of performing chemistry at a radiotracer scale is that reactions that proceed only poorly or sluggishly on a typical synthetic scale (micromole to millimole scale) can be driven to completion much more readily and rapidly by the addition of a vast excess of other reagents, which can be present in  $10^5$ -fold excess or more.

## **1.6 Specific aims of this thesis**

The aims of this thesis are as follows:

- 1) The synthesis and enzymatic evaluation of new fluorosugars that act as mechanism-based inactivators for retaining glycosidases. This will be accomplished by separately studying both the location and number of fluorine atoms incorporated in the sugar ring, and also by searching for novel activated aglycones that can be incorporated into an activated fluorosugar to generate more specific or efficient inactivators.
- 2) The synthesis and enzymatic evaluation of more efficient and/or more selective activated fluorosugars that are covalent inactivators of two lysosomal enzymes:



human glucocerebrosidase and human iduronidase. This will be accomplished by applying to both enzymes the successful strategies from the first objective.

- 3) The testing of any compounds determined to be useful from the second objective as potential pharmacological chaperones of either glucocerebrosidase or iduronidase.
- 4) The development of a radiosynthetic route for the generation of a radioactively-labelled activated fluorosugar to be used as a PET imaging probe for monitoring enzyme replacement therapy for the treatment of Gauchers disease or Mucopolysaccharidosis I in an animal model.

**Chapter 2: Development of Fluorinated Carbohydrates as**  
**Covalent Inactivators of Glycosidases**

## 2.1 Model glycosidases: introduction

### 2.1.1 *Agrobacterium* sp. $\beta$ -glucosidase (Abg)

*Agrobacterium* sp.  $\beta$ -glucosidase (Abg, EC 3.2.1.21) is a family GH1 retaining *exo*-glycosidase that is believed to have evolved to assist in cello-oligosaccharide degradation.<sup>116</sup> Abg has proven to be a useful model enzyme in the Withers group owing to its high stability under a variety of conditions, its tolerance for a variety of substrates, its ease of expression and purification, and its high catalytic efficiency with artificial substrates,<sup>14,117</sup> and has been extensively studied by site-directed mutagenesis,<sup>118-121</sup> and inactivator studies.<sup>57,58,122-124</sup> The gene coding for Abg (*abg*) was first cloned in 1988, and the recombinant protein can be readily overexpressed and purified from *E. coli* cells.<sup>14,116</sup> There is no experimentally determined three dimensional structure of Abg, although a homology model has been constructed based on the three dimensional structures solved by X-ray crystallography of other family GH1  $\beta$ -glucosidases.<sup>125</sup> Abg was also the first enzyme to be converted to a glycosynthase, a class of enzyme that can no longer act as a glycoside hydrolase, but can be used to catalyze the formation of new glycosidic linkages.<sup>126-128</sup> This is accomplished by replacement of the enzymatic nucleophile with a non-nucleophilic residue. When reacted with a glycosyl fluoride of the opposite configuration to the natural substrate along with a suitable acceptor, efficient glycoside synthesis is achieved. Abg was also used as a model enzyme to assist in the development and study of many fluorosugar inactivators.<sup>57,58,122,124,129,130</sup>

### 2.1.2 Yeast $\alpha$ -glucosidase (Yag)

Yeast  $\alpha$ -glucosidase (Yag, EC 3.2.1.20) is a family GH13, commercially-available retaining *exo*-glucosidase from *Saccharomyces cerevisiae* that is involved in the degradation of maltosides. It has been used as a representative retaining  $\alpha$ -glucosidase in many studies of potential glucosidase inhibitors,<sup>23</sup> as well as being an important enzyme for studying the mechanism of this class of enzyme.<sup>5</sup> While no three-dimensional structure for Yag is available, there are three-dimensional structures solved by X-ray crystallography for other GH13 glycosidases.<sup>131-133</sup> It was chosen as a model enzyme for the studies with activated

fluorosugar derivatives described in this chapter since it was the enzyme used to help develop 5-fluoro-glycosyl fluorides as inactivators of retaining  $\alpha$ -glucosidases.<sup>129,134</sup>

### 2.1.3 $\beta$ -Mannosidase from *Cellulomonas fimi* (Man2A)

The  $\beta$ -mannosidase from *Cellulomonas fimi* (Man2A, EC 3.2.1.25) is a family GH2 mannosidase involved in the degradation of mannan,<sup>135</sup> and was chosen as a representative retaining  $\beta$ -mannosidase for inactivator studies because it is very stable, has a high catalytic efficiency with artificial substrates, and has been shown to be inactivated by 2-deoxy-2-fluoro- $\beta$ -D-mannosyl fluoride.<sup>136,137</sup> The gene encoding Man2A (*man2A*) has been identified, and a recombinant form of the enzyme has been overexpressed and purified from *E. coli* cells.<sup>135</sup> There is no three dimensional protein structure of Man2A, although the X-ray crystallographic structures of other family GH2 glycosidases have been solved, such as the *E. coli*  $\beta$ -galactosidase<sup>138</sup> (discussed below), the human  $\beta$ -glucuronidase<sup>139</sup> and a  $\beta$ -mannosidase from *Bacteroides thetaiotaomicron*.<sup>140,141</sup> A nucleophile mutant of Man2A (Glu519Ser) has been shown to act as a glycosynthase.<sup>142</sup> Interestingly, a mutant Man2A enzyme in which the catalytic acid/base residue has been mutated (Glu429Ala) that is treated with an activated 2,4-dinitrophenyl  $\beta$ -D-mannopyranoside and a high concentration of fluoride ion has been shown to form  $\beta$ -D-mannopyranosyl fluoride *in situ*, which has possible implications in the design of an enzyme capable of catalyzing the formation of C-F bonds.<sup>143</sup>

### 2.1.4 Jack bean $\alpha$ -mannosidase (JBAM)

*Canavalia ensiformis* or Jack bean  $\alpha$ -mannosidase (JBAM, 3.2.1.24) is a commercially available retaining  $\alpha$ -mannosidase<sup>144</sup> that is used as a representative retaining  $\alpha$ -mannosidase to study the interaction between putative inhibitors and this class of enzyme.<sup>145,146</sup> Neither its primary sequence nor its three dimensional structure have been reported. However, it is known that JBAM has a wide substrate specificity and readily hydrolyzes linkages between mannosides and a wide variety of aglycones.<sup>147</sup> Additionally, it is known that 5-fluoro- $\beta$ -L-gulosyl fluoride is a covalent inactivator of JBAM, and trapping

and identification of the catalytic nucleophile allowed the assignment of JBAM as a family GH38 glycosidase.<sup>148</sup> The three-dimensional crystal structure of two family GH38 glycosidases are known, the bovine<sup>149</sup> and drosophila<sup>150</sup>  $\alpha$ -mannosidases. JBAM was chosen as a model glycosidase because it is commercially available and the catalytic nucleophile has already been trapped with an activated fluorosugar reagent.<sup>148</sup>

### 2.1.5 *E. coli* $\beta$ -galactosidase (*E. coli* $\beta$ -gal)

*E. coli*  $\beta$ -galactosidase (*E. coli*  $\beta$ -gal, EC 3.2.1.23) is a commercially available family GH2 retaining  $\beta$ -galactosidase involved in the degradation of lactose. The *lacZ* gene of the *lac* operon in *E. coli* is responsible for its expression, and has become an extremely powerful tool in molecular biology for the overexpression of proteins in *E. coli* cells by fusion of the desired gene to the *Z* promoter gene and treatment of the cells with isopropyl  $\beta$ -D-1-thiogalactopyranoside (IPTG) to induce protein expression. *E. coli*  $\beta$ -gal gene expression and catalytic activity have also been used as reporters in many other experiments studying gene expression, in combination with a chromogenic substrate such as 5-bromo-4-chloro-3-indoyl- $\beta$ -D-galactopyranoside (X-Gal).<sup>92</sup> The three-dimensional structure of the enzyme has been solved, and shows an open active site necessary to accommodate the varied natural substrates of the enzyme, lactose and allo-lactose.<sup>92,138</sup> The catalytic nucleophile residue for this enzyme was initially mis-identified as Glu-461 by labelling studies using Conduritol epoxide-C,<sup>151</sup> and subsequent kinetic studies.<sup>152</sup> Later studies using a more specific reagent, 2,4-dinitrophenyl  $\beta$ -D-galactopyranoside correctly identified the nucleophile residue as Glu-537.<sup>153,154</sup>

## 2.2 An introduction to fluorosugars as glycosidase inactivators

### 2.2.1 Properties of fluorinated organic compounds

Fluorinated carbohydrates, or “fluorosugars”, are a broad class of molecules in which a hydroxyl group or a hydrogen atom has been replaced with a fluorine atom. The C-F bond

is a strong covalent bond (on average between 440-486 kJ/mol), which means that when bonded to a chemically unactivated carbon atom, the C-F bond is exceedingly stable.<sup>155</sup> However, because of its high electronegativity, fluorine can be a good leaving group when it is bonded to a chemically activated carbon atom.

Owing to its small size, the replacement of a hydroxyl group by fluorine is a reasonably conservative replacement, as the average C-O bond length in a hydroxyl group (1.52 Å) is quite close to the C-F bond length (between 1.41-1.47 Å).<sup>155</sup> However, due to its extreme electronegativity, introduction of a fluorine into a molecule can greatly perturb the distribution of electron density in a molecule. When replacing a hydroxyl group by fluorine, the ability to donate hydrogen bonds is completely abolished and the ability to accept hydrogen bonds is also severely attenuated.<sup>156-159</sup>

Fluorinated organic compounds have potentially very polar bonds arising from the large difference in electronegativity between the carbon and fluorine atoms, however the small size of the fluorine atom means that its valence electrons are held tightly to the nucleus which means it forms a very non-polarizable surface. The net effect is that the bond, while polar, is not very polarizable. This means that in a polar solvent system, fluorinated compounds are not as soluble as might be expected, since other solvent molecules contain more polarizable bonds that preferentially form interactions through dispersion forces. This, combined with their poor ability to hydrogen-bond, means that highly fluorinated organic compounds are often poorly soluble in polar protic solvents such as water.<sup>160,161</sup>

### **2.2.2 Activated fluorosugars as glycosidase inactivators**

A fluorosugar is deemed to be “activated” when it has a good leaving group at the anomeric center, therefore making it chemically reactive towards substitution at the anomeric center. Activated fluorosugars have been found to be highly efficient covalent inactivators of a variety of glycosidases, as discussed below. They invariably function by forming a covalent bond to the catalytic nucleophile; no other enzymatic residues have been demonstrated to bond to this family of reagents.<sup>12,13</sup>

### 2.2.2.1 2-Deoxy-2-fluoro glycosides

The activated 2-deoxy-2-fluoro glycosides (Figure 2.1, a)) were the first to be tested, and were found to be specific inactivators of a variety of retaining  $\beta$ -glycosidases.<sup>57,58,122</sup> The appropriately configured 2-deoxy-2-fluoro  $\alpha$ -glycosyl fluorides are not inactivators for retaining  $\alpha$ -glycosidases, and only act as slow substrates for these enzymes.<sup>57</sup> The 2-deoxy-2-fluoro substitution leads to a destabilization of both the glycosylation and deglycosylation transition states in the retaining glycosidase catalytic mechanism, thereby slowing both the formation of the glycosyl-enzyme intermediate and its hydrolysis. This destabilization of the oxocarbenium ion-like transition state arises both from inductive effects of fluorine and from the removal of hydrogen-bonding interactions ordinarily formed with the O2 on the pyranose ring in the transition state. The incorporation of a good leaving group (often a dinitrophenolate or fluoride) accelerates the glycosylation step, leading to the accumulation of the covalent glycosyl-enzyme intermediate (Figure 2.2). This species can be moderately stable, with observed life-times ranging from seconds to months.<sup>13</sup>

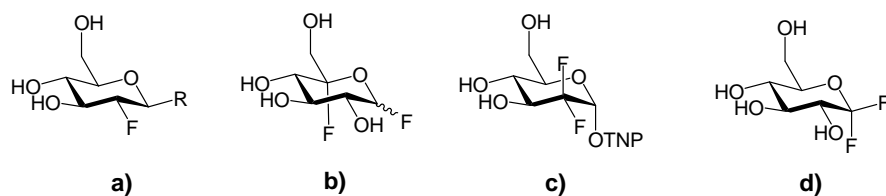


**Figure 2.1.** Structures of activated fluorosugar glycosidase inactivators, represented as glucosides. a) 2-deoxy-2-fluoro glycosides, b) 5-fluoro glycosyl fluorides, c) trinitrophenyl 2-deoxy-2,2-difluoro glycosides, and d) 1-fluoro glycosyl fluorides. R = F, dinitrophenyl; TNP = trinitrophenyl.

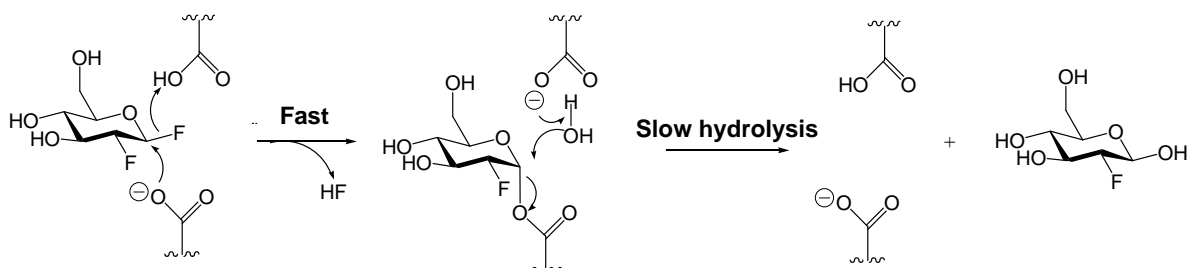


**Figure 2.2.** Mechanism of inactivation of a retaining  $\beta$ -glucosidase using 2-deoxy-2-fluoro- $\beta$ -D-glucosyl fluoride through accumulation of the stable covalent glycosyl-enzyme intermediate.

The activity of enzymes inactivated in this fashion can be recovered either through hydrolysis of the covalent glycosyl-enzyme intermediate, or by transglycosylation onto a suitable acceptor substrate to restore a catalytically competent enzyme. If the acceptor substrate molecule has an affinity for the enzyme's aglycone binding site, then the transglycosylation onto that acceptor will be accelerated. Such acceleration of transglycosylation activity can be used as a probe to examine the interactions between the aglycone binding site and the acceptor molecule (Figure 2.3).<sup>57</sup> As a consequence of this recovery of activity, this class of molecule is formally better described as being a very slow substrate rather than a true inactivator. However, the trapped intermediates are usually sufficiently long-lived that, for all practical purposes, these reagents function as inactivators and will generally be referred to as such.

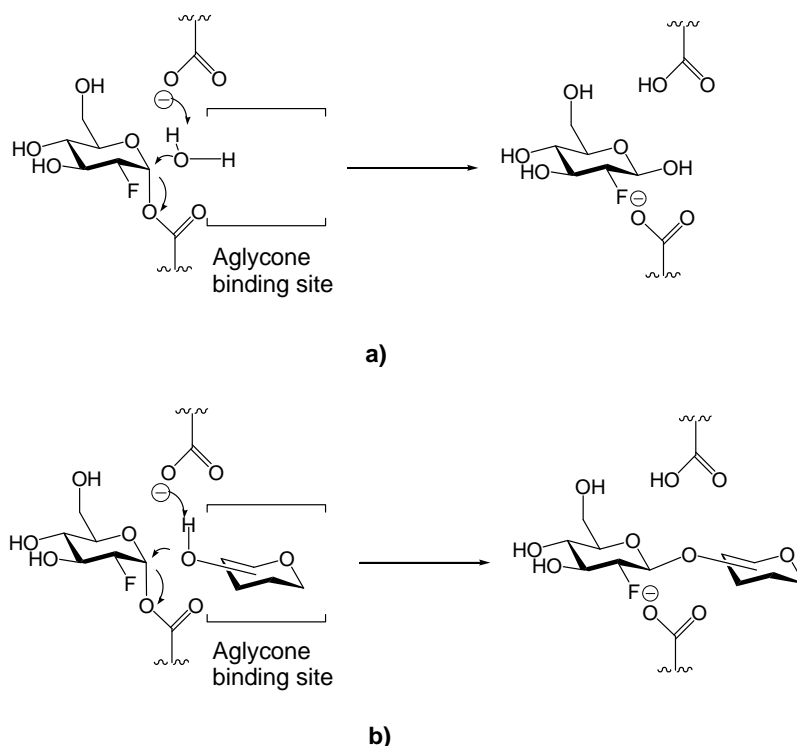


**Figure 2.3.** Turnover of covalent glycosyl-enzyme intermediate by a) hydrolysis and b) transglycosylation.



#### 2.2.2.2 5-Fluoro glycosides

Activated 5-fluoro glycosides (Figure 2.1, b)) are also covalent inactivators of glycosidases, working by a similar mechanism to that of the activated 2-deoxy-2-fluoro glycosides. One structural difference between the two classes lies in the replacement of a hydrogen atom by fluorine, as opposed to the replacement of a hydroxyl group with fluorine in the 2-deoxy-2-fluoro glycosides. This change would be expected to be more strongly destabilizing to both glycosylation and deglycosylation transition states, on the basis of the larger change in electronegativity arising from replacement of hydrogen with fluorine. However, the replacement of an oxygen atom with fluorine in the 2-deoxy-2-fluoro glycosides also strongly attenuates the hydrogen-bonding interactions at that position, which have been shown to be very important in both the glycosylation and deglycosylation transition states.<sup>117</sup> No such loss of hydrogen-bonding interactions is incurred by 5-fluoro substitution. The combined effect of these two competing factors is that, in the context of inhibitory activity against retaining  $\beta$ -glycosidases, the 5-fluoro glycosides tend to have both higher glycosylation and higher deglycosylation rates than the analogous 2-deoxy-2-fluoro glycosides. Indeed, they often function as slow substrates for which the second step (deglycosylation) is rate-limiting and the intermediate accumulates. Kinetically, this is revealed in very low  $K_m$  values (if monitored as a substrate) or apparent very tight binding (low  $K_i$  values) if monitored as a reversible inhibitor. For a more detailed discussion, see Mosi and Withers, 2002.<sup>12</sup> Interestingly, and in contrast to what is found with the 2-deoxy-2-fluoro glycosides, the appropriately activated 5-fluoro glycosides are capable of inactivating retaining  $\alpha$ -glycosidases. Kinetic, mechanistic and structural studies have confirmed that this inactivation is indeed due to the accumulation of a stable 5-fluoroglycosyl-enzyme species.<sup>129,134,148,162</sup> By contrast, the 2-deoxy-2-fluoro  $\alpha$ -glycosides act as slow substrates for  $\alpha$ -glycosidases since the deglycosylation step remains faster than glycosylation. The origin of this selectivity, based on the site of fluorination, is not entirely clear, although it is thought to be related to the relative distribution of partial positive charge between the anomeric carbon and the ring oxygen in the transition state of the reaction.<sup>5</sup>

#### 2.2.2.3 2-Deoxy-2,2-difluoro glycosides

Activated 2-deoxy-2,2-difluoro glycosides (Figure 2.1, c)) have also been used to trap the covalent glycosyl-enzyme intermediate in retaining  $\alpha$ -glycosidases.<sup>163-166</sup> Since the appropriately configured 2-deoxy-2-fluoro glycosyl fluorides had been demonstrated to behave as slow substrates for retaining  $\alpha$ -glycosidases,<sup>57</sup> the introduction of a second fluorine atom at C2 was pursued to further inductively destabilize the two positively-charged transition states. Therefore, the presence of multiple fluorine atoms on the sugar ring has an additive destabilizing effect on the energy of the transition states. However, a more chemically activated aglycone such as chloride<sup>165</sup> or trinitrophenol (TNP)<sup>163-166</sup> is necessary to sufficiently accelerate the glycosylation step to permit the accumulation of a significant steady-state population of the covalent glycosyl-enzyme intermediate. This class of inactivator has not been as widely adopted as either the activated 2-deoxy-2-fluoro glycosides or activated 5-fluoro glycosides owing to the challenges surrounding their synthesis.

#### 2.2.2.4 1-Fluoro-glycosyl fluorides

The final class of activated fluorosugars that have been investigated as potential time-dependent inactivators of glycosidases are the 1-fluoro glycosyl fluorides (Figure 2.4, d)). However, when 1-fluoro glucosyl fluoride was tested as a potential inactivator with a variety of retaining  $\alpha$ - and  $\beta$ -glucosidases, no time dependent inactivation was observed, and the compound was observed to act simply as a substrate for the enzymes tested, with turnover of the covalent glycosyl-enzyme intermediate being relatively fast.<sup>166-168</sup> The fluorine atom at the anomeric center in the 1-fluoro glycosyl fluorides is closer to the build-up of positive charge than is the case for the C-2 fluorine in the 2-deoxy-2-fluoro glycosyl fluorides, so it may at first seem counterintuitive that the former act as substrates while the latter act as covalent inactivators for the retaining  $\beta$ -glycosidases. However, the hydrogen bonding interactions in both of the enzyme-catalyzed transition states are an extremely important stabilizing interaction.<sup>5,117</sup> Therefore, it was suggested that the behaviour of 2-deoxy-2-fluoro glycosides as inactivators for retaining  $\beta$ -glycosidases arises as much from their removal of specific hydrogen-bonding interactions between O2 on the sugar ring and the enzyme as

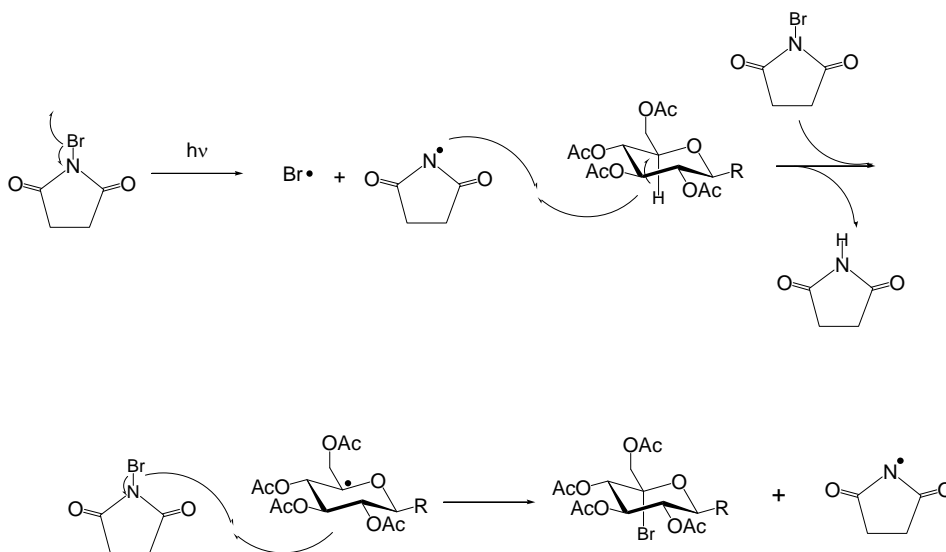
from the electron withdrawing effects of the fluorine atom.<sup>167</sup> Additionally, while the fluorine atom at C-1 will inductively withdraw electron density from the developing positive charge in the transition state, it is capable of resonance donation from its lone pair of electrons to stabilize the developing empty orbital, which is a stabilizing effect.

To date, no other general class of fluorosugar has been reported to act as a time-dependent inactivator of a retaining glycosidase, though 3-,4- and 6-deoxyfluoro sugar derivatives have all been synthesized and their behaviour with retaining glycosidases examined.<sup>117,154,169</sup>

### **2.2.3 General synthetic approaches to activated fluorosugars**

#### **2.2.3.1 5-Fluoro and 1-fluoro glycosides**

Different synthetic approaches are required to install fluorine atoms at different locations on the sugar ring. There have been two methods reported for the installation of a 5-fluoro moiety, both of which rely upon the nucleophilic attack of a fluoride ion. The C5 carbon is activated towards nucleophilic attack either as the C5-bromide<sup>129,134,170-176</sup> or as a C5-C6 epoxide,<sup>177</sup> although this latter method has not been widely adopted. The generation of a C5 bromide is the most common strategy in the synthesis of 5-fluoro glycosyl fluorides, and is accomplished by a light-catalyzed free-radical bromination reaction using *N*-bromosuccinimide (NBS) as the bromine atom source (Scheme 2.1). The regioselectivity of the free-radical bromination reaction is the key in the synthesis of both the 5-fluoro- and 1-fluoro glycosides. Ferrier first reported this reaction and found that in O-linked glycosides, the bromination was selective for C5 over C1 although significant by-products arising from bromination at other sites, in particular the methyl groups on the acetate protecting groups, were also observed.<sup>175,176</sup> The introduction of a bromine atom at C5 makes C5 an anomeric center, and the bromine atom preferentially adopts an axial configuration due to the anomeric effect of the ring oxygen. Praly later reported that the presence of a chlorine atom or a  $\pi$ -acceptor such as a nitrile group at the anomeric center changed the selectivity of the bromination reaction to give predominantly bromination at C1.<sup>178</sup>



**Scheme 2.1.** Light catalyzed free-radical generation of a C5 bromide by *N*-bromosuccinimide (NBS).  
 R = OAc, OPh, OMe.

The regioselectivity of the bromination reaction is best explained by considering the stability of the intermediate free-radical formed at either C1 or C5. The radicals formed on either center can be stabilized by interactions with the lone pair of electrons on the ring oxygen. Normally carbon-based radical stability increases with a higher degree of substitution on that carbon atom.<sup>179</sup> Therefore, radicals at C5 on a sugar ring are more stable than radicals at C1, which explains the observed preference for formation of the C5 bromide in most cases, as reported by Ferrier. This is shown by the fact that the bromination reaction proceeded more smoothly and in higher yield on protected uronic acids, which contain a radical-stabilizing ester group at C6, than on sugars with a hydroxymethyl group at C6, such as in normal glucosides.<sup>175,176</sup> However, introduction of a  $\pi$ -acceptor such as a nitrile at C1 increases the stability of radicals at that position and thus alters the regioselectivity of the bromination. The presence of an equatorial chlorine atom at C1 also appears to greatly stabilize radicals at this center, as  $\beta$ -chlorides react under free radical conditions to give 1-bromo- $\beta$ -glycosyl chlorides.<sup>178,180</sup>

Following the introduction of a bromine atom at either C5 or C1, the fluorine atom is introduced via the nucleophilic displacement of the bromide with a fluoride ion, usually

using a silver salt. The formation of the 1-fluoro glycosyl fluorides requires greater than two equivalents of silver fluoride to displace both the bromine and chlorine atoms at the anomeric center;<sup>178,180</sup> both 1-fluoro-glucosyl fluoride<sup>178</sup> and 1-fluoro-galactosyl fluoride<sup>180</sup> have been synthesized using this methodology.

In the context of the synthesis of activated 5-fluoro glycosides, the fluoride source and solvent both play key roles in controlling the stereochemistry of the C-5 fluoride formed. If the C-5 fluoride has the opposite configuration to that of the starting bromide, then the resulting glycoside is an L-sugar. Generation of these unnatural L-configured sugars is achieved by treatment of the 5-bromide with silver fluoride in acetonitrile, which yields the kinetic product arising from inversion at C5.<sup>129,134,144,148,162,170-174,181-183</sup> The 5-fluoro-D-glycosyl fluoride, which arises from retention of configuration at C5 is more challenging to synthesize, and requires equilibrating conditions to obtain the axial (thermodynamically favoured) product. The original method used to obtain this class of compound involved treatment of the L-sugar, the product of inversion, with hydrogen fluoride/pyridine to obtain the thermodynamically favoured D-sugar.<sup>129</sup> However, treatment of the 5-bromide species with silver tetrafluoroborate in diethyl ether was found to yield a mixture of both the inversion and retention products, which are usually separable by chromatography.<sup>170,172,174</sup>

#### 2.2.3.2 2-Deoxy-2-fluoro glycosides

The synthesis of 2-deoxy-2-fluoro glycosides relies on either the addition of an electrophilic fluorine atom to an electron rich glycal,<sup>184-188</sup> or the activation of the C2-hydroxyl group to make it a very good leaving group followed by displacement with a nucleophilic fluoride ion.<sup>185,189</sup> This latter method of fluorination is the strategy adopted for the synthesis of [<sup>18</sup>F] fluorodeoxyglucose (FDG, **1.12**), which is the most widely used radiopharmaceutical in the world<sup>109,190,191</sup>, see Section 1.5.4.1 for a more complete discussion of FDG and radiochemistry).

The most common method to introduce the fluorine atom at C2 that is amenable to large-scale synthesis is the reaction of the appropriate glycal with Selectfluor<sup>TM</sup>.

Selectfluor<sup>TM</sup> (1-chloromethyl-4-fluoro-1,4-diazonia-bicyclo[2.2.2]octane

bis(tetrafluoroborate)) is a convenient reagent due to its ease of handling, commercial availability, safety and relatively low cost. This reagent introduces the fluorine atom only at C2, although the stereoselectivity achievable with Selectfluor<sup>TM</sup> depends on the specific glycal used. Equatorial fluorination is favoured in systems with an axial group at C4, likewise increasing steric bulk at either the 3 or 6 positions also leads to increased selectivity for equatorial fluorination.<sup>186-188,192,193</sup> There are numerous examples in the literature of activated 2-deoxy-2-fluoro-glycosides being prepared and used; for some representative examples, see<sup>13,57,58,136,193-197</sup>

The 2-deoxy-2,2-difluoro glycosides represent the most synthetically challenging of the activated fluorosugars. They were originally prepared by the addition of an electrophilic fluorine atom from acetyl hypofluorite to a 2-fluoro glycal.<sup>163,164,166,197</sup> More recently, it has been shown that by appropriate choice of solvent, Selectfluor<sup>TM</sup> can be used as the fluorinating reagent<sup>165</sup>, which makes the preparation of 2-deoxy-2,2-difluoro glycosides considerably easier and safer. However, since the precursor for the second fluorination, the 2-fluoro glycal, requires a prior fluorination step, this class of fluorosugar is still the most synthetically challenging to access. Further, the resultant sugars are so deactivated towards displacement at the anomeric center that installation of the desired leaving group can be challenging.

## 2.3: Chemical synthesis of difluorosugar fluorides

### 2.3.1 Target compounds

As described above, the different fluorination states of the sugar ring result in decreases in the rates of glycosylation and deglycosylation in a glycosidase active site by different amounts. The fluorosugar variants chosen as synthetic targets are shown in Figure 2.4. The target fluorosugar variants **2.4** and **2.6-2.8** were chosen to explore the effect of simultaneously incorporating two of the fluorosugar modifications described above. The D-*gluco*- and L-*ido*-configured sugars were chosen to test this idea since they are readily

synthetically manipulated, and the chemistry for making the above four modifications to the glucose ring is known.

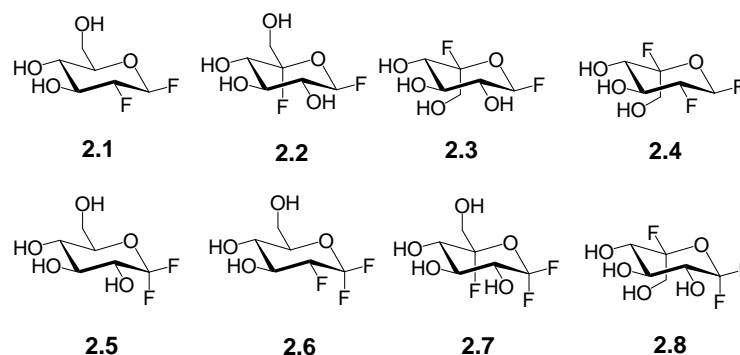


**Figure 2.4.** Fluorosugar variants chosen as synthetic targets.

Compounds **2.1**, **2.2** and **2.3** are all known inactivators of Abg,<sup>57,129</sup> and it is known that the covalent glycosyl-enzyme intermediate formed by Abg and the *L-ido*-configured **2.3** is longer-lived than that formed by the *D-gluco*-configured **2.2**. The covalent 2-deoxy-2-fluoro-glucosyl-enzyme is the most stable intermediate formed of these three, thus compound **2.4** was chosen as a target since it combines the 2-fluoro and 5-fluoro modifications. Since inactivation of Abg with the *L-ido*-configured **2.3** has already been demonstrated, we hypothesized that **2.4** could conceivably bind to the active site of Abg, and form the covalent glycosyl-enzyme intermediate. The analogous *D-gluco*-configured compound was not targeted since the effect of incorporation of fluorine at both C2 and C5 could be adequately studied with compound **2.4**.

Compound **2.5** has not been specifically tested as an inactivator of Abg, although it has been shown to be a slow substrate for other retaining  $\beta$ -glucosidases, as well as for  $\alpha$ -glucosidases.<sup>166-168</sup> Compounds **2.6**, **2.7** and **2.8** were chosen to combine the anomeric gem-difluoro modification with a 2-deoxy-2-fluoro-(**2.6**) and 5-fluoro-(**2.7** and **2.8**) glucosyl fluoride, and to study the effect on the rates of formation and breakdown of the proposed covalent glycosyl-enzyme intermediates.

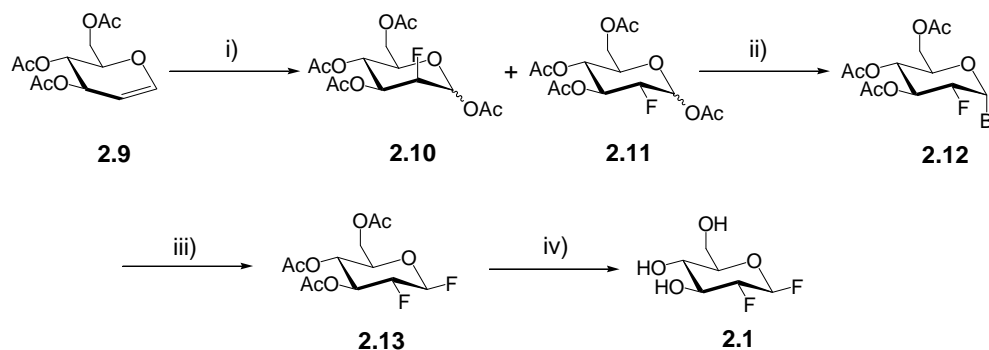
One important consideration is that fluoride may not be a sufficiently chemically activated leaving group to permit these compounds to function as time-dependent

inactivators since all of the novel compounds proposed (**2.4**, **2.6**, **2.7** and **2.8**) incorporate a higher degree of fluorination than their parent compounds. As a consequence, they would all be predicted to have slower rates of both glycosylation and deglycosylation, as the electronegative fluorine(s) destabilize both of the positively charged transition states. Despite this potential drawback, fluoride was still chosen as the aglycone for these target compounds as this allowed direct comparison of the enzymatic activity of the novel compounds **2.4**, **2.6**, **2.7** and **2.8** with that of the known compounds **2.1**, **2.2**, **2.3** and **2.5**. Furthermore, the chemistry employed in the synthetic introduction of the chosen fluorination modifications was readily amenable to the presence of an equatorial anomeric fluoride. Finally, the only other aglycone that has been widely used to inactivate retaining  $\beta$ -glycosidases is 2,4-dinitrophenol (DNP), which has approximately the same leaving group ability as fluoride as discussed in Section 2.5.

### 2.3.2 Chemical synthesis

#### 2.3.2.1 2-Deoxy-2-fluoro- $\beta$ -D-glucopyranosyl fluoride (**2.1**)

Compound 2-deoxy-2-fluoro- $\beta$ -D-glucopyranosyl fluoride (**2.1**) was prepared as shown in Scheme 2.2.



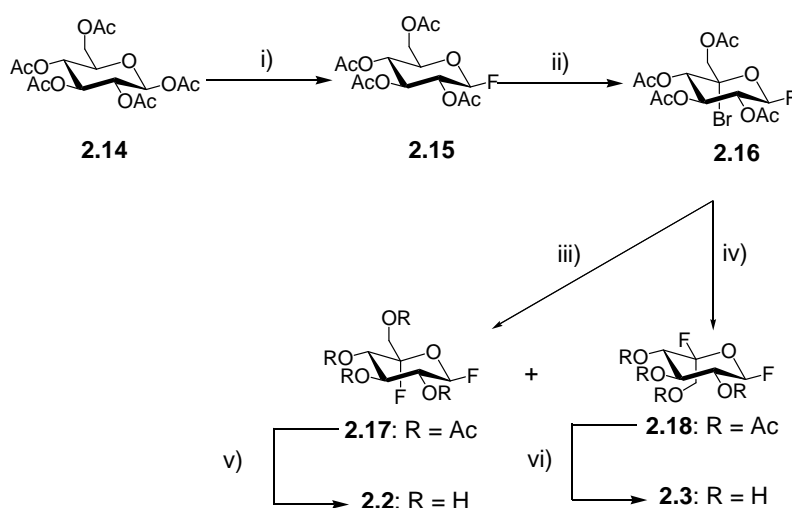
**Scheme 2.2.** The synthesis of 2-deoxy-2-fluoro-glucosyl fluoride (**2.1**). i) Selectfluor<sup>TM</sup>, MeCN, AcOH **2.10**: 20%, **2.11** 19%; ii) 33% (w/v) HBr/AcOH, 92%; iii) AgF, MeCN, 90%; iv) NaOMe, MeOH, 98%.



Tri-*O*-acetyl glucal was reacted with Selectfluor<sup>TM</sup> in the presence of acetic acid to yield anomeric mixtures of both the *manno*- (**2.10**) and *gluco*- (**2.11**) configured 1,3,4,6-tetra-*O*-acetyl-2-deoxy-2-fluoro-D-glycopyranoses in approximately a 1:1 ratio, which were separable by flash chromatography.<sup>186,188</sup> The anomeric acetate of compound **2.11** was converted to a bromide by treatment with HBr/AcOH (33% w/v), followed by displacement with a fluoride ion using silver fluoride in acetonitrile to yield **2.13**.<sup>198</sup> The final product (**2.1**) was obtained easily by Zemplen deacetylation.

### 2.3.2.2 5-Fluoro-β-D-glucopyranosyl fluoride (**2.2**) and 5-fluoro-α-L-idopyranosyl fluoride (**2.3**)

5-Fluoro-β-D-glucopyranosyl fluoride (**2.2**) and 5-fluoro-α-L-idopyranosyl fluoride (**2.3**) were prepared according to literature methods<sup>170</sup> as shown in Scheme 2.3.



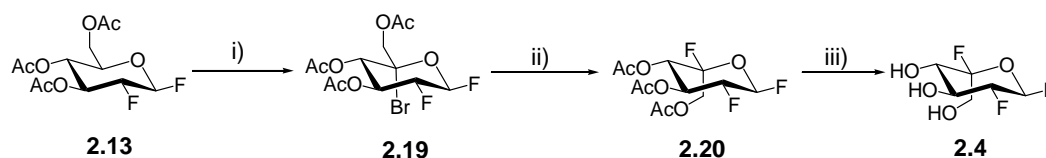
**Scheme 2.3.** Synthesis of 5-fluoro-β-D-glucosyl fluoride (**2.2**) and 5-fluoro-α-L-idosyl fluoride (**2.3**). i) 33% (w/v) HBr/AcOH, then AgF, MeCN, 68%; ii) NBS, CCl<sub>4</sub>, hv; iii) AgBF<sub>4</sub>, Et<sub>2</sub>O, **2.17**: 3% (from **2.15**), **2.18**: 3% (from **2.15**); iv) AgF, MeCN, 23%; v) NH<sub>3</sub>, MeOH, 76%; vi) NH<sub>3</sub>, MeOH, 59%.

1,2,3,4,6-Penta-*O*-acetyl-β-D-glucopyranose was converted to its β-fluoride under Koenigs-Knorr conditions<sup>199</sup> to yield compound **2.15**, which was subsequently photobrominated to yield **2.16**. This molecule was found to be moderately labile under

ambient conditions, and the material was therefore used crude for the subsequent fluorination steps. Treatment of crude **2.16** with silver fluoride in acetonitrile yielded solely the *L-ido*-configured 5-fluoro glycosyl fluoride (**2.18**) in 23% yield, whereas treatment of crude **2.16** with silver tetrafluoroborate, gave a mixture of epimeric *D-gluco*- (3%) and *L-ido*-configured (3%) glycosyl fluorides. While these yields were lower than previously reported, they still furnished sufficient material to facilitate subsequent deprotection and enzymatic testing. *L-ido*-configured compounds such as **2.3** are drawn in the  ${}^4C_1$  chair conformation for ease of identification, though it is understood that these compounds typically adopt a skew-boat or  ${}^1C_4$  conformation in solution.<sup>200</sup>

#### 2.3.2.3. 2-Deoxy-2,5-difluoro- $\alpha$ -*L*-idopyranosyl fluoride (**2.4**)

2-Deoxy-2,5-difluoro- $\alpha$ -*L*-idopyranosyl fluoride (**2.4**) was prepared as shown in Scheme 2.4.



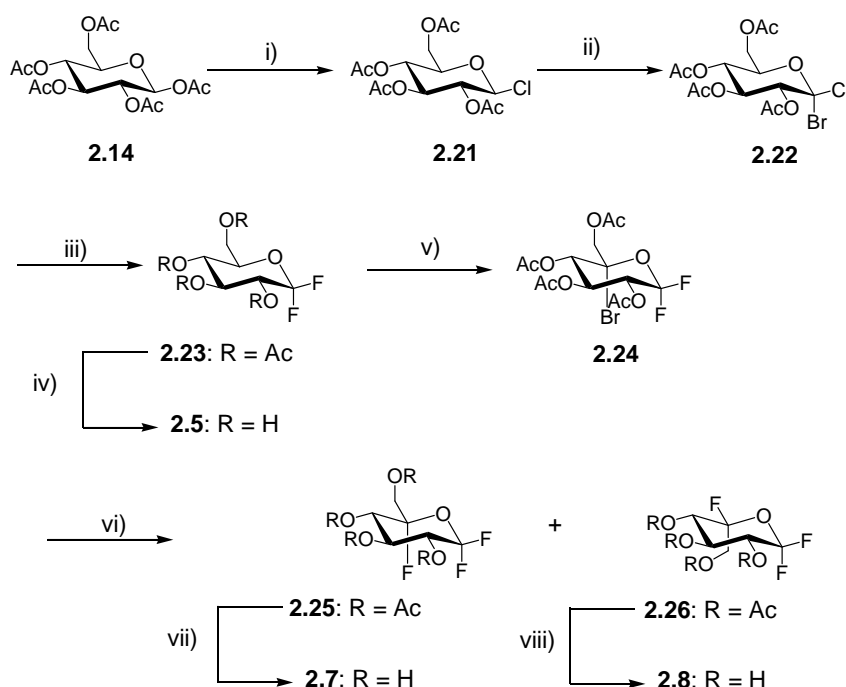
**Scheme 2.4.** Synthesis of 2-deoxy-2,5-difluoro- $\alpha$ -*L*-idopyranosyl fluoride (**2.4**). i) NBS,  $CCl_4$ , hv; ii) AgF, MeCN, 28% from **2.13**; iii)  $NH_3$ , MeOH, 95%.

Compound **2.13** was subjected to photobromination conditions to generate the C5 bromide. The regiochemistry was assigned by the disappearance of the H5 signal in the  ${}^1H$  NMR spectrum. Since **2.19** proved to be somewhat unstable, the crude **2.19** was fluorinated at C5 using silver fluoride and acetonitrile to yield the *L-ido*-configured **2.20**, in a modest yield. The presence of the 2-fluoro substituent did not appear to have any impact on the radical bromination or subsequent nucleophilic fluorination reactions at C5. The configuration was assigned as being *ido* on the basis of the small observed ring proton coupling constants (eg.  $J_{H1-H2} = 3.1$  Hz), which are indicative of the fact that the product no longer adopts a  ${}^4C_1$  chair conformation. Likewise, no large F-5/H-4 coupling constant ( $J_{H4-F5}$

= 8.4 Hz) was observed, as would be the case for the D-*gluco* isomer. Deprotection of **2.20** was accomplished using ammonia in methanol to yield the desired compound **2.4**.

#### 2.3.2.4 1-Fluoro-D-glucopyranosyl fluoride (**2.5**), 1,5-difluoro-D-glucopyranosyl fluoride (**2.7**) and 1,5-difluoro-L-idopyranosyl fluoride (**2.8**)

The known<sup>167</sup> compound 1-fluoro-D-glucopyranosyl fluoride **2.5** and the novel compounds 1,5-difluoro-D-glucopyranosyl fluoride **2.7** and 1,5-difluoro-L-idopyranosyl fluoride **2.8** were prepared as shown in Scheme 2.5.



**Scheme 2.5.** Synthesis of 1-fluoro-D-glucopyranosyl fluoride (**2.5**), 1,5-difluoro-D-glucopyranosyl fluoride (**2.7**) and 1,5-difluoro-L-idopyranosyl fluoride (**2.8**). i)  $\text{AlCl}_3$ ,  $\text{CHCl}_3$ , 80%; ii) NBS,  $\text{CCl}_4$ , hv, 33%; iii)  $\text{AgF}$ , MeCN, 84%; iv) NaOMe, MeOH, 76%; v) NBS,  $\text{CCl}_4$ , hv; vi)  $\text{AgBF}_4$ ,  $\text{Et}_2\text{O}$ , **2.25**: 5% from **2.23**, **2.26**: 3% from **2.23**; vii) NaOMe, MeOH, 89%; viii) NaOMe, MeOH, 90%.

1,2,3,4,6-Penta-*O*-acetyl- $\beta$ -D-glucopyranoside was readily converted to the  $\beta$ -chloride using aluminum trichloride.<sup>201</sup> Photobromination of the  $\beta$ -chloride yielded the 1,1-mixed dihalo species **2.22** in a modest yield (33%) as reported previously.<sup>178</sup> In contrast to

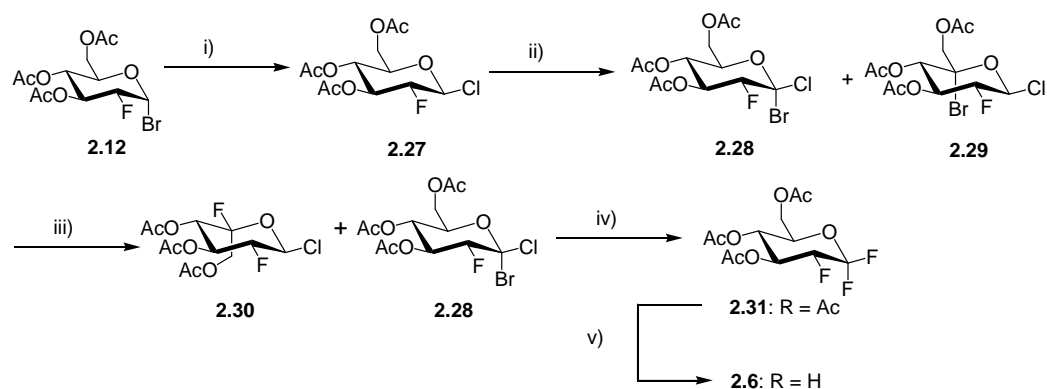
the previous report, the author was unable to obtain **2.22** as a crystalline solid,<sup>178</sup> thus the mixed dihalo species was used shortly after synthesis to avoid decomposition. Treatment with an excess of silver fluoride in acetonitrile led to the 1,1-gem-difluoro species **2.23** in a good yield (84%). It is worth noting that in this class of compound the anomeric center is not stereogenic, meaning the compound lacks either an  $\alpha$ - or  $\beta$ - designation. The known<sup>178</sup> compound **2.5** was thus obtained in good yield (74%) following Zemplen deprotection.

Treatment of **2.23** with *N*-bromosuccinimide under photobromination conditions led to radical photobromination at C5. The presence of the 1,1-gem difluoro moiety resulted in a dramatic decrease in the rate of radical bromination relative to a  $\beta$ -configured fluoride or chloride. The starting material was consumed after 48 hours, compared with 2 hours for the synthesis of **2.22**. The formation of the desired 5-bromide **2.24** was accompanied by the formation of multiple, uncharacterized, side products which presumably arise from the bromination of the acetate methyl groups.<sup>176</sup>

Compound **2.24** was found to be considerably less reactive than the other 5-bromo species prepared. In particular, the bromide did not react under standard silver fluoride/acetonitrile conditions, and could only be fluorinated by silver tetrafluoroborate. This reaction gave only a very poor yield of the desired compounds **2.25** (5%) and **2.26** (3%). This reaction also led to the formation of a major by-product, which is presumed to be the product of elimination of HBr across the C4-C5 bond, on the basis of crude mass spectral data and TLC analysis. However, the desired compounds **2.7** and **2.8** were obtained in sufficient quantities to facilitate enzymatic testing following deacetylation.

#### 2.3.2.5 2-Deoxy-1,2-difluoro-D-glucopyranosyl fluoride (**2.6**)

The novel compound 2-deoxy-1,2-difluoro-D-glucopyranosyl fluoride (**2.6**) was synthesized according to the procedure shown in Scheme 2.6.



**Scheme 2.6.** Synthesis of 2-deoxy-1,2-difluoro-D-glucopyranosyl fluoride (**2.6**). i) AgCl, MeCN, 77%; ii) NBS, CCl<sub>4</sub>, hv; iii) AgF, MeCN, overnight, **2.30**: 7% from **2.27**; iv) AgF, MeCN, 10 days; v) NaOMe, MeOH, 10% from **2.27**.

Treatment of **2.12** with silver chloride for 4 days led to the β-chloride **2.27** in good yield (77%). This reaction was challenging to monitor, since both the starting material and product had identical R<sub>f</sub> values by TLC analysis under all conditions tested. Fortunately, **2.27** was found to be a crystalline solid, aiding purification. Treatment of **2.27** with *N*-bromosuccinimide under photobromination conditions led to an inseparable mixture of **2.28** and **2.29**, which were not fully characterized at this stage. Treatment of the crude mixture of **2.28** and **2.29** with silver fluoride in acetonitrile led to the selective fluorination of **2.29** only. Flash chromatography was used to separate unreacted **2.28** from the newly formed **2.30**, which was isolated in a 7% overall yield from **2.27**.

The unreacted **2.28** that was isolated was fluorinated to yield **2.31** by using silver fluoride over an extended reaction time of 10 days. This suggests that the substituent at C2 has a profound impact on the reactivity of the dihalo C1 center towards nucleophilic substitution. When an O-acetyl group is present at C2, as in the synthesis of **2.23** from **2.21**, the reaction time is less than twelve hours. Thus the electronegative fluorine atom has the expected impact of destabilizing the developing positive charge in the transition state of the displacement reaction. Compound **2.31** could not be fully isolated from other minor impurities present, but could be detected by its very distinctive <sup>1</sup>H and <sup>19</sup>F NMR spectra. However, deprotection of the mixture gave **2.6** in 10% overall yield from **2.27**, which was readily separated from all other impurities that could be detected by TLC, NMR and MS.

## 2.4: Enzymatic testing of difluorosugar fluorides

### 2.4.1 Kinetic analysis of the inactivation of Abg by 2.1 and 2.4-2.8

#### 2.4.1.1 2-Deoxy-2-fluoro- $\beta$ -D-glucopyranosyl fluoride (2.1)

Compounds **2.1**, **2.2** and **2.3** are all known inactivators of Abg.<sup>57,122,129</sup> Compound **2.1** was evaluated as a covalent inactivator of Abg, as a control. The resulting activity vs. time curves for various concentrations of inactivator fitted to an exponential decay equation, and a second replot of the individual  $k_{\text{obs}}$  values as a function of inactivator concentration are shown in Figure 2.5. Studies at higher inactivator concentrations were not possible owing to the rapidity of inactivation at these concentrations. As a consequence of this, saturation was not observed and only a second order  $k_i/K_i$  rate constant was obtained. However, since the second order rate constant of  $13.8 \text{ min}^{-1}\text{mM}^{-1}$  obtained in the present study agrees very closely with the previously published value of  $14.6 \text{ min}^{-1}\text{mM}^{-1}$ , this serves as a useful control experiment to show that the results obtained below can be directly compared with previously published values.

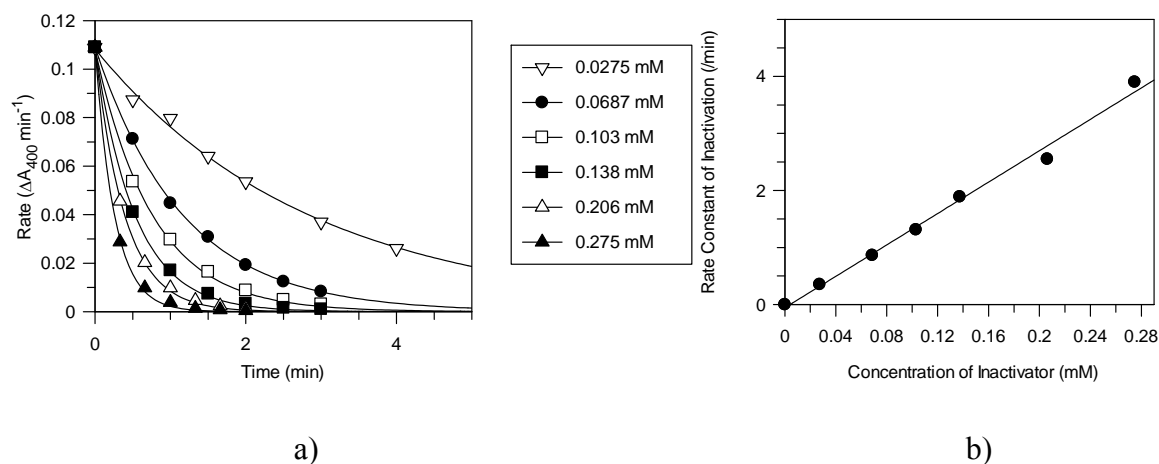


**Figure 2.5.** Inactivation of Abg with **2.1**. a) Non-linear plot of residual enzyme activity versus time at the indicated inactivator concentrations fitted to an exponential decay equation. b) Plot of the observed rate constants of inactivation versus concentration of inactivator.

The covalent glycosyl-enzyme intermediate formed following the treatment of Abg with **2.1** was isolated and when treated with a suitable transglycosylation agent could be reactivated. Following separation of the inactivated Abg from excess small molecule inactivator, the enzyme was treated with 20 mM thiophenyl  $\beta$ -D-glucopyranoside and the residual enzyme activity was measured as a function of incubation time (Figure 2.6). The observed rate constant for reactivation at this concentration of thiophenyl  $\beta$ -D-glucopyranoside was  $0.013 \text{ min}^{-1}$ . The absence of recovery of enzyme activity in the absence of acceptor (data not shown) demonstrates that thiophenyl  $\beta$ -D-glucopyranoside is an effective transglycosylation agent for the reactivation of the covalent glycosyl-enzyme intermediate of Abg.

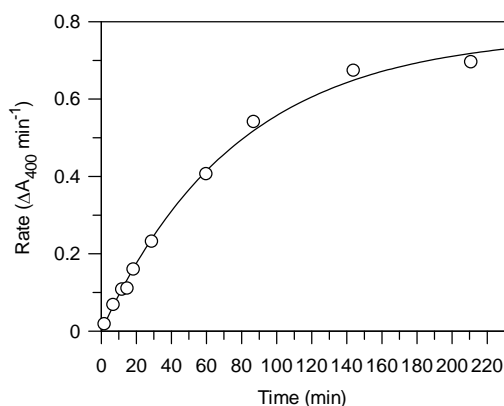
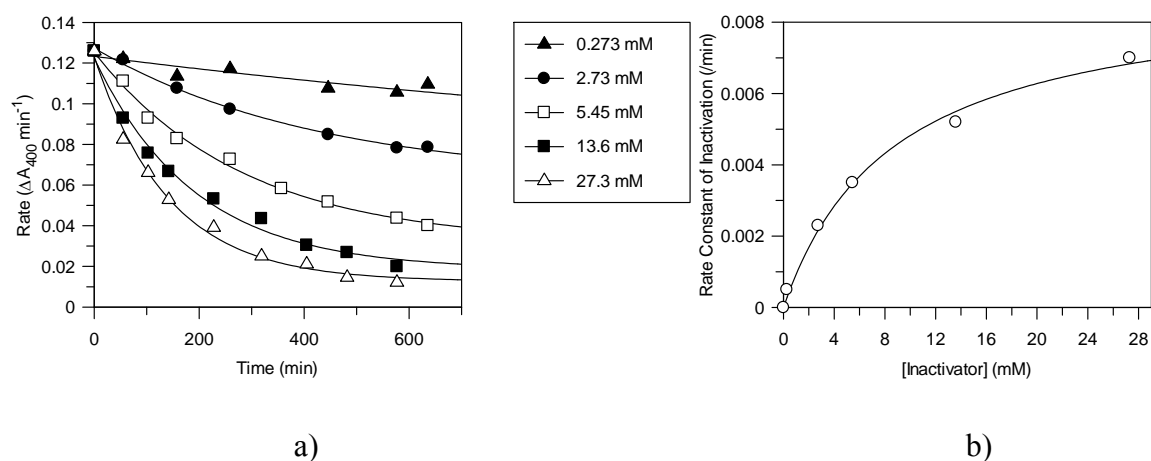


**Figure 2.6.** Residual enzymatic activity versus time curve for the reactivation of covalent 2-deoxy-2-fluoro-glucosyl-Abg intermediate following incubation with 20 mM thiophenyl  $\beta$ -D-glucopyranoside

Compounds **2.2** and **2.3** were not re-evaluated as covalent inactivators of Abg, but were instead used in later experiments (see Section 3.1.6.3).

#### 2.4.1.2 2-Deoxy-2,5-difluoro- $\alpha$ -L-idopyranosyl fluoride (**2.4**)

The novel compound **2.4** behaved as an apparent covalent inactivator of Abg, showing time-dependent inactivation of the enzyme in a *pseudo*-first order manner, as shown in Figure 2.7.

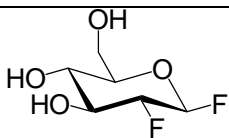
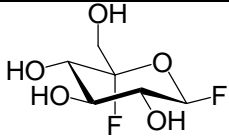
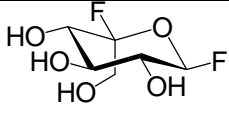


**Figure 2.7.** Apparent inactivation of Abg with **2.4**. a) Non-linear plot of residual enzyme activity versus time at the indicated inactivator concentrations fitted to an exponential decay equation. b) Plot of the observed rate constants of inactivation versus concentration of inactivator.

However, inactivation of Abg by **2.4** was found to require very high concentrations (concentration of inactivator varies between 1-27 mM) and long incubation times (>600 min at an inactivator concentration of 27.3 mM) before the inactivation reaction approaches completion. From these data, it is possible to derive a second order rate constant for the inactivation process of  $0.001 \text{ min}^{-1} \text{ mM}^{-1}$ . Table 2.1 shows the kinetic parameters for the previously known inactivators of Abg: **2.1**, **2.2** and **2.3**. The apparent second order rate constant for inactivation of Abg by **2.4** ( $0.001 \text{ min}^{-1} \text{ mM}^{-1}$ ) is 3000 fold lower than the  $k_i/K_i$  value for **2.3** ( $3.0 \text{ min}^{-1} \text{ mM}^{-1}$ ), and 13,800 fold lower than the  $k_i/K_i$  value for **2.1** ( $13.8 \text{ min}^{-1} \text{ mM}^{-1}$ ). This decreased rate of inactivation would be consistent with the cumulative, destabilizing electron-withdrawing effects of both the 2-deoxy-2-fluoro- and 5-fluoro-modifications on the glycosylation transition state. Indeed, the presence of two fluorines at the 2-position in 2,4,6-trinitrophenyl 2-deoxy-2,2-difluoro- $\alpha$ -D-maltoside lowered the rate of formation of the glycosyl-enzyme intermediate on  $\alpha$ -amylase by almost  $10^6$ -fold relative to  $\alpha$ -maltosyl fluoride.<sup>163</sup> If this is the case, then both the rate of formation (glycosylation) and breakdown (deglycosylation) of the covalent glycosyl-enzyme intermediate should be affected by roughly equal amounts, since both proceed through similar, positively charged transition states. Since the inactivation kinetics only report on the rate of formation of the



covalent glycosyl-enzyme intermediate, it is also necessary to examine the effect of the incorporation of multiple fluorine atoms on the rate of the breakdown of the presumed intermediate.

Compound	$k_i$ ( $\text{min}^{-1}$ )	$K_i$ (mM)	$k_i/K_i$ ( $\text{min}^{-1}\text{mM}^{-1}$ )	Reference
 <b>2.1</b>	5.9	0.40	14.8	57,122
 <b>2.2</b>	--	--	660	129
 <b>2.3</b>	--	--	3.0	200

**Table 2.1.** Kinetic parameters for selected inactivators of Abg.

Following incubation of Abg with a high concentration of **2.4** (21.8 mM) for 18 hours, <10% residual enzyme activity could be detected. The inactivated enzyme was separated from excess small molecule inactivator using a 10 kDa molecular weight cut-off filter, and the inactivated enzyme was incubated in the presence of 20 mM thiophenyl  $\beta$ -D-glucopyranoside and the rate of recovery of enzymatic activity monitored. A plot of residual enzyme activity as a function of incubation time is shown in Figure 2.7.

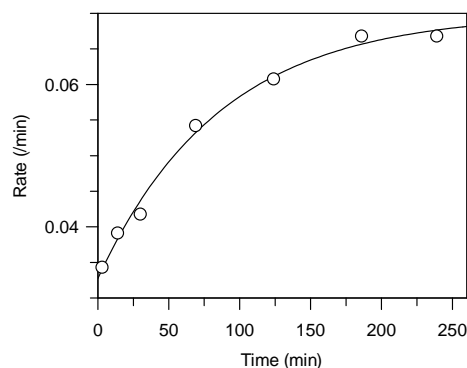


**Figure 2.7.** Residual activity versus time for Abg treated with 20 mM  $\beta$ -Glc-SPh, following treatment of Abg with **2.4**.

The most striking observation is that the rate of recovery ( $k_{\text{obs}} = 0.012 \text{ min}^{-1}$ ) of enzyme activity of the presumed 2-deoxy-2,5-difluoro-idosyl-enzyme intermediate of Abg in the presence of 20 mM thiophenyl  $\beta$ -D-glucopyranoside is very similar to that observed for the known 2-deoxy-2-fluoro-glucosyl-enzyme intermediate under the same conditions ( $k_{\text{obs}} = 0.013 \text{ min}^{-1}$ ), which is obtained by treatment of Abg with **2.1**. While it is possible that the rates of recovery of the two (presumed) covalent glycosyl-enzyme intermediates are coincidentally the same under the reactivation conditions, this seems exceedingly unlikely given the vast electronic differences between the two compounds and the differences observed in the rates of inactivation of Abg. A more likely explanation is that the sample of **2.4** is contaminated with a small amount of a highly reactive impurity, such as **2.1**, and that the desired compound **2.4** does not behave as a covalent inactivator of Abg.

#### 2.4.1.3 Testing a sample of **2.4** for the presence of a highly reactive inhibitory impurity

This problem of a reactive contaminant within the inactivator preparation is not unprecedented,<sup>29</sup> and indeed it is probably quite common but undetected. An excellent test for the presence of a low concentration of a reactive impurity involves the reaction of a very high concentration of the enzyme with inactivator. Ideally an enzyme concentration approaching that of the “inactivator” is used. In reality, if the enzyme concentration is greater than the concentration of the reactive contaminant, and under those conditions complete

inactivation is still observed, then this shows that the contaminant cannot be responsible for the inactivation and that the active compound is likely indeed the desired compound. This experiment thus uses the enzyme as a stoichiometric reagent to titrate out the active compound that behaves as the covalent inactivator.

Incubation of **2.4** (21.8 mM) with either a low (6 nM) or a high (6  $\mu$ M) concentration of Abg showed the expected inactivation at the low enzyme concentration (Figure 2.8), but very little inactivation at the higher concentration of Abg. This demonstrates that **2.4** is not acting as the covalent inactivator, but instead a small amount of another contaminating small molecule is acting in that capacity.

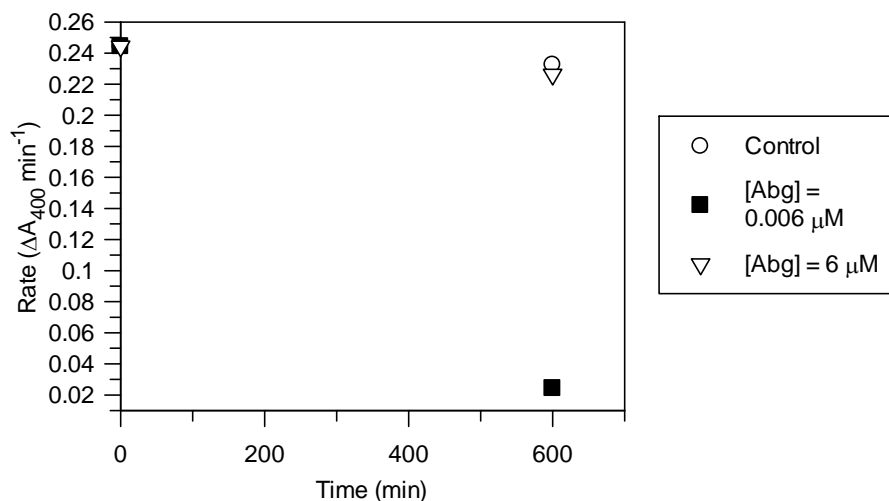
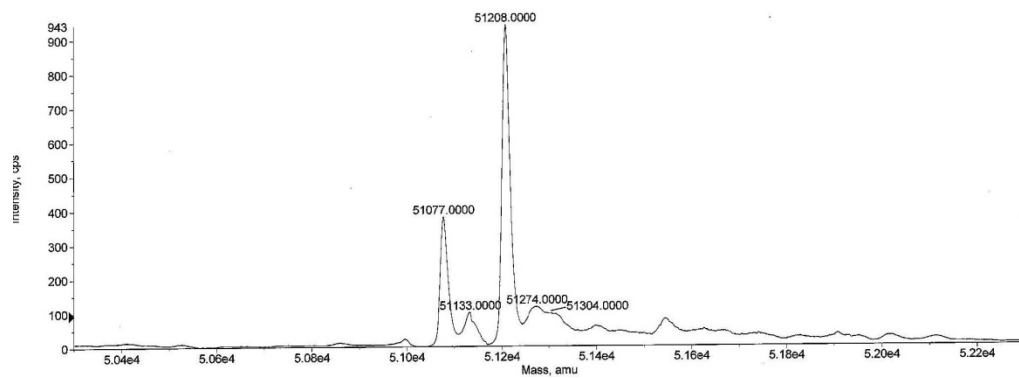


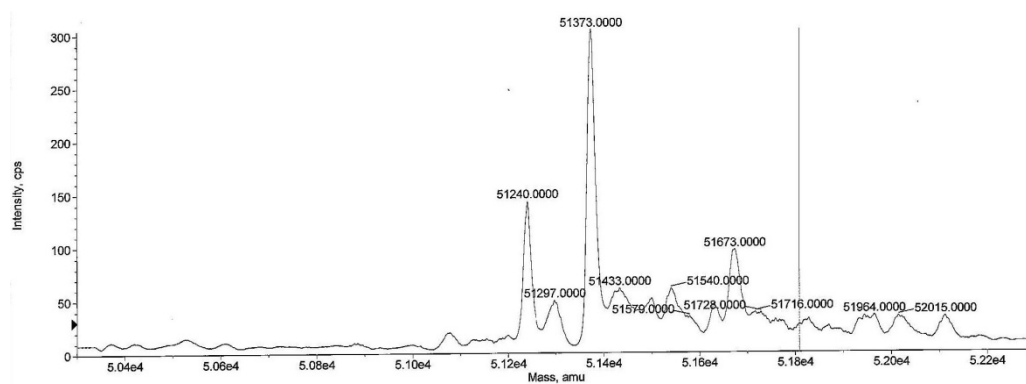
**Figure 2.8.** Test for the presence of a contaminating impurity in the preparation of **2.4** using different concentrations of Abg.

Confirmation that the inactivator was not **2.4** came from mass spectrometric analysis of the inactivated protein (Figure 2.9). Its mass of  $51,372 \pm 5$  is 164 mass units higher than that of unlabelled enzyme ( $51,208 \pm 5$ ) and identical, within error, to that of Abg inactivated with **2.1** ( $51,373 \pm 5$ ). Inactivation with **2.4** would have resulted in an increase in  $m/z$  of 184. This experiment shows that the active contaminant is some sort of activated 2-deoxy-2-fluoro-glycoside, such as **2.1**, consistent with the observed rate of recovery of enzyme activity in the reactivation experiments (Figure 2.7). Given that the per-acetylated precursor to **2.1**, compound **2.13**, is an intermediate in the synthetic scheme leading to **2.4**, it is

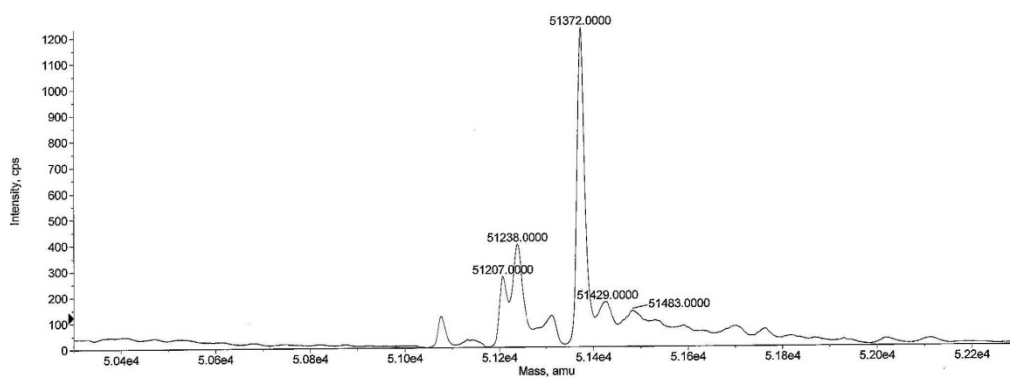
reasonable to assume that the active contaminant is indeed **2.1** that results from unreacted **2.13** inadvertently carried through the later synthetic steps in a very low concentration.



a)



b)



c)

**Figure 2.9.** ESI-MS analysis of a) Abg, b) Abg inactivated with **2.1**, and c) Abg inactivated with **2.4**.

The approximate degree of contamination can be estimated at between 0.03% and 0.0003%, since **2.1** forms a covalent glycosyl-enzyme intermediate with Abg in a one-to-one inactivator-to-enzyme ratio. In the experiment to test for the presence of a contaminant described above, the concentration of Abg ( $\sim 6 \mu\text{M}$ ) therefore represents the maximum concentration of contamination in the solution of **2.4**, which is present at 21.6 mM, since Abg was not fully inactivated at this concentration. However, a lower limit for the degree of contamination is  $\sim 60 \text{ nM}$ , since at this concentration of enzyme Abg was fully inactivated. Thus, in a solution of **2.4** = 21.6 mM, the contaminant is present at a concentration between  $<6 \mu\text{M}$  and  $>60 \text{ nM}$ , or between 0.03 % and 0.0003 % of the total material. This degree of contamination is far beyond the detection ability of the commonly used analytical techniques used to assess purity such as high-field NMR or TLC analysis.

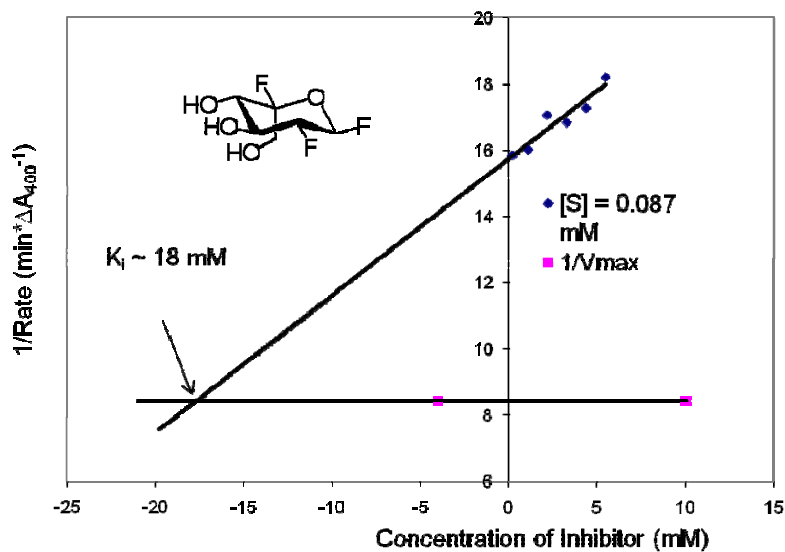
#### 2.4.1.4. 2-Deoxy-1,2-difluoro-D-glucopyranosyl fluoride (**2.6**), 1,5-difluoro-D-glucopyranosyl fluoride (**2.7**) and 1,5-difluoro-L-idopyranosyl fluoride (**2.8**)

2-Deoxy-1,2-difluoro-D-glucopyranosyl fluoride (**2.6**), 1,5-Difluoro-D-glucopyranosyl fluoride (**2.7**) and 1,5-difluoro-L-idopyranosyl fluoride (**2.8**) were each individually tested as covalent inactivators of Abg. In each case, the presence of a highly reactive impurity was detected as described for **2.4** above. Thus, none of these three compounds acted as a covalent inactivator of Abg.

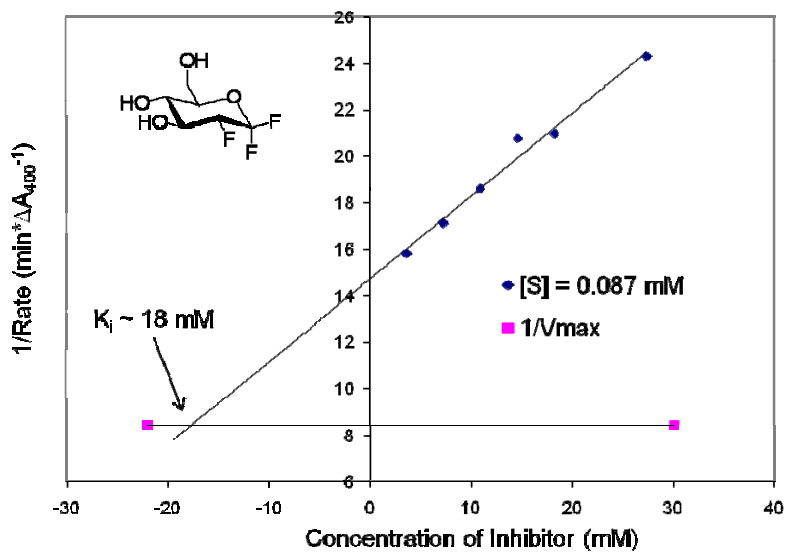
#### 2.4.1.5 Enzymatic evaluation of **2.4**, **2.6**, **2.7** and **2.8** as reversible inhibitors of Abg

Since inactivation by the contaminant was very slow, it proved possible to measure  $K_i$  values for reversible binding of **2.4** and **2.5-2.8** to Ab in the usual manner by avoiding prolonged incubations. A solution of Abg was individually incubated with the substrate pNP- $\beta$ -D-Glc (0.089 mM,  $\sim K_m$ ) and varying amounts of inhibitor, and the rate of enzyme-catalyzed substrate hydrolysis monitored for  $<2$  minutes. It was important to monitor the enzyme activity at short time spans, since at longer incubation times ( $>30$  minutes) the enzyme activity began to decrease in a time dependent manner because of the presence of the highly reactive impurity described in Section 2.4.1.3. The resulting data were plotted as a

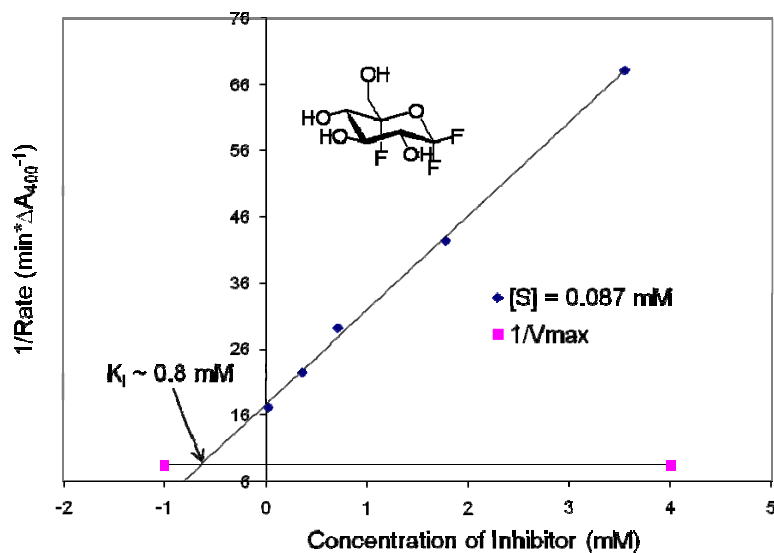
Dixon plot (inverse of rate as a function of inhibitor concentration), and is shown in Figure 2.10. During the course of these and such similar studies, it was assumed that the compounds of interest behaved kinetically as competitive inhibitors.



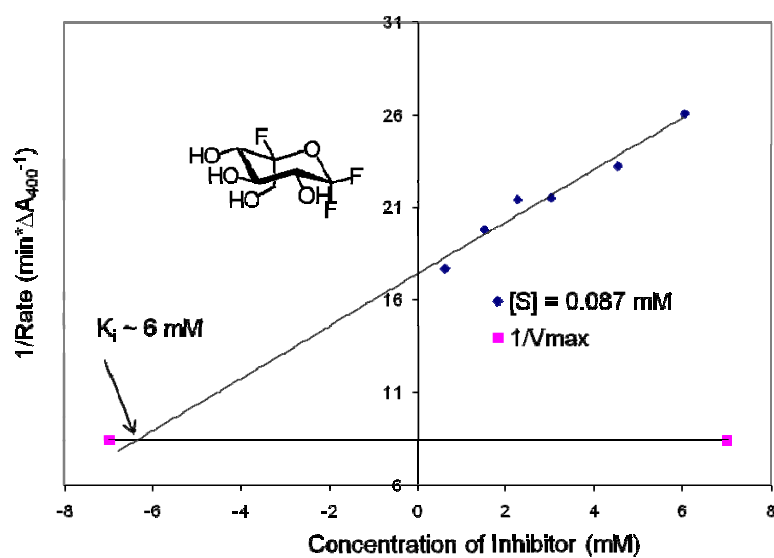
a)



b)



c)



d)

**Figure 2.10.** Dixon plot representation of compounds a) **2.4**, b) **2.6**, c) **2.7** and d) **2.8** tested as reversible inhibitors of Abg.

From the Dixon plot, the intercept between the inverse  $V_{\max}$  and  $[S] = 0.087 \text{ mM}$  gives  $-K_i$ . Solving for the intercept gives  $K_i$  values of  $\sim 18 \text{ mM}$ ,  $18 \text{ mM}$ ,  $0.6 \text{ mM}$  and  $6 \text{ mM}$  for compounds **2.4**, **2.6**, **2.7** and **2.8** respectively. In the analysis of compounds **2.4** and **2.8**, it



was not possible to sample higher inhibitor concentrations approaching or above  $K_i$  owing to the scarcity of material remaining. Clearly, all four compounds bind poorly; presumably the disruption of the hydrogen-bonding interactions at C2 (in the case of **2.4** and **2.6**) and the changes in conformation arising from the *L-ido* configuration (in the case of **2.4** and **2.8**) lower the affinity of these compounds for the enzyme active site, and make them poor inhibitors.

#### 2.4.1.6 1-Fluoro-D-glucopyranosyl fluoride (**2.5**)

Compound **2.5** was also tested as a covalent inactivator of Abg at concentrations ranging from 0.066-6.6 mM. Under the standard conditions used to test for inactivation, no time-dependent inactivation was observed.

In previous studies of this compound as an inhibitor of other retaining  $\beta$ -glycosidases, the rate of turnover of the covalent glycosyl-enzyme intermediate was found to be comparable to the rate of glycosylation.<sup>166-168</sup> This similarity in rates means that **2.5** behaves like a slow substrate, rather than a covalent inactivator. Therefore, **2.5** was tested as a substrate for Abg as follows.

Abg-catalyzed hydrolysis of the chromogenic substrate, *para*-nitrophenyl  $\beta$ -D-glucopyranoside (pNP-Glc,  $K_m = 75 \mu\text{M}$ ) can be monitored by the increase in UV absorbance at 400 nm arising from the increase in the concentration of *para*-nitrophenol.<sup>14</sup> The presence of a competing substrate (**2.5**) in solution that cannot be observed by a change in UV absorbance lowers the effective concentration of enzyme free to hydrolyze pNP-Glc, which is revealed kinetically as competitive inhibition. When **2.5** was tested under steady-state conditions with the concentration of substrate = 0.1 mM, it was found to behave as a competitive inhibitor for Abg with an apparent  $K_i$  value ( $K_i'$ ) of approximately 5 mM (Figure 2.12). This  $K_i'$  value for **2.5** behaving as a competitive inhibitor for Abg is the same as the  $K_m$  value of the compound acting as a substrate for the enzyme, since both processes effectively reduce the concentration of free enzyme in solution.

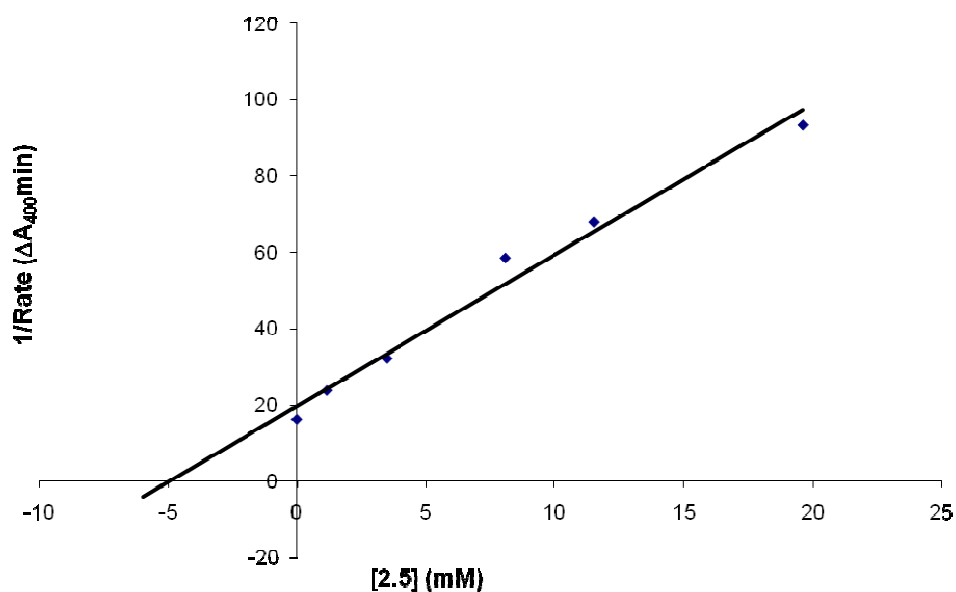


**Figure 2.12.** Dixon plot representation of the testing of **2.5** as a competitive inhibitor of Abg.

Interestingly, while no time-dependent inactivation was observed using the standard assay, inhibition of activity was observed following longer incubation times (>10 mins, Figure 2.13). This likely occurs because the ultimate product of enzyme catalyzed hydrolysis, gluconolactone, is a known<sup>14</sup> inhibitor of Abg ( $K_i = 0.0014$  mM, see Figure 2.14). This is further supported by the observation that the rate of hydrolysis of pNP- $\beta$ -Glc following prolonged incubation in the presence of **2.5** is much lower than in its absence, which is consistent with the time-dependent build-up of a highly potent competitive inhibitor.

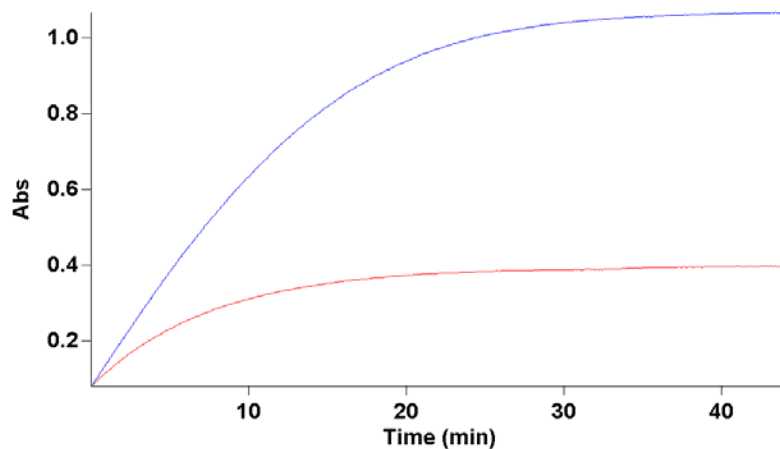


**Figure 2.13.** Observed absorbance vs. time data for the hydrolysis of pNP-β-Glc by Abg in the presence (red) and absence (blue) of **2.5**.

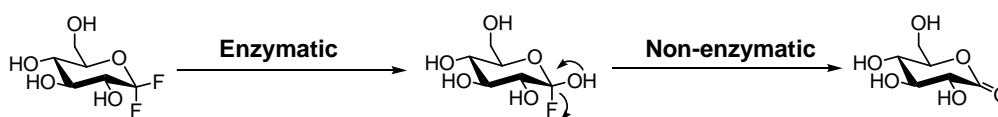


**Figure 2.14.** Mechanism of production of gluconolactone by sequential enzymatic and non-enzymatic reactions.

Although it is possible to measure a  $k_{\text{cat}}$  value for many glycosyl fluorides using a fluoride ion-selective electrode, this was not possible with **2.5** owing to the continuous production of a competitive inhibitor as described above. Since the known  $K_i$  value (0.0014 mM) for the inhibitor, gluconolactone, is below the limit of detection using the fluoride electrode (1 mM), it is not possible to measure the  $k_{\text{cat}}$  value for **2.5** using this method since gluconolactone produced will begin to inhibit the enzyme before the fluoride release can be detected.

#### 2.4.2 Kinetic analysis of the inactivation of Yag by 2.6, 2.7 and 2.8

As described in Section 2.3.1, 2-deoxy-1,2-difluoro-D-glucopyranosyl fluoride (**2.6**), 1,5-difluoro-D-glucopyranosyl fluoride (**2.7**) and 1,5-difluoro-L-idopyranosyl fluoride (**2.8**) are also potential covalent inactivators of retaining  $\alpha$ -glucosidases, owing to the presence of an axial anomeric fluoride. All three compounds were tested against yeast  $\alpha$ -glucosidase (Yag) to see if time-dependent inactivation could be observed. While time-dependent inactivation was observed for compounds **2.7** and **2.8**, in both cases this inactivation activity was determined to arise from the presence of a highly reactive impurity, using a similar method to that described in Section 2.4.1.3. No time-dependent inactivation was observed for **2.6**.

In an attempt to see if it was possible to determine the identity of the impurity, the following experiment was performed. Yag was treated with a large excess of either **2.7** or **2.8** overnight, until  $<5\%$  residual enzyme activity was detected. The enzyme was then separated from the small molecule using a 10 kDa molecular weight cut-off filter, and incubated in buffer at 37 °C. Aliquots were withdrawn from this solution at time intervals and assayed for the recovery of enzyme activity. The reactivation curves for Yag treated with a solution of **2.7** and **2.8** (Figure 2.15) are shown below.

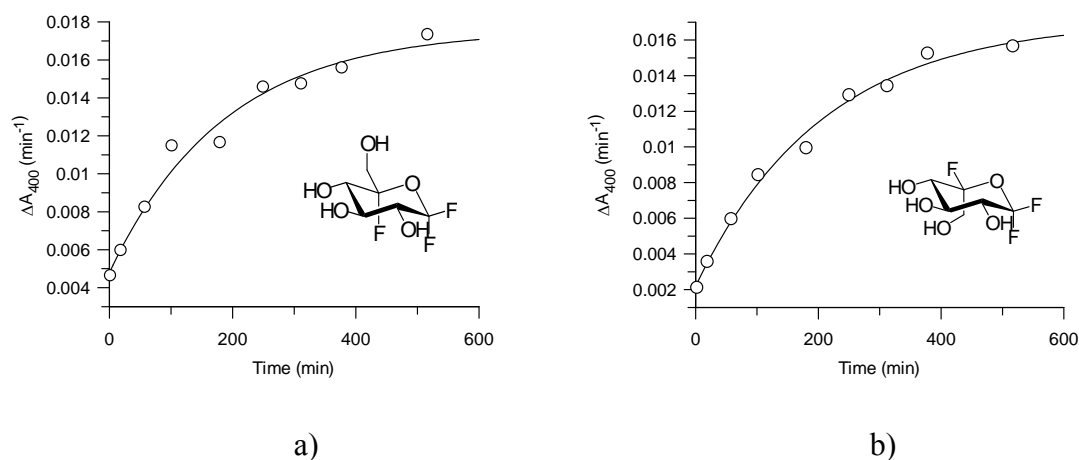


**Figure 2.15.** Recovery of enzyme activity as a function of time for Yag treated with a) **2.7** and b) **2.8**.

The reactivation curves for Yag treated with either **2.7** or **2.8** yield the same values for the rate constant of recovery of enzyme activity ( $k_{\text{obs}} = 0.005 \text{ min}^{-1}$  for enzyme treated with **2.7**, and  $k_{\text{obs}} = 0.005 \text{ min}^{-1}$  for enzyme treated with **2.8**) which suggests that the covalent glycosyl-enzyme intermediate in both cases is the same species. Presumably, this means both compounds are contaminated by the same impurity which is plausible since the synthesis of the two compounds proceeds through common intermediates, so an impurity resulting from an earlier step could be carried forward in the final synthetic steps for both compounds. It is also important to note that the observed rate of reactivation for the covalent glycosyl-enzyme intermediate for Yag treated with either **2.7** or **2.8** ( $k_{\text{obs}} = 0.005 \text{ min}^{-1}$ ) is similar to the previously observed value for the reactivation of the covalent glycosyl-enzyme intermediate of Yag treated with 5-fluoro- $\beta$ -L-idosyl fluoride ( $k_{\text{obs}} = 0.002 \text{ min}^{-1}$ ).<sup>134</sup> This suggests that the contaminating species in the preparation of both **2.7** and **2.8** could be 5-fluoro- $\beta$ -L-idosyl fluoride.

#### 2.4.3 General conclusions for the difluorosugar fluorides

None of the novel compounds described here functioned as time-dependent inactivators against either a retaining  $\beta$ -glucosidase (Abg) or a retaining  $\alpha$ -glucosidase (Yag). In fact, all four novel compounds (**2.4**, **2.7**, **2.8** and **2.6**) tested as potential inactivators of Abg were found to be contaminated with a small amount ( $<0.03\%$ ) of a highly reactive impurity, hypothesized to be the known inactivator 2-deoxy-2-fluoro- $\beta$ -D-glucopyranosyl fluoride (**2.1**). Two of the three potential inactivators of Yag (**2.7** and **2.8**) were also found to be contaminated with a highly reactive impurity ( $<0.03\%$ ), which was proposed to be the known inactivator 5-fluoro- $\beta$ -L-idosyl fluoride. The final potential inactivator of Yag, **2.6**, showed no time-dependent inactivation.

It is important to note that the presence of these impurities is undetectable by analytical techniques employed in standard synthetic characterization, and the compounds would be deemed “pure” using generally accepted criteria in the synthetic organic chemistry community. This demonstrates that caution must be used in assessing molecules possessing biological activity at such potentially low levels (a 1:1 stoichiometry with the enzyme of

interest in this instance), and shows how easy it is for such miniscule concentrations of contaminants to give false-positive results when they contaminate a compound otherwise possessing little or none of the desired activity.<sup>29</sup>

The fact that an impurity present in such incredibly small quantities is more active than the desired compound, present in a vast excess, clearly demonstrates the lack of reactivity of these novel compounds as glycosidase inactivators. All four compounds were shown to bind to the active site of Abg as reversible inhibitors, albeit poorly. Therefore, the most likely explanation for the lack of reactivity of these novel compounds is that the higher degree of fluorination on the sugar ring electronically destabilizes the oxocarbenium ion-like transition state in the enzymatic reaction to a level inaccessible to the enzyme. If this is true, the fluoride leaving group is not a powerful enough leaving group to accommodate glycosylation of the enzyme.

In the compounds described thus far, the only leaving group (aglycone) that has been used is fluoride. As can be seen from the difluorosugar fluorides (**2.4**, **2.6**, **2.7** and **2.8**), fluoride does not appear to be the optimal leaving group. As a consequence of this restriction, it was decided to examine the possibility of other leaving groups for use in the context of a covalent glycosidase inactivator.

## **2.5 Previous studies on the role of aglycones in activated fluorosugars**

### **2.5.1 General aglycone considerations**

When considering different groups as potential aglycones in the design of covalent inactivators of glycosidases, the primary consideration is the reactivity, or the leaving group ability, of the group in question. It is necessary to have a good leaving group to increase the rate of glycosylation, and allow an accumulation of a large population of the covalent glycosyl-enzyme intermediate.<sup>122</sup> As discussed above, this is one possible explanation for why compounds **2.4**, **2.6**, **2.7** and **2.8** were not successful as covalent inactivators of Abg. It is possible that the fluoride group was insufficiently chemically activated to act as a leaving

group for the enzymatic reaction with these compounds since the high degree of fluorination slowed down the glycosylation rate, such that a large steady-state concentration of the covalent glycosyl-enzyme intermediate cannot accumulate. It is also important that an aglycone is not too chemically reactive, or the compound will react spontaneously with the solvent and decompose. It is therefore necessary to strike a balance between having a group that is sufficiently activated that it will accelerate the glycosylation step when reacting with the glycosidase, but not so reactive that it will spontaneously decompose through reaction with solvent under ambient conditions.

One measure of an aglycone's leaving group ability is its  $pK_a$  value. However, while leaving group ability and  $pK_a$  usually show a direct correlation, other factors such as steric hindrance may mean that a compound with a high  $pK_a$  value can still act as a very effective leaving group. Furthermore, specific interactions with an enzymatic active site may turn a poorly activated leaving group into a very effective one.<sup>130</sup> Therefore, while  $pK_a$  values offer a rough guide for leaving group ability, caution must be employed when drawing direct comparisons between  $pK_a$  and leaving group ability.<sup>202</sup>

### **2.5.2 Fluoride aglycones**

One of the most commonly used and successful aglycones for fluorosugar inactivators is fluoride.<sup>12,13</sup> The  $pK_a$  of HF in water is 3.1. The small fluorine atom presumably makes few if any specific interactions with the enzymatic active site, and its activation of a fluorosugar for enzymatic reaction may therefore be presumed to arise almost entirely from the electron withdrawing ability of the fluorine atom.

### **2.5.3 2,4-Dinitrophenol aglycones**

2,4-Dinitrophenyl (DNP) is the other commonly used aglycone for activated fluorosugars as glycosidase inactivators. Unlike fluoride, it has only been reported in the design of covalent inactivators of retaining  $\beta$ -glycosidases using 2-deoxy-2-fluoroglycosides.<sup>13</sup> This narrower application of the DNP aglycone arises because the

photochemistry commonly used to synthesize the 5-fluoro glycosides is not compatible with the DNP ring, and the conditions necessary for the removal of commonly employed protecting groups that are compatible with the DNP group (acidic conditions), are incompatible with the 5-fluoro glycosides, which are very sensitive towards acidic conditions.<sup>129</sup> The  $pK_a$  value for 2,4-dinitrophenol is 4.0, which suggests that the DNP aglycone may be slightly less chemically activated than the fluoride aglycone. However, the aromatic DNP ring has the potential to make interactions with the enzyme active site, which may in certain cases make it a more efficient inactivator relative to the more highly chemically activated fluorine aglycone.<sup>122</sup> Additionally, a dinitrophenyl ring offers the possibility of introducing additional substituents to try to harness specific interactions with the enzyme active site.

#### **2.5.4 2,4,6-Trinitrophenol aglycones**

2,4,6-Trinitrophenyl (TNP) aglycones have not seen wide application as an aglycone for an activated fluorosugar, and have only been used as a leaving group with the 2-deoxy-2,2-difluoro glycosides as inactivators of retaining  $\alpha$ -glycosidases.<sup>12,163-166</sup> This narrow application of the TNP leaving group in the context of activated fluorosugars arises from the fact that TNP-glycosides have only been demonstrated to be stable towards spontaneous solvolysis when used as a leaving group for the 2-deoxy-2,2-difluoro glycosides. Because its  $pK_a$  value is 0.5, TNP-glycosides are much more reactive towards spontaneous decomposition. Additionally, TNP is synthetically much more challenging to incorporate, and trinitrophenyl groups (or picric acid derivatives) are also known to be highly explosive.

#### **2.5.5 Chloride aglycones**

Similar to the TNP aglycones discussed above, glycosyl chlorides have only seen application as a potential glycosidase inactivator in two classes of compounds, the 2-deoxy-2,2-difluoro glycosides and the 2-chloro-2-deoxy-2-fluoro glycosides.<sup>165</sup> For 2-deoxy-2,2-difluoro glycosides, it was previously predicted that fluoride ( $pK_a$  of the conjugate acid = 3.1) was insufficiently chemically activated to act as a good aglycone for displacement



reactions at the anomeric center of 2-deoxy-2,2-difluoro glycosides,<sup>197</sup> therefore, the more chemically activated chloride ( $\text{pK}_a$  of the conjugate acid = -7) was chosen. In that case, while both classes of anomeric chloride could be successfully deprotected and were stable towards spontaneous hydrolysis, only one of the two retaining  $\alpha$ -glycosidases with which these compounds were tested was successfully inactivated.<sup>165</sup>

### 2.5.6 Natural aglycones

There are currently only two examples of a fluorosugar that behaves as an inactivator of a glycosidase where the leaving group is not chemically activated. In the first example, the enzyme myrosinase was inactivated by treatment with 2-deoxy-2-fluoro-glucosyl tropaeolin (Figure 2.16, a)), which is an analogue of the natural substrate for the enzyme, glucotropaeolin.<sup>203</sup> In the second example, 2'-deoxy-2'-fluoro-cellobiose (Figure 2.16, b)) was prepared and shown to be a covalent inactivator of Abg.<sup>130</sup> The inactivator was proposed to harness specific interactions between the aglycone and the enzyme active site so effectively, that no chemical activation of the aglycone is necessary to make the covalent glycosyl-enzyme intermediate kinetically accessible. However, for this general class of fluorosugars with chemically unactivated aglycones to function as covalent inactivators, it was shown that the second (deglycosylation) step must be the rate-determining step in the enzyme-catalyzed reaction of the natural substrate.<sup>130</sup>

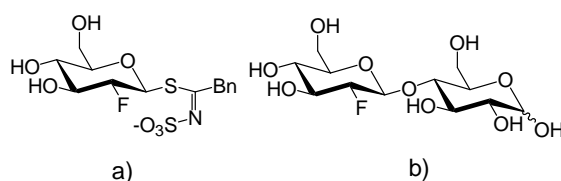


**Figure 2.16.** Structures of the fluorosugar inactivators incorporating natural aglycones. a) 2-deoxy-2-fluoro-glucosyl tropaeolin and b) 2'-deoxy-2'-fluoro-cellobiose.

## 2.6: Chemical synthesis of activated fluorosugars bearing novel aglycones

### 2.6.1 Target compounds

One goal of this project was to find new aglycones that would act as good leaving groups for activated fluorosugars used as covalent glycosidase inactivators. Although it is not always true that the  $pK_a$  value of the corresponding free acid of the aglycone will correlate directly with the leaving group ability of that group in a glycosidase active site, aglycone  $pK_a$  values do offer some ability to predict relative leaving group ability. Therefore, the  $pK_a$  value of the aglycone was used as a predictive guide in selecting aglycones chosen as synthetic targets.

The structures of the first two target compounds are shown in Figure 2.17: 2-deoxy-2-fluoro- $\beta$ -D-glucopyranosyl chloride (**2.32**) and 2-deoxy-2,5-difluoro- $\alpha$ -L-idopyranosyl chloride (**2.33**). Both of these compounds were selected so as to test whether a fluorosugar bearing an equatorial chlorine at the anomeric center would survive deprotection and be stable in aqueous buffer, and if it would act as a sufficiently good leaving group to create a successful covalent inactivator. While a chlorine atom has been installed and tested as an axial substituent,<sup>165</sup> there has been no report of a glycoside bearing an equatorial chlorine atom being successfully deprotected and tested as a covalent glycosidase inactivator to date.

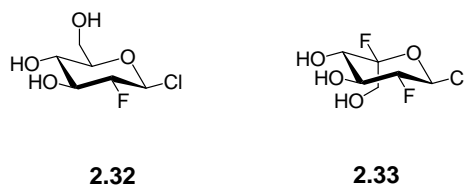


**Figure 2.17.** Structures of the target compounds bearing an equatorial anomeric chloride as the aglycone.

The structures of the next six target compounds are shown in Figure 2.18. These are: methyl-(2-deoxy-2-fluoro- $\beta$ -D-glucopyranosyl)-sulfonate (**2.34**), *para*-toluene-(2-deoxy-2-fluoro- $\beta$ -D-glucopyranosyl)-sulfonate (**2.35**), *para*-toluene-(2-deoxy-2-fluoro- $\beta$ -D-glucopyranosyl)-sulfinate (**2.36**), dimethyl (2-deoxy-2-fluoro- $\beta$ -D-glucopyranosyl) phosphate

(**2.37**), methyl methyl-(2-deoxy-2-fluoro- $\beta$ -D-glucopyranosyl) phosphonate (**2.38**), and dimethyl-(2-deoxy-2-fluoro- $\beta$ -D-glucopyranosyl) phosphinate (**2.39**).

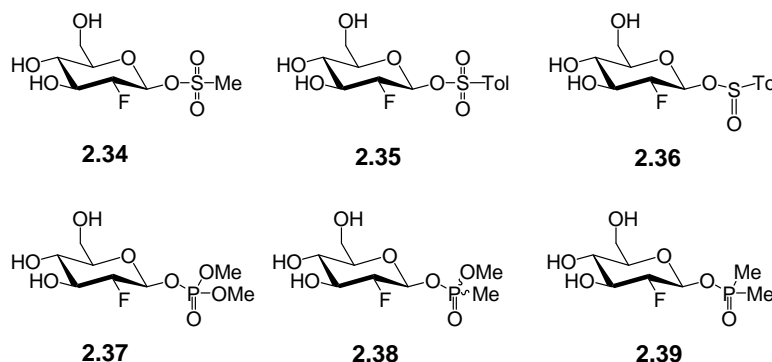


**Figure 2.18.** Structures of the target aglycone variants incorporating sulfur- and phosphorus-based aglycones.

The two sulfonate compounds (**2.34** and **2.35**) were selected to see if a sulfonate leaving group would satisfy the chosen criteria. However, given that the  $pK_a$  values for the corresponding sulfonic acids are considerably lower than the  $pK_a$  values for the known aglycones ( $pK_a$  HF = 3.1,  $pK_a$  HODNP = 4.0 vs.  $pK_a$  MsOH = -2.0,  $pK_a$  TsOH = -6.5), it is also entirely possible that these groups will be too electron withdrawing, and the resulting target compounds too unstable towards spontaneous decomposition. To help address this question, a sulfinic acid derivative (**2.36**) was also considered as the  $pK_a$  value for the free sulfinic acid is 2.0. In all three cases, the selection of the R group attached to the sulfur atom of the aglycone was made based on the synthetic route chosen (see below) and the availability of the precursor free acids or sulfonyl chlorides.

The three phosphorus-based compounds were chosen on the basis of the ability to modulate the  $pK_a$  values based on the number of oxygen atoms directly bonded to the phosphorus atom. The target compound **2.38** also introduces a new stereocenter at the phosphorus atom. It was decided that no effort to control the stereochemistry at this center would initially be made, since that would greatly increase the complexity of the synthetic route required.

## 2.6.2 Synthesis

### 2.6.2.1 Attempted synthesis of 2-deoxy-2-fluoro- $\beta$ -D-glucopyranosyl chloride (**2.32**) and 2-deoxy-2,5-difluoro- $\alpha$ -L-idopyranosyl chloride (**2.33**)

The protected versions of both compounds (**2.27** and **2.30**) were already available as intermediates from the synthesis of **2.6** (Section 2.3.2.5). In both cases, attempts to deprotect both **2.27** and **2.30** using ammonia in methanol were unsuccessful, leading only to the product of methanolysis at the anomeric center in the case of **2.27**, or decomposition in the case of **2.30** (Figure 2.19)

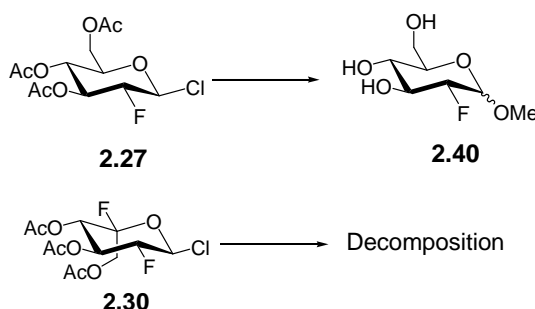
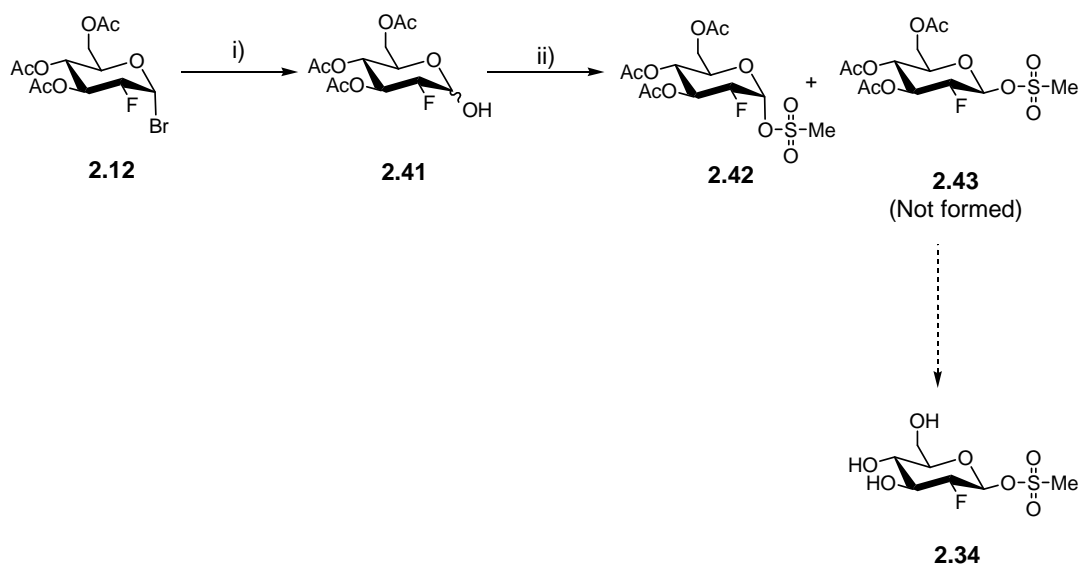


**Figure 2.19.** Decomposition of both **2.27** and **2.30** when treated with  $\text{NH}_3$  in MeOH.

This indicates that chloride is too good a leaving group. Despite the increased reactivity of L-idosides compared to D-glucosides, the presence of the additional fluorine at C5 in **2.30** would be expected to make displacement reactions at the anomeric center much more difficult owing to the destabilization of a positively charged transition state. This is indeed observed in the behaviour of **2.4** towards enzymatic attack at the anomeric center (see Sections 2.4.1.2 and 2.4.1.3). The present results suggests that despite this increased stabilization towards displacement, the chloride leaving group is still too labile to be useful in the context of fluorosugar inactivators other than 2-deoxy-2,2-dihalo glycosides.

2.6.2.2 Attempted synthesis of methyl-(2-deoxy-2-fluoro- $\beta$ -D-glucopyranosyl)-sulfonate (**2.34**), para-toluene-(2-deoxy-2-fluoro- $\beta$ -D-glucopyranosyl)-sulfonate (**2.35**), para-toluene-(2-deoxy-2-fluoro- $\beta$ -D-glucopyranosyl)-sulfinatate (**2.36**)

The synthetic route used to try and prepare methyl-(2-deoxy-2-fluoro- $\beta$ -D-glucopyranosyl)-sulfonate (**2.34**) is shown in Scheme 2.7.

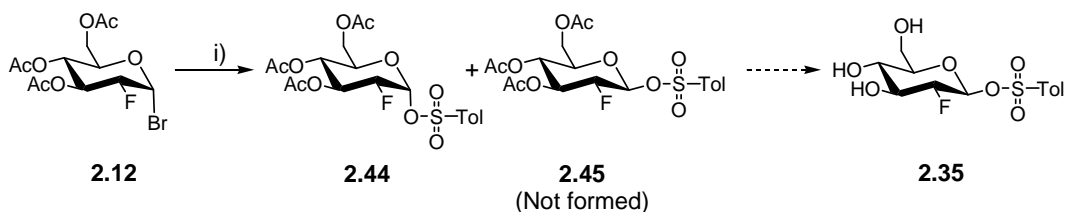


**Scheme 2.7.** Attempted synthesis of methyl-(2-deoxy-2-fluoro- $\beta$ -D-glucopyranosyl)-sulfonate (**2.34**).

i)  $\text{Ag}_2\text{CO}_3$ ,  $\text{H}_2\text{O}$ , Acetone, 67%; ii) Mesyl chloride, pyridine,  $\text{CH}_2\text{Cl}_2$ .

The known<sup>204</sup> compound **2.41** was prepared by the hydrolysis of bromide **2.12**. Treatment of **2.41** with mesyl chloride and pyridine under a variety of reaction conditions yielded only the  $\alpha$ -linked sulfonyl compound **2.42**, with no trace of the  $\beta$ -linked compound **2.43** detected by  $^1\text{H}$ -NMR spectroscopy. This suggests one of two possibilities: 1) that the presumably less reactive but more thermodynamically stable alpha anomer of the free hemiacetal is the one that is reacting with the mesyl chloride under these conditions, or 2) that the kinetically favoured  $\beta$ -linkage is isomerized to the thermodynamically more stable  $\alpha$ -linkage under the reaction conditions.

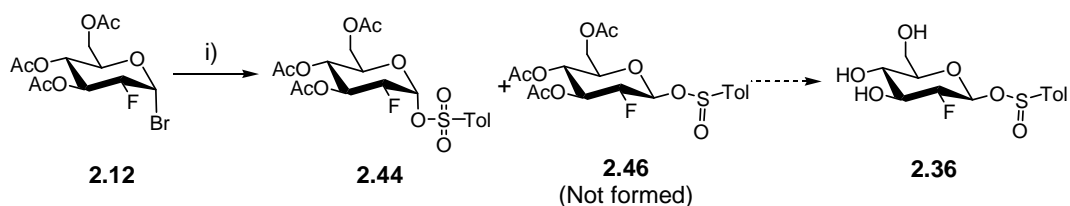
To test these two possibilities, the synthesis of para-toluene-(2-deoxy-2-fluoro- $\beta$ -D-glucopyranosyl)-sulfonate (**2.35**) was attempted as shown in Scheme 2.8.



**Scheme 2.8.** Attempted synthesis of *para*-toluene-(2-deoxy-2-fluoro- $\beta$ -D-glucopyranosyl)-sulfonate (**2.35**). i) AgOTs, MeCN.

Using a nucleophilic displacement of the  $\alpha$ -bromide ensures that the kinetic product initially formed is the desired  $\beta$ -linked **2.45**. However, under the conditions employed, only the  $\alpha$ -linked **2.44** was observed following purification, which suggests that the initially formed  $\beta$ -tosylate is readily isomerized to the thermodynamically more stable  $\alpha$ -tosylate. Given the lack of success experienced in deprotecting the other series of fluorosugars bearing highly electronegative aglycones, the  $\beta$ -chlorides described above, it was decided to abandon these targets.

An attempted synthesis of *para*-toluene-(2-deoxy-2-fluoro- $\beta$ -D-glucopyranosyl)-sulfinate (**2.36**) is shown in Scheme 2.9.



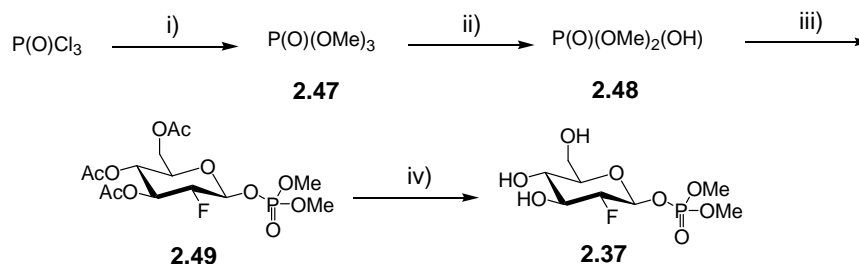
**Scheme 2.9.** Attempted synthesis of *para*-toluene-(2-deoxy-2-fluoro- $\beta$ -D-glucopyranosyl)-sulfinate (**2.36**). i) *para*-Toluene sulfinic acid, Ag<sub>2</sub>CO<sub>3</sub>, MeCN.

Displacement of the  $\alpha$ -bromide **2.12** using *para*-toluene sulfinic acid did not lead to the desired compound **2.46**, instead, only **2.44** was observed. This suggests that any **2.46** that had been formed was oxidized to the  $\beta$ -linked sulfonate, which has already been shown to be kinetically unstable relative to the  $\alpha$ -linked **2.44**, during the work-up and purification steps. This facile oxidation suggested that should **2.36** be successfully prepared, it could only be

handled in an anaerobic environment, thereby severely limiting its usefulness. Thus, the synthesis of **2.36** was abandoned.

### 2.6.2.3 Synthesis of dimethyl (2-deoxy-2-fluoro- $\beta$ -D-glucopyranosyl) phosphate (**2.37**), and attempted syntheses of methyl methyl-(2-deoxy-2-fluoro- $\beta$ -D-glucopyranosyl) phosphonate (**2.38**), and dimethyl (2-deoxy-2-fluoro- $\beta$ -D-glucopyranosyl) phosphinate (**2.39**)

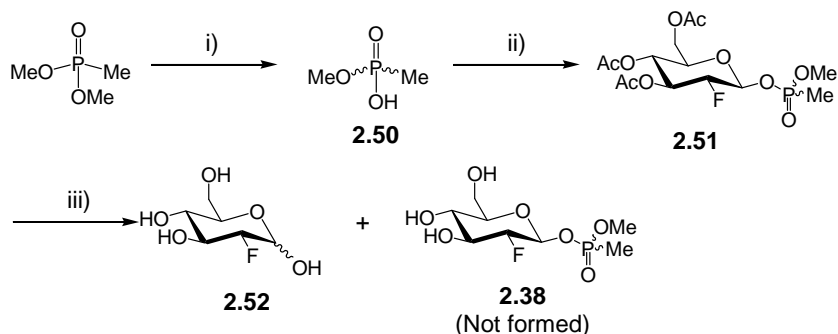
The synthesis of dimethyl (2-deoxy-2-fluoro- $\beta$ -D-glucopyranosyl) phosphate (**2.37**) is shown in Scheme 2.10.



**Scheme 2.10.** Synthesis of dimethyl (2-deoxy-2-fluoro- $\beta$ -D-glucopyranosyl) phosphate (**2.37**). i) MeOH,  $\text{NEt}_3$ ,  $\text{CH}_2\text{Cl}_2$ ; ii) LiBr, MeCN, then Amberlite IR-120 ( $\text{H}^+$ ), 77%; iii) **2.12**,  $\text{Ag}_2\text{CO}_3$ , MeCN, 87%; iv) NaOMe, MeOH, 71%.

Dimethyl phosphoric acid was prepared by reaction of phosphorus oxychloride with methanol, followed by removal of one methyl group using lithium bromide in acetonitrile. The reaction of dimethyl phosphoric acid with bromide **2.12** gave **2.49** in good yield (87%), as only the  $\beta$ -anomer. Basic deprotection gave **2.37** (71%), although this compound was found to be moderately unstable to spontaneous solvolysis in polar protic solvents such as methanol or water. The relative stabilities of these compounds are discussed in Section 2.7.3.

The attempted synthesis of methyl methyl-(2-deoxy-2-fluoro- $\beta$ -D-glucopyranosyl) phosphonate (**2.38**) is shown in Scheme 2.11.



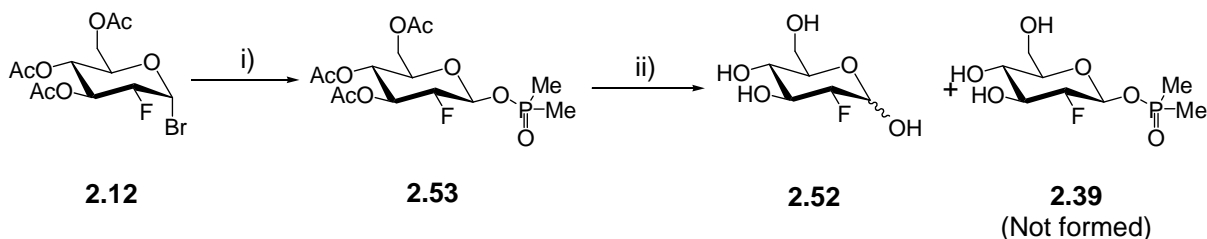
**Scheme 2.11.** Attempted synthesis of methyl methyl-(2-deoxy-2-fluoro-β-D-glucopyranosyl) phosphonate (**2.38**). i) LiBr, MeCN, then Amberlite IR-120 ( $\text{H}^+$ ), 74%; ii) **2.12**,  $\text{Ag}_2\text{CO}_3$ , MeCN, 82%; iii) NaOMe, MeOH or AcCl, MeOH.

Racemic **2.50** was prepared from the commercially available dimethyl methylphosphonate in a reasonable yield (74%).<sup>205</sup> Displacement of bromide from **2.12** proceeded smoothly, giving **2.51** in 82% yield as an equimolar mixture of diastereomers at the phosphorus center. The  $^{13}\text{C}$  NMR spectrum was extremely complex owing to two sets of extremely similar signals from the two diastereomers that are further complicated by the couplings to  $^{19}\text{F}$ - and  $^{31}\text{P}$ -nuclei. However, the high resolution mass spectrum, and the pattern of chemical shifts observed in the  $^1\text{H}$ - and  $^{19}\text{F}$ -NMR spectra, are consistent with structure **2.51**.

All attempts to remove the acetate protecting groups under basic (NaOMe/MeOH or  $\text{NH}_3/\text{MeOH}$ ) and acidic (HCl/MeOH) conditions failed. The only product observed, **2.52**, arose from cleavage of the phosphonate aglycone. The mechanism for this decomposition is discussed in Section 2.6.2.4.

The attempted synthesis of dimethyl (2-deoxy-2-fluoro-β-D-glucopyranosyl) phosphinate (**2.39**) is shown in Scheme 2.12.





**Scheme 2.12.** Attempted synthesis of dimethyl (2-deoxy-2-fluoro-β-D-glucopyranosyl) phosphinate (**2.39**). i) Dimethylphosphinic acid,  $\text{Ag}_2\text{CO}_3$ , MeCN, 83%; ii) NaOMe, MeOH or AcCl, MeOH.

The commercially available dimethylphosphinic acid was reacted with bromide **2.12** to give **2.53** in a good yield (83%). Unlike compound **2.51**, the NMR spectra for **2.53** were easier to interpret since the phosphorus atom is not stereogenic, as in **2.51**. However, as with **2.51**, attempted removal of the acetate groups led only to the formation of the free hemiacetal **2.52**, with no trace of the desired compound **2.39**.

#### 2.6.2.4 Proposed mechanism for decomposition of methyl methyl-(3,4,6-tri-O-acetyl-2-deoxy-2-fluoro-β-D-glucopyranosyl) phosphonate (**2.51**), and dimethyl (3,4,6-tri-O-acetyl-2-deoxy-2-fluoro-β-D-glucopyranosyl) phosphinate (**2.53**) under acidic or basic conditions

During the design of these phosphorus-based compounds, it was predicted that the stability of the target glycoside would correlate inversely with the number of oxygen atoms bonded directly to the phosphorus. This was based on the assumption that these compounds decompose in an  $\text{S}_{\text{N}}1$ -like process, where leaving group departure is the rate-limiting step and the compound with the best leaving group would be the most reactive and therefore least stable. Based on this reasoning, it was predicted that the target phosphate **2.37** would be the least stable compound, and that the target compound **2.39** would be the most stable. Instead, the opposite trend during the deprotection of the acetate protecting groups was actually observed.

One noteworthy feature of the failed deprotections is that the free hemiacetal product was the only product observed, rather than the expected methyl glycoside. If the loss of the phosphorus-based aglycone was occurring through displacement of this group by solvent at

the anomeric center, significant amounts of the methyl glycoside would have been expected. This potential mechanism has been labelled as mechanism of decomposition 1 in Figure 2.20. Such a mechanism was observed in the case of the decomposition of the anomeric chlorides **2.27** and **2.30** (Section 2.6.2.1). While it is possible to explain the presence of some of the free hemiacetal as arising from the attack of a small amount of water present in the methanol solution, it seems exceedingly unlikely that water acts as the nucleophile in the presence of a vast excess of methanol.

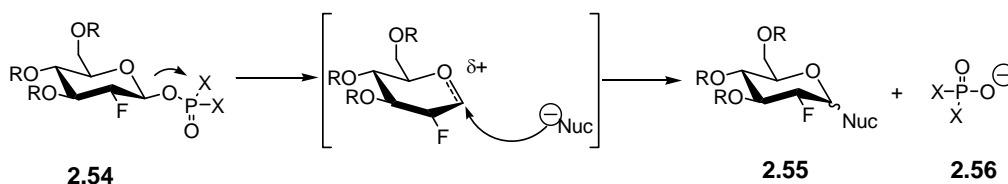


**Figure 2.20.** Schematic depiction of the mechanism of decomposition 1 for **2.51** and **2.53**.

An alternative mechanism for decomposition that could explain the observed product has been labelled mechanism of decomposition 2, and is depicted schematically in Figure 2.21. The observed product may arise from direct attack of solvent at the phosphorus center, and the anomeric oxygen atom act as a leaving group.

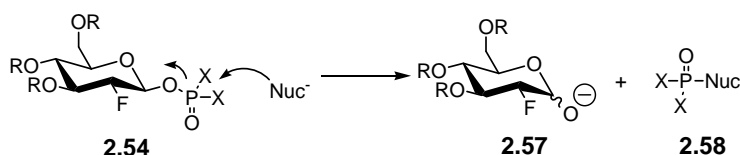


**Figure 2.21.** Schematic depiction of the mechanism of decomposition 2 for **2.51** and **2.53**.

This mechanism would account for the presence of a free hemiacetal on the observed product and the lack of the methyl glycoside. Additionally, this mechanism gives rise to a phosphoester resulting from the attack of solvent at the phosphorus center, leading to either a phosphodiester or phosphomonoester depending on the starting aglycone. Most importantly, if **2.51** and **2.53** were decomposing by this mechanism under the deprotection conditions, it would readily explain why the predicted increase in stability towards spontaneous solvolysis

with decreasing oxidation state was not being observed. The original hypothesis had been that decreasing the oxidation state of the phosphorus would increase the stability of the resulting glycosides towards spontaneous hydrolysis in aqueous solution, which should occur by mechanism 1. However, if the decomposition during deprotection instead proceeds via mechanism 2, then this does not disprove the original hypothesis regarding stability towards spontaneous hydrolysis. By analogy, this proposed mechanism resembles the known mechanism for decomposition observed for 2,4-dinitrophenyl glycosides such as 2,4-dinitrophenyl-(3,4,6-tri-O-acetyl- $\beta$ -D-glucopyranoside), which have been shown to break down by a nucleophilic aromatic substitution reaction on the dinitrophenyl ring under basic conditions, as shown in Figure 2.22.<sup>206</sup>

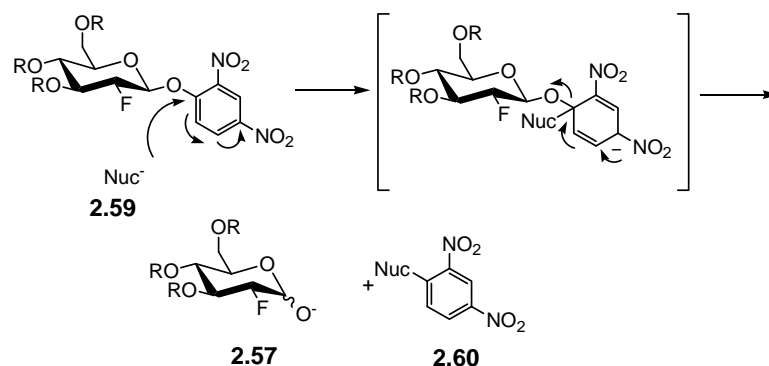


**Figure 2.22.** Mechanism of decomposition for DNP-glycosides under basic conditions.

To test which mechanism of decomposition was occurring, the crude reaction mixture for the reaction of **2.53** with sodium methoxide/methanol was examined by ESI-MS and NMR spectroscopy. In the negative ion ESI-MS, a peak was observed at  $m/z = 107.9$ , which is consistent with the  $[\text{M-H}]^-$  ion of the proposed phosphinate ester product. Significantly, no peak was observed at  $m/z = 97$ , which would be the expected peak if **2.53** was decomposing according to mechanism 1.

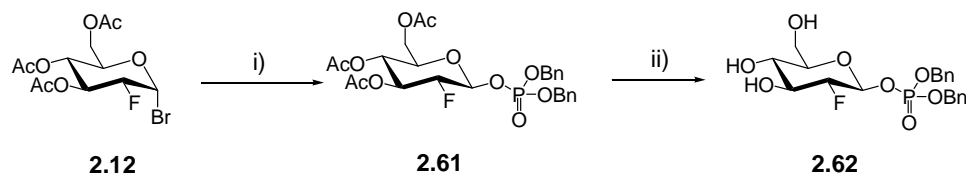
Examination of the crude  $^1\text{H}$ -NMR spectrum of the crude reaction mixture from methoxide-treated **2.53** reveals a large doublet at 3.73 ppm ( $J = 13.1$  Hz), which collapses to a singlet when the  $^{31}\text{P}$  nucleus is decoupled. This chemical shift is typical of an alkyl group directly bonded to oxygen, and the coupling constant is consistent with a three-bond coupling

to phosphorus. Furthermore, if the reaction is carried out in deuterated methanol ( $\text{CD}_3\text{OD}$ ), then this signal is absent entirely since no protons are present. Finally, a  $^{31}\text{P}$ -NMR spectrum of this mixture shows the same peak as an authentic sample of dimethyl-methylphosphonate. On the basis of these experimental results, it was concluded that both phosphonate **2.51** and phosphinate **2.53** decomposed according to mechanism of decomposition 2 under basic conditions. While the deprotection reaction was not studied under acidic conditions, a very similar mechanism of decomposition at the phosphorus atom could be proposed to account for the inability to deprotect these compounds under acidic conditions. The reasons for this increased susceptibility towards nucleophilic attack for both **2.51** and **2.53** compared to **2.39** are not clear, although it may be related to greater electron-electron repulsion between the incoming nucleophile and the lone pairs on the phosphate oxygen atoms.

2.6.2.5 Synthesis of dibenzyl (2-deoxy-2-fluoro- $\beta$ -D-glucopyranosyl) phosphate (**2.62**), benzyl benzyl-(2-deoxy-2-fluoro- $\beta$ -D-glucopyranosyl) phosphonate (**2.67**), and dibenzyl (2-deoxy-2-fluoro- $\beta$ -D-glucopyranosyl) phosphinate (**2.70**)

The instability of phosphonate **2.51** and phosphinate **2.53** to deprotection under acidic or basic conditions meant the problem of the instability of dimethyl phosphate derivative **2.37** towards spontaneous hydrolysis in methanol and water remained. Since the inability to deprotect either **2.51** or **2.53** was hypothesized to arise from nucleophilic attack at the phosphorus center, it was decided to try to increase the stability of the phosphonate and phosphinate derivatives towards nucleophilic attack by increasing the steric bulk around the phosphorus atom. Benzyl groups were therefore chosen, since the desired aglycone precursors were synthetically accessible.<sup>207,208</sup> In addition, there was the potential that a benzyl group in the aglycone may interact with aromatic residues in the enzyme active site.

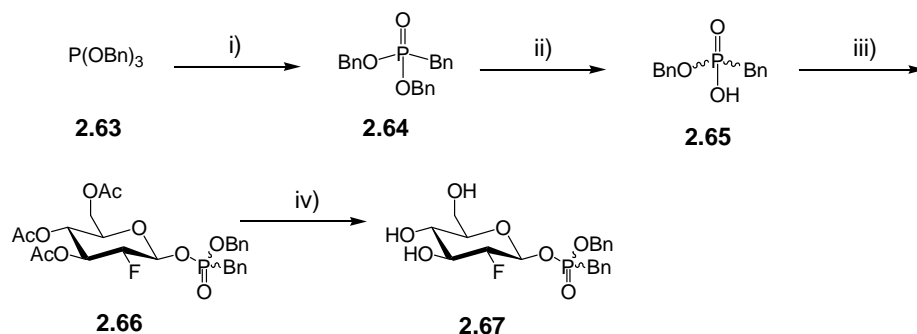
The synthesis of dibenzyl (2-deoxy-2-fluoro- $\beta$ -D-glucopyranosyl) phosphate (**2.62**) is shown in Scheme 2.13.



**Scheme 2.13.** Synthesis of dibenzyl (2-deoxy-2-fluoro-β-D-glucopyranosyl) phosphate (**2.62**). i) Dibenzyl phosphoric acid, Ag<sub>2</sub>CO<sub>3</sub>, MeCN, 53%; ii) NaOMe, MeOH, 65%.

Commercially available dibenzyl phosphoric acid was coupled to bromide **2.12**, to yield **2.61** in an acceptable 53% yield. It was found that the proton adduct of the phosphoric acid was required as the lithium salt was completely unreactive under otherwise identical conditions. One possible explanation for this difference in reactivity may be that the free acid readily reacts with silver carbonate to create the silver salt *in situ*. Indeed, when the silver salt of dibenzyl phosphate was separately prepared and treated with **2.12** in acetonitrile, the same product **2.61** was observed. Deprotection under basic conditions gave **2.62** (65%).

The synthesis of benzyl benzyl-(2-deoxy-2-fluoro-β-D-glucopyranosyl) phosphonate (**2.67**) is shown in Scheme 2.14.



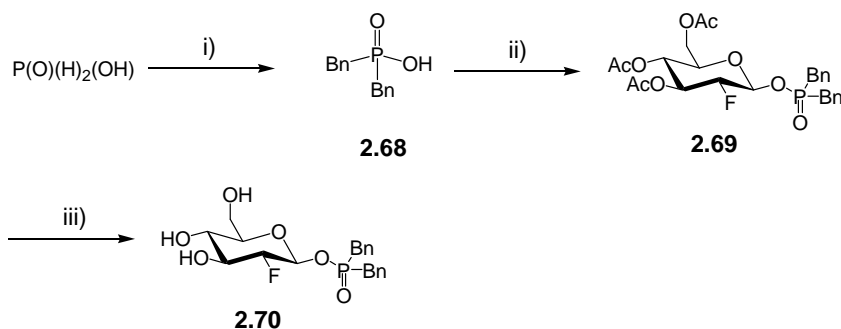
**Scheme 2.14.** Synthesis of benzyl benzyl-(2-deoxy-2-fluoro-β-D-glucopyranosyl) phosphonate (**2.67**). i) BnCl, 73%; ii) LiBr, MeCN, then Amberlite IR-120 (H<sup>+</sup>), 95%; iii) **2.12**, Ag<sub>2</sub>CO<sub>3</sub>, MeCN, 63%; iv) NaOMe, MeOH, 83%.

Compound **2.63** was prepared as previously described.<sup>208</sup> It was found that strict anaerobic conditions were required during the synthesis of **2.63** to prevent the oxidation of the phosphite to a phosphotriester. Heating neat **2.63** with benzyl chloride led to the

formation of phosphonate **2.64** in 73% yield via a Michaelis-Arbuzov rearrangement.<sup>208,209</sup> Racemic **2.65** was obtained by selective removal of a single benzyl group using lithium bromide in acetonitrile (95%).<sup>205</sup> When treated with bromide **2.12**, **2.66** is formed as a mixture of diastereomers at the phosphorus center in an acceptable yield (63%). As was the case with the methyl methylphosphonate **2.51**, the compound was best characterized by studying the <sup>1</sup>H-, <sup>19</sup>F-, and <sup>31</sup>P-NMR chemical shifts in addition to the mass spectral data, since the signals for individual diastereomers overlapped and could not be completely resolved.

Treatment of **2.66** with sodium methoxide in methanol led to the desired compound **2.67** in very good yield (83%), with no trace of the free hemiacetal by-product. This greater stability of the benzyl benzylphosphonate ester compared to the methyl methylphosphonate ester under basic conditions supports the hypothesis that increased steric bulk at the phosphorus center leads to increased stability towards nucleophilic displacement by solvent.

The synthesis of dibenzyl-(2-deoxy-2-fluoro-β-D-glucopyranosyl) phosphinate (**2.70**) is shown in Scheme 2.15.



**Scheme 2.15.** Synthesis of dibenzyl-(2-deoxy-2-fluoro-β-D-glucopyranosyl) phosphinate (**2.70**). i) TMSCl, diisopropyl ethylamine, CH<sub>2</sub>Cl<sub>2</sub>, then BnBr, 36%; ii) **2.12**, Ag<sub>2</sub>CO<sub>3</sub>, MeCN, 83%; iii) NaOMe, MeOH.

The aglycone **2.68** was readily prepared in excellent yield (84%) according to a literature procedure.<sup>207</sup> Its reaction with bromide **2.12** was slower than was the case with the other benzyl-containing phosphorus derivatives, giving only a 36% yield of product after stirring overnight, along with 49% recovered starting material. The protected phosphinate

**2.69** was subjected to deprotection by sodium methoxide in methanol. The majority of the isolated material was a mixture in which the dibenzyl phosphinate ester had been cleaved and one or more acetate groups remained (determined by ESI-MS and crude NMR spectra). This suggests that the rates of attack of methoxide on the phosphinate ester and that at the acetate carbonyl are very similar. However, some of the desired **2.70** was isolated.

Unfortunately, this material was contaminated with a modest amount (approximately 30% by  $^1\text{H}$ -NMR spectra) of material in which the phosphinate aglycone was cleaved, and two of the three acetates had been removed (Figure 2.23). Its structure was determined on the basis of the  $^{31}\text{P}$ -NMR spectrum (only one  $^{31}\text{P}$ -NMR signal was observed in the mixture of two compounds) and on the basis of the  $m/z$  observed in the ESI-MS. Fortunately, the presence of this impurity was not predicted to interfere with the enzymatic testing of **2.70** as an inactivator, since it lacks an activated aglycone, and is unlikely to bind non-covalently to the enzyme active site owing to the presence of the acetate.

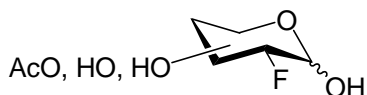


**Figure 2.23.** General structure for the proposed impurity in the preparation of **2.70**.

## 2.7 Enzymatic testing of fluorosugars bearing phosphorus-based aglycones

### 2.7.1 Kinetic analysis of the inactivation of Abg by **2.37**, **2.62**, **2.67** and **2.70**

#### 2.7.1.1 Dimethyl (2-deoxy-2-fluoro- $\beta$ -D-glucopyranosyl) phosphate (**2.37**)

Dimethyl phosphate derivative **2.37** was evaluated as a potential time-dependent covalent inactivator of Abg. A range of concentrations of **2.37** were incubated with Abg, and the reaction mixtures assayed at time intervals for residual enzyme activity. The resulting activity versus time plot for various concentrations of inactivator, and a re-plot of the individual  $k_{\text{obs}}$  values plotted as a function of inhibitor concentration are shown in Figure 2.24.

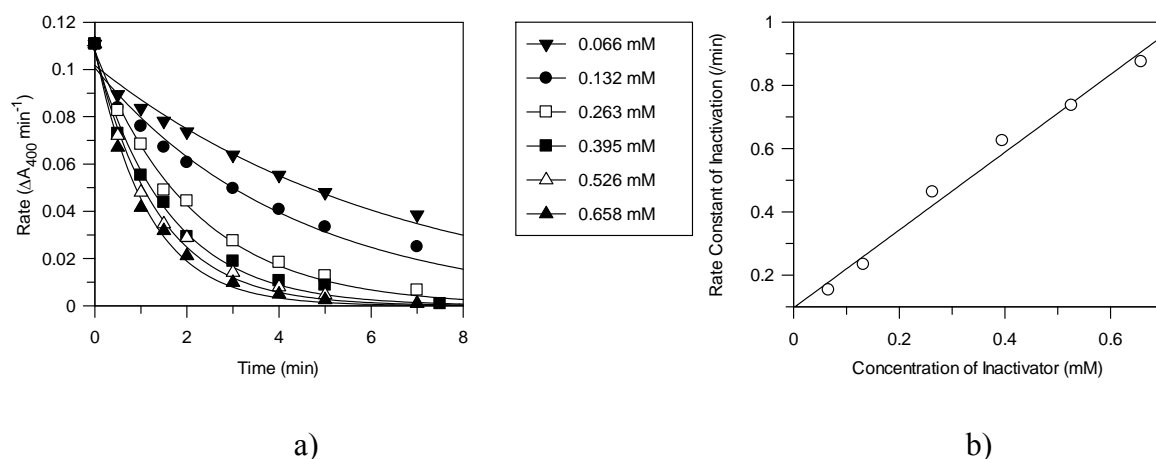


**Figure 2.24.** Inactivation of Abg with **2.37**. a) Non-linear plot of residual enzyme activity versus time at the indicated inactivator concentrations fitted to an exponential decay equation. b) Plot of the observed rate constants ( $k_{\text{obs}}$ ) of inactivation versus concentration of inactivator.

The measurement of inactivation rates at saturating concentrations of inactivator was not possible owing to very rapid inactivation, thus only concentrations up to 0.66 mM could be measured. A second order rate constant of inactivation,  $k_i/K_i$  of  $1.23 \text{ min}^{-1}\text{mM}^{-1}$  was derived from the slope of the linear plot obtained.

Given the difficulties arising from the presence of a highly reactive contaminant previously encountered, the test for such an active impurity was carried out. Unlike the previous studies where inactivation was only observed at very high concentrations and after long incubation times, it was possible to definitively prove that **2.37** was the reactive compound. Abg ( $17 \text{ }\mu\text{M}$ ) was incubated with a 10-fold excess of inhibitor ( $165 \text{ }\mu\text{M}$ ) for 6 min, after which the reaction was halted by dilution and the residual enzyme activity was determined to be 23% of the starting activity. This is essentially identical to the 25% residual enzyme activity observed in control experiments when using a vast excess of inactivator ( $165 \text{ }\mu\text{M}$ ) relative to enzyme ( $0.017 \text{ }\mu\text{M}$ ). The fact that the inhibitor solution is still able to inactivate Abg at these relative concentrations means that a potential highly reactive contaminant, should it be present, would have to constitute at least 10% of the inactivator preparation, an amount that would be readily detected by both TLC and NMR analyses.



To demonstrate that the time-dependent inactivation of Abg by **2.37** was active site-directed, the inactivation process was studied in the presence and absence of a competitive inhibitor, gluconolactone ( $K_i = 1.4 \mu\text{M}$ ,<sup>14</sup> Figure 2.25). The activity versus time plot generated is shown in Figure 2.26 for samples of Abg incubated in the presence and absence of  $2.5 \mu\text{M}$  gluconolactone. The  $k_{\text{obs}}$  for Abg in the presence of  $0.66 \text{ mM}$  **2.37** was  $0.88 \text{ min}^{-1}$ , which was reduced to  $0.48 \text{ min}^{-1}$  in the presence of  $2.5 \mu\text{M}$  gluconolactone.

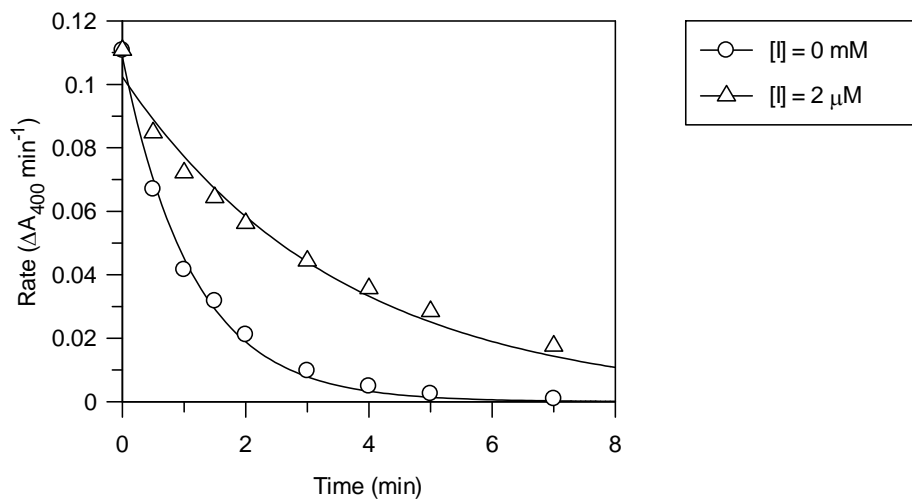


**Figure 2.25.** Inactivation of Abg and **2.37** in the presence (triangles) and absence (circles) of  $2.5 \mu\text{M}$  gluconolactone.

The only structural difference between **2.37** and **2.1** lies in the identity of the aglycone portion of the molecule, dimethyl phosphate versus fluoride. As a result, while the two compounds demonstrate different kinetics of inactivation ( $k_i/K_i = 13.8 \text{ min}^{-1}\text{mM}^{-1}$  for **2.1**,  $k_i/K_i = 1.23 \text{ min}^{-1}\text{mM}^{-1}$  for **2.37**), they should show the same rate of turnover of the covalent glycosyl-enzyme intermediate, since the species formed by both are identical. To test this, a sample of Abg treated with an excess of **2.37** was separated from excess small molecule, and incubated with  $20 \text{ mM}$  thiophenyl  $\beta$ -D-glucopyranoside. The recovery of enzymatic activity was monitored and the resulting activity versus time plot from this experiment is shown in Figure 2.26. The rate of reactivation observed under these conditions,  $k_{\text{obs}} = 0.020 \pm 0.004 \text{ min}^{-1}$ , is the same, within error, to the rate of reactivation observed for the covalent glycosyl-enzyme intermediate generated by treatment of Abg with **2.1** ( $k_{\text{obs}} =$

$0.013 \pm 0.003 \text{ min}^{-1}$ ). This result demonstrates that the same covalent glycosyl-enzyme intermediate is generated by treatment of Abg with either species.

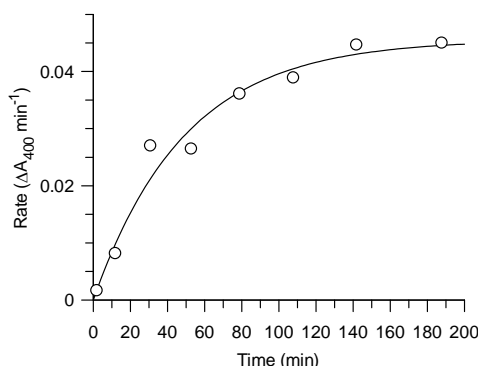


**Figure 2.26.** Residual activity versus time for Abg incubated with 20 mM Glc-SPh, following treatment of Abg with **2.37**.

#### 2.7.1.2 Dibenzyl (2-deoxy-2-fluoro- $\beta$ -D-glucopyranosyl) phosphate (**2.62**)

Compound **2.62** was tested as a covalent inactivator of Abg but was found to be only sparingly soluble in water at millimolar concentrations, thus stock solutions were made in methanol. Fortunately however, while the compound was not soluble enough to make stock solutions, it was sufficiently soluble in water at the concentrations needed for the inactivation assay with Abg. This behaviour was observed for all phosphorus-based aglycone derivatives described with the exception of **2.37**, and all were treated in a similar manner. The resulting activity versus time plot for various concentrations of inactivator, and a second re-plot of the individual  $k_{\text{obs}}$  values plotted as a function of inhibitor concentration are shown in Figure 2.27.

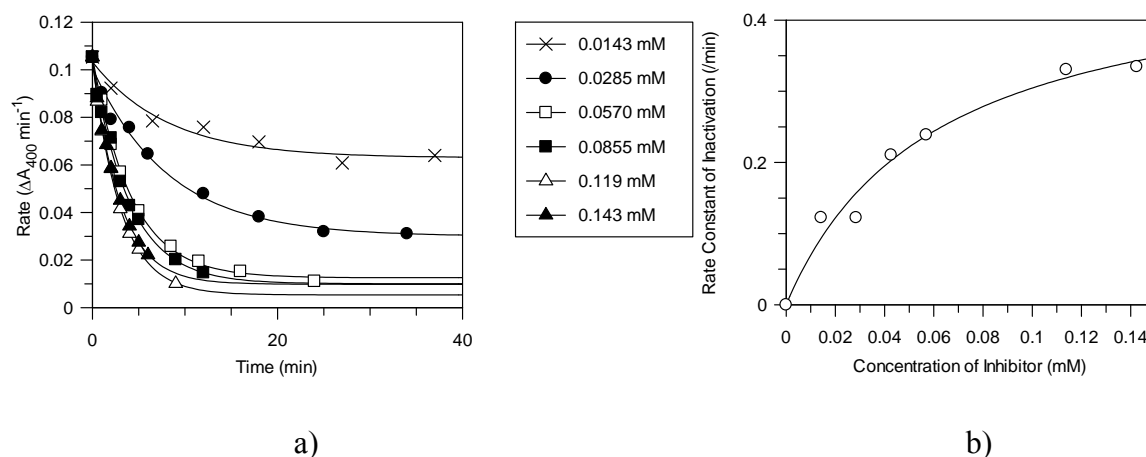


**Figure 2.27.** Inactivation of Abg with **2.62**. a) Non-linear plot of residual enzyme activity versus time at the indicated inactivator concentrations fitted to an exponential decay equation. b) Plot of the observed rate constants of inactivation versus concentration of inactivator.

In this instance, it was possible to calculate the individual  $k_i$  ( $0.47 \text{ min}^{-1}$ ) and  $K_i$  ( $0.059 \text{ mM}$ ) values for **2.62**, in addition to the second order rate constant  $k_i/K_i = 8.0 \text{ min}^{-1} \text{ mM}^{-1}$  since inactivation was slow enough to allow measurements at concentrations approaching saturation. This is unlike the cases of the previously tested **2.1** and **2.37** wherein only the second order rate constants,  $k_i/K_i$ , were obtained.

Compound **2.62** was tested for the presence of a highly active contaminant in a similar manner to that used for **2.37**. Abg ( $17 \text{ } \mu\text{M}$ ) was incubated with an  $\sim 8$ -fold excess of inhibitor ( $142 \text{ } \mu\text{M}$ ) for 20 minutes, after which the reaction was halted by dilution and the residual enzyme activity was determined to be 5% of the starting activity. This is essentially identical to the 9% residual enzyme activity observed in control experiments when using a vast excess of inactivator ( $142 \text{ } \mu\text{M}$ ) relative to enzyme ( $0.017 \text{ } \mu\text{M}$ ). The fact that the inhibitor solution is still able to inactivate Abg at these relative concentrations means that a potential highly reactive contaminant, should it be present, would have to constitute at least 10% of the inactivator preparation, an amount that would be readily detected by both TLC and NMR analyses.

### 2.7.1.3 Benzyl benzyl-(2-deoxy-2-fluoro- $\beta$ -D-glucopyranosyl) phosphonate (**2.67**)

A diastereomeric mixture (at phosphorus) of **2.67** was tested as a covalent inactivator of Abg. The resulting activity versus time plot for various concentrations of inactivator and a re-plot of the individual  $k_{\text{obs}}$  values plotted as a function of inactivator concentration are shown in Figure 2.28.

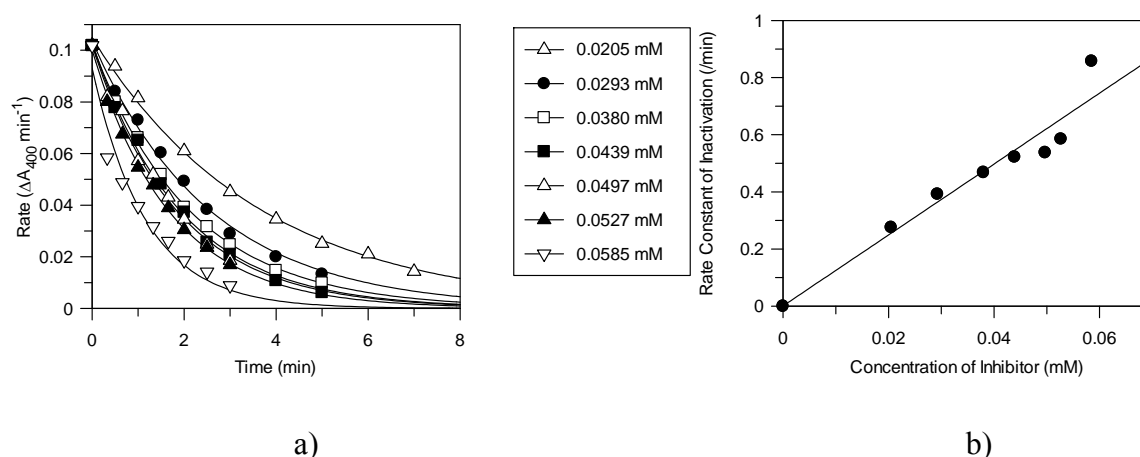


**Figure 2.28.** Inactivation of Abg with **2.67**. a) Non-linear plot of residual enzyme activity versus time at the indicated inactivator concentrations fitted to an exponential decay equation. b) Plot of the observed rate constants of inactivation versus concentration of inactivator.

In this instance, it was not possible to calculate the individual  $k_i$  and  $K_i$  values for **2.67**, as inactivation was too rapid at concentrations approaching saturation. The resulting data points are best fitted using a single exponential decay curve, and not a double exponential. This suggests either that the two diastereomers inactivate the enzyme at identical or near-identical rates, or else that one diastereomer inactivates the enzyme and that the other diastereomer is not accommodated in the enzyme active site. Given that Abg is thought not to have a rigid specificity for the aglycone,<sup>14</sup> it seems unlikely that the enzyme would have an absolute specificity for the two very similar benzyl groups (P-Bn vs. P-OBn). Therefore, these two diastereomers were treated as having similar or identical properties with respect to their interactions with the enzyme active site, and they are therefore treated as a single compound for the duration of this analysis. Therefore, a second order  $k_i/K_i$  value =  $11 \text{ min}^{-1} \text{ mM}^{-1}$  was obtained from linear fitting of a re-plot of the individual rate constants of

inactivation. This was found to be true for the other benzyl benzylphosphonate derivatives described (Section 2.9).

Compound **2.67** was also tested for the presence of a highly active contaminant in a manner similar to that used for **2.37**. Abg (17  $\mu\text{M}$ ) was incubated with an  $\sim 9$ -fold excess of inhibitor (146  $\mu\text{M}$ ) for 5 minutes, after which the reaction was halted by dilution and the residual enzyme activity was determined to be 3% of the starting activity. This is essentially identical to the 1% residual enzyme activity observed in control experiments when using a vast excess of inactivator (146  $\mu\text{M}$ ) relative to enzyme (0.017  $\mu\text{M}$ ). The fact that the inhibitor solution is still able to inactivate Abg at these relative concentrations means that a potential highly reactive contaminant, should it be present, would have to constitute at least 10% of the inactivator preparation, an amount that would be readily detected by both TLC and NMR analyses.

#### 2.7.1.4 Dibenzyl (2-deoxy-2-fluoro- $\beta$ -D-glucopyranosyl) phosphinate (**2.70**)

Compound **2.70** was tested as a mixture, since it was not possible to separate the desired compound from an identifiable impurity as discussed in Section 2.6.2.5. However, this mixture of **2.70** and the undesired by-product was tested for the mixture's ability to inactivate Abg in a time-dependent fashion. As discussed in Section 2.6.2.5, it was predicted that the identified impurity would not interact in any significant manner with the enzyme, and so would not interfere with the analysis of the desired compound **2.70**.

Therefore, the mixture containing **2.70** was tested as a covalent inactivator of Abg. The resulting activity vs. time plot for various concentrations of inactivator and a second plot of the individual  $k_{\text{obs}}$  values plotted as a function of inactivator concentration are shown in Figure 2.29.

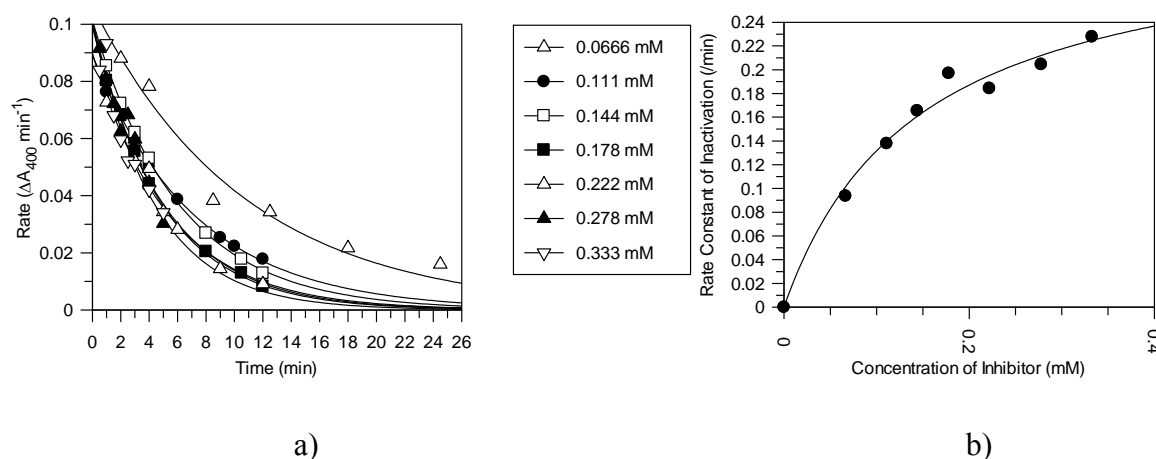


**Figure 2.29.** Inactivation of Abg with the impure solution of **2.70**. a) Non-linear plot of residual enzyme activity versus time at the indicated inactivator concentrations fitted to an exponential decay equation. b) Plot of the observed rate constants of inactivation versus concentration of inactivator.

The resulting data points in Figure 2.29 a) can be best fitted using a single exponential decay curve. This observation supports the prediction that the known contaminant will not behave as a time dependent inactivator of Abg. No effort was made to correct the obtained values of  $k_i = 0.32 \text{ min}^{-1}$ ,  $K_i = 0.15 \text{ mM}$  or  $k_i/K_i = 2.1 \text{ min}^{-1} \text{ mM}^{-1}$  from the re-plot of the observed rate constants of inactivation for the presence of the inactive impurity. As a result, the values obtained should be assumed to be underestimates of the true values of  $k_i$ ,  $K_i$  and  $k_i/K_i$ .

Compound **2.70** was also tested for the presence of a highly active contaminant in a manner similar to that used for **2.37**. Abg ( $17 \mu\text{M}$ ) was incubated with an  $\sim 9$ -fold excess of inhibitor ( $144 \mu\text{M}$ ) for 10 minutes, after which the reaction was halted by dilution and the residual enzyme activity was determined to be 20% of the starting activity. This is essentially identical to the 24% residual enzyme activity observed in control experiments when using a vast excess of inactivator ( $144 \mu\text{M}$ ) relative to enzyme ( $0.017 \mu\text{M}$ ). The fact that the inhibitor solution is still able to inactivate Abg at these relative concentrations means that a potential highly reactive contaminant, should it be present, would have to constitute at least 10% of the inactivator preparation, an amount that would be readily detected by both TLC and NMR analyses.

### 2.7.3 Tests for the stability of glucosides bearing phosphorus-based aglycones towards spontaneous hydrolysis

As discussed in Section 2.6.1, part of the goal in the design of compounds **2.62**, **2.67** and **2.70** was to modulate the reactivity of the fluorosugar derivative to control its spontaneous solvolysis. Direct monitoring of the breakdown of these compounds by NMR spectroscopy was not possible, owing to the poor solubility of these compounds in water. At the concentrations necessary to monitor decomposition using NMR, the compounds precipitated out of aqueous solution. While it could be possible to study the kinetics of decomposition using NMR in a non-aqueous solvent, it is the stability in water that is important for assessing the usefulness of these compounds for potential biological applications. It was not possible to directly monitor the breakdown of these compounds spectrophotometrically either, since they lack a distinctive chromophore whose absorption wavelength changes significantly upon solvolysis.

The assay that was developed to monitor breakdown of the compound in solution used residual Abg activity as the readout for inactivator decomposition as follows. The inactivator of interest was incubated in aqueous buffer (pH = 6.8), and at time intervals an aliquot of this solution was removed, and added to a second solution containing assay buffer and Abg. The initial concentration of inactivator in the first solution was chosen such that it was as close to the limit of solubility as possible, but would still readily inactivate Abg upon dilution. The second tube containing Abg and inactivator was incubated for a defined amount of time (5 min) to permit the remaining small molecule to partially inactivate Abg. Finally, an aliquot of this solution was added to the standard enzymatic assay cuvette containing substrate (pNP-Glc) and the residual enzyme activity was assayed. The residual amount of Abg activity is an indirect way of measuring the relative amount of small-molecule inactivator remaining in the initial solution as a function of incubation time, and hence the degree of hydrolysis.

The resulting plots of incubation time vs. residual enzyme activity are shown for compounds **2.62**, **2.67** and **2.70** in Figure 2.30 a), b) and c) respectively.

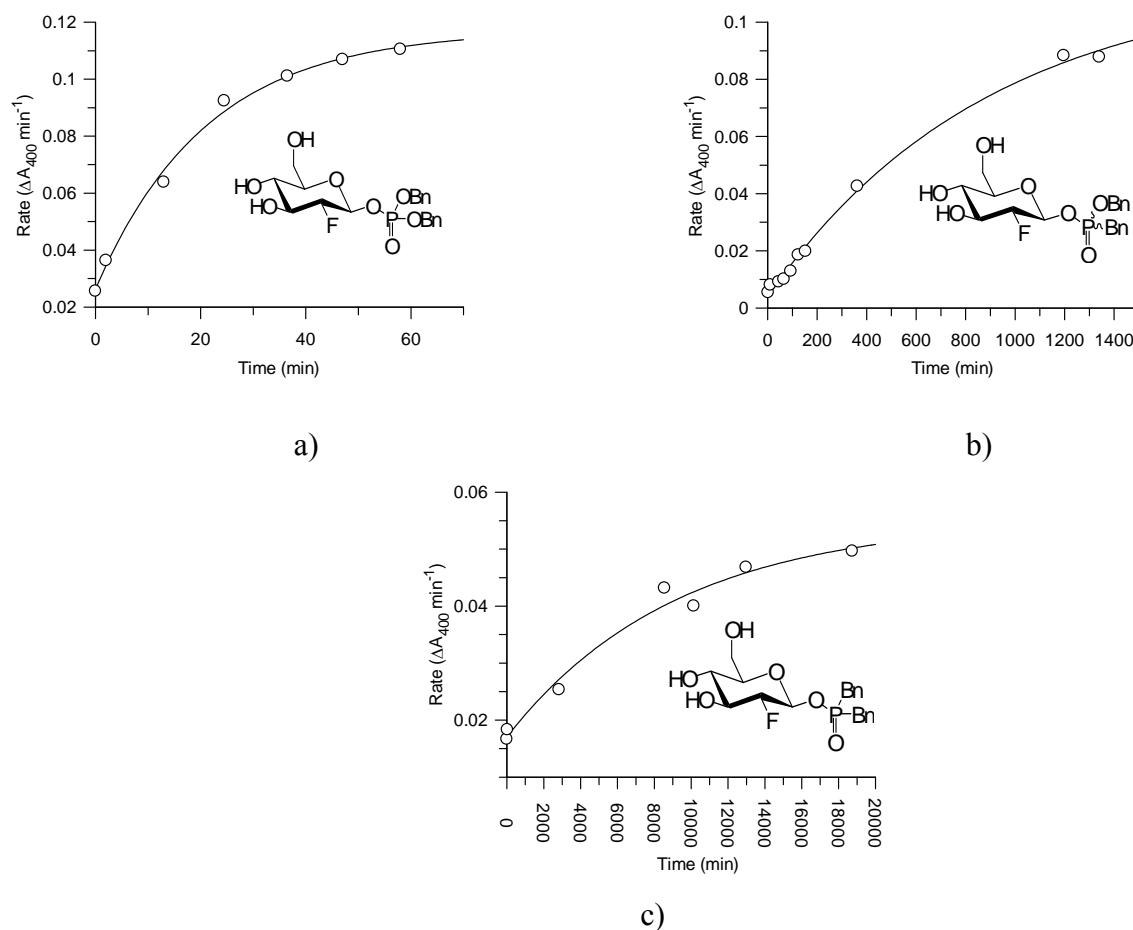


**Figure 2.30.** Monitoring stability of a) **2.62**, b) **2.67** and c) **2.70** by measuring residual enzyme activity as a function of inactivator incubation time.

It is obvious from the relative time-scales of the three plots that there is a significant difference in stability between the three compounds. The most labile compound, **2.62** [Figure 2.30, a)], has a  $k_{\text{obs}}$  of decomposition =  $0.047 \text{ min}^{-1}$ , or a half life ( $t_{1/2}$ ) of approximately 15 minutes. The next most stable compound, **2.67** [Figure 2.30, b)], has a  $k_{\text{obs}}$  of decomposition =  $0.0011 \text{ min}^{-1}$ , or a half life ( $t_{1/2}$ ) of approximately 630 minutes. The most stable compound, **2.70** [Figure 2.30, c)], has a  $k_{\text{obs}}$  of decomposition =  $0.00011 \text{ min}^{-1}$ , or a half life ( $t_{1/2}$ ) of approximately 6300 minutes. These results support the hypothesis that higher degrees of oxygenation correlate with lesser stability towards spontaneous decomposition for structurally similar aglycones.



## 2.7.4 General conclusions for aglycone variants

### 2.7.4.1 Considerations of aglycone properties

In attempting to evaluate the leaving group ability of different activated aglycones in the context of fluorosugars, two factors must be taken into account: the electron-withdrawing ability of the leaving group, and the energetics of binding of the aglycone in the enzyme active site.

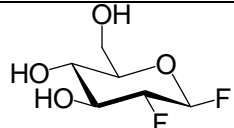
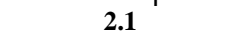
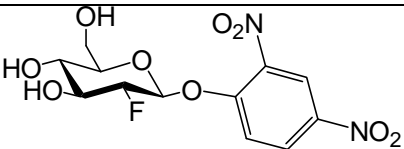
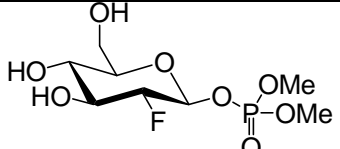
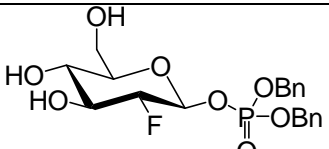
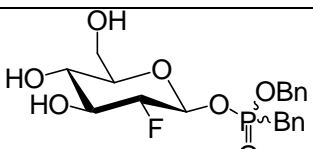
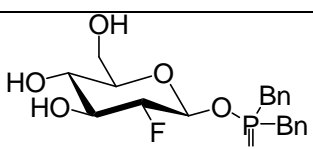
The  $pK_a$  value for the conjugate acid of an aglycone can be taken as one measure of the electron-withdrawing ability of a leaving group, but this is not an absolute measurement since  $pK_a$  values also take into account the strength of the orbital overlap between the proton and the species in question. As an example, the  $pK_a$  value for HF (3.1) is actually higher than the  $pK_a$  value for HCl ( $\sim 7$ ), despite the fact that fluorine is more electronegative than chlorine. This is a reflection of the poorer bonding between the proton and the chlorine atom relative to the bonding of the proton and the fluorine atom, arising from less favourable orbital overlap. In the present context, the aglycones being compared all lie within the same row on the periodic table, meaning that the  $pK_a$  value of the aglycone will be a very good reflection of its electron-withdrawing ability. Furthermore, with the exception of the fluoride leaving group in **2.1**, the rest of the compounds all have an oxygen atom directly attached to the anomeric center, and so comparison of the  $pK_a$  values of these compounds directly reflects the electron-withdrawing ability of the groups attached to the oxygen atom.

Evaluating the contribution of specific interactions of the aglycone with the enzyme active site (eg. hydrogen bond interactions, charge-charge interactions, hydrophobic interactions etc.) is considerably more difficult, and is reflected in the enthalpic contribution to binding. This type of analysis is also complicated by the entropic gain inherent in removing a hydrophobic compound from solution. This will be reflected in a further increase in the apparent binding affinity of the inactivator to the enzyme active site. To fully understand the contribution of specific interactions between the aglycone and the enzyme, and the entropic contributions to binding, requires detailed studies involving the thermodynamic parameters of binding ( $\Delta H$ ,  $\Delta S$ , and  $\Delta G$ ). These types of experiments are beyond the scope of this work. For the purposes of this discussion, relative contributions from specific interactions between the enzyme and the aglycone, and entropic contributions

to binding, will be considered together and can be roughly estimated on the basis of the kinetic parameters of inactivation of the compound in question.

#### 2.7.4.2 Summary of kinetic parameters for inactivation of Abg using the fluorosugar variants with novel aglycones

The kinetic parameters for a selected group of Abg inactivators are shown in Table 2.2.

Compound	$k_i$ ( $\text{min}^{-1}$ )	$K_i$ (mM)	$k_i/K_i$ ( $\text{min}^{-1}\text{mM}^{-1}$ )	Reference
 <b>2.1</b>	5.9	0.40	14.8	57,122
 <b>2.1</b>	--	--	12.6	This work
 <b>3.3</b>	25	0.05	500	58,122
 <b>2.37</b>	--	--	1.23	This work
 <b>2.62</b>	0.47	0.059	8.0	This work
 <b>2.67</b>	--	--	11	This work
 <b>2.70</b>	0.32*	0.15*	2.1*	This work

\* = Contaminated with ~30% of an inactive compound

**Table 2.2.** Kinetic parameters for selected fluorosugars as inactivators of Abg.

It was not possible to obtain individual  $k_i$  and  $K_i$  values for all compounds, as discussed previously. However, some structure-activity relationships can still be made through comparison of the second order rate constants  $k_i/K_i$ .

The previously known compound **3.3** is one of the most efficient inactivators of Abg. A comparison purely on the basis of  $pK_a$  values between **3.3** and **2.1** would suggest that **2.1** should be a more efficient inactivator. Instead, **3.3** is a more efficient inactivator by more than 30-fold. The high efficiency of **3.3** has been postulated to arise from stacking interactions between the aromatic dinitrophenyl ring and an aromatic residue in the +1 binding subsite in the enzyme-inactivator complex and in the glycosylation transition state.<sup>122</sup> The DNP ring therefore harnesses some of the interactions between the enzyme and the natural sugar substrate. In contrast, a small fluoride is incapable of forming any sort of stacking interactions, and is an extremely poor hydrogen-bond acceptor.

The dimethyl phosphate derivative **2.37** is a modest inactivator of Abg; it is approximately 10-fold poorer than the fluoride derivative, and over 400-fold worse than the DNP derivative **3.3**. This is despite the fact that the  $pK_a$  value for dimethyl phosphoric acid is 1.8, and 2.7 units lower than those of either HF or dinitrophenol respectively, so despite being a more chemically activated species, incorporation of the dimethyl phosphate aglycone leads to a less efficient inactivator. This discrepancy must again arise from a difference in interactions in the +1 subsite. So while **3.3** is a more efficient inactivator than **2.1** on the basis of favourable enzymatic interactions, **2.37** may be a less efficient inactivator than either **3.3** or **2.1** because of unfavourable interactions between the enzyme and the aglycone.

The two methyl groups attached to the phosphate in **2.37** are among the more sterically conservative substituents that could be introduced. The dibenzyl phosphate derivative **2.62** has two benzyl groups, which are more sterically demanding by design (see Section 2.6.2.5), so it is interesting to note that **2.62** is actually a slightly better inactivator of Abg than **2.37**. It is not readily apparent whether this slight increase in efficiency arises from an increase in specific contacts between the aglycone and the enzyme, or simply from the entropic gain in desolvating a larger and more hydrophobic aglycone group when binding in the active site.

Individual  $k_i$  and  $K_i$  values were obtained for compound **2.62**, allowing a better evaluation of the origin of the efficiency of the phosphate leaving group as an activated aglycone. The  $k_i$  value ( $0.47 \text{ min}^{-1}$ ) represents the rate constant for the rate-determining step for the inactivation reaction, which is likely the glycosylation step of the inactivation reaction. Despite the phosphate aglycone being more chemically activated than either fluoride or dinitrophenolate, this reactivity is not observed in the relative  $k_i$  values. This likely means that the phosphate leaving group is not as well accommodated in the enzymatic transition state as either the fluoride or dinitrophenolate aglycones.

The increased affinity of the aglycone group for the enzyme active site is partly reflected in the lower  $K_i$  value observed for **2.62**,  $0.059 \text{ mM}$ . This is closer to the  $K_i$  value for **3.3** ( $0.05 \text{ mM}$ ) than the  $K_i$  value for **2.1** ( $0.40 \text{ mM}$ ), which supports the hypothesis that this compound's increased efficiency as an inactivator arises from favourable interactions (enthalpic or entropic) between the aglycone and the enzyme.

Finally, the phosphonate derivative **2.67** and the phosphinate derivative **2.70** both have second order rate constants of inactivation ( $k_i/K_i = 11 \text{ min}^{-1}\text{mM}^{-1}$  and  $k_i/K_i = \text{at least } 2.1 \text{ min}^{-1}\text{mM}^{-1}$ , respectively) that are very close to the  $k_i/K_i$  value for **2.62** ( $8.0 \text{ min}^{-1}\text{mM}^{-1}$ ). The decreased distance between the phosphorus atom and the benzyl group(s) arising from the removal of one or both intervening oxygen atoms does not appear to have dramatically affected the ability of the compound to act as an inactivator. This is a strange result, given that the  $\text{pK}_a$  of the corresponding free acids decreases by approximately 1  $\text{pK}_a$  unit for each additional oxygen directly bonded to the phosphorus center. Therefore, because **2.62** has a leaving group that should be nearly 100-fold more chemically activated than **2.70**, it is surprising to find that the rates of inactivation by the two compounds differ by only 4-fold. The reason for this discrepancy is not readily apparent.

#### 2.7.4.3 Stability considerations

Selection of the ideal phosphorus-based aglycone for a fluorosugar designed as a glycosidase inactivator depends on two factors. First of all, increasing degrees of oxygenation led to increasingly chemically activated aglycones, which are therefore more

susceptible to spontaneous solvolysis via glycosidic fission. However, as discussed in Section 2.6.2.4, decreasing levels of oxygenation also correlate with an increasing susceptibility to nucleophilic attack at the phosphorus atom under strongly acidic or basic conditions, such as those encountered during acetate deprotection.

While it was possible to kinetically evaluate **2.62** as an Abg inactivator, its instability towards spontaneous decomposition means that it is largely unsuitable for most of the desired applications for this new class of glycosidase inactivator, as discussed in Chapter 3. In contrast, **2.70** proved to be extremely stable towards spontaneous decomposition but was difficult to access synthetically owing to its susceptibility to decomposition during acetate removal. Therefore, obtaining large quantities of pure material represented a significant challenge. Benzyl benzyl-phosphonate **2.67** represented an ideal balance between stability towards spontaneous solvolysis and stability towards decomposition during acetate removal. Therefore, the benzyl benzyl-phosphonate aglycone was chosen for further study.

## **2.8 Expanding the scope of fluorosugars bearing phosphorus-based aglycones as inactivators of other enzymes**

### **2.8.1 Target compounds**

Given that phosphate-, phosphonate- and phosphinate-based aglycones had been demonstrated to be useable in the design of mechanism-based inactivators for a retaining  $\beta$ -glucosidase, the next step was to expand the scope of this novel leaving group to other classes of retaining glycosidases.

The compounds chosen as synthetic targets are depicted in Figure 2.31.

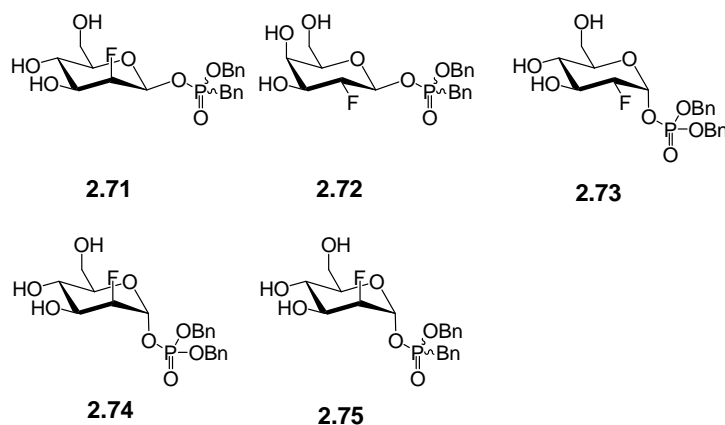


**Figure 2.31.** Structures of target compounds chosen as inactivators of other glycosidases.

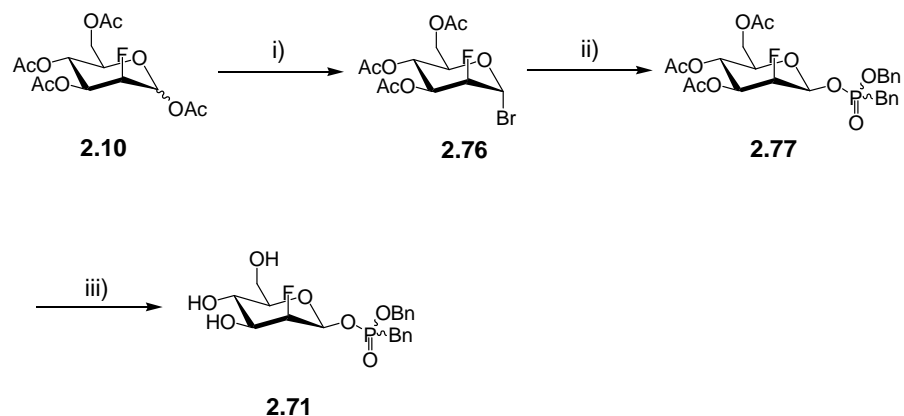
The compounds **2.71** and **2.72** were chosen as potential inactivators of other retaining  $\beta$ -glycosidases, in this case, a retaining mannosidase and galactosidase respectively. The benzyl benzylphosphonate leaving group was used since it showed the optimal balance between stability under deprotection conditions and stability towards spontaneous hydrolysis.

The target compounds **2.73**, **2.74** and **2.75** are all potential  $\alpha$ -glycosidase inactivators. It is already known that appropriately configured 2-fluoro- $\alpha$ -glycosyl fluorides do not act as covalent inactivators of retaining  $\alpha$ -glycosidases. The rate of hydrolysis of the covalent glycosyl-enzyme intermediate is too high relative to the rate of formation, and so these compounds are better classified as slow substrates rather than true inactivators.<sup>12</sup> The covalent glycosyl-enzyme intermediate produced by the target compounds **2.73**, **2.74** and **2.75** would be identical to those produced by the analogous 2-fluoro- $\alpha$ -glycosyl fluorides. Therefore, the rate of turnover of the glycosyl-enzyme intermediate would be the same as that observed with the 2-fluoro- $\alpha$ -glycosyl fluorides. Since  $pK_a$  arguments would suggest that dibenzyl phosphate is a better leaving group than fluoride, the glycosylation step would be predicted to be accelerated relative to the deglycosylation step. As a result there should be an increase in the steady-state concentration of the covalent glycosyl-enzyme intermediate, leading to inactivation of the enzyme, if this is the dominant factor.

## 2.8.1 Chemical synthesis

### 2.8.1.1 Synthesis of benzyl benzyl-(2-deoxy-2-fluoro- $\beta$ -D-mannopyranosyl) phosphonate (**2.71**)

The synthesis of benzyl benzyl-(2-deoxy-2-fluoro- $\beta$ -D-mannopyranosyl) phosphonate (**2.71**) is shown in Scheme 2.16.



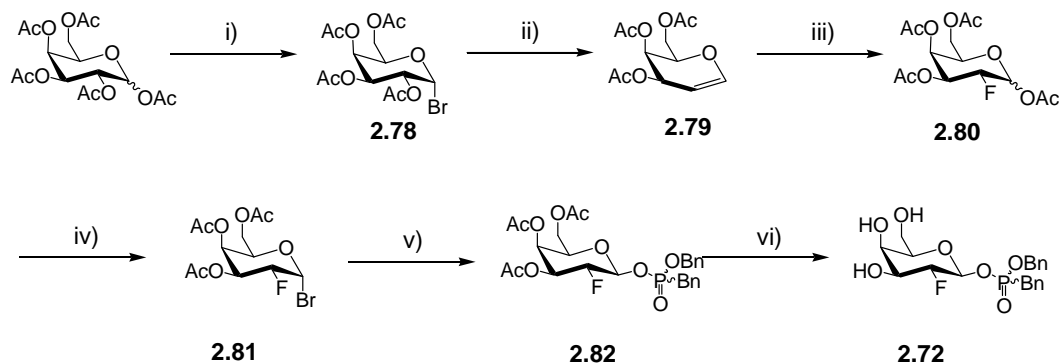
**Scheme 2.16.** Synthesis of benzyl benzyl-(2-deoxy-2-fluoro- $\beta$ -D-mannopyranosyl) phosphonate (**2.71**). i) 33% (w/v) HBr/AcOH, 90%; ii) **2.65**, Ag<sub>2</sub>CO<sub>3</sub>, MeCN, 63%; iii) NaOMe, MeOH, 77%.

Bromide **2.76**, a known<sup>198</sup> compound which was available from the synthesis of **2.1**, was glycosylated as outlined in the synthesis of **2.67**, to give **2.77** in an acceptable yield (63%). **2.77** was readily deprotected using sodium methoxide in methanol to give **2.71** (77%).

### 2.8.1.2 Synthesis of benzyl benzyl-(2-deoxy-2-fluoro- $\beta$ -D-galactopyranosyl) phosphonate (**2.72**)

The synthesis of benzyl benzyl-(2-deoxy-2-fluoro- $\beta$ -D-galactopyranosyl) phosphonate (**2.72**) is shown in Scheme 2.17.



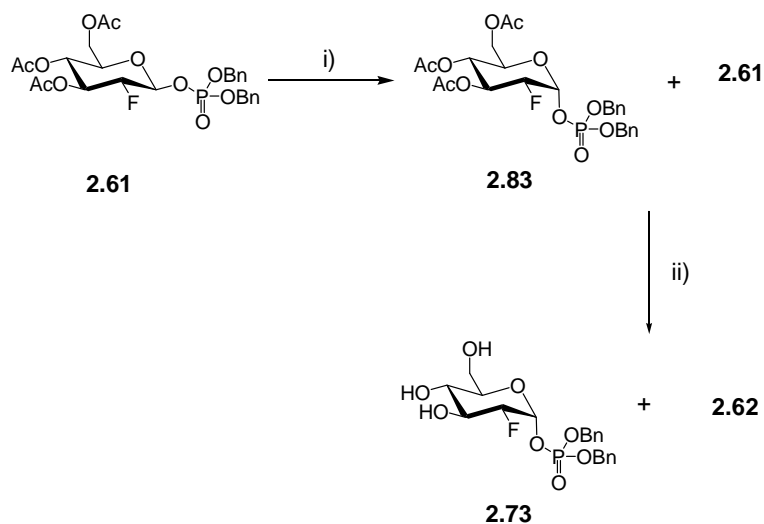


**Scheme 2.17.** Synthesis of benzyl benzyl-(2-deoxy-2-fluoro- $\beta$ -D-galactopyranosyl) phosphonate (**2.72**). i) 33% (w/v) HBr/AcOH; ii) Zn, AcOH, H<sub>2</sub>O, 48% over two steps; iii) Selectfluor<sup>TM</sup>, MeCN, AcOH, 21%; iv) 33% (w/v) HBr/AcOH; v) **2.65**, Ag<sub>2</sub>CO<sub>3</sub>, MeCN, 80% from **2.80**; vi) NaOMe, MeOH, 98%.

Glycal **2.79** was fluorinated using Selectfluor<sup>TM</sup>, and subsequently converted to the bromide **2.81** under standard conditions. The coupling of benzyl benzylphosphonic acid (**2.65**) and bromide **2.81** proceeded smoothly to give the desired compound **2.82** in good yield (80% over two steps). Deprotection gave **2.72** in excellent yield (98%).

#### 2.8.1.3 Synthesis of dibenzyl (2-deoxy-2-fluoro- $\alpha$ -D-glucopyranosyl) phosphate (**2.73**)

The acetylated precursor of **2.73** has been previously been reported by Wong and co-workers en route to Uridine-diphospho-2-deoxy-2-fluoro- $\alpha$ -D-glucopyranoside.<sup>210</sup> Despite repeated attempts at reproducing their results, the author was unable to produce the title compound using the methodology described. Instead, only the  $\beta$ -linked product **2.61** could be isolated. Owing to the difficulty in producing the desired compound in the published manner, a different synthetic route was used to prepare **2.73** as shown in Scheme 2.18.



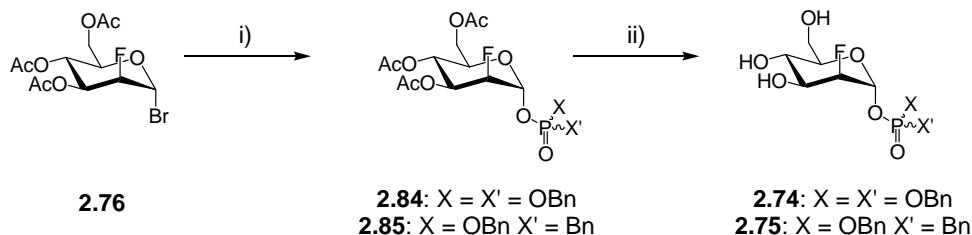
**Scheme 2.18.** Synthesis of dibenzyl (2-deoxy-2-fluoro- $\alpha$ -D-glucopyranosyl) phosphate (**2.73**). i) Dibenzyl phosphoric acid, toluene, 22%; ii) NaOMe, MeOH, 77%.

This route utilizes the greater thermodynamic stability of  $\alpha$ - over  $\beta$ -glycosides when the aglycones are electron-withdrawing groups, to produce **2.83** from **2.61**. To accomplish this anomerization, **2.61** was treated with dibenzyl phosphoric acid in refluxing toluene for 2 days. A 4:1 mixture of the desired **2.83** to **2.61** was obtained. Prolonged treatment under these conditions did not lead to any change in this ratio of products, suggesting that the reaction had reached equilibrium under these conditions within two days.

The inseparable mixture of **2.83** and **2.61** was deprotected under basic conditions to yield a 19:1 mixture of the desired product **2.73** to the beta anomer **2.62** (77% total yield). The fact that the  $\alpha$ -anomer is enriched relative to the  $\beta$ -anomer during this deprotection is expected, since the  $\beta$ -anomer would be predicted to be the more labile anomer, and therefore to decompose more readily during the deprotection reaction. The anomeric mixture was again found to be inseparable. Since this mixture was to be tested against an  $\alpha$ -glucosidase, the presence of the  $\beta$ -anomer should not be a problem as it should not be a substrate. This was confirmed by testing the enzyme with a previously prepared sample of **2.62** (data not shown).

2.8.1.4 Synthesis of dibenzyl (2-deoxy-2-fluoro- $\alpha$ -D-mannopyranosyl) phosphate (**2.74**) and benzyl benzyl-(2-deoxy-2-fluoro- $\alpha$ -D-mannopyranosyl) phosphonate (**2.75**)

The synthetic route used to prepare both **2.74** and **2.75** is shown in Scheme 2.19.



**Scheme 2.19.** Synthesis of dibenzyl (2-deoxy-2-fluoro- $\alpha$ -D-mannopyranosyl) phosphate (**2.74**) and benzyl benzyl-(2-deoxy-2-fluoro- $\alpha$ -D-mannopyranosyl) phosphonate (**2.75**). i) **2.65**, Ag<sub>2</sub>CO<sub>3</sub>, toluene (for **2.84**), MeCN (for **2.85**), **2.84**: 7%, **2.85**: 37%; ii) NaOMe, MeOH, **2.74**: 76%, **2.75**: 83%.

Both **2.84** and **2.85** were prepared by treatment of **2.76** with the appropriate phosphoric (**2.84**, 7%) or phosphonic (**2.85**, 37%) acid in the appropriately optimized solvent. The solvents used are directly contrary to the previous report from Wong and co-workers which described toluene as being the best solvent for formation of the  $\alpha$ -linked phosphodiester,<sup>210</sup> while in the author's hands the  $\beta$ -linked phosphoester (18%) was the favoured product. Despite multiple attempts, the author could reproduce neither the yields nor the selectivity outlined in that patent for the synthesis of **2.74**. Despite the difficulty in obtaining an efficient synthesis for either protected precursor, sufficient material for deprotection under basic conditions was obtained (76% for **2.74**, 83 % for **2.75**) for enzymatic testing.

## 2.9 Enzymatic testing of fluorosugars bearing phosphorus-based aglycones as inactivators of other enzymes

### 2.9.1 Kinetic analysis of the inactivation of Abg by **2.71** and **2.72**

#### 2.9.1.1 Benzyl benzyl-(2-deoxy-2-fluoro- $\beta$ -D-mannopyranosyl) phosphonate (**2.71**)

Abg is known to hydrolyze both mannosides and galactosides.<sup>14</sup> Therefore, a diastereomeric mixture (at phosphorus) of benzyl benzyl-(2-deoxy-2-fluoro- $\beta$ -D-mannopyranosyl) phosphonate (**2.71**) was evaluated as an inactivator of Abg. The resulting activity versus time curve for various concentrations of inactivator and a re-plot of the individual  $k_{\text{obs}}$  values as a function of inactivator concentration is shown in Figure 2.32. pNP- $\beta$ -D-fucoside was used as the substrate for this assay<sup>14</sup> since accurate results cannot be obtained using pNP- $\beta$ -Glc as the substrate, as follows. The 2-fluoro-mannosyl covalent intermediate formed is considerably less stable than the 2-fluoro-glucosyl covalent intermediate with Abg ( $k_{\text{hyd}} = 1 \times 10^{-3} \text{ min}^{-1}$  and  $k_{\text{hyd}} = 1.2 \times 10^{-5} \text{ min}^{-1}$  respectively), meaning that if pNP- $\beta$ -Glc is used as the substrate, turnover of the covalent glycosyl-enzyme intermediate can be observed over the course of the assay through transglycosylation onto the O4 hydroxyl of pNP- $\beta$ -Glc.<sup>122</sup> Therefore, measurement of the residual enzyme activity is quite challenging, since the amount of active enzyme changes over the course of the assay. Since pNP- $\beta$ -D-fucoside does not have the equatorial O4 hydroxyl needed for turnover of the intermediate by transglycosylation and is still a good substrate for Abg, it is a good substrate for assays in which turnover of the intermediate via transglycosylation is problematic.

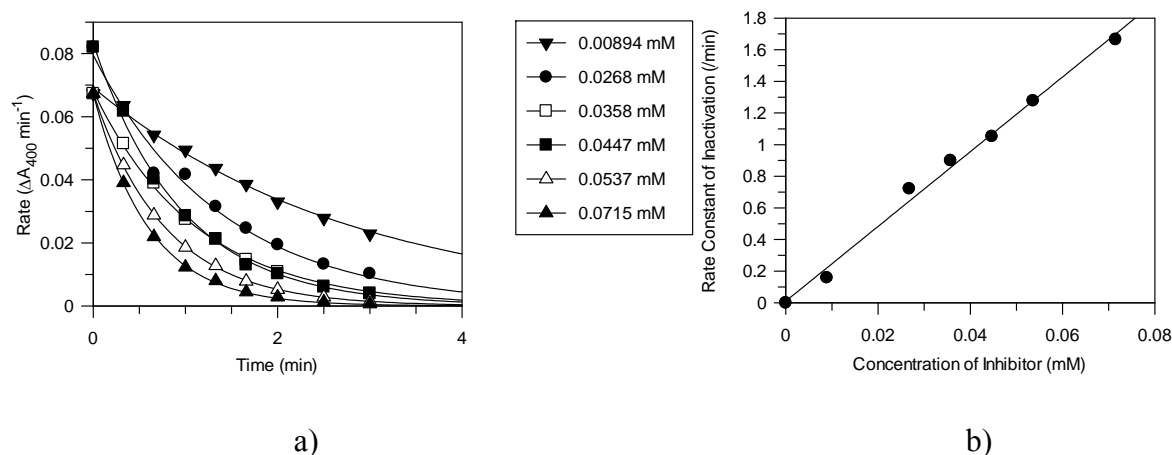
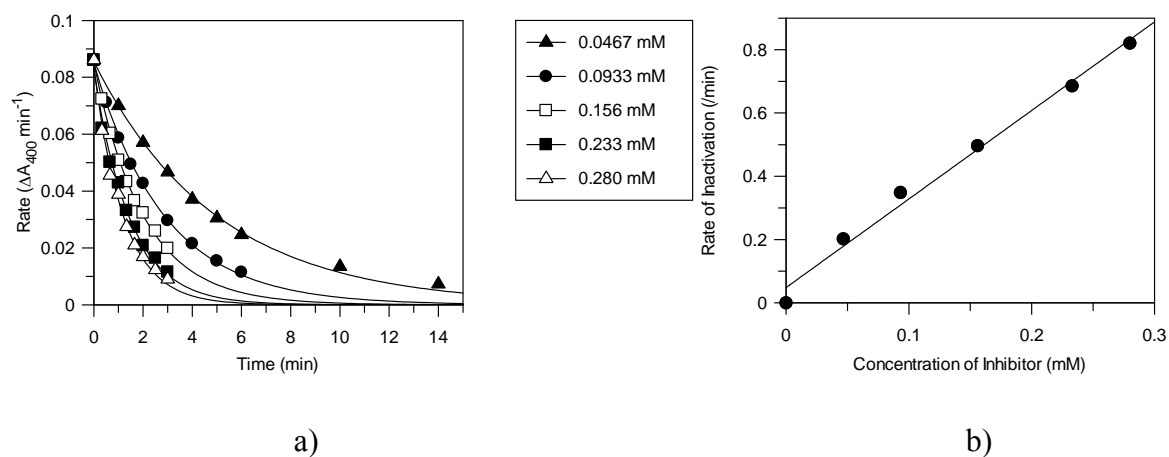


**Figure 2.32.** Inactivation of Abg with **2.71**. a) Non-linear plot of residual enzyme activity versus time at the indicated inactivator concentrations fitted to an exponential decay equation. b) Plot of the observed rate constants of inactivation versus concentration of inactivator.

In this instance, it was not possible to calculate the individual  $k_i$  and  $K_i$  values for **2.71**, since inactivation was too rapid at concentrations approaching saturation to allow sampling. However, a second order rate constant of inactivation ( $k_i/K_i = 23.9 \text{ min}^{-1}\text{mM}^{-1}$ ) was obtained from linear fitting of the re-plot of the rate constants of inactivation. This makes **2.71** the most efficient of the novel Abg inactivators tested, and is the only compound described thus far in the course of these studies that is a more potent inactivator than the fluoride derivative **2.1**, although neither of these compounds are as efficient as the DNP-derivative **3.3**.

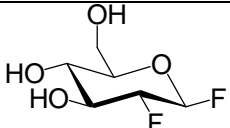
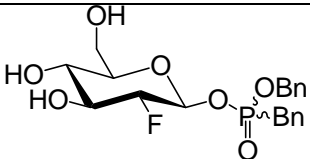
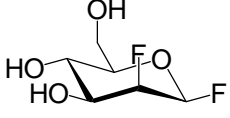
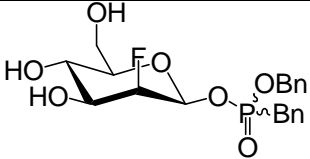
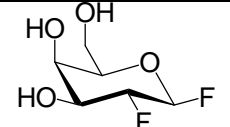
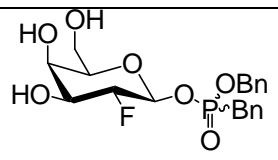
#### 2.9.1.2 Benzyl benzyl-(2-deoxy-2-fluoro-β-D-galactopyranosyl) phosphonate (**2.72**)

A diastereomeric mixture (at the phosphorus atom) of benzyl benzyl-(2-deoxy-2-fluoro-β-D-galactopyranosyl) phosphonate (**2.72**) was also tested as an inactivator of Abg (Figure 2.33). As described above for the assay involving **2.71**, it was necessary to use pNP-β-D-fucoside as the substrate in these assays.



**Figure 2.33.** Inactivation of Abg with **2.72**. a) Non-linear plot of residual enzyme activity versus time at the indicated inactivator concentrations fitted to an exponential decay equation. b) Plot of the observed rate constants of inactivation versus concentration of inactivator.

As described for **2.71**, only a second-order rate constant of inactivation ( $k_i/K_i = 2.8 \text{ min}^{-1}\text{mM}^{-1}$ ) was obtained for **2.72**. The kinetic parameters for inactivation of Abg by the three benzyl benzylphosphonate derivatives and their fluoride counterparts are summarized in Table 2.3.

Compound	$k_i$ ( $\text{min}^{-1}$ )	$K_i$ (mM)	$k_i/K_i$ ( $\text{min}^{-1}\text{mM}^{-1}$ )	Reference
 <b>2.1</b>	5.9 --	0.40 --	14.8 12.6	57,122 This work
 <b>2.67</b>	--	--	2.8	This work
 <b>2.76</b>	5.6	1.2	4.7	57,122
 <b>2.71</b>	--	--	23.9	This work
 <b>2.77</b>	2.6	3.2	0.81	57,122
 <b>2.72</b>	--	--	2.8	This work

**Table 2.3.** Kinetic parameters for selected fluorosugars as inactivators of Abg.

### 2.9.2 Kinetic analysis of the inactivation of Man2A by **2.71**

Benzyl benzyl-(2-deoxy-2-fluoro- $\beta$ -D-mannopyranosyl) phosphonate (**2.71**) was tested as an inactivator of Man2A. The resulting activity versus time plot for various concentrations of inactivator and a re-plot of the individual  $k_{\text{obs}}$  values plotted as a function of inactivator concentration is shown for **2.71** in Figure 2.34.

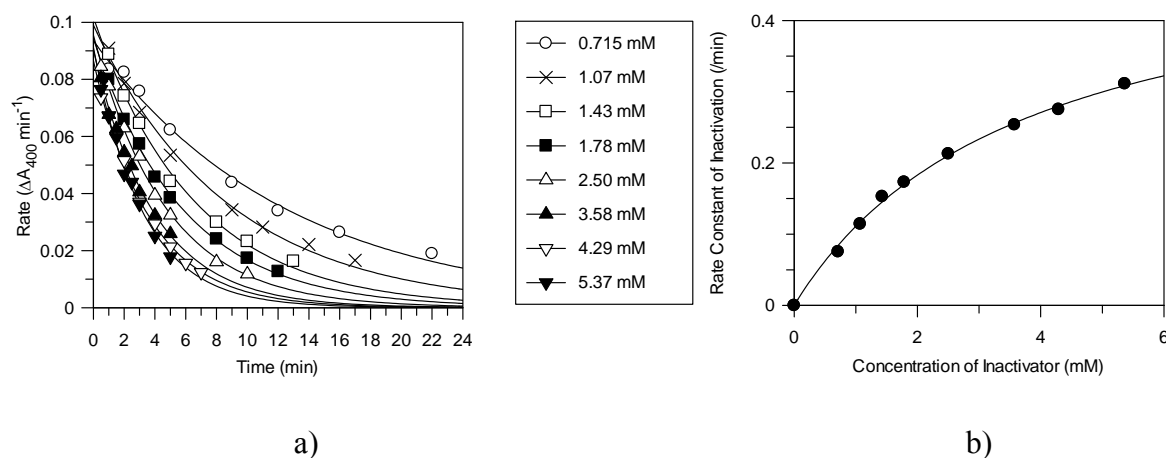


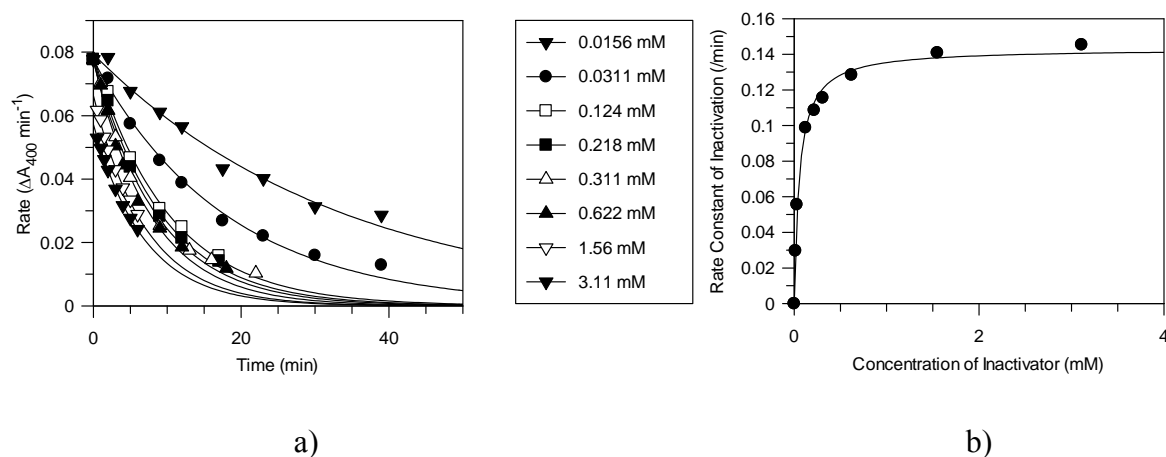
**Figure 2.34.** Inactivation of Man2A by **2.71**. a) Non-linear plot of residual enzyme activity versus time at the indicated inactivator concentrations fitted to an exponential decay equation. b) Plot of the observed rate constants of inactivation versus concentration of inactivator.

Compound **2.71** behaves as a covalent inactivator of Man2A, and individual values for  $k_i = 0.52 \text{ min}^{-1}$ ,  $K_i = 3.7 \text{ mM}$ , and  $k_i/K_i = 0.14 \text{ min}^{-1}\text{mM}^{-1}$  were obtained. A comparison of the kinetic parameters for this compound with the previously known inactivator of Man2A, 2-deoxy-2-fluoro- $\beta$ -D-mannopyranosyl fluoride ( $k_i = 0.57 \text{ min}^{-1}$ ,  $K_i = 0.41 \text{ mM}$ , and  $k_i/K_i = 1.4 \text{ min}^{-1}\text{mM}^{-1}$ )<sup>137</sup> reveals a 10-fold loss of inactivator specificity. This is almost entirely owing to an increase in  $K_i$ , which suggests that the benzyl benzylphosphonate aglycone is less well accommodated in the active site than the much smaller fluoride aglycone. However, there does not appear to be a significant effect on the energies of the two transition states relative to their respective ground states, as the  $k_i$  values are extremely close in magnitude.



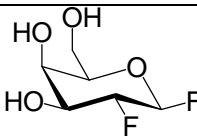
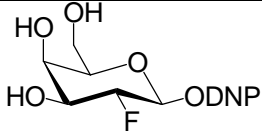
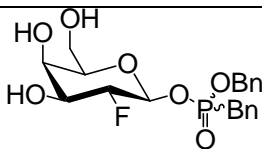
### 2.9.3 Kinetic analysis of the inactivation of *E. coli* $\beta$ -Gal by **2.72**

Benzyl benzyl-(2-deoxy-2-fluoro- $\beta$ -D-galactopyranosyl) phosphonate (**2.72**) was tested as a covalent inactivator of *E. coli*  $\beta$ -Gal. The resulting activity versus time plot for various concentrations of inactivator and a re-plot of the individual  $k_{\text{obs}}$  values plotted as a function of inactivator concentration is shown in Figure 2.35.



**Figure 2.35.** Inactivation of *E. coli*  $\beta$ -Gal with **2.72**. a) Non-linear plot of residual enzyme activity versus time at the indicated inactivator concentrations fitted to an exponential decay equation. b) Plot of the observed rate constants of inactivation versus concentration of inactivator.

Compound **2.72** was an efficient inactivator of *E. coli*  $\beta$ -Gal, with kinetic parameters of  $k_i = 0.14 \text{ min}^{-1}$ ,  $K_i = 0.058 \text{ mM}$ , and  $k_i/K_i = 2.5 \text{ min}^{-1}\text{mM}^{-1}$ . These values are presented in Table 2.4 along with the kinetic parameters for two known inactivators of *E. coli*  $\beta$ -Gal, 2-deoxy-2-fluoro- $\beta$ -D-galactopyranosyl fluoride (**2.77**) and 2,4-dinitrophenyl  $\beta$ -D-galactopyranoside (**2.78**).

Compound	$k_i$ ( $\text{min}^{-1}$ )	$K_i$ (mM)	$k_i/K_i$ ( $\text{min}^{-1}\text{mM}^{-1}$ )	Reference
 <b>2.77</b>	13.2	1.3	10.2	153
 <b>2.78</b>	0.66*	0.89*	0.74*	154
 <b>2.72</b>	0.14	0.058	2.5	This work

\* Data recorded at 25 °C

**Table 2.4.** Kinetic parameters for selected fluorosugars as inactivators of *E. coli*  $\beta$ -Gal.

It is difficult to make direct comparisons between 2,4-dinitrophenyl 2-deoxy-2-fluoro- $\beta$ -D-galactopyranoside and **2.72** since the kinetic parameters for 2,4-dinitrophenyl 2-deoxy-2-fluoro- $\beta$ -D-galactopyranoside were obtained at 25 °C rather than at 37 °C. However, if the values are taken as lower limits for the parameters at 37 °C (since the enzyme is more active at 37 °C than at 25 °C), then some interesting comparisons can still be made.

Fluoride appears to be the aglycone that is best accommodated in the glycosylation transition state, as can be seen from a comparison of the relative  $k_i$  values. The benzyl benzylphosphonate appears to be the aglycone least accommodated by the enzyme in the transition state of glycoside fission, as it has the lowest  $k_i$  value among all three compounds. However, the benzyl benzylphosphonate aglycone appears to be the one that binds tightest to

the enzyme in the ground state, as it has the lowest  $K_i$  value. It is not known to what extent this binding is enthalpically or entropically driven, although this observation can be explained by the fact that *E. coli*  $\beta$ -Gal is known to have a relatively open active site that can accommodate both of the natural substrates, allo-lactose and lactose.<sup>138</sup>

#### 2.9.4 Kinetic evaluation of **2.73** as a covalent inactivator of Yag

Dibenzyl (2-deoxy-2-fluoro- $\alpha$ -D-glucopyranosyl) phosphate (**2.73**) was tested as a covalent inactivator of Yag. No accumulation of the covalent intermediate was observed at 37 °C. To test whether accumulation could be observed kinetically, both the incubation and the assay temperatures were lowered to 4 °C to slow the rate of turnover of any covalent glycosyl-enzyme intermediate formed enough to be observed kinetically. This method has been used to observe the covalent glycosyl-enzyme intermediate formed between 5-fluoro- $\beta$ -L-idosyl fluoride and Yag.<sup>129,134</sup> However, even at 4 °C, no time-dependent decrease in enzyme activity was observed.

To test whether the compound was acting as a substrate for Yag, a TLC assay was used to observe the formation of 2-deoxy-2-fluoro-glucose released by the enzyme, as can be seen in Figure 2.36.

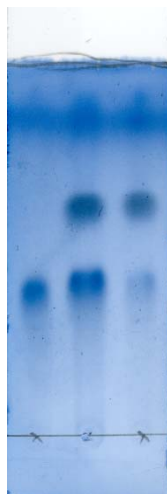


**Figure 2.36.** TLC analysis of hydrolysis of **2.73** by Yag, 18 minutes incubation at 37 °C. Lane 1 = positive control (2-deoxy-2-fluoro-glucose). Lane 2 = **2.73** + Yag. Lane 3 = negative control, **2.73** only.

The fastest running spot can be identified as intact **2.73** both by its  $R_f$  and by co-spot with an authentic standard (data not shown). The middle spot corresponds to the product of hydrolysis of **2.73**, 2-deoxy-2-fluoro-glucose. The darker product spot in the middle lane (containing enzyme) relative to the right-hand lane (containing no-enzyme) shows that **2.73** is hydrolyzed in an enzyme-dependent manner. This suggests that **2.73** is a substrate for Yag. Therefore, **2.73** was tested as a competitive substrate for Yag under steady state conditions, as described previously for **2.5** and Abg. The resulting inverse rate versus inhibitor concentration plot can be seen in Figure 2.37.

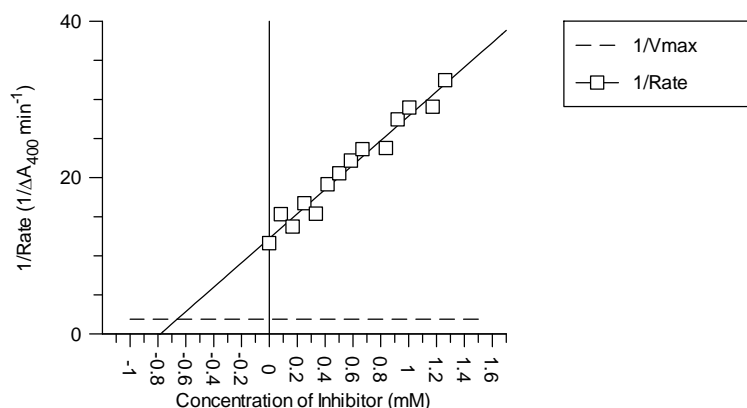


**Figure 2.37.** Testing of **2.73** as a competitive substrate for Yag by plotting 1/rate of pNP- $\alpha$ -Glc hydrolysis catalyzed by Yag vs. concentration of **2.73**.

An apparent  $K_i'$  value for **2.73** for Yag of approximately 0.7 mM can be obtained from the intersection of the 1/rate and  $1/V_{\max}$  lines, which should correspond to the  $K_m$  value for this compound as a substrate.

### 2.9.5 Kinetic evaluation of **2.74** as a covalent inactivator of JBAM

Dibenzyl (2-deoxy-2-fluoro- $\alpha$ -D-mannopyranosyl) phosphate (**2.74**) and benzyl benzyl-(2-deoxy-2-fluoro- $\alpha$ -D-mannopyranosyl) phosphonate (**2.75**) were both evaluated as potential inactivators of JBAM. However, no accumulation of the covalent intermediate was

observed at 37 °C. To test whether accumulation could be observed kinetically, both the incubation and the assay temperatures were lowered to 4 °C to slow the rate of turnover of any covalent glycosyl-enzyme intermediate formed enough to be observed kinetically, as described for the evaluation of **2.73** as a potential inactivator of Yag above. However, even at 4 °C, no time-dependent decrease in enzyme activity was observed with either **2.74** or **2.75**. To test whether either compound is a substrate for JBAM, a TLC assay was used to test for the presence of the product of hydrolysis, 2-deoxy-2-fluoro-mannose. The image of the TLC plate for **2.74** in the presence (right lane) and absence (left lane) of JBAM is shown in Figure 2.38.

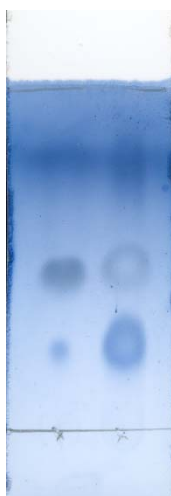


**Figure 2.38.** TLC plate showing **2.74** incubated in the presence (right lane) and absence (left lane) of JBAM. The top spot is intact inactivator, and the middle spot is 2-deoxy-2-fluoro-glucose (both confirmed by co-spot analysis, not shown).

This TLC assay shows that **2.74** is hydrolyzed at an increased rate in the presence of enzyme. Therefore, dibenzyl phosphate derivative **2.74** was evaluated as a competitive substrate for JBAM under steady-state conditions. The resulting graph of inverse rate versus concentration of **2.74** is shown in Figure 2.39.

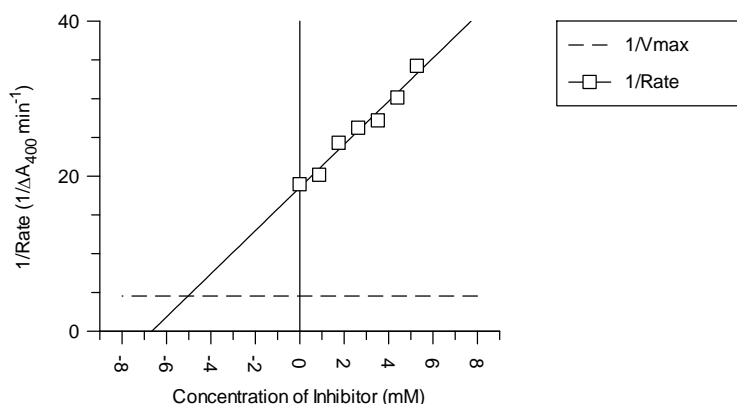


**Figure 2.39.** Testing of **2.74** as a competitive substrate for JBAM by plotting 1/rate of DNP- $\alpha$ -Man hydrolysis catalyzed by JBAM vs. concentration of **2.74**.

From this graph, a  $K_i'$  value (corresponding to the  $K_m$  value for **2.74** as a substrate) of ~5 mM can be obtained. This, coupled with the TLC data, demonstrates that **2.74** behaves as a substrate for JBAM, rather than a covalent inactivator.

Treatment of the other compound, benzyl benzylphosphonate derivative **2.75** with JBAM, even for extended periods of time (30 mins), showed no increase in the amount of hydrolysis observed above the control reaction. Therefore, it was concluded that this compound does not act as a substrate for JBAM. To test whether **2.75** was still capable of binding to the active site of the enzyme, it was tested as a competitive inhibitor of the substrate, DNP- $\alpha$ -Man. No reduction in the rate of hydrolysis of DNP- $\alpha$ -Man was observed at the highest concentration of **2.75** tested (6 mM). This result is quite surprising, given that the phosphate analogue **2.74** was shown to bind to the enzyme active site and acted as a substrate for the enzyme. However, given that **2.74** has a relatively high  $K_m$  value as a substrate, ~5 mM, then it is possible that the change from a P-OBn bond to P-Bn bond in **2.75** introduces sufficient unfavourable interactions with the enzyme so that it no longer binds to the enzyme at the concentrations tested.

## **2.10: General conclusions regarding scope and usefulness of various aglycones in fluorosugars as inactivators of glycosidases**

Attempts to prepare fluorosugars bearing an equatorial chloride leaving group as potential inactivators of retaining  $\beta$ -glycosidases were unsuccessful. Both the 2-deoxy-2-fluoro- $\beta$ -D-glucopyranosyl chloride **2.32** and the more highly fluorinated 2-deoxy-2,5-difluoro- $\alpha$ -L-idopyranosyl chloride **2.33** proved too prone to spontaneous decomposition during base-catalyzed removal of the acetate protecting groups from their acetylated precursors to be isolated. Likewise, attempts to make fluorosugars bearing sulfur-based aglycones were unsuccessful. The glycosides with sulfonate-based aglycones (**2.34** and **2.35**) proved to be too unstable to prepare, while the attempt to prepare a glycoside bearing a sulfinato-based aglycone (**2.36**) was unsuccessful, leading only to products arising from spontaneous atmospheric oxidation of the sulfinato ester to the sulfonate ester.

Fluorosugars bearing phosphorus-based aglycones have been shown to act as covalent inactivators of a variety of retaining  $\beta$ -glycosidases. None of the compounds tested proved to be significantly superior to their respective fluoride- or DNP-bearing fluorosugars as covalent inactivators of the enzymes against which they were tested. However, one advantage that this novel class of aglycones offers is in the potential ability to alter the lipophilicity of fluorosugars bearing these aglycones by altering the lipophilicity of the substituents on the phosphorus center, which could have future implications for design of this class of molecule as a potential drug. Furthermore, this novel aglycone also permits the design of fluorosugars bearing aglycones that show specificity for the +1 subsite of the enzyme, which may be harnessed to increase either the selectivity or efficiency of the inactivator. This idea is explored further in Chapter 3.

## **Chapter 3: Development of More Efficient Covalent Inactivators** **for Two Lysosomal Enzymes**



## 3.1 Glucocerebrosidase (GCase)

### 3.1.1 General introduction

Glucocerebrosidase (GCase) is a membrane-associated retaining  $\beta$ -glucosidase that belongs to the sequence-related family GH30 (<http://www.cazy.org/>). Its enzymatic nucleophile has been identified as Glu 340 using an active site-directed covalent inactivator<sup>211</sup> as described in Section 3.1.2, and the acid/base as Glu 235. This glycoprotein is responsible for cleaving the  $\beta$ -linked glucosyl residue from the glycolipid substrate glucosyl ceramide, as described in Section 1.4.3. The presence of the activator protein Saposin C is required for activity *in vivo*,<sup>212</sup> and though the exact mechanism by which this small activator protein (80 amino acid residues) functions is not clear, it appears that Saposin C promotes association between GCase and the lipid membrane by altering the membrane structure so as to promote binding of GCase to those regions.<sup>213</sup> This proposed mechanism of activation is consistent with structural studies on both the Saposin-C protein,<sup>214-216</sup> and GCase.<sup>217</sup> The three-dimensional structure of GCase was first solved by X-ray crystallography in 2003,<sup>218</sup> and subsequent structural studies have focused on different glycosylation states of the enzyme<sup>219-221</sup> and on co-crystallization in the presence of ligands bound to the enzyme either covalently<sup>222</sup> or non-covalently.<sup>223,224</sup>

While the activator protein Saposin C is required for GCase activity *in vivo*, other additives have been explored for the *in vitro* activation of GCase. These are generally divided into two categories: bile salts and detergents, and negatively charged phospholipids.<sup>212</sup> Detergents such as Triton<sup>®</sup> X-100 or sodium dodecyl sulfate (SDS) appear to assist in GCase activity through micelle formation to help co-solubilise the enzyme and substrate, while bile salts such as sodium taurocholate appear to enhance enzyme activity through a specific charge-mediated interaction with the enzyme. X-ray crystallographic studies on the three dimensional structure of GCase appear to support the idea that the enzyme readily adopts two conformations, one of which is catalytically active, and one which is not.<sup>224</sup> Sodium taurocholate appears to form specific contacts with the GCase enzyme that favour the catalytically active conformation. Negatively charged phospholipids such as phosphatidylserine have also been shown to activate GCase,<sup>225</sup> and it has been suggested that this class of molecule may also serve, alongside Saposin C, as the natural

activators of GCase.<sup>226</sup> A recombinant form of GCase is available commercially as Cerezyme®, which is used clinically in ERT for the treatment of Gauchers disease, which is discussed further in Section 4.1.1.1.

### 3.1.2 Known inactivators of GCase

#### 3.1.1.1 Conduritol B-epoxide

Conduritol B-epoxide (**3.1**, Figure 3.1) is an epoxide-containing polyhydroxylated cyclohexane derivative. It covalently inactivates GCase through activation of the oxygen atom of the epoxide ring by proton donation from one enzymatic carboxylic acid residue, followed by nucleophilic attack on one of the carbon atoms of the epoxide ring by a second enzymatic carboxylic acid residue to open the epoxide ring, as depicted in Scheme 3.1. Owing to the *pseudo*-C<sub>2</sub> symmetry of **3.1**, it is possible for either carboxylic acid, either the catalytic acid/base or catalytic nucleophile, to covalently bond to **3.1**.

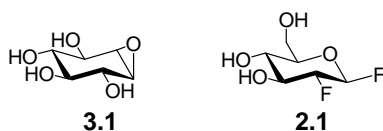
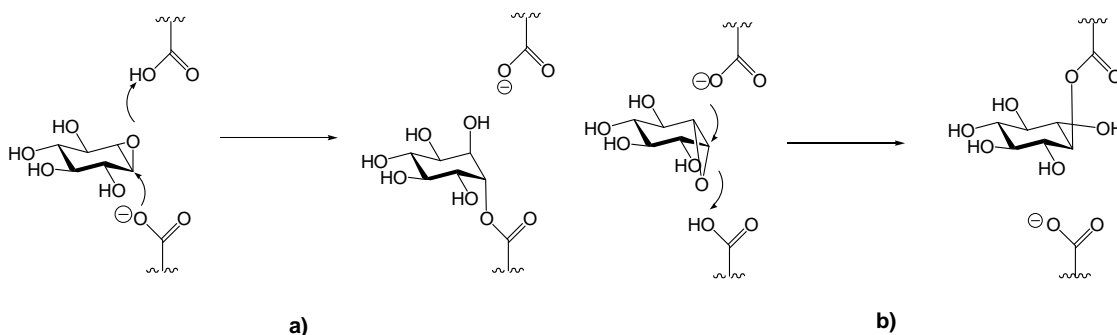


**Figure 3.1.** Structures of two known covalent inactivators of GCase.



**Scheme 3.1.** Mechanism of inactivation of GCase by **3.1** through covalent bond formation to the a) catalytic nucleophile and b) catalytic acid/base residue.

Compound **3.1**, and its derivatives and analogues, have been extensively studied as covalent inactivators of glycosidases.<sup>39</sup> Epoxide **3.1** has been shown to be a selective inactivator of human GCase while not reducing the enzymatic activity of other known mammalian  $\beta$ -glucosidases.<sup>227</sup> This is an important feature that is exploited in the enzymatic assays for GCase activity in liver homogenates,<sup>227</sup> as well as in efforts to discover and characterize novel mammalian  $\beta$ -glucosidases since **3.1** can be added to crude enzyme mixtures to selectively inactivate GCase, allowing other  $\beta$ -glucosidase activities to be examined.<sup>228-230</sup> **3.1** has also been exploited as a probe in cell-based assays to mimic the state of Gauchers cells for a number of different purposes,<sup>97,231-236</sup> and in otherwise healthy mice to selectively ablate GCase activity<sup>30,237</sup> in an attempt to create an animal model for Gauchers disease. One important result from these latter studies was the finding that the lower limit of normal GCase activity necessary for an individual to be asymptomatic is 12-16%.<sup>30</sup> It was necessary to use mice treated with **3.1** as an animal model for Gauchers for many years, since the generation of a Gauchers mouse through genetic engineering was very challenging,<sup>94-96,238-242</sup> and only recently has a viable animal model been produced through the generation of a conditional knockout that maintains some enzyme activity in the brain.<sup>240,243</sup>

#### 3.1.1.2 2-Deoxy-2-fluoro- $\beta$ -D-glucosyl fluoride

More recently, 2-deoxy-2-fluoro- $\beta$ -D-glucosyl fluoride (**2.1**) has also been shown to be a covalent inactivator of GCase.<sup>211</sup> This reagent has seen far less application *in vivo* compared to conduritol-B-epoxide (**3.1**) owing to the lack of selectivity for GCase relative to other retaining  $\beta$ -glucosidases. However, the use of **2.1** was critical in correctly identifying the catalytic nucleophile in GCase.<sup>211</sup> This was achieved through the labelling of the nucleophilic residue in the intact protein with **2.1**, followed by proteolysis of the protein and identification of the labelled residue by mass spectrometry. This is a general strategy<sup>40</sup> that has been successfully applied in the identification of the catalytic nucleophile for a number of glycosidases. In the case of GCase, the catalytic nucleophile had previously been mistakenly identified as Asp 443, using a <sup>3</sup>H-labelled derivative of **3.1**,<sup>244</sup> and it was only after re-examination of the identity of the nucleophile using **2.1** that Glu 340 was correctly identified as the enzymatic nucleophile.<sup>211</sup> The ability of **2.1** to stabilize the folded

conformation of treated GCase has also been investigated,<sup>245</sup> which represents an important first step in testing the ability of activated fluorosugars to act as pharmacological chaperones, as discussed in Section 4.1.

### 3.1.3 General considerations for GCase inactivators

The search for a more efficient and selective GCase inactivator was one of the eventual goals in the development of new activated fluorosugar inactivators in Chapter 2. The results from Sections 2.3 and 2.4 yielded no promising lead compounds as a result of additional fluorination on the sugar ring, although the search for a new aglycone for activated fluorosugars did lead to the development of the phosphorus-based aglycones as discussed in Sections 2.6-2.9. Therefore, efforts to increase the selectivity and efficiency of activated fluorosugars as inactivators of GCase focused on altering the activated aglycone rather than altering the fluorination state of the sugar ring, with a particular emphasis on exploring the use of fluorosugars containing appropriate phosphorus-based aglycones to accomplish this goal.

In terms of substrate mimicry, the 2-deoxy-2-fluoro-glucoside portion of fluorosugar inactivator **2.1** already closely resembles the glucopyranoside ring in the natural substrate, glucosyl ceramide (**3.2**, Figure 3.2). However, the fluorine aglycone in compound **2.1** is not a good mimic of the ceramide moiety as it lacks the size, hydrophobicity and specifically oriented-functional groups of the ceramide chain. Therefore, in searching for more efficient GCase inactivators, it was decided to focus on synthesizing activated fluorosugars with aglycones that might have more significant interactions with the enzyme active site by mimicry of the ceramide aglycone in the natural substrate.

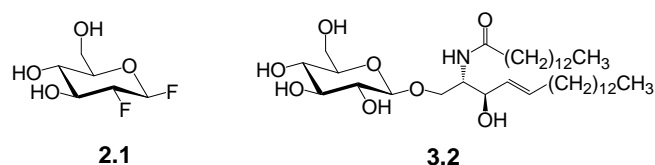


**Figure 3.2.** Structures of the known GCase inactivator 2-deoxy-2-fluoro- $\beta$ -D-glucosyl fluoride (**2.1**) and the natural substrate of GCase, glucosyl ceramide (**3.2**).

### 3.1.4 Target compounds

It was anticipated that incorporation of very specific mimicry of the ceramide aglycone with its stereogenic hydroxyl, amide and alkene functional groups would be extremely challenging. Additionally, it was not necessarily obvious how to incorporate these specifically positioned functional groups in the context of a chemically activated aglycone. Therefore, the focus during the design of the target compounds shifted to the installation of simple hydrophobic groups within the activated aglycone of 2-deoxy-2-fluoro- $\beta$ -D-glucopyranosides, as shown in Figure 3.3.

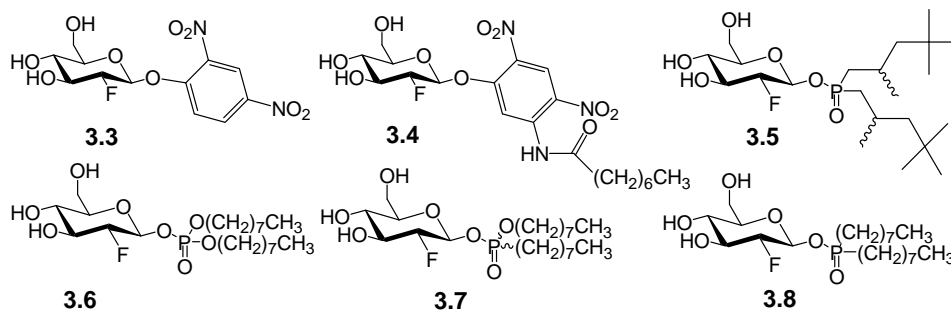


**Figure 3.3.** Structures of the GCase-targeted aglycone variants.

To date, the only activated aglycone that has been used in an activated fluorosugar tested as an inactivator for GCase is fluoride.<sup>211</sup> Surprisingly, the other commonly used activated aglycone, DNP, has not been used as the aglycone in a covalent inactivator for GCase. Therefore, compound **3.3** was chosen as a synthetic target to see if the presence of a hydrophobic DNP aglycone would make **3.3** a more efficient GCase inactivator. A simple derivative of **3.3**, compound **3.4**, was also chosen as a target, where a hydrophobic alkyl

chain had been appended to C5 of the aromatic ring. The choice of an amide as the linker group at the C5 position was made on the basis of the ready availability of the precursor starting materials.

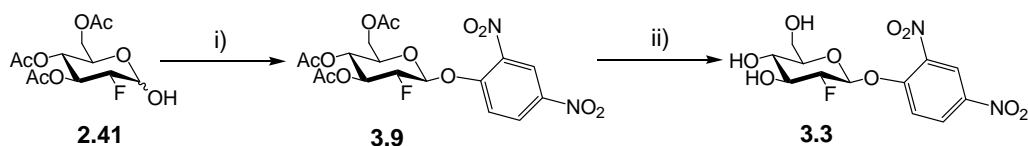
Fluorosugars bearing phosphorus-based aglycones were shown to act as covalent inactivators of a variety of retaining  $\beta$ -glycosidases (Sections 2.6-2.9), therefore a series of phosphate, phosphonate and phosphinate esters with octyl chains attached to the phosphorus atoms were chosen as synthetic targets in an attempt to design novel fluorosugar inactivators of GCase. It was hypothesized that the presence of the two hydrophobic chains might mimic the hydrocarbon chains in the ceramide, thus increasing the specificity and efficiency of these compounds as covalent inactivators of GCase.

Compound **3.5** was chosen as a synthetic target for two reasons. The first reason is that the diisooctyl phosphinic acid precursor is commercially available, so a derivative containing it should be easily prepared. The second reason **3.5** was chosen as a target was as a test of the ability of the GCase active site to accommodate a sterically bulky group that had approximately the same degree of hydrophobicity as **3.8**. Compounds **3.6**, **3.7**, and **3.8** were chosen as synthetic targets since the *n*-octyl chains could potentially act as mimics of the two alkyl chains in the ceramide aglycone in the natural substrate.

### 3.1.5 Chemical synthesis

#### 3.1.4.1 Synthesis of 2,4-dinitrophenyl 2-deoxy-2-fluoro- $\beta$ -D-glucopyranoside (**3.3**) and 5-amido-octyl-2,4-dinitrophenyl 2-deoxy-2-fluoro- $\beta$ -D-glucopyranoside (**3.4**)

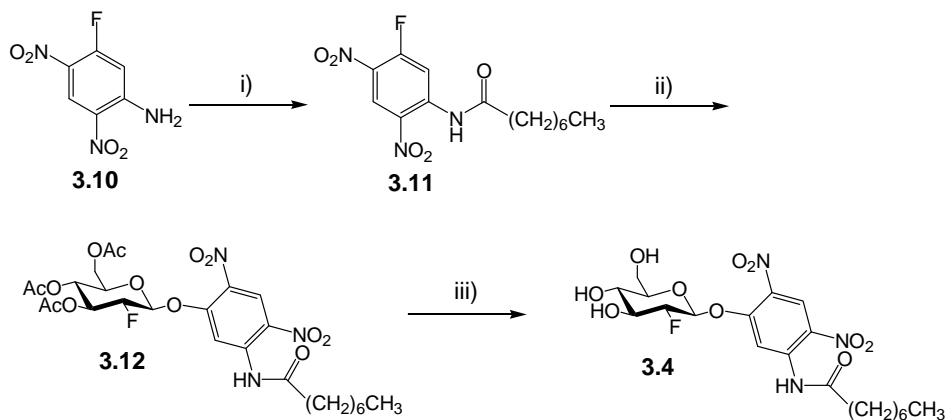
Compound **3.3** was prepared using a previously known<sup>58</sup> synthetic route, as seen in Scheme 3.2.



**Scheme 3.2.** Synthesis of 2,4-dinitrophenyl 2-deoxy-2-fluoro-β-D-glucopyranoside (**3.3**). i) DNFB, DABCO, DMF, 52%; ii) AcCl, MeOH, 74%.

The free hemiacetal **2.41**, available from the attempted synthesis of **2.34**, was reacted with 2,4-dinitrofluorobenzene (DNFB) to give **3.9** (52%). The acetate protecting groups were removed using HCl/MeOH to give **3.3** in reasonable yield (74%). It was necessary to use acidic conditions for the removal of the acetate groups, as under basic conditions the bond between the glycosidic oxygen and the aromatic ring is cleaved through a nucleophilic aromatic substitution reaction.

A similar synthetic route was used to construct **3.4**, as seen in Scheme 3.3.



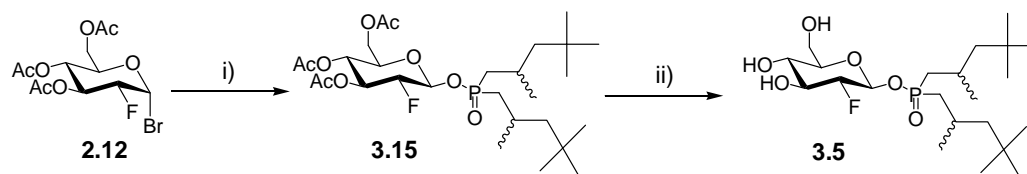
**Scheme 3.3.** Synthesis of 5-amido-octyl-2,4-dinitrophenyl 2-deoxy-2-fluoro-β-D-glucopyranoside (**3.4**). i) Octanoyl chloride, pyridine, toluene, 91%; ii) **2.41**, DABCO, DMF, 43%; iii) AcCl, MeOH, 11%.

The commercially available compound **3.10** was treated with octanoyl chloride and 1 equivalent of pyridine in refluxing toluene for 6 days. The aniline group in **3.10** is an exceptionally poor nucleophile, owing to the presence of three electron-withdrawing groups on the aromatic ring. However, use of a stronger base such as DBU in an attempt to

accelerate the coupling reaction led exclusively to decomposition of **3.10**, possibly arising from polymerization of **3.10** from an intermolecular nucleophilic aromatic substitution reaction. Treatment of **3.11** with the free hemiacetal **2.41** led to the formation of the desired compound **3.12** (43%) along with the unwanted  $\alpha$ -anomer (15%). Removal of the acetate protecting groups using HCl/MeOH did not proceed smoothly, as the major product of the reaction was the deacetylated product in which the amide bond had also been cleaved to yield the free aniline. Attempts to control the rate of this amide bond cleavage side-reaction by varying the reaction time or reaction temperature were unsuccessful, which suggests that the rate of methanol attack at the amide is approximately the same as the corresponding rate of attack on the esters of the acetate groups. Although nucleophilic acyl substitution reactions normally occur much more quickly at esters than amides, this particular amide has a highly electron withdrawing aromatic group attached to it, which renders it considerably more susceptible to nucleophilic acyl substitution. As a result of this significant side reaction, only a small amount (11%) of the desired compound **3.4** was isolated.

3.1.4.2 Synthesis of diisooctyl (2-deoxy-2-fluoro- $\beta$ -D-glucopyranosyl) phosphinate (**3.5**), synthesis of dioctyl (2-deoxy-2-fluoro- $\beta$ -D-glucopyranosyl) phosphate (**3.6**), attempted synthesis of octyl octyl-(2-deoxy-2-fluoro- $\beta$ -D-glucopyranosyl) phosphonate (**3.7**), and attempted synthesis of dioctyl (2-deoxy-2-fluoro- $\beta$ -D-glucopyranosyl) phosphinate (**3.8**).

Compound **3.5** was successfully prepared as a mixture of four diastereomers using the synthetic route shown in Scheme 3.5.



**Scheme 3.5.** Synthesis of diisooctyl (2-deoxy-2-fluoro- $\beta$ -D-glucopyranosyl) phosphinate (**3.5**). i) Diisooctyl phosphinic acid,  $\text{Ag}_2\text{CO}_3$ , MeCN, 67%; ii) NaOMe, MeOH, 78%.



The reaction of the bromide **2.12** with commercially available diisooctyl phosphinic acid, which is available as a mixture of three diastereomers furnished **3.15** in 67% yield as a mixture of four diastereomers. The acetate groups were removed cleanly using NaOMe/MeOH to give **3.5** (78%), also as a mixture of four diastereomers. The aglycone precursor for **3.15**, diisooctyl phosphinic acid, contains three stereogenic centers: at the phosphorus atom, and at both of the tertiary carbons on the two alkyl chains. As a result, there are eight possible stereoisomers for this compound, which are depicted as a series of mirror image compounds using Fischer diagrams in Figure 3.4.

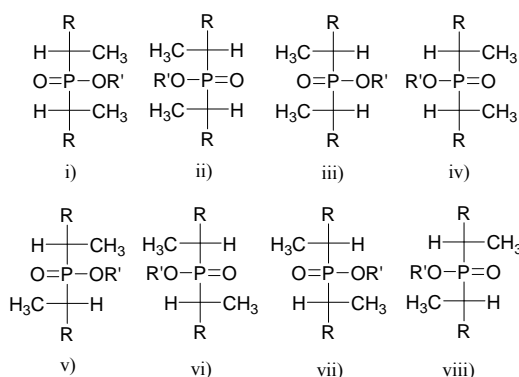


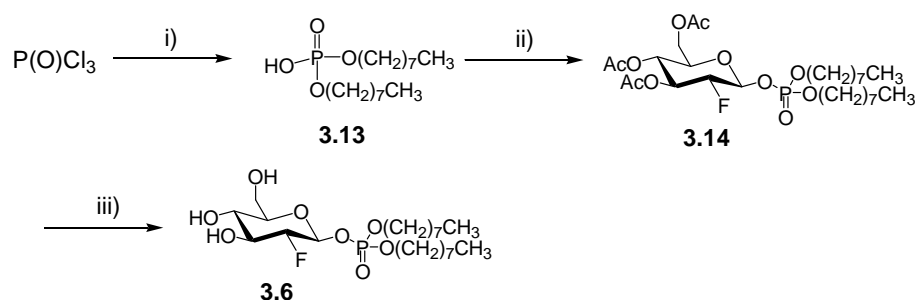
**Figure 3.4.** Fischer diagrams depicting potential stereoisomers of a) diisooctyl phosphinic acid,  $R=CH_2C(CH_3)_3$ ,  $R'=H$  and b) **3.15**,  $R=CH_2C(CH_3)_3$ ,  $R'$ =tetra-O-acetyl-2-deoxy-2-fluoro- $\beta$ -D-glucopyranoside.

The eight possible compounds depicted in Figure 3.4 are drawn beside their potential enantiomeric (mirror-image) compound. However, for structures i), ii), iii) and iv), a plane of symmetry exists through the phosphorus atom, making these structures *meso* and therefore achiral. As a result, structures i) and ii) depict the same stereoisomer, as also do structures iii) and iv). If structure i) is rotated  $180^\circ$ , then it can be seen that this depicts the same structure as ii). Similarly, a  $180^\circ$  rotation shows that structures v) and viii) depict the same structures, as do vi) and vii). In the case of diisooctyl phosphinic acid, the acidic proton can readily bond to either oxygen atom on the phosphorus center and in solution presumably rapidly interconverts between bonding to either oxygen atom, or tautomerizes. Thus, for diisooctyl phosphinic acid in solution, structures i) and iii) will rapidly tautomerize, meaning there are only three distinct stereoisomers present in solution. However, for compound **3.15**, the

phosphinate ester bond does not rapidly interconvert between the two oxygen atoms, meaning there are four distinct stereoisomers present, which can be represented by structures i), iii), v) and vi).

Because both **3.15** and **3.5** were prepared as a mixture of 4 diastereomers, they were characterized by examining their  $^1\text{H}$ ,  $^{19}\text{F}$ , and  $^{31}\text{P}$  NMR spectra, as well as by ESI-MS and EA. The  $^{13}\text{C}$  NMR spectrum was extremely complicated arising both from splitting of the  $^{13}\text{C}$  signals by both the  $^{19}\text{F}$  and  $^{31}\text{P}$  nuclei, and the number of overlapping signals from chemically similar carbon nuclei, making the interpretation of the spectrum obtained exceedingly difficult. It is interesting to note that during the base-catalyzed deprotection of phosphinate **3.5**, no decomposition resulting from attack at the phosphorus center was observed. This result supports the hypothesis that increasing the degree of steric bulk around the phosphorus atom increases the stability of the phosphinate ester towards nucleophilic attack (Section 2.6.2.4).

Compound **3.6** was prepared according to the synthetic route shown in Scheme 3.4.



**Scheme 3.4.** Synthesis of dioctyl (2-deoxy-2-fluoro- $\beta$ -D-glucopyranosyl) phosphate (**3.6**). i) 2 eq. octanol, 1 eq.  $\text{H}_2\text{O}$ ,  $\text{CH}_2\text{Cl}_2$ ; ii)  $\text{Ag}_2\text{CO}_3$ , MeCN, **2.12**, 15% from **2.12**; iii) NaOMe, MeOH, 86%.

The aglycone precursor **3.13** was prepared using a known<sup>246</sup> procedure, then the crude material was coupled with the bromide **2.12** to give compound **3.14** in a poor yield (15% from **2.12**). This low yield arises from the generation of a variety of products in the first step, which generates a mixture of mono-, di- and tri-phosphoric acids, all of which can react with **2.12**. Removal of the acetyl protecting groups proceeded smoothly to give the desired compound **3.6** in an excellent yield (86%).

All attempts to generate the precursor octyl octylphosphonate in a similar fashion to the preparation of the benzyl benzylphosphonic acid **2.65** were unsuccessful. Trioctyl phosphite could not be induced to undergo a Michaelis-Arbuzov rearrangement using octyl iodide or octyl bromide, despite prolonged heating or the addition of acid catalysts. Similarly, the synthetic method used to prepare dibenzyl phosphinic acid (**2.68**) was unsuccessful in preparing dioctyl phosphinic acid. This is presumably due to the fact that the alkyl bromide, such as in octyl bromide, is much less reactive towards displacement reactions compared to the benzylic bromide.

### 3.1.6 Kinetic analysis of the inactivation of Abg by **3.4**, **3.5** and **3.6**

Compounds **3.4**, **3.5** and **3.6** were tested as inactivators of Abg since Abg is known to have a relaxed tolerance towards substrates and inhibitors with lipophilic aglycones.<sup>14,116</sup> However, since Abg and GCase belong to different sequence-related families (families GH1 and GH30 respectively), their active site architectures are presumably different, particularly with respect to the aglycone subsites. This is seen in structural studies with the homology model constructed for Abg<sup>125</sup> (based on the X-ray crystal structures of other GH1 glycoside hydrolases) and the X-ray crystal structures of GCase,<sup>218-220,222-224</sup> showing substantial differences in the residues in the active sites. This is a consequence of the differences in the natural substrates of the two enzymes. Thus, compounds that are considerably more potent inactivators of GCase than of Abg are assumed to interact more favourably with the GCase aglycone binding site.

#### 3.1.5.1 5-Amidooctyl-2,4-dinitrophenyl 2-deoxy-2-fluoro- $\beta$ -D-glucopyranoside (**3.4**)

5-Amidooctyl-2,4-dinitrophenyl 2-deoxy-2-fluoro- $\beta$ -D-glucopyranoside (**3.4**) was tested as an inactivator of Abg. Compound **3.4** was only sparingly soluble in water at millimolar concentrations, thus stock solutions were made in methanol. Fortunately however, while the compound was not soluble enough to make stock solutions, it was sufficiently soluble in water at the concentrations needed for the inactivation assay with Abg. The resulting activity versus time plot for various concentrations of inactivator, and a re-plot of

the individual  $k_{\text{obs}}$  values plotted as a function of inhibitor concentration are shown in Figure 3.5.

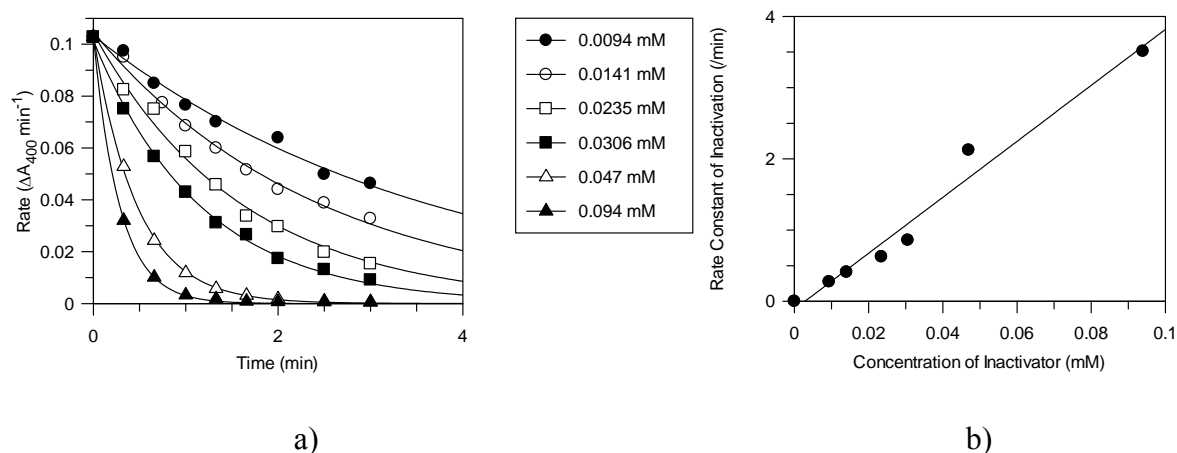


**Figure 3.5.** Inactivation of Abg with **3.4**. a) Non-linear plot of residual enzyme activity versus time at the indicated inactivator concentrations fitted to an exponential decay equation. b) Plot of the observed rate constants of inactivation versus concentration of inactivator.

The measurement of inactivation rates at saturating concentrations of inactivator was not possible owing to very rapid inactivation, thus only concentrations up to 0.094 mM could be studied. A second order rate constant of inactivation,  $k_i/K_i$  of  $40 \text{ min}^{-1}\text{mM}^{-1}$  was derived from the slope of the linear plot obtained, making **3.4** the third most efficient fluorosugar inactivator reported for Abg (after 2,4-dinitrophenyl  $\beta$ -D-glucopyranoside **3.3**,  $k_i/K_i = 500 \text{ min}^{-1}\text{mM}^{-1}$  and 5-fluoro- $\beta$ -D-glucopyranosyl fluoride **2.2**,  $k_i/K_i = 660 \text{ min}^{-1}\text{mM}^{-1}$ ). The addition of the hydrophobic octyl chain bonded to the dinitrophenyl ring in **3.4** leads to a 12.5-fold decrease in inactivator efficiency compared to the parent dinitrophenyl glucoside **3.3**. Since the presence of this alkyl chain makes **3.4** a more hydrophobic molecule than **3.3**, it had been hoped that this would increase the affinity of **3.4** for the enzyme active site. The fact that the more hydrophobic **3.4** is actually a less efficient inactivator than **3.3** suggests that the octyl amide on C5 of the DNP ring forms unfavourable steric and/or electronic interactions with the enzyme active site.

To test for the presence of a highly reactive impurity, Abg (17  $\mu\text{M}$ ) was incubated with a 10-fold excess of inhibitor (118  $\mu\text{M}$ ) for 14 min, after which the reaction was halted

by dilution and the residual enzyme activity was determined to be 4% of the starting activity. This is essentially identical to the 1% residual enzyme activity observed in control experiments when using a vast excess of inactivator (118  $\mu$ M) relative to enzyme (0.017  $\mu$ M). The fact that the inhibitor solution is still able to inactivate Abg at these relative concentrations means that a potential highly reactive contaminant, should it be present, would have to constitute at least 10% of the inactivator preparation, an amount that would be readily detected by both TLC and NMR analyses. Therefore it is concluded that **3.4** is the true inactivator.

#### 3.1.5.2 Diisooctyl (2-deoxy-2-fluoro- $\beta$ -D-glucopyranosyl) phosphinate (**3.5**)

The mixture of four diastereomers of diisooctyl (2-deoxy-2-fluoro- $\beta$ -D-glucopyranosyl) phosphinate (**3.5**) was tested as an inactivator of Abg. Unfortunately, the only time-dependent inactivation of Abg that was observed could be traced to the presence of a highly reactive contaminant. When a solution of **3.5** was tested as a reversible inhibitor of Abg in a similar manner to the testing of **2.4**, **2.6**, **2.7** and **2.8** as inhibitors of Abg (Section 2.4.1.5), no inhibition could be observed at the highest concentration tested (0.564 mM). On the basis of these results, it was concluded that **3.5** does not bind to the active site of Abg, presumably as a consequence of the sterically demanding isooctyl groups not being accommodated by the enzyme.

#### 3.1.5.3 Dioctyl (2-deoxy-2-fluoro- $\beta$ -D-glucopyranosyl) phosphate (**3.6**)

Dioctyl (2-deoxy-2-fluoro- $\beta$ -D-glucopyranosyl) phosphate (**3.6**) was tested as an inactivator of Abg. Compound **3.6** was only sparingly soluble in water at millimolar concentrations, thus stock solutions were made in methanol. Fortunately however, while the compound was not soluble enough to make stock solutions, it was sufficiently soluble in water at the concentrations needed for the inactivation assay with Abg. The resulting activity vs. time curve for various [I] and a re-plot of the individual  $k_{\text{obs}}$  values plotted as a function of inhibitor concentration are shown for **3.6** in Figure 3.6.

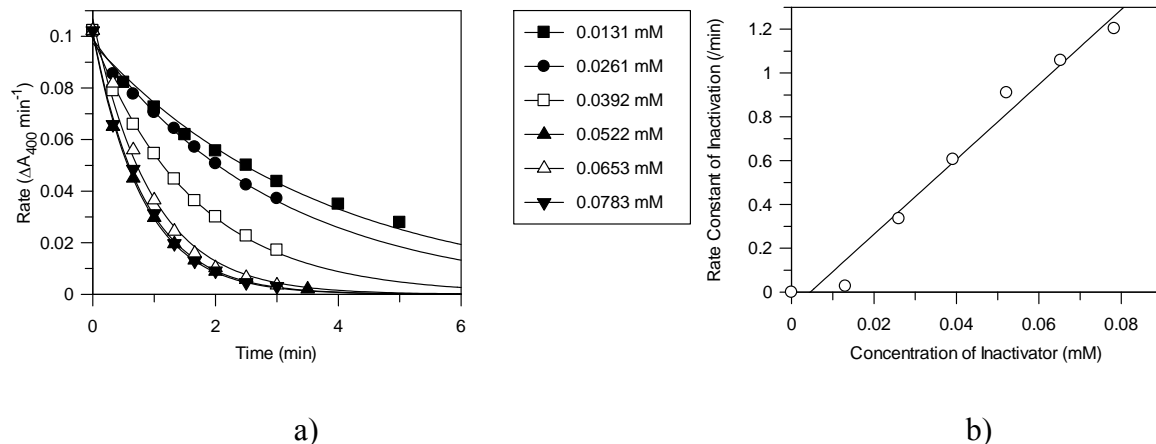


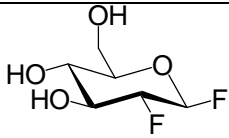
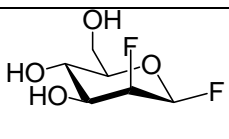
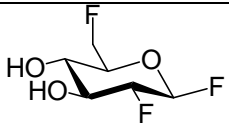
**Figure 3.6.** Inactivation of Abg with **3.6**. a) Non-linear plot of residual enzyme activity versus time at the indicated inactivator concentrations fitted to an exponential decay equation. b) Plot of the observed rate constants of inactivation versus concentration of inactivator.

The measurement of inactivation rates at saturating concentrations of inactivator was not possible owing to very rapid inactivation, thus only concentrations up to 0.078 mM could be measured. A second order rate constant of inactivation,  $k_i/K_i$  of  $17 \text{ min}^{-1}\text{mM}^{-1}$  was derived from the slope of the linear plot obtained. The fact that the straight-chain octyl groups in **3.6** were well-tolerated by the enzyme, while the branched-chain octyl groups in **3.5** were not, supports the hypothesis that the enzyme is unable to accommodate bulky groups such as the isooctyl chains.

Compound **3.6** is the most efficient of the phosphorus-based aglycone inactivators of Abg tested, although the difference between the most efficient (**3.6**,  $k_i/K_i = 17 \text{ min}^{-1}\text{mM}^{-1}$ ) and least efficient (**2.37**,  $k_i/K_i = 1.23 \text{ min}^{-1}\text{mM}^{-1}$ ) is small. Despite the significant chemical differences between methyl, benzyl and octyl groups, only a 14-fold difference in inactivator efficiency was observed. This suggests that the phosphorus-based inactivators do not specifically interact with the enzyme's aglycone subsite.

### 3.1.6 Kinetic analysis of the inactivation of GCase by 2.2, 2.3, 2.37, 2.62, 2.67, 2.70, 2.71, 3.3, 3.4, 3.5 and 3.6.

Unlike Abg, GCase has only been tested with a small number of fluorosugar inactivators. Table 3.1 summarizes the known activated fluorosugar inactivators of GCase, along with their respective kinetic parameters of inactivation. It is worth noting that the covalent inactivator with the highest efficiency against GCase, **2.1**, is still more than 600 times less efficient as an inactivator of GCase than it is of Abg, as judged by the magnitude of the respective  $k_i/K_i$  values.

Compound	$k_i$ ( $\text{min}^{-1}$ )	$K_i$ (mM)	$k_i/K_i$ ( $\text{min}^{-1}\text{mM}^{-1}$ )	Reference
 <b>2.1</b>	--	--	0.0227	211
 <b>3.16</b>	--	--	0.0019	247
 <b>3.17</b>	0.17	101	0.0017	248

**Table 3.1.** Kinetic parameters for known activated fluorosugar inactivators of GCase.

Since GCase cleaves mannosides in addition to glucosides, all of the *gluco*- and *manno*- configured inhibitors prepared in Sections 2.6 and 2.8 were also tested as

inactivators of GCase. All the results of these experiments are presented in Table 3.2 (page 150).

### 3.1.6.1 2,4-Dinitrophenyl 2-deoxy-2-fluoro- $\beta$ -D-glucopyranoside (**3.3**)

2,4-Dinitrophenyl 2-deoxy-2-fluoro- $\beta$ -D-glucopyranoside (**3.3**) was tested as an inactivator of GCase. The resulting activity vs. time curve for various [I] and a re-plot of the individual  $k_{\text{obs}}$  values plotted as a function of inhibitor concentration are shown for **3.3** in Figure 3.7.

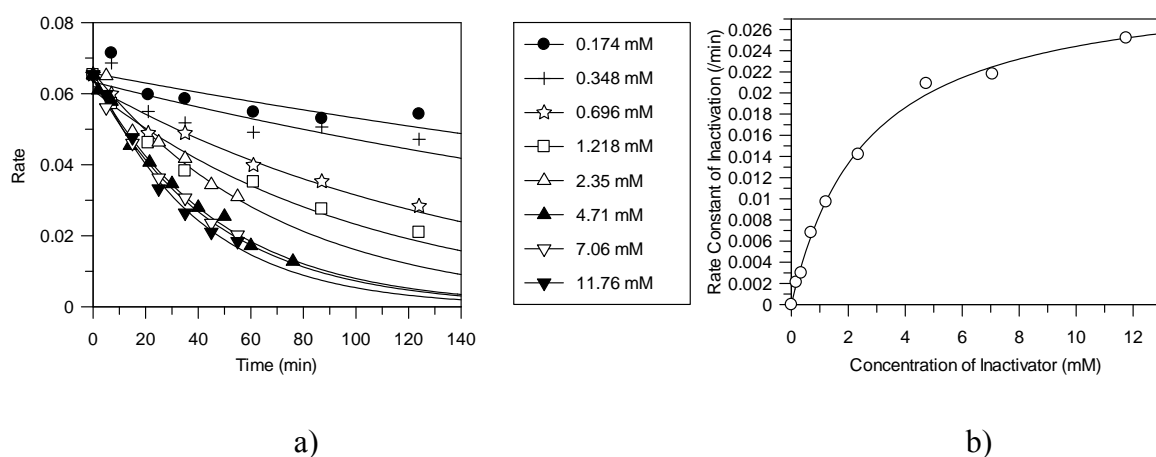


**Figure 3.7.** Inactivation of GCase with **3.3**. a) Non-linear plot of residual enzyme activity versus time at the indicated inactivator concentrations fitted to an exponential decay equation. b) Plot of the observed rate constants of inactivation versus concentration of inactivator.

Gcase is inactivated only two-fold less efficiently by **3.3** than by **2.1** ( $k_i/K_i = 0.012 \text{ min}^{-1}\text{mM}^{-1}$  and  $k_i/K_i = 0.023 \text{ min}^{-1}\text{mM}^{-1}$ , respectively). However, while concentrations approaching saturation could not be tested owing to the rapidity of inactivation by **2.1**, individual values of  $k_i = 0.030 \text{ min}^{-1}$  and  $K_i = 2.5 \text{ mM}$  could be obtained for **3.3** as an inactivator of GCase. The fact that individual kinetic parameters could be obtained for **3.3**, but not for **2.1**, allows some guesses to be made regarding the nature of the interactions that these two aglycones make with the enzyme active site. Because there is only a two-fold



difference in second-order rate constants of inactivation for both compounds, relative comparisons should be possible. Since saturation is observed for **3.3**, this means that the  $K_i$  value for **2.1** must be higher than for **3.3**. Therefore, the  $k_i$  value for **2.1** should be higher than for **3.3**, since inactivation becomes too rapid at higher concentrations that are still below saturation for **2.1**. This is supported by the fact that 2,6-dideoxy-2,6-difluoro- $\beta$ -D-glucopyranosyl fluoride (**3.17**), which is a less efficient inactivator than **3.3**, still has a higher  $k_i$  value ( $0.17 \text{ min}^{-1}$ ) than does **3.3** ( $0.030 \text{ min}^{-1}$ ). This suggests that the efficiency of **3.3** arises from a more favourable  $K_i$  value (2.5 mM) than for **2.1**, and that the DNP ring is bound in the GCCase active site tighter than fluoride. Conversely, the efficiency of **2.1** as an inactivator must arise from the fluoride leaving group being better accommodated in the enzymatic active site during the glycosylation transition state, which is reflected as a higher value for  $k_i$ .

#### 3.1.6.2 5-Amidooctyl-2,4-dinitrophenyl 2-deoxy-2-fluoro- $\beta$ -D-glucopyranoside (**3.4**)

5-Amidooctyl-2,4-dinitrophenyl 2-deoxy-2-fluoro- $\beta$ -D-glucopyranoside (**3.4**) was tested as an inactivator of GCCase. Owing to the poor solubility of **3.4** in water at millimolar concentrations, stock solutions were made up in methanol. Unfortunately, no time-dependent inactivation was observed, even at the highest concentration of **3.4** tested (4.70 mM). It was not possible to test yet higher concentrations of inactivator owing to the poor solubility of the compound, and the fact that high levels of methanol from the inactivator stock solution strongly inhibited enzyme activity. Compound **3.4** was also tested as a reversible inhibitor of GCCase in a similar manner to that described in Section 2.4.1.5. At the highest concentration tested (4.70 mM), the only inhibition was traced to the presence of methanol in the solution which came from the stock solution of **3.4**. Therefore, it was concluded that this compound does not bind to the active site of GCCase.

The finding that **3.4** is not an inactivator of GCCase and was only a modest inactivator of Abg are disappointing and indicate that bulky substituents on the aromatic ring are not well tolerated. Owing to the lack of success in finding a more potent GCCase inactivator using

the strategy of appending hydrophobic groups onto the aromatic ring of the DNP aglycone, further derivatives in this class of compound were not explored.

#### 3.1.6.3 5-Fluoro- $\beta$ -D-glucopyranosyl fluoride (**2.2**) and 5-fluoro- $\alpha$ -L-idopyranosyl fluoride (**2.3**)

5-Fluoro- $\beta$ -D-glucopyranosyl fluoride (**2.2**) and 5-fluoro- $\alpha$ -L-idopyranosyl fluoride (**2.3**) were both tested as inactivators of GCCase. Surprisingly, neither compound showed any time-dependent inactivation of GCCase, even at the highest concentrations tested (5.12 mM and 6.47 mM, respectively). Given that 5-fluoro glycosyl fluorides are more labile compounds towards spontaneous decomposition in aqueous solution than 2-deoxy-2-fluoro glycosyl fluorides, it was possible that the more acidic GCCase assay buffer (pH 5.5) was causing these compounds to hydrolyze much more rapidly than in the Abg assay buffer (pH 6.8). To test this possibility, separate samples of **2.2** ( $[2.2] = 35.4 \mu\text{M}$ ) were incubated in either GCCase assay buffer at pH 5.5 or in Abg assay buffer at pH 6.8 for 10 minutes. The samples so treated were then diluted into pH 6.8 buffer containing Abg, and incubated for 2 minutes before assaying residual Abg activity. The residual Abg activity observed for inactivator incubated in pH 6.8 buffer was 3%, which was essentially identical to the residual enzyme activity for inactivator incubated in pH 5.5 buffer (2%). This demonstrates that the inability of these compounds to behave as covalent inactivators of GCCase is not due to spontaneous hydrolysis in the acidic assay buffer.

It is also possible that both compounds act as substrates for GCCase rather than inactivators, and thus the rate of formation of the covalent glycosyl-enzyme intermediate is approximately equal to the rate of its hydrolysis. To test this possibility, a TLC assay of GCCase incubated with either **2.2** or **2.3** was performed. In both cases, the rates of hydrolysis of **2.2** or **2.3** were the same in the presence and absence of enzyme, indicating that the hydrolysis is not enzyme-catalyzed. Both compounds were tested as reversible inhibitors of GCCase in a similar manner to that described in Section 2.4.1.5, but neither compound showed any inhibition of GCCase activity. This inability of **2.2** and **2.3** to bind to GCCase is somewhat

surprising given that the 5-fluoro-glycosyl fluorides **2.2** and **2.3** are effective inactivators of Abg.

#### 3.1.6.4 Dimethyl (2-deoxy-2-fluoro- $\beta$ -D-glucopyranosyl) phosphate (**2.37**)

Dimethyl (2-deoxy-2-fluoro- $\beta$ -D-glucopyranosyl) phosphate (**2.37**) was tested as a time-dependent covalent inactivator of GCCase. The resulting activity vs. time curves for various [I] and a re-plot of the individual  $k_{\text{obs}}$  values as a function of inhibitor concentration are shown for **2.37** in Figure 3.8.

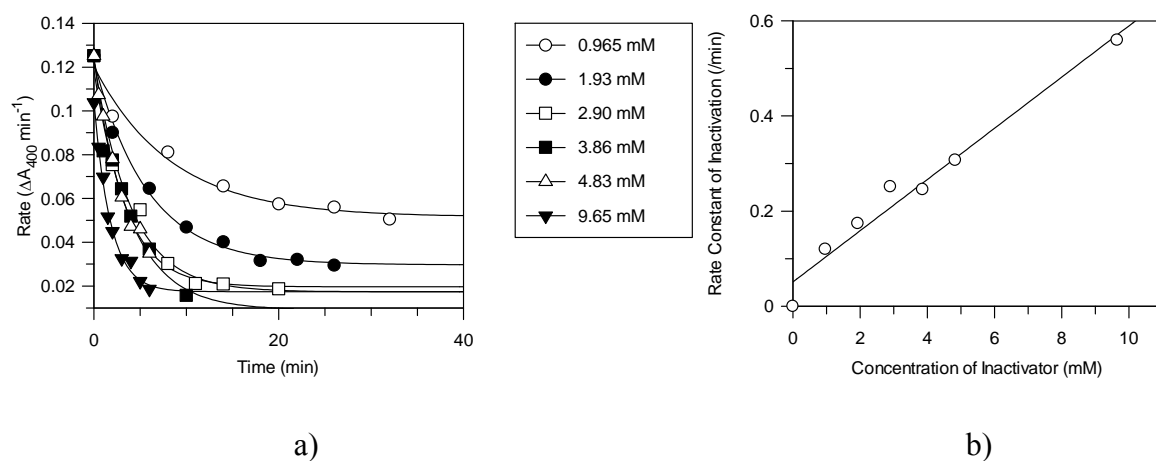


**Figure 3.8.** Inactivation of GCCase with **2.37**. a) Non-linear plot of residual enzyme activity versus time at the indicated inactivator concentrations fitted to an exponential decay equation. b) Plot of the observed rate constants of inactivation versus concentration of inactivator.

Measurement of inactivation rates at saturating concentrations of inactivator was not possible owing to very rapid inactivation, thus only concentrations up to 9.65 mM could be measured. However, a second order rate constant of inactivation,  $k_i/K_i$  of  $0.052 \text{ min}^{-1}\text{mM}^{-1}$  was derived from the slope of the linear plot obtained. Compound **2.37** is therefore a somewhat more efficient inactivator of GCase than either **2.1** or **3.3**. This result stands in contrast to those with Abg, for which almost all the phosphorus-based aglycones were comparatively less efficient inactivators of the enzyme. This may mean that the tetra-coordinate phosphorus atom in the aglycone of **2.37** is better accommodated in the GCase active site than in the active site of Abg.

#### 3.1.6.5 Dibenzyl (2-deoxy-2-fluoro- $\beta$ -D-glucopyranosyl) phosphate (**2.62**), benzyl benzyl-(2-deoxy-2-fluoro- $\beta$ -D-glucopyranosyl) phosphonate (**2.67**) and dibenzyl (2-deoxy-2-fluoro- $\beta$ -D-glucopyranosyl) phosphinate (**2.70**)

Dibenzyl (2-deoxy-2-fluoro- $\beta$ -D-glucopyranosyl) phosphate (**2.62**) was tested as a covalent inactivator of GCase. The resulting activity vs. time curve for various  $[I]$  and a re-plot of the individual  $k_{\text{obs}}$  values as a function of inhibitor concentration are shown for **2.62** in Figure 3.9.

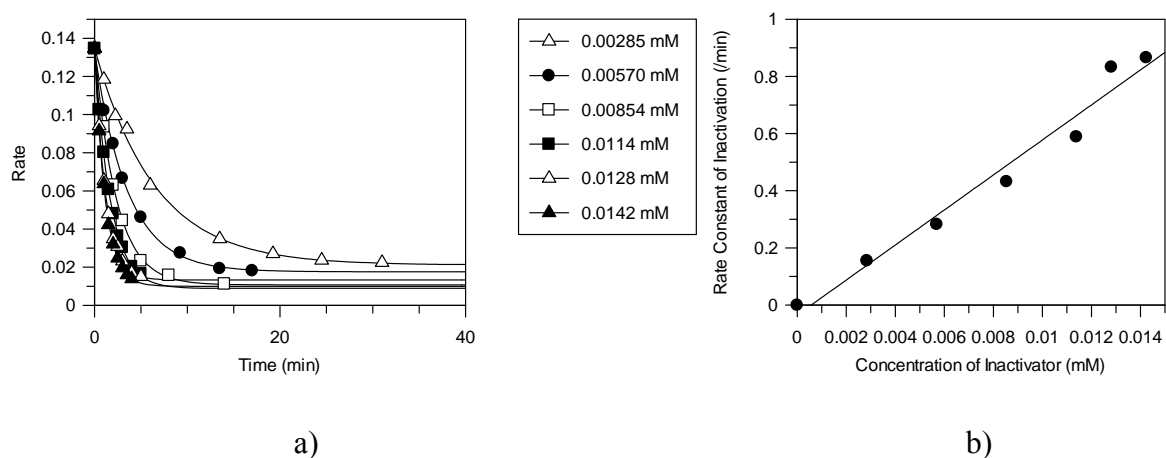


**Figure 3.9.** Inactivation of GCase with **2.62**. a) Non-linear plot of residual enzyme activity versus time at the indicated inactivator concentrations fitted to an exponential decay equation. b) Plot of the observed rate constants of inactivation versus concentration of inactivator.

Dibenzyl phosphate derivative **2.62** was a highly efficient time-dependent inactivator of GCase; indeed measurement of inactivation rates at saturating concentrations of inactivator was not possible owing to very rapid inactivation, thus only concentrations up to 0.0142 mM could be studied. However, a second order rate constant of inactivation of  $k_i/K_i = 61 \text{ min}^{-1}\text{mM}^{-1}$  was derived from the slope of the linear plot obtained. Remarkably, **2.62** is a >1100-fold more efficient inactivator than the dimethyl derivative **2.37**, and is >2600-fold more efficient than **2.1**, the previously most effective inactivator of GCase. This huge gain in inactivator efficiency is almost certainly due to the formation of specific interactions between the dibenzyl phosphate aglycone and the enzyme active site and stands in contrast to the slight increase in efficiency between the dimethyl phosphate ( $k_i/K_i = 1.23 \text{ min}^{-1}\text{mM}^{-1}$ ) and dibenzyl phosphate ( $k_i/K_i = 8.0 \text{ min}^{-1}\text{mM}^{-1}$ ) derivatives as inactivators of Abg. The effectiveness of compound **2.62** as an inactivator of GCase is an excellent demonstration of the ability to build specificity for a given enzyme active site into the phosphorus-based aglycone.

Benzyl benzyl-(2-deoxy-2-fluoro- $\beta$ -D-glucopyranosyl) phosphonate (**2.67**) and dibenzyl (2-deoxy-2-fluoro- $\beta$ -D-glucopyranosyl) phosphinate (**2.70**) were also found to be excellent time-dependent covalent inactivators of GCase. The resulting activity vs. time curve for various [I] and a re-plot of the individual  $k_{\text{obs}}$  values plotted as a function of inhibitor concentration are shown for **2.67** in Figure 3.10, and for **2.70** in Figure 3.11.

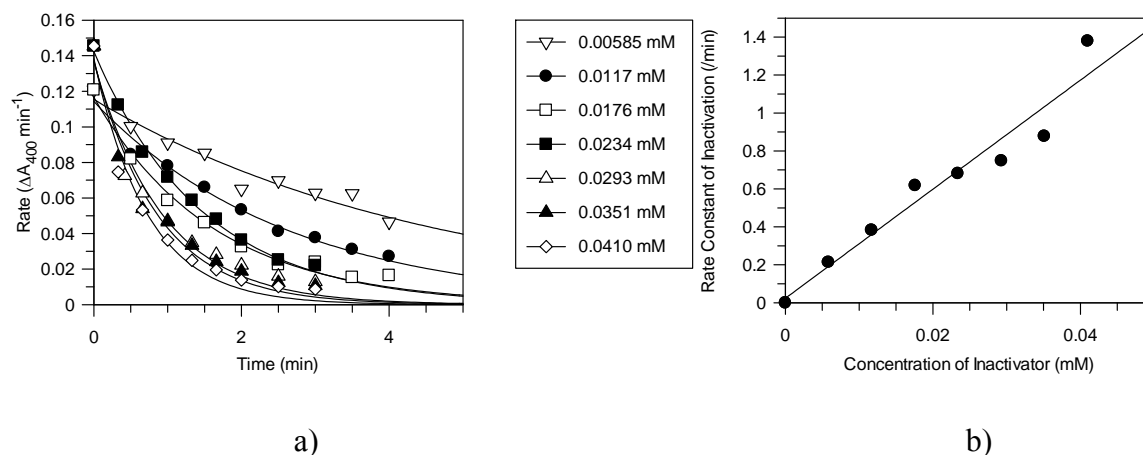


**Figure 3.10.** Inactivation of GCase with **2.67**. a) Non-linear plot of residual enzyme activity versus time at the indicated inactivator concentrations fitted to an exponential decay equation. b) Plot of the observed rate constants of inactivation versus concentration of inactivator.

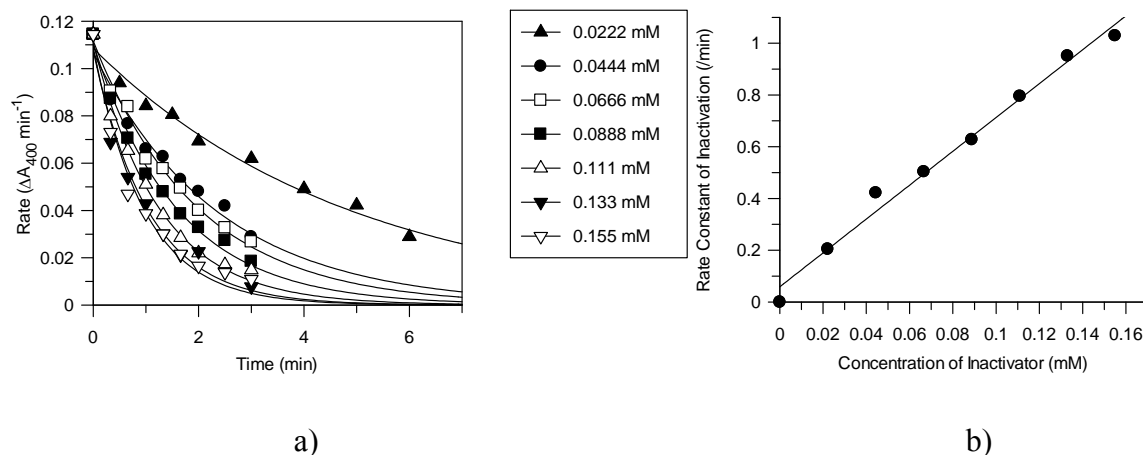


**Figure 3.11.** Inactivation of GCase with **2.70**. a) Non-linear plot of residual enzyme activity versus time at the indicated inactivator concentrations fitted to an exponential decay equation. b) Plot of the observed rate constants of inactivation versus concentration of inactivator.

Compound **2.67**, tested as a mixture of diastereomers at the phosphorus atom as previously described for Abg (Section 2.7.1.3), is also a remarkably effective inactivator of GCase. Again, measurement of inactivation rates at saturating concentrations of inactivator was not possible owing to very rapid inactivation, but a second order rate constant of inactivation  $k_i/K_i = 29 \text{ min}^{-1}\text{mM}^{-1}$  was derived from the slope of the linear plot obtained at

concentrations up to 0.041 mM. Thus, **2.67** inactivated GCase only two-fold slower than **2.62**, despite the presumed difference in leaving group ability between the phosphate and phosphonate leaving groups. The phosphinate **2.70** was tested as an impure mixture as previously described (Section 2.7.1.4), and again measurement of inactivation rates at saturating concentrations of inactivator was not possible owing to very rapid inactivation, thus only concentrations up to 0.22 mM could be measured. A second order rate constant of inactivation of  $k_i/K_i = 6.5 \text{ min}^{-1}\text{mM}^{-1}$  was derived from the slope of the linear plot obtained. As previously noted, this value should be taken as a lower limit of the true inactivation constant, since the mixture is known to contain approximately 30% of an enzymatically-inactive compound as determined by  $^1\text{H}$  NMR.

This series of fluorosugars bearing phosphorus-based aglycones containing two benzyl groups shows the expected trend in reactivity with GCase predicted by the relative  $\text{pK}_a$  values of the corresponding free acids, with fluorosugars bearing aglycones with lower  $\text{pK}_a$  values being more efficient inactivators. It is tempting to ascribe these differences in enzymatic reactivity directly to the presumed differences in chemical reactivity, as reflected by  $\text{pK}_a$  values. However, it is the  $k_i$  value that is reflective of the transition state energies relative to the ground state energies, and none of the three compounds tested (**2.62**, **2.67** and **2.70**) as inactivators of GCase yielded individual kinetic parameters for  $k_i$  or  $K_i$ , only the second-order rate constant of inactivation,  $k_i/K_i$ . Since  $k_i/K_i$  is a measure of the rate of free enzyme and free inactivator forming the covalent complex, the affinity of the enzyme for the phosphate, phosphonate or phosphinate must also be taken into account in this type of analysis. It was seen with Abg for the two compounds in which individual  $k_i$  and  $K_i$  values could be obtained, **2.62** and **2.70**, that differences in the apparent dissociation constant  $K_i$  appeared more significant than differences in the transition state energy, as reflected in  $k_i$ . Therefore, the factors contributing to the observed trend in reactivity of **2.62**, **2.67** and **2.70** acting as inactivators of GCase cannot be individually identified.

#### 3.1.6.6 Dioctyl (2-deoxy-2-fluoro- $\beta$ -D-glucopyranosyl) phosphate (**3.6**)

Dioctyl (2-deoxy-2-fluoro- $\beta$ -D-glucopyranosyl) phosphate (**3.6**) proved to be the best time-dependent covalent inactivator of GCase yet; the activity vs. time curve for various  $[\text{I}]$

and a re-plot of the individual  $k_{\text{obs}}$  values as a function of inhibitor concentration are shown for **3.6** in Figure 3.12 and these yielded a second order rate constant of  $k_i/K_i = 98 \text{ min}^{-1}\text{mM}^{-1}$ . Thus, **3.6** is a 4300-fold faster inactivator of GCase than is the fluoride **2.1**, but only 1.6-fold faster than the dibenzyl phosphate derivative **2.62**. Since the benzyl (seven carbons) and octyl (eight carbons) substituents are of similar hydrophobicity, it would appear that hydrophobicity is the major determining factor in the efficiency of inactivation. However, the synthesis of the dibenzyl derivatives is considerably simpler.

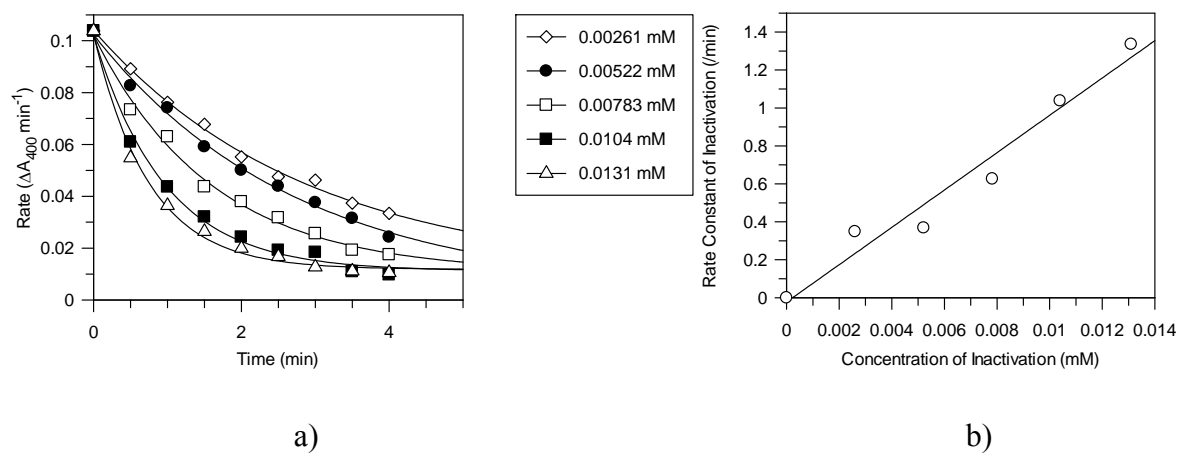


**Figure 3.12.** Inactivation of GCase with **3.6**. a) Non-linear plot of residual enzyme activity versus time at the indicated inactivator concentrations fitted to an exponential decay equation. b) Plot of the observed rate constants of inactivation versus concentration of inactivator.

#### 3.1.6.7 Benzyl benzyl-(2-deoxy-2-fluoro- $\beta$ -D-mannopyranosyl) phosphonate (**2.71**)

The activity vs. time curve for various  $[I]$ , and a re-plot of the individual  $k_{\text{obs}}$  values plotted as a function of inhibitor concentration, are shown in Figure 3.13 for the testing of benzyl benzyl-(2-deoxy-2-fluoro- $\beta$ -D-mannopyranosyl) phosphonate (**2.71**) as an inactivator of GCase. Measurement of inactivation rates at saturating concentrations of inactivator was not possible owing to very rapid inactivation, and only a second order rate constant of inactivation  $k_i/K_i = 40 \text{ min}^{-1}\text{mM}^{-1}$  was derived from the slope of the linear plot obtained from testing of concentrations up to 0.0715 mM. This slight increase in efficiency for the *manno*-configured inactivator **2.71** compared to the *gluco*-configured inactivator **2.67** ( $k_i/K_i = 29 \text{ min}^{-1}\text{mM}^{-1}$  versus GCase) was also observed when these two compounds were tested as



inactivators of Abg. This is slightly puzzling, because this trend is not observed for the analogous compounds with fluoride as the leaving group (compounds **2.1** and **3.16**). Therefore, this unexpected efficiency of **2.71** as an inactivator of GCase and Abg may reflect increased steric compression in the ground state between the fluorine at C2 and the bulky dibenzyl phosphorus aglycone at the anomeric center.

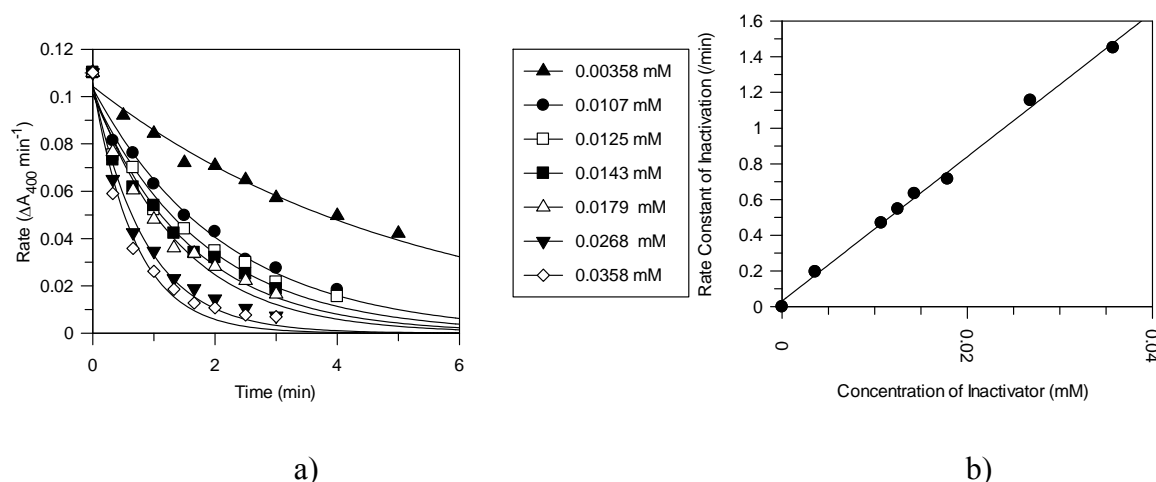


**Figure 3.13.** Inactivation of GCase with **2.71**. a) Non-linear plot of residual enzyme activity versus time at the indicated inactivator concentrations fitted to an exponential decay equation. b) Plot of the observed rate constants of inactivation versus concentration of inactivator.

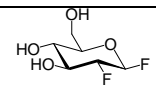
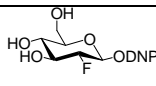
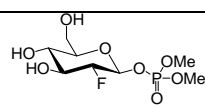
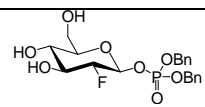
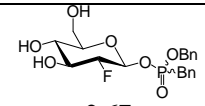
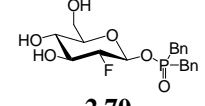
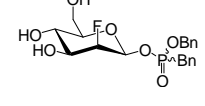
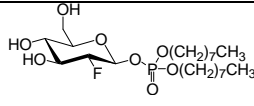
#### 3.1.6.8 Diisooctyl (2-deoxy-2-fluoro- $\beta$ -D-glucopyranosyl) phosphinate (**3.5**)

Diisooctyl (2-deoxy-2-fluoro- $\beta$ -D-glucopyranosyl) phosphinate (**3.5**) proved not to be a time-dependent inactivator, even at the highest concentration tested (4.16 mM). Nor was it a reversible inhibitor of GCase, the only inhibition detected at a concentration of 4.16 mM being traced to the presence of methanol. This shows that **3.5** does not bind to the active site of GCase, presumably as a consequence of the sterically demanding isooctyl groups.

When a solution of **3.5** was previously tested as an inactivator of Abg it was found that the preparation was contaminated with a very minute amount of a highly active impurity, as described in Section 3.1.5.2. The presence of the impurity could not be detected when tested against GCase. This would be expected if the impurity is a compound which is much more highly active against Abg than against GCase, such as **2.1**.

### **3.1.8 Conclusions and future considerations**

The kinetic parameters of inactivation for the compounds which successfully inactivated GCase are summarized in Table 3.2.

Compound	$k_i$ ( $\text{min}^{-1}$ )	$K_i$ (mM)	$k_i/K_i$ ( $\text{min}^{-1}\text{mM}^{-1}$ )	Reference
 <b>2.1</b>	--	--	0.0227	211
 <b>3.3</b>	0.030	2.5	0.012	This work
 <b>2.37</b>	--	--	0.052	This work
 <b>2.62</b>	--	--	61	This work
 <b>2.67</b>	--	--	29	This work
 <b>2.70</b>	--	--	6.5*	This work
 <b>2.71</b>	--	--	40	This work
 <b>3.6</b>	--	--	98	This work

\* = Contaminated with ~30% of an inactive compound

**Table 3.2.** Kinetic parameters for selected activated fluorosugars as inactivators of GCCase.

Compound **3.6** is the most efficient covalent inactivator of GCCase found to date. However, phosphate-based aglycones are only modestly stable towards spontaneous hydrolysis via glycosidic bond fission, shown in Section 2.7.3 where the half-life in aqueous solution for the dibenzyl phosphate derivative **2.62** was shown to be approximately 15 minutes. Attempted syntheses of dioctyl phosphonate- and phosphinate-based aglycones were unsuccessful. Since there was only a 1.6-fold difference in inactivator efficiency ( $k_i/K_i$ ) for GCCase between the dibenzyl phosphate **2.62** and the dioctyl phosphate **3.6**, it was decided that phosphorus-based aglycones bearing benzyl groups represented an excellent compromise between inactivator efficiency and ease of synthetic access. Within the series of compounds bearing two benzyl groups on the phosphorus-based aglycone, **2.67** represented an excellent balance between stability towards spontaneous hydrolysis and efficiency as an inactivator of GCCase, and was therefore chosen as the compound of interest to pursue in pharmacological chaperone studies with GCCase (Chapter 4).

## 3.2 $\alpha$ -L-Iduronidase (Idua)

### 3.2.1 General introduction

Human  $\alpha$ -L-iduronidase (Idua) is a soluble glycosidase belonging to family GH39 (<http://www.cazy.org/>) that cleaves terminal iduronic acid residues with retention of stereochemistry at the anomeric center. This lysosomal glycoprotein has been postulated to exist as part of a multi-enzyme complex<sup>249,250</sup> that is responsible for the degradation of heparan sulfate and dermatan sulfate, as described in Section 1.4.5. It does not appear to require any activators or cofactors for enzyme activity either *in vivo* or *in vitro*.<sup>101,250-253</sup> On the basis of bioinformatics studies, some of the active site residues of Idua have been predicted,<sup>254</sup> and experimentally confirmed by kinetic analysis of mutants.<sup>255</sup> The enzymatic nucleophile was identified by these approaches as Glu 299, and experimentally confirmed by using an active-site directed covalent inactivator,<sup>173</sup> as described in Section 3.2.2.

To date, no experimentally determined three dimensional structure of Idua has been reported. Preliminary studies to obtain crystals suitable for X-ray crystallography have only

led to aggregated Idua that has amyloid-like properties.<sup>256,257</sup> A three dimensional computer-generated homology model of Idua has been constructed on the basis of the experimentally determined X-ray crystal structure of a sequence-related xylosidase from *Thermoanaerobacterium saccharolyticum*, which also belongs to family GH39.<sup>258</sup> This homology model has offered some insights into possible genotype-phenotype correlations,<sup>259</sup> although such correlations are complicated by many other factors in a patient's genetic background.<sup>102</sup>

### 3.2.2 History of activated fluorosugars as Idua inactivators

Human  $\alpha$ -L-iduronidase (Idua) has proven to be a challenging enzyme to inactivate using activated fluorosugars. To date, there are only two examples of activated fluorosugars being tested as covalent inactivators of Idua, 2-deoxy-2-fluoro- $\alpha$ -L-iduronyl fluoride (**3.16**, Figure 3.14) and 5-fluoro- $\alpha$ -L-iduronyl fluoride (**3.17**).<sup>173</sup>

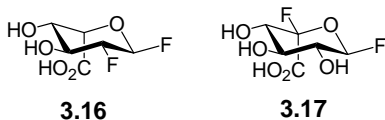


**Figure 3.14.** Structures of activated fluorosugars previously tested as covalent inactivators of Idua.

Treatment of Idua with either compound (**3.16** or **3.17**) did not lead to the accumulation of a long-lived covalent intermediate, and a corresponding time-dependent loss of enzyme activity. Rather, in the presence of either compound, the enzyme activity immediately dropped to constant values, that were dependent on the concentration of **3.16** or **3.17** in solution. This behaviour was consistent with considering both compounds acting as slow substrates of the enzyme rather than true inactivators, with rates of enzymatic glycosylation and deglycosylation being very similar. When analyzed as apparent reversible inhibitors of the enzyme rather than as time-dependent inactivators,  $K_i'$  values of 4.6  $\mu$ M and 1.2  $\mu$ M were obtained for **3.16** and **3.17** respectively. These low  $K_i'$  values indicate the steady-state accumulation of a high concentration of the covalent glycosyl-enzyme intermediate. Incubation of either compound with Idua resulted in a time-dependent release

of fluoride ion, which is consistent with continuous turnover of the activated fluorosugar by the enzyme. However, by careful handling of a sample of Idua treated with either **3.16** or **3.17**, it was possible to label and identify the catalytic nucleophile of Idua as Glu 299 by proteolysis followed by HPLC-mass spectrometry on the peptides generated.<sup>173</sup>

The conclusion from testing of both **3.16** and **3.17** was that neither a 2-deoxy-2-fluoro- or a 5-fluoro-activated fluorosugar was alone capable of leading to sufficient destabilization of the deglycosylation transition state to result in accumulation of a long-lived covalent glycosyl-enzyme intermediate. Therefore, the design and synthesis of activated fluorosugars that form more stable glycosyl-enzyme intermediates with Idua was desirable in the context of designing new biological probes for Idua in whole cell or *in vivo* applications, such as potential pharmacological chaperones of Idua.

### 3.2.3 Chemical synthesis of difluorosugar fluorides as potential inactivators of Idua

#### 3.2.2.1 Target compounds

Two compounds that may behave as covalent inactivators of Idua were selected as synthetic targets, both of which are shown in Figure 3.15.

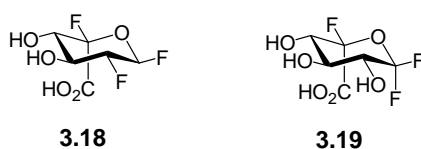


**Figure 3.15.** Structures of difluorosugar fluoride targets chosen as potential Idua inactivators.

2-Deoxy-2,5-difluoro- $\alpha$ -L-idopyranosyl uronic acid fluoride (**3.18**) was chosen as a synthetic target because it combines structural features of the previously known 2-deoxy-2-fluoro- $\alpha$ -L-idopyranosyl uronic acid fluoride (**3.16**) and 5-fluoro- $\alpha$ -L-idopyranosyl uronic acid fluorides (**3.17**), both of which are known to form short-lived covalent glycosyl-enzyme intermediates.<sup>173</sup> The goal was to see whether the electron-withdrawing effects of simultaneously incorporating both a 2-deoxy-2-fluoro and a 5-fluoro moiety in the context of

an iduronyl fluoride would be cumulative, and would therefore lead to generation of a covalent glycosyl-enzyme intermediate with a much longer lifetime.

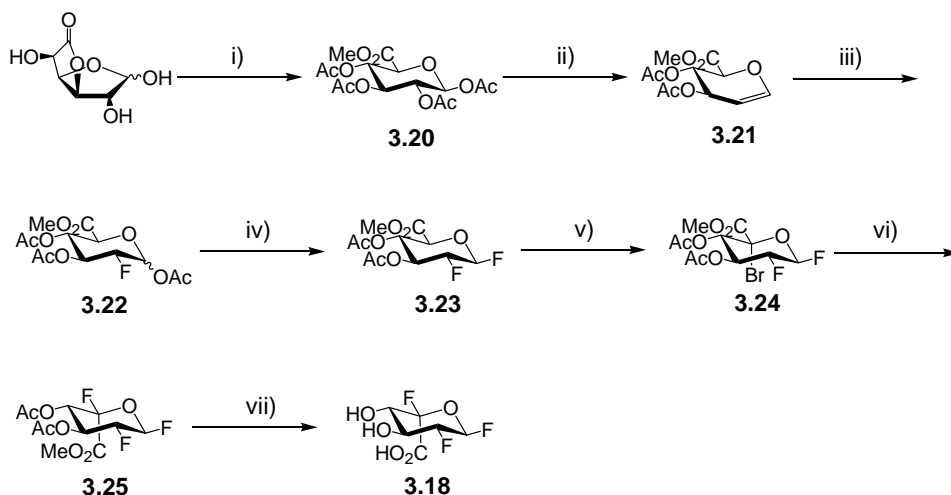
1,5-Difluoro-L-idopyranosyl uronic acid fluoride (**3.19**) was chosen as a synthetic target for similar reasons and because it was deemed readily synthetically accessible, based on the chemistry used to synthesize 1,5-difluoro-L-idopyranosyl fluoride (**2.8**). While idopyranosyl fluoride **2.8** was not a time-dependent inactivator of either Abg or Yag, these studies were undertaken at the same time as the experiments described in Section 2.4, and so the conclusions from those experiments were not available until near the end of this investigation. Additionally, it was possible that Idua, an enzyme unrelated by sequence, and presumably therefore structure, to Abg or Yag might be able to accommodate the 1,1-difluoro group both sterically and electronically, especially given the large tolerance for C5 substitution within this family.

The strategy in the design of both target compounds **3.18** and **3.19** was to increase the degree of fluorination on the sugar ring in an attempt to further destabilize the oxocarbenium ion-like transition states in both the glycosylation and deglycosylation steps of the reaction of these compounds with Idua. The design of these compounds accepted at the outset that the fluoride leaving group might not be sufficiently chemically activated to overcome the electron-withdrawing effects of the presence of two other fluorine atoms on the sugar ring. However, since the challenge in the design of covalent inactivators for Idua previously encountered in studies employing **3.16** and **3.17** was the high rate of turnover of the covalent glycosyl-enzyme intermediate, synthetic efforts were initially focused on possible solutions to that problem, as described above.

#### 3.2.2.2 Synthesis of 2-deoxy-2,5-difluoro- $\alpha$ -L-idopyranosyl uronic acid fluoride (**3.18**)

Compound **3.18** is structurally similar to the previously reported 2-deoxy-2-fluoro- $\alpha$ -L-idopyranosyl uronic acid fluoride,<sup>173</sup> with the difference lying in the identity of the substituent at C5 (H vs. F). The key step in the previously described synthesis is a TEMPO-mediated oxidation of 2-deoxy-2-fluoro- $\beta$ -D-glucosyl fluoride followed by formation of the phenacyl ester.<sup>173</sup> The author found that oxidations using TEMPO proved to be challenging

reactions that did not lead to reproducible results or consistent yields. As a result, a different synthetic route was used for the synthesis of **3.18**, as shown in Scheme 3.6.



**Scheme 3.6.** Synthesis of 2-deoxy-2,5-difluoro- $\alpha$ -L-idopyranosyl uronic acid fluoride (**3.18**). i) NaOH (cat), MeOH, then Ac<sub>2</sub>O, Py, 39%; ii) 33% (w/v) HBr/AcOH, then Zn<sub>(s)</sub>, AcOH, H<sub>2</sub>O, 74%; iii) Selectfluor<sup>TM</sup>, MeCN, H<sub>2</sub>O, then Ac<sub>2</sub>O, I<sub>2</sub>, 9%; iv) 33% (w/v) HBr/AcOH, then AgF, MeCN, 75%; v) NBS, CCl<sub>4</sub>, hv; vi) AgF, MeCN; vii) NaOMe, MeOH, then NaOH, H<sub>2</sub>O, 9% from **3.23**.

The starting material, 3,6-glucuronolactone, is a useful starting material for this synthesis, because it is commercially available and inexpensive. Despite the poor yield (39%), the known<sup>260</sup> intermediate **3.20** was synthesized on a large scale (~40 g) without difficulty. **3.20** was then readily converted to the  $\alpha$ -bromide and then reduced using Zn<sub>(s)</sub> in acetic acid/H<sub>2</sub>O to give the glycol **3.21** in very good yield (74% over two steps). The fluorination step using Selectfluor<sup>TM</sup> was very inefficient, giving the desired *glucurono*-configured **3.22** in only a disappointing 9% yield. While the Selectfluor<sup>TM</sup> reaction with acetylated glycols is not always a high-yielding reaction, the yield obtained here seems unusually low when compared to the Selectfluor<sup>TM</sup> reaction on tri-O-acetyl-D-glucal, which yields the *gluco*-configured product in 22% yield, as seen during the synthesis of **2.1**. One possible explanation for this lower yield is the decreased steric bulk at C6. It is known that having sterically bulky groups at either C3 or C6 leads to much higher equatorial:axial selectivity in fluorinations using Selectfluor<sup>TM</sup>, presumably by favouring approach of the electrophilic fluorine on the bottom face of the glycol ring.<sup>186</sup> In this case, the planar ester at

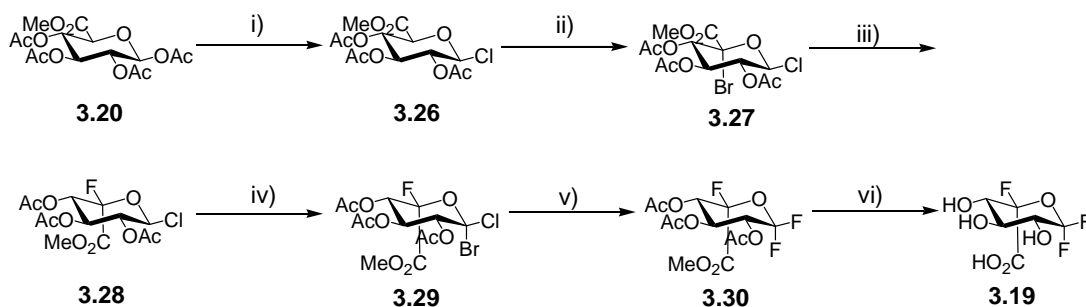


C6 would presumably offer less steric hindrance to the approaching electrophile than would an acetylated hydroxymethyl group, as was the case in the synthesis of **2.1**. TLC analysis of the crude reaction mixture following addition of Selectfluor<sup>TM</sup> did show one other major compound that was not isolated, but could be the *manno*-configured analogue.

Despite the poor yield for the fluorination at C2, sufficient material for the subsequent steps was produced owing to the ability to efficiently generate large amounts of the precursor glycal. The anomeric fluoride could be installed with little difficulty to give **3.23** (75%), which was then treated with NBS under radical photobromination conditions to give the 5-bromo compound **3.24**. The <sup>1</sup>H NMR spectrum of the crude material indicated that the radical bromination reaction had indeed occurred at C5 since no signal corresponding to H5 was present. However, since 5-bromo compounds such as **3.24** are often moderately unstable, compound **3.24** was used in subsequent steps following only partial purification. Treatment of bromide **3.24** with silver fluoride in acetonitrile yielded the *ido*-configured **3.25** through an inversion of stereochemistry at C5, although this product was contaminated with a small amount of another impurity. Nonetheless, the <sup>1</sup>H- and <sup>19</sup>F-NMR spectra could both still be acquired, and these confirmed the presence of the newly installed fluorine atom, covalently bonded to C5 by the appearance of a new signal in the <sup>19</sup>F NMR spectrum at -107 ppm, which is a characteristic region of the spectrum for equatorial fluorine atoms bound to C5. They also confirmed that the newly formed compound had the *ido* configuration, as judged by the small vicinal <sup>1</sup>H coupling constants (eg. J<sub>H2-H1</sub> = 1.9 Hz). Deprotection of the two acetyl groups and hydrolysis of the methyl ester yielded pure **3.18** in 9% overall yield starting from **3.23**.

#### 3.2.2.3 Synthesis of 1,5-difluoro-L-idopyranosyl uronic acid fluoride (**3.19**)

The synthetic route used to prepare 1,5-difluoro-L-idopyranosyl uronic acid fluoride (**3.19**) is shown in Scheme 3.7.



**Scheme 3.7.** Synthesis of 1,5-difluoro-L-idopyranosyl uronic acid fluoride (**3.19**). i)  $\text{BF}_3\text{-OEt}_2$ ,  $\text{CHCl}_2\text{OCH}_3$ , 76%; ii) NBS,  $\text{CCl}_4$ , hv; iii)  $\text{AgF}$ , MeCN, 29% from **3.26**; iv) NBS,  $\text{CCl}_4$ , hv; v)  $\text{AgBF}_4$ ,  $\text{Et}_2\text{O}$ ; vi) NaOMe, MeOH,  $\text{H}_2\text{O}$ , 12% from **3.28**.

An early intermediate from the previous synthesis, **3.20**, was used as the starting material for the synthesis of **3.19**. The best yield of the  $\beta$ -chloride **3.26** (76%) was obtained by treatment of **3.20** with  $\text{BF}_3\text{-OEt}_2$  in dichloromethyl methylether. Subsequent reaction of **3.26** under radical photobromination conditions gave almost exclusively the product arising from bromination at C5, and only trace amounts of the product arising from bromination at the anomeric center. Although the resulting bromide **3.27** was not isolated, treatment of the mixture of compounds with silver fluoride in acetonitrile yields **3.28** as the major product (29%) after purification. Radical bromination reactions usually occur at C5 in a normal pyranose ring, as this proceeds through a tertiary radical intermediate that is stabilized by the lone pair of electrons on the ring oxygen.<sup>176</sup> In the case of the uronic acids, the presence of the nearby  $\pi$ -system of electrons in the C6 ester also serves to further stabilize a radical at C5, further directing the radical bromination to C5.<sup>173-175,196</sup> On the other hand, the presence of an equatorial chlorine atom at the anomeric center has been found to stabilize radical formation at the anomeric center and, on pyranose sugars lacking the uronic acid functionality, alters the regioselectivity of the radical reaction to favour bromination at C1 over C5.<sup>178</sup> In this case, it appears that the stabilizing effect of the nearby  $\pi$ -system in the C6 ester stabilizes the radical more than the equatorial chlorine, as the major product is the C5-bromo species.

A radical bromination reaction on compound **3.28** led to the formation of the mixed anomeric-dihalo species **3.29** as seen by the disappearance of the signal for H-1 in the crude

<sup>1</sup>H NMR spectrum. Treatment of the crude mixture of **3.29** with silver fluoride in acetonitrile resulted in monofluorination at the anomeric center, presumably yielding the product with the newly installed fluorine atom in the equatorial orientation. Difluorination at the anomeric center of **3.29** required the use of silver tetrafluoroborate in ether, as was used for the synthesis of compounds **2.7** and **2.8** (Section 2.3.2.4). In this instance, the fluorination reaction using silver tetrafluoroborate was accompanied by the formation of modest amounts of what was presumed to be the glycal formed by elimination across C1-C2. This proved to be inseparable from the desired product **3.30**. Removal of the protecting groups using methoxide in wet methanol led to pure **3.19** in 12% yield from **3.28**.

#### 3.2.4 Enzymatic evaluation of **3.18** and **3.19** as inhibitors of Idua

2-Deoxy-2,5-difluoro- $\alpha$ -L-idopyranosyl uronic acid fluoride (**3.18**) was evaluated as a potential covalent inactivator of Idua. Unfortunately, even at the highest concentration tested (9.95 mM) no time-dependent loss of enzyme activity was observed. TLC analysis of reaction mixtures of **3.18** incubated in the presence of Idua revealed no hydrolysis of the compound, suggesting that it was not a substrate for the enzyme. Therefore, compound **3.18** was tested as a competitive inhibitor of Idua-catalyzed hydrolysis of 4-methylumbelliferyl  $\alpha$ -L-iduronide (MUI, [S] = 0.056 mM). The resulting data were plotted as a Dixon plot (inverse of rate as a function of inhibitor concentration), as is shown in Figure 3.16.

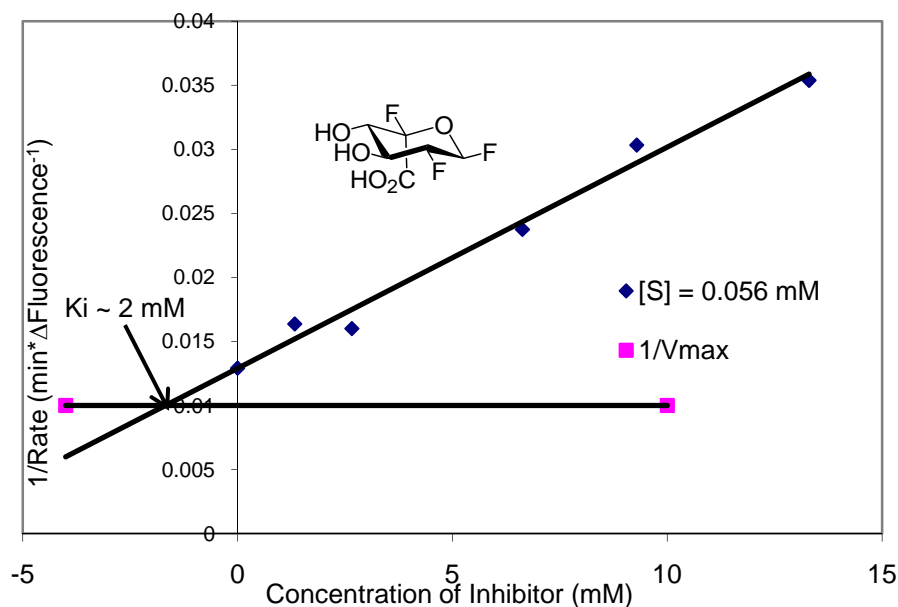


**Figure 3.16.** Dixon plot representation of inhibition of Idua by **3.18**.

The intercept in the Dixon plot gives a  $K_i$  value of  $\sim 2$  mM, assuming competitive inhibition. Thus **3.18** binds to the active site of Idua, but is not turned over by the enzyme. Presumably, the fluoride leaving group at the anomeric center is not sufficiently chemically activated to act as a good leaving group and accelerate the glycosylation step sufficiently to allow accumulation of the covalent glycosyl-enzyme intermediate.

1,5-Difluoro-L-idopyranosyl uronic acid fluoride (**3.19**) was evaluated as a time-dependent inactivator of Idua in a similar manner, but unfortunately no loss of enzyme activity was observed, even at the highest concentration tested (13.60 mM). A TLC assay of **3.19** incubated in the presence of Idua showed no hydrolysis of **3.19**, suggesting that this compound does not act as a substrate for Idua. Finally, evaluation of **3.19** as a competitive inhibitor of Idua showed no inhibition of enzyme activity, even at the highest concentration tested (6.80 mM), suggesting that **3.19** does not bind to the Idua active site, presumably as a consequence of the *gem*-difluoro moiety at the anomeric center.

### 3.2.5 Conclusions and future considerations

The two compounds previously tested as time-dependent inactivators of Idua, 2-deoxy-2-fluoro- and 5-fluoro- $\alpha$ -L-iduronyl fluoride (**3.16** and **3.17** respectively) were both shown to behave as slow substrates for the Idua enzyme, but with turnover of the covalent glycosyl-enzyme intermediate being rapid relative to the time-scale of the assay.<sup>173</sup> In an attempt to generate a time-dependent inactivator of Idua with a longer-lived covalent glycosyl-enzyme intermediate, two compounds bearing extra fluorine substituents, 2-deoxy-2,5-difluoro- $\alpha$ -L-idopyranosyl uronic acid fluoride (**3.18**) and 1,5-difluoro-L-idopyranosyl uronic acid fluoride (**3.19**), were synthesized by radical-bromination/nucleophilic fluoride displacement sequences. Unfortunately, neither compound functioned as a covalent inactivator of Idua. Further, neither compound was cleaved by the enzyme and only compound **3.18** was shown to bind to the Idua active site, albeit with only a modest affinity ( $K_i = \sim 2$  mM). This lack of time-dependent inactivation of Idua by **3.18** presumably arises because the fluoride aglycone is insufficiently chemically activated to act as a leaving group in the enzyme-catalyzed reaction, similar to the behaviour seen for compounds **2.4**, **2.6**, **2.7** and **2.8** when tested as potential inactivators of Abg (Section 2.4.1). The lack of inhibition by compound **3.19** is largely due to poor binding caused by the axial fluorine atom at the anomeric center, since the analogue with a hydrogen atom at this position (5-fluoro- $\alpha$ -L-iduronyl fluoride, **3.17**) is known to be a potent inhibitor of Idua activity.<sup>173</sup> This could be easily caused by unfavourable steric or electronic interactions with the catalytic nucleophile. This means that no compound suitable for testing as a chaperone for Idua or as a potential active site labelling agent for PET imaging studies of ERT was found.

## **Chapter 4: Testing of Fluorinated Carbohydrates as Potential Therapeutic and Diagnostic Tools for Gauchers Disease**

## 4.1: Investigating pharmacological chaperones for GCase

### 4.1.1 Current therapeutic strategies in the treatment of Gauchers disease

#### 4.1.1.1 Enzyme replacement therapy (ERT)

Enzyme replacement therapy (ERT) was first proposed as a treatment for Gauchers disease almost 30 years ago.<sup>261</sup> ERT involves the intravenous infusion of a recombinant form of the deficient enzyme. The enzyme is then trafficked throughout the body and, following cellular uptake, sorted to the lysosome. In the lysosome, the recombinant enzyme catalytically degrades the built-up substrate, and therefore helps to alleviate disease symptoms.<sup>67</sup> Current therapeutic use of ERT for Gauchers disease is restricted to Type I (non-neuronopathic) Gauchers disease, as the recombinant form of the enzyme does not effectively cross the blood-brain barrier. However, despite this restriction, there are promising results from animal models that suggest that the more severe forms of Gauchers disease (Type II and Type III) that have neural cell involvement may be treatable using ERT,<sup>73,243,262</sup> once concerns surrounding safety and the means of delivery have been addressed.

ERT has been used clinically to treat Gauchers disease since 1991,<sup>71,263</sup> and has proven successful in the treatment of Type I Gauchers disease. During the course of the development of this therapy, significant challenges surrounding the production,<sup>221,264</sup> purification,<sup>265</sup> and targeting<sup>266-269</sup> of the recombinant GCase enzyme were solved, and improvements in these features of ERT remain of interest. One important development in ERT has been in targeting the recombinant enzyme to macrophage cells, which show the greatest storage of substrate.<sup>64</sup> It was demonstrated that remodelling of the three complex *N*-linked glycan chains to expose the core  $\alpha$ -mannosyl residues greatly increases uptake of the recombinant enzyme into the desired tissues.<sup>266-269</sup> It is partly this glycan remodelling that leads to the high cost of ERT, estimated at between \$100,000-\$300,000 USD/patient/year.<sup>270-</sup>

<sup>272</sup> An additional complicating factor is that there is no general consensus on the minimum dosing regimen needed to attain the desired therapeutic goals.<sup>72,77,273</sup> Both of these factors contribute to the drive to find alternative therapies to reduce the cost of treatment of Gauchers disease, or better diagnostic tools to help assess the efficacy of ERT treatment.<sup>272</sup>

#### 4.1.1.2 Substrate reduction therapy (SRT)

An alternative therapy for the treatment of Gauchers disease is called Substrate reduction therapy (SRT). In SRT, the therapeutic strategy is to reduce the rate of substrate synthesis through the addition of a small molecule inhibitor of the biosynthetic enzyme. SRT takes advantage of the fact that Gauchers patients retain a low residual level of GCase activity, and therefore a reduction in the influx of substrate into the degradation pathway to a level that the residual GCase activity can still accommodate is beneficial.<sup>274</sup> To date, the most successful example of SRT is in the use of *N*-butyldeoxynojirimycin (**4.1**, Figure 4.1), which is used clinically in the treatment of Gauchers disease under the trade name Zavesca®.<sup>22,65,78,79,275,276</sup> **4.1**, and related derivatives, are inhibitors of the ceramide glucosyltransferase, and thus reduce the level of synthesis of glucosylceramide. This in turn leads to reduced substrate storage and alleviation of patient symptoms. Interestingly, **4.1** has also been shown to act as a Pharmacological Chaperone (PC, Section 4.1.1.4) for GCase, although it is not known whether this other activity is clinically significant.<sup>277</sup> SRT is currently recommended for patients unwilling or unable to undergo ERT. The advantage of the use of a small molecule such as **4.1** in the context of SRT for Gauchers disease is the fact that the small molecule is orally available and can potentially cross the blood-brain barrier, making it a candidate for treatment of Types II and III Gauchers disease although there are no reports of **4.1** being used to successfully treat these patients. The reported side-effects of **4.1** include diarrhoea and tremors.<sup>64</sup>

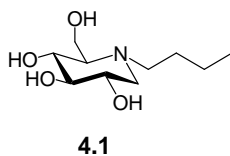


**Figure 4.1.** Structure of *N*-butyldeoxynojirimycin (**4.1**).



#### 4.1.1.3 Other potential treatments

Other potential therapies that have been examined for the treatment of Gauchers disease include bone marrow transplantation (BMT) and gene therapy. In both approaches, the therapeutic strategy is to introduce cells in the body that will produce a healthy form of the GCase enzyme that can be trafficked to the affected organs and degrade the accumulated substrate. The difference between the two therapies lies in the mechanism of introduction of the modified cells. In BMT, the bone marrow cells of the patient are destroyed and replaced with marrow from a healthy, compatible donor. This therapy has shown promise in the treatment of patients with severe (Type III) Gauchers disease, although it is extremely invasive. Treatment must be initiated very early in life to show benefits and there is a high risk of morbidity and mortality.<sup>278,279</sup>

Gene therapy is a potential treatment for Gauchers disease that holds a great deal of promise.<sup>68</sup> In gene therapy, a vector containing a gene encoding healthy GCase is inserted into a retrovirus, which infects the Gauchers patient and inserts copies of the gene into the host genome, which will then express a functional form of the enzyme. The promise of gene therapy is that a single treatment course can potentially offer a lifetime of therapy, since the GCase will be continuously produced in the host. However, despite some promising initial results in animal studies,<sup>243,280,281</sup> there are still significant safety concerns surrounding current gene therapy approaches in humans.<sup>282,283</sup>

#### 4.1.1.4 Enzyme enhancement therapy (EET) through the use of pharmacological chaperones (PC)

The other therapeutic option for the treatment of Gauchers disease that is attracting increasing attention is enzyme enhancement therapy (EET) through the use of pharmacological chaperones (PCs). As discussed in the general introduction (Section 1.4.3), PCs represent a promising new strategy in the treatment of protein misfolding diseases such as Gauchers disease by assisting in the proper folding of the mutant enzyme and permitting

its passage through the endoplasmic reticulum quality control (ERQC) to the lysosome, thereby avoiding endoplasmic reticulum associated degradation (ERAD).

The majority of compounds that have been tested as PCs for GCase have been azasugar analogues containing a nitrogen atom that is presumably protonated under physiological pH. This positive charge helps these analogues interact favourably with the negatively-charged GCase active site,<sup>218</sup> and may mimic the positive charge that develops in the transition state of enzyme-catalyzed glycoside cleavage. There have also been some reports of compounds that act as a PC for GCase that do not structurally resemble a sugar ring.<sup>33,284</sup> Representative structures of some of the compounds shown to act as PCs<sup>33,277,284-289</sup> for GCase are shown in Figure 4.2.

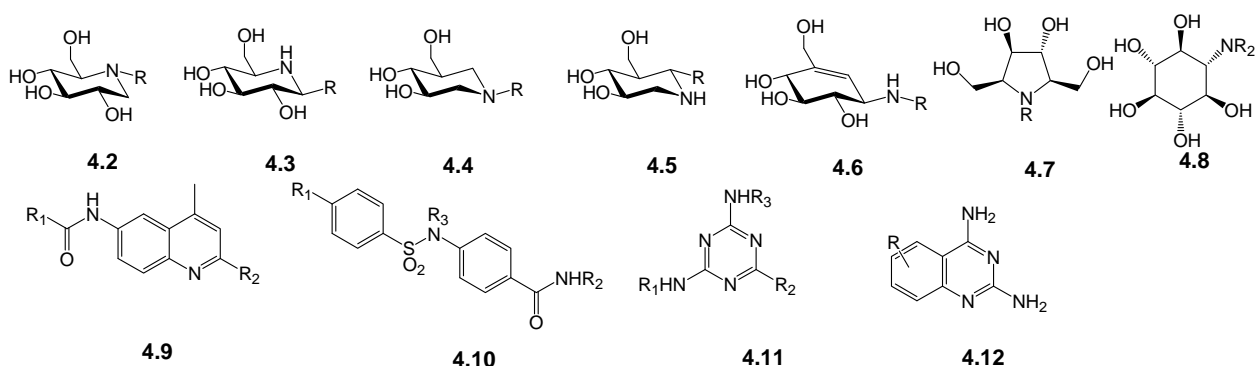


**Figure 4.2.** Representative structures of some compounds shown to act as PCs for GCase.

Out of the core structures represented in Figure 4.2, the individual compound that currently shows the most promise as a PC for GCase<sup>33,224,285,286,289-292</sup> is isofagomine (**4.4**, R=H). Isofagomine has shown an ideal chaperone profile, where inhibition, and thus binding of the inhibitor to the enzyme, is stronger at neutral pH, as encountered in the ER during GCase synthesis, but weaker at the more acidic pH of the lysosome where the enzyme needs to be catalytically active.<sup>286</sup> The exact mechanism by which this compound acts as a chaperone has been investigated. While the major mechanism by which this compound increases GCase activity in the lysosome is through increased levels of properly folded

enzyme reaching the lysosome, it was also demonstrated that once there isofagomine-treated GCase showed a lower pH optimum of activity in the Asn370Ser mutant, along with an altered sensitivity to SDS.<sup>286</sup> A subsequent structural study has confirmed that isofagomine helps GCase adopt the catalytic conformation and, analysis of changes in the melting temperature also proved that isofagomine stabilizes GCase towards denaturation.<sup>293</sup> This compound has successfully undergone Phase II clinical trials for treatment of Type I Gauchers disease,<sup>294</sup> and further clinical studies are underway. If testing of this compound proves successful in a clinical context, this will represent the first demonstration of the use of a PC for treatment of a LSD.

#### **4.1.2 An introduction to activated fluorosugars as potential PCs**

The key feature of a PC is that it must be capable of binding to, and stabilizing, the folded conformation of the target protein. It has been previously demonstrated that a sample of Abg that has a covalently bound 2-deoxy-2-fluoro-glucopyranosyl moiety in the active site is stabilized towards urea denaturation,<sup>295</sup> and more importantly that a sample of GCase that has a covalently bound 2-deoxy-2-fluoro-glucopyranosyl moiety in the active site is stabilized towards chemical denaturation using guanidinium hydrochloride.<sup>245</sup> These results demonstrate that a covalent intermediate arising from treatment of a glycosidase with an activated fluorosugar is more stable than the native form of the enzyme, and hence this type of species may function as a PC for GCase.

The use of activated fluorosugars as potential PCs for GCase differs from the use of noncovalent inhibitors of GCase as PCs in one important aspect. When using noncovalent inhibitors of GCase such as isofagomine (**4.4**, R=H) the concentration of inhibitor is critical; at extremely low concentrations, no chaperone effect is observed, while at extremely high concentrations chaperone activity may be observed, but the concentration of inhibitor is still high enough to inhibit lysosomal enzyme activity. This means that following washout of the inhibitor, enzymatic activity returns as the inhibitor is displaced from the enzyme active site by the high concentration of built-up substrate in the lysosome. This recovery of activity depends on the rate of dissociation of the enzyme-inhibitor complex, which can be very slow

for a tightly bound inhibitor.<sup>296</sup> In one cell-based experiment, it was reported that enzyme activity recovered by almost 50% 4 hours after isofagomine treatment, and had completely recovered within 24 hours.<sup>286</sup> However, GCase activity following treatment with a covalent inactivator such as **2.1** recovers much more slowly *in vitro*, with a  $t_{1/2} = 1300$  min corresponding to hydrolysis of the covalent glycosyl-enzyme intermediate.<sup>211</sup> Indeed, animal studies on the rates of recovery of  $\beta$ -glucosidase activity in rats following treatment with **2.1** showed hydrolytic breakdown of the covalent glycosyl-enzyme intermediate was the primary mechanism of recovery of  $\beta$ -glucosidase activity.<sup>297</sup> This decreased rate of recovery of enzyme activity following treatment with a covalent inactivator compared to a noncovalent inhibitor may be a beneficial feature, as this would permit the slow release of a low steady-state concentration of free enzyme in the lysosome rather than a more rapid increase in concentration of free enzyme following washout of a noncovalent inhibitor.

Compounds **2.1** and **2.67** (whose structures are shown again in Figure 4.3) were selected for testing as potential PCs of GCase. **2.1** was selected as a potential chaperone since previous *in vivo* studies on this compound administered to rats have shown that it inhibited the *in vivo*  $\beta$ -glucosidase activity in brain, spleen, liver and kidney, demonstrating the ability of this compound to traffic into all of these organs.<sup>297</sup> The drawback of **2.1** is that it is not a particularly efficient inactivator of GCase, and may require relatively high concentrations to show PC activity. Additionally, since it contains only a fluoride aglycone it is unlikely to show any selectivity for GCase over other mammalian  $\beta$ -glucosidases.<sup>228,298-300</sup> Compound **2.67** was also selected as a potential chaperone because it is almost 1000-fold more efficient as an inactivator of GCase than compound is **2.1**. Phosphonate derivative **2.67** was chosen over the dibenzyl phosphate derivative **2.62** and dioctyl phosphate derivative **3.6** because, while the latter two compounds are both more efficient inactivators of GCase, they are considerably less stable towards spontaneous decomposition in aqueous solution as described in Section 2.7.3. Therefore, **2.67** represented an excellent compromise between stability towards spontaneous decomposition, efficiency of inactivation, and synthetic accessibility. Finally, the greater efficiency of inactivation of GCase may mean that, at lower concentrations, there might be increased selectivity for GCase over other mammalian  $\beta$ -

glucosidases. Unfortunately, purified sources of these other mammalian glucosidases were unavailable during the course of these studies, so this hypothesis could not be tested *in vitro*.

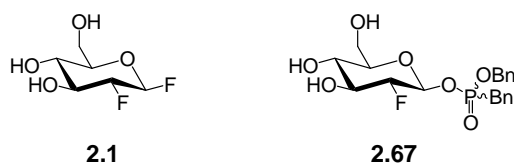


**Figure 4.3.** Structures of activated fluorosugars tested as PCs for GCase.

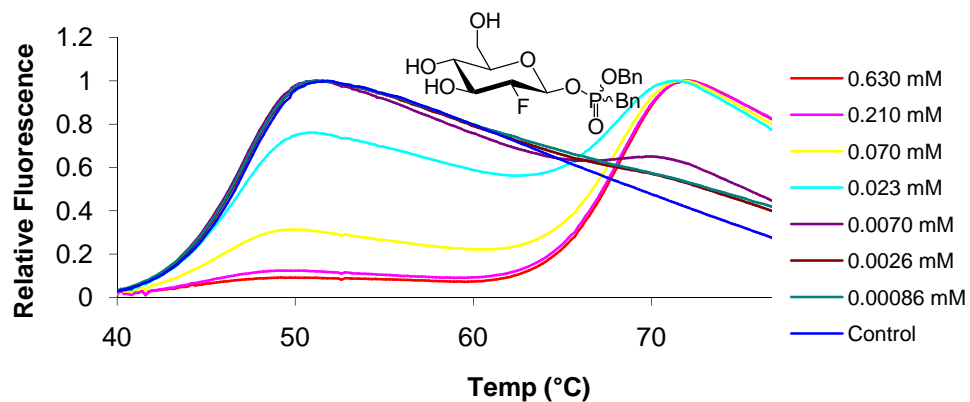
#### 4.1.3 Testing of **2.1** and **2.67** as PC for GCase in a cell-based system

Note: These experiments were performed by Dr. Michael Tropak, Mr. Justin Buttner and Ms. Sayuri Yonegawa at the Hospital for Sick Children, University of Toronto.

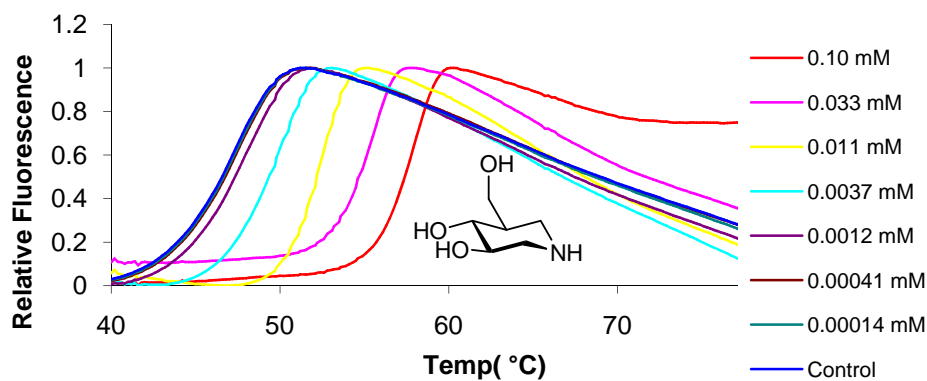
##### 4.1.3.1 Testing the ability of **2.1** and **2.67** to raise the melting temperature of GCase *in vitro*

Prior to testing the ability of both **2.1** and **2.67** to function as PCs of GCase in cell lines, both compounds were tested for their ability to stabilize wild-type GCase towards thermal denaturation. Following incubation of GCase with **2.1**, **2.67** or isofagomine (**4.4** R=H) for thirty minutes, the sample of enzyme was treated with NanoOrange® and the fluorescence of each sample monitored as a function of temperature. When the NanoOrange® binds to hydrophobic patches of the protein, the intensity of its fluorescence increases; hence, as the protein unfolds, the observed fluorescence should increase. Figure 4.4 shows the fluorescence intensity versus temperature curves for GCase treated with the indicated concentrations of **2.1**, **2.67** or isofagomine. Isofagomine was included in this analysis as a positive control, since it is a known<sup>286</sup> PC for GCase, and it binds to and stabilizes the folded conformation of the enzyme.<sup>290</sup>

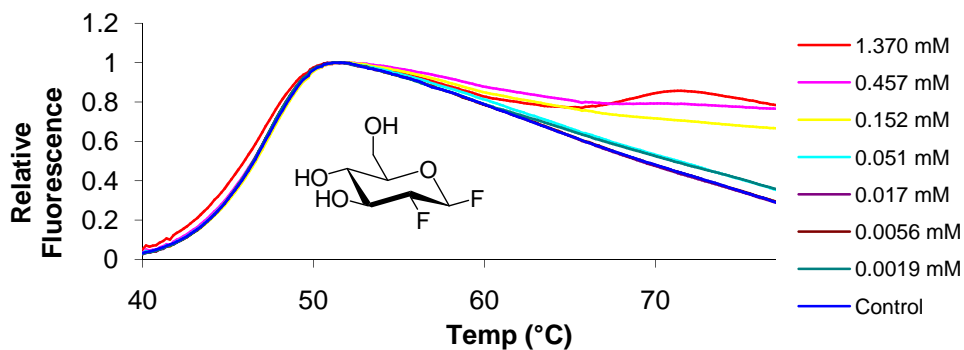
a)



b)



c)



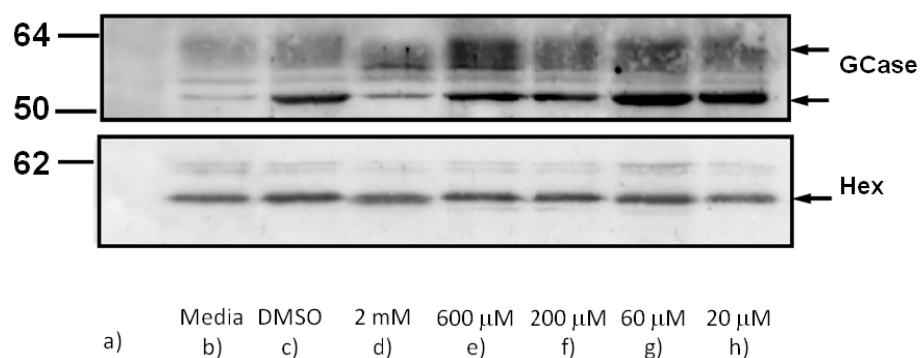
**Figure 4.4.** Relative fluorescence versus temperature curves for GCase incubated for 30 minutes in the presence of a) **2.67**, b) isofagomine, and c) **2.1**. Note that these experiments were carried out in the absence of both Triton-X100 and sodium taurocholate, both of which function to increase enzyme activity.

Figure 4.4 (a) shows that incubation of GCase in the presence of a variety of concentrations of **2.67** for thirty minutes prior to analysis of the melting temperature causes a remarkable 21 °C increase in melting temperature of GCase that has been completely inactivated by **2.67** (210 µM and 610 µM) relative to native GCase when measured at pH = 7. It is important to note that in these experiments, the incubation was carried out in the absence of Triton X-100 and sodium taurocholate, both of which are normally included in *in vitro* GCase activity assays because they increase the enzyme activity considerably, which explains the necessity of using concentrations much higher than those observed in Section 3.1.6.5. Experiments were carried out at pH = 7 since this mimics the pH of the ER where GCase is synthesized and where the mutant enzyme is targeted for ERAD. Experiments carried out at intermediate concentrations of **2.67** show the presence of two distinct melting temperatures, which correspond to the presence of both native GCase ( $T_m = 47$  °C) and GCase that has been inactivated by **2.67** ( $T_m = 68$  °C). By comparison, the known chaperone isofagomine increases the  $T_m$  by a maximum of 10 °C at pH = 7 [Figure 4.4, (b)]. In contrast to the two states observed in the melting curve of GCase incubated with **2.67**, the melting temperature of GCase in the presence of isofagomine increases as a function of inhibitor concentration to intermediate values. This represents a concentration-dependent exchange process that leads to a global stabilization of the pool of GCase molecules during the unfolding process. This experiment shows that **2.67** stabilizes the wild-type GCase towards thermal denaturation by 10 °C more than the maximum stabilization imparted by isofagomine at the highest concentration tested. It is interesting to note that under the conditions of this experiment, **2.67** is a more potent stabilizing agent than is **2.1** [Figure 4.5, (c)], which is expected given the 1000-fold difference in the relative efficiencies of these two compounds as inactivators of GCase *in vitro*. At the highest concentration of **2.1** tested (1370 µM), two protein unfolding events can be seen at 47 °C and 68 °C, which correspond to the unfolding of the native and inactivated states of the enzyme, respectively. Under these experimental conditions, only a small proportion of GCase is inactivated (and hence stabilized) by **2.1**. This is the expected result given the absence of both Triton-X100 and sodium taurocholate in the incubation buffer. If the incubation times were extended further so that GCase is fully inactivated by **2.1** under these conditions, the same degree of

stabilization of the enzyme would be observed since the covalent glycosyl-enzyme intermediate formed between GCase and either **2.1** or **2.67** is identical.

#### 4.1.3.2 Preliminary testing of **2.1** as a PC for GCase

Compound **2.1** was tested as a PC in patient fibroblasts containing GCase bearing the Asn370Ser mutation, the most common point mutation that causes Type I Gauchers disease. Fibroblasts are cells in the connective tissue that are responsible for synthesizing the extracellular matrix and collagen, as well as playing a key role in healing wounds. The patient fibroblasts were treated with **2.1**, and the cells lysed after seven days. The GCase in the cell lysates was subjected to Western blot analysis, and the levels of protein expression were compared to those of untreated cells, as seen in Figure 4.5.



**Figure 4.5.** Western blot analysis of GCase from fibroblast cells bearing an Asn370Ser point mutation. a) Position of molecular weight markers (not seen in this figure); cells treated with b) cell media only, c) DMSO only, d) 2000  $\mu$ M **2.1** dissolved in DMSO, e) 600  $\mu$ M **2.1** dissolved in DMSO, f) 200  $\mu$ M **2.1** dissolved in DMSO, g) 60  $\mu$ M **2.1** dissolved in DMSO, and h) 20  $\mu$ M **2.1**, dissolved in DMSO. The two bands in the upper box correspond to different glycosylation states of GCase, while the bands in the lower box correspond to lysosomal  $\beta$ -hexosaminidase, used as a control to judge the amount of sample loaded in each lane.

GCase appears as more than one indistinct band in these Western blot experiments, since it exists in the cell in a number of glycosylation states whose mobilities under the gel conditions differ, shown in the upper box in Figure 4.5. The lower box shows the levels of lysosomal  $\beta$ -hexosaminidase that was used in these experiments as a loading control.



Interestingly, DMSO showed a chaperone effect, as seen in comparing lane c) to lane b). This is not an entirely unexpected result since it has been observed in other systems that DMSO can stabilize the folded conformation of a protein.<sup>90</sup> Since the solutions of **2.1** were dissolved in DMSO, the intensity of the GCCase bands in lane c) represent the baseline level against which the chaperone potential of **2.1** should be judged. At concentrations of **2.1** that were >60  $\mu\text{M}$  [lanes d), e) and f)], the cells grew very poorly, showing that **2.1** is toxic to the cells at these concentrations. This may arise from inactivation of other cellular  $\beta$ -glycosidases by **2.1**, whose normal function is required for cell viability. For the purposes of analysis of the potential use of **2.1** as a PC, this cellular toxicity means that lanes d), e) and f) can be ignored. However, cells treated with low levels of **2.1** [ $\leq 60 \mu\text{M}$ , lanes (g) and (h)] contain higher levels of the properly folded mutant GCCase enzyme than do cells in the DMSO treated experiment in lane c), as judged by the intensities of the bands in the upper box that reflect the amount of GCCase. The level of increase in GCCase as evaluated by Western blot analysis is modest at best, although the level of increase is comparable to similar experiments previously reported which analyzed the ability of isofagomine to act as PC for GCCase by Western blot.<sup>286</sup>

An enzymatic assay on the crude cell lysates for GCCase activity<sup>212,227</sup> showed no increase in enzyme activity in cells treated with **2.1** over the level of the control cells. However, as discussed in Section 4.1.2, if **2.1** is behaving as a PC for GCCase, an immediate increase in enzyme activity following treatment with **2.1** would not be expected since the covalent glycosyl-enzyme intermediate species has a half life of reactivation ( $t_{1/2}$ ) = 1300 minutes. Further experiments testing the ability of **2.1** to increase GCCase activity are planned which incorporate a recovery phase following treatment with **2.1** (a pulse-chase experiment).

#### 4.1.3.3 Preliminary testing of **2.67** as a PC for GCCase

Compound **2.67** was also tested as a PC for GCCase in a similar manner to that described for the testing of **2.1**. The ability of **2.67** to act as a chaperone was evaluated by Western blot analysis, and the results of this experiment can be seen in Figure 4.6.

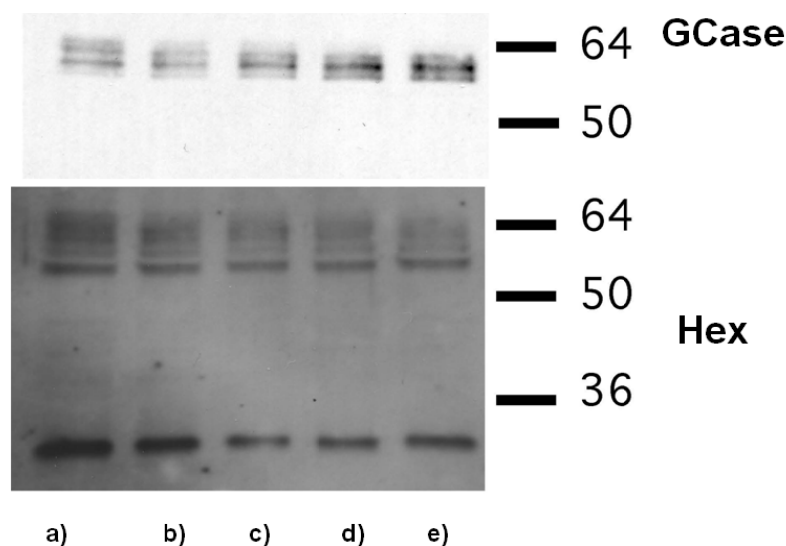


**Figure 4.6.** Western blot analysis of GCase from patient fibroblast cells bearing an Asn370Ser point mutation. Cells treated with a) 0  $\mu\text{M}$  **2.67**, b) 3.9  $\mu\text{M}$  **2.67**, c) 12  $\mu\text{M}$  **2.67**, d) 35  $\mu\text{M}$  **2.67**, and e) 105  $\mu\text{M}$  **2.67**. The two bands in the upper box correspond to different glycosylation states of GCase, while the bands in the lower box correspond to lysosomal  $\beta$ -hexosaminidase, used as a control to judge the amount of sample loaded in each lane.

Unlike was the case of cells treated with **2.1**, no cellular toxicity was observed for fibroblast cells treated with **2.67** even at the highest level tested (105  $\mu\text{M}$ ). Levels of GCase are progressively higher in fibroblasts that express GCase bearing the Asn370Ser point mutation when treated with increasing levels of **2.67**, suggesting that **2.67** is acting as a PC for the mutant enzyme. Despite the fact that **2.67** is an approximately 1000-fold more efficient inactivator of GCase *in vitro*, it does not appear to function as a more efficient PC for GCase, as judged by the minimum concentration necessary to achieve a noticeable increase in the intensities of the GCase bands in their respective Western blots, chosen as 20  $\mu\text{M}$  and 12  $\mu\text{M}$  for **2.1** and **2.67** respectively by visual analysis of the Western blots in Figures 4.5 and 4.6. This may suggest that **2.1** crosses the cell membrane more readily than does **2.67** and enters the ER, where GCase is synthesized. Cells treated with **2.67** for five days also did not show any increase in GCase enzyme activity over the time period studied, which correlates with the results seen for the analogous experiment employing **2.1**.

#### 4.1.3.4 Conclusions and future directions for the use of **2.1** and **2.67** as PC of GCase

In the present set of experiments, we wished to test whether the covalent glycosyl-enzyme intermediate formed by reaction of an activated fluorosugar and GCase could function as a PC for GCase in a cell-based system. On the basis of the Western blot analysis of human fibroblasts expressing GCase bearing the Asn370Ser point mutation, which is the most common mutation leading to Gauchers disease, both **2.1** and **2.67** increased the levels of GCase in the cells in a concentration-dependent fashion. At concentrations >60  $\mu$ M, **2.1** was found to be toxic to the cells. This effect presumably arises from **2.1** inactivating other glycosidases that are required for proper cellular function. In contrast, compound **2.67** showed no toxicity at the highest concentration tested (105  $\mu$ M) which may indicate that **2.67** is a more specific inactivator of GCase than is **2.1**.

No increase in enzyme activity was seen upon treatment of mutant GCase with either **2.1** or **2.67**. Under the conditions of continuous treatment of the cells with either **2.1** or **2.67**, it would be expected that no significant steady-state population of free enzyme accumulates as any free enzyme that is generated by the hydrolysis of the covalent glycosyl-enzyme intermediate is immediately inactivated again. It is expected that a pulse-chase experiment with an appropriate concentration of inactivator may show increased enzyme activity, as during the pulse phase, inactivated GCase can accumulate in the lysosome, and during the chase phase, the enzyme can reactivate through hydrolysis of the covalent intermediate. An experiment to test this hypothesis is planned.

It was shown that the Asn370Ser GCase mutant was inactivated in a cell-based system through treatment with either **2.1** or **2.67**. As a consequence of this inactivation, the mutant GCase was thermodynamically stabilized, as shown by the *in vitro* melting temperature experiments, and hence was more resistant to ERAD. However, the stabilized enzyme did not reactivate during the course of the experiment, under the conditions used, to generate catalytically active enzyme. This raises the possibility of using **2.1** or **2.67** as potential probes of the diseased cell state to study the relative effects of cellular stress arising from the Unfolded Protein Response<sup>87</sup> as a consequence of the large amount of protein undergoing ERAD in a GCase deficient cell, versus the biochemical consequences of substrate accumulation which would be unchanged in cells treated with **2.1** or **2.67**. The

relative contributions of these two factors towards the cellular stress and hence the disease state could be effectively studied with a covalent inactivator of GCase such as **2.1** or **2.67**.

The results from these experiments suggest that a better activated fluorosugar for use as a PC for GCase might be designed in two ways. First, a fluorosugar with a faster rate of hydrolysis for the covalent glycosyl-enzyme intermediate would show a quicker recovery of enzyme activity, which means a shorter “chase” time is necessary during the pulse-chase type of experiments (or cycles of therapy in a pharmaceutical context). Second, manipulation of the groups attached to the phosphorus may allow for a derivative with better cellular uptake to be designed.

## **4.2 Development of activated fluorosugars as PET imaging agents for monitoring ERT in Gauchers disease**

### **4.2.1 Objectives in development of a PET imaging agent**

Positron Emission Tomography (PET) imaging is a non-invasive imaging modality that can permit the imaging of many different biological processes in a whole organism.<sup>109,112,301</sup> PET is capable of quantitatively imaging the localization of a given PET imaging agent to particular organs or regions of the organism while also allowing these processes to be studied as a function of time. In the context of ERT for the treatment of Gauchers disease, a PET imaging agent that permits monitoring of the biodistribution of recombinant GCase injected into a patient (Cerezyme®) could be a valuable diagnostic tool in tailoring the dose of GCase given to an individual patient, monitoring the course of therapy over time and any development of an immune response to the ERT.

While there have been many studies on the biodistribution of recombinant GCase in animals,<sup>73,266,269,302,303</sup> there have been few studies on humans. This arises because the most common method for assessing distribution is through measurement of enzyme activity in tissue homogenates from sacrificed animals, an approach that is obviously not suitable for human studies. To date, there has only been one successful published attempt to label and

study the distribution of GCase in human subjects. In this study, GCase was labelled with  $^{123}\text{I}$  through an acylation reaction with surface lysine residues, and the distribution analyzed with a  $\gamma$ -scintigraphical camera. This study showed uptake of the recombinant enzyme into many organs including the liver, spleen and bone marrow.<sup>304</sup> However,  $\gamma$ -scintigraphy produces only a two-dimensional image of low resolution, making it less desirable than other imaging modalities. Additionally, this study required modification of one or more surface residues, which may well lead to an immune response and/or to biodistribution patterns that are different from those of the unmodified enzyme.

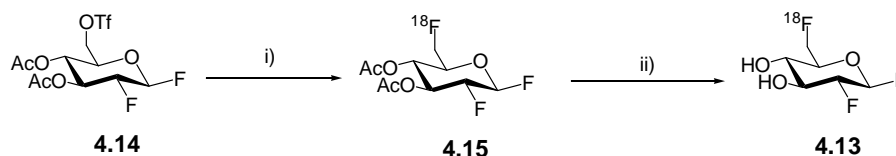
The approach for radiolabelling GCase that was adopted in the present study was to employ activated fluorosugars that act as active site-directed inactivators of GCase as probes. If an activated fluorosugar bearing a radionuclide were reacted with GCase *in vitro*, then the covalent glycosyl-enzyme intermediate thus generated could be injected into a small animal such as a mouse or rat and the distribution of the enzyme monitored using PET imaging. The advantage that this approach would have over other approaches is that the site of radiolabelling would be in the interior of the protein (the active site), making this a much more conservative structural perturbation that is less likely to change the biodistribution of the labelled enzyme. Since the rate of reactivation through hydrolysis of the covalent 2-deoxy-2-fluoro-glucosyl-enzyme intermediate is already known to be long ( $t_{1/2} = 1300$  min),<sup>211</sup> this species should be sufficiently stable over the time course necessary to acquire a PET image.

#### **4.2.2 Previous attempts to radiolabel GCase**

As mentioned above, there has already been one successful published attempt at radiolabelling GCase,<sup>304</sup> although this method does suffer from significant drawbacks. There have also been two previous attempts to radiolabel GCase using activated fluorosugars, as described below.

#### 4.2.2.1 2,6-Dideoxy-2-fluoro-6-[<sup>18</sup>F]-fluoro-β-D-glucosyl fluoride (**4.13**)

The first attempt to radiolabel GCase used 2,6-dideoxy-2-fluoro-6-[<sup>18</sup>F]-fluoro-β-D-glucopyranosyl fluoride (**4.13**) and was carried out by Dr. Alex Wong, then a graduate student in the Withers group. The synthetic route used is shown in Scheme 4.1.



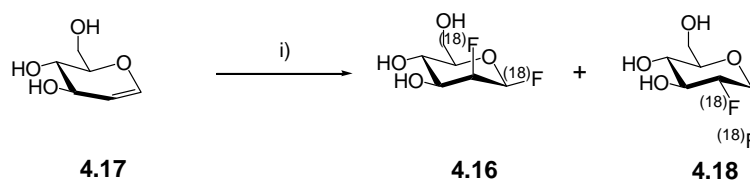
**Scheme 4.1.** Radiosynthesis of 2,6-dideoxy-2-fluoro-6-[<sup>18</sup>F]-fluoro-β-D-glucosyl fluoride (**4.13**). i) <sup>18</sup>F<sup>-</sup>, [2.2.2]-Kryptofix, MeCN; ii) NaOMe, MeOH, 9% radiochemical yield. Adapted from Wong *et al.*<sup>248</sup>

The decision to incorporate the radionuclide at C6 of the sugar ring was made because the precursor **4.14** was readily synthetically accessible, and because this allowed the use of <sup>18</sup>F<sup>-</sup> as the source of [<sup>18</sup>F], which has a higher specific activity than [<sup>18</sup>F]F<sub>2</sub>.<sup>108,110,112</sup> In addition, having a deoxy-fluoro modification at C6 also meant that this compound was not a substrate for hexokinase, and therefore **4.13** would not act as an FDG mimic (Section 1.5.4.1) which would lead to a signal from metabolic imaging that would overwhelm the desired image. This was a goal in the design of **4.13** since at the time Dr. Wong sought to use **4.13** as a radiotracer in imaging GCase levels *in vivo*, an experiment that was later abandoned.<sup>305</sup> Unfortunately, the attempted radiolabelling of GCase using **4.13** was unsuccessful, and at the time two possible explanations were offered. The first possible explanation is that hydrolysis of the triflate in **4.14** by contaminating water would lead to the generation of (cold) **2.1** following acetate removal, which is a much more efficient inactivator of GCase ( $k_i/K_i = 0.0227 \text{ min}^{-1}\text{mM}^{-1}$  and  $0.0017 \text{ min}^{-1}\text{mM}^{-1}$  for **2.1**<sup>211</sup> and **3.17**<sup>248</sup> respectively). This greater than 10-fold higher efficiency of **2.1** compared to **3.17** (and **4.13**) means that the enzyme will preferentially react with any contaminating **2.1**, leading to poor reaction with the desired radiolabel **4.13**. The second possible explanation for the lack of success in this experiment was that the inactivator has too poor an affinity for the enzyme active site at the relatively low concentration of inactivator relative to enzyme used in the radiolabelling attempt.<sup>305</sup>

To validate these results, a second attempt to radiolabel GCase using this approach was undertaken by the author and Dr. Chris Phenix, a postdoctoral fellow in the Withers lab. It was again observed that **4.13** did not radiolabel GCase under any of the experimental conditions tested. Model studies using **4.13** and Abg supported the hypothesis that modest amounts of **2.1** were generated during the radiosynthetic procedure outlined in Scheme 4.1, since increasing the concentration of **4.13** relative to the concentration of Abg actually led to a decrease in radiolabelling efficiency of Abg. This result was consistent with increased generation of contaminating **2.1**, but would not be expected if the problem encountered was that the concentration of inactivator was too low. Ultimately, owing to the problems encountered with contamination of **2.1** in preparations of **4.13**, a search was started for an alternative small molecule suitable for radiolabelling GCase.

#### 4.2.2.2 2-Deoxy-2- $^{18}\text{F}$ fluoro- $\beta$ -D-mannopyranosyl $^{18}\text{F}$ -fluoride (**4.16**)

The second attempt to radiolabel GCase was carried out by Dr. Neil Lim, a postdoctoral fellow in the Withers group using 2-deoxy-2- $^{18}\text{F}$ fluoro- $\beta$ -D-mannopyranosyl  $^{18}\text{F}$ -fluoride (**4.16**). The synthetic route used has been previously reported,<sup>247</sup> and is shown in Scheme 4.2.



**Scheme 4.2.** Radiosynthesis of 2-deoxy-2- $^{18}\text{F}$ fluoro- $\beta$ -D-mannopyranosyl  $^{18}\text{F}$ -fluoride (**4.16**). i)  $^{18}\text{F}\text{F}_2$ , MeCN, 1:2 **4.16** : **4.18**, 12% radiochemical yield **4.16**. Adapted from McCarter *et al.*<sup>247</sup> Note that each individual molecule of **4.16** or **4.18** only incorporates one  $^{18}\text{F}$  nucleus at either the anomeric center or at C2, and thus the fluorine atoms at these positions are marked with brackets to reflect this.

Dr. Lim reported that, although the desired compound **4.16** was synthesized and could successfully radiolabel Abg as shown by both TLC and size-exclusion HPLC analyses, all attempts at formation of the covalent glycosyl-enzyme intermediate following treatment

of **4.16** with GCase were unsuccessful.<sup>306</sup> It was not clear whether the difficulty in radiolabelling the enzyme arose from the lower specific activity of **4.16** owing to the use of [<sup>18</sup>F]F<sub>2</sub> as the source of [<sup>18</sup>F] (which is known to have low specific activity),<sup>108,110,112</sup> or the known low rate of reaction of the [<sup>19</sup>F] analogue of **4.16**, 2-deoxy-2-fluoro-β-D-mannosyl fluoride (**3.16**), with GCase ( $k_i/K_i = 0.0019 \text{ min}^{-1}\text{mM}^{-1}$ ).<sup>247</sup> Additionally, half of the radioactivity would in theory be lost upon treatment with a retaining β-glycosidase such as GCase, since statistically half of the radioactive fluorine atoms in **4.16** would be bonded to the anomeric center, and hence would be lost upon enzymatic reaction. Therefore, these drawbacks meant that a superior radiolabel was sought.

### **4.2.3 Radiolabelling of GCase with 2,4-dinitrophenyl 2-deoxy-2-[<sup>18</sup>F]-fluoro-β-D-glucopyranoside (**4.19**) and PET imaging results**

Note: These experiments were performed by the author in collaboration with Dr. Chris Phenix, a postdoctoral fellow in the Withers lab.

#### 4.2.3.1 Radiosynthesis of 2,4-dinitrophenyl 2-deoxy-2-[<sup>18</sup>F]-fluoro-β-D-glucopyranoside (**4.19**)

To try to address the issues that arose in the previous attempts to radiolabel GCase with an activated fluorosugar, a new target compound was sought. The ideal compound would:

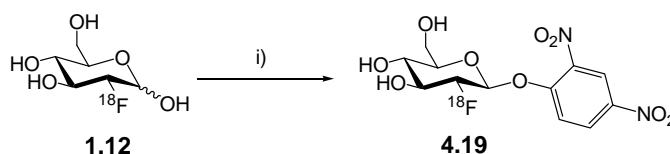
- 1) have a high specific activity;
- 2) be an efficient inactivator for GCase; and
- 3) not get contaminated during radiosynthesis with a more efficient cold inactivator.

Possible radiosynthetic routes towards a radiolabelled version of 2-deoxy-2-fluoro-β-D-glucopyranosyl fluoride (**2.1**), starting from **1.12**, were explored. Unfortunately, the necessary reactions appeared too sluggish, and required too many handling steps, to furnish the desired compound in sufficient amounts and high enough specific activities. Similarly,



radiolabelled derivatives containing phosphorus-based aglycones faced the same barriers, so their radiosyntheses were not attempted.

An examination of the literature revealed a report by Sharma *et al.* that described the one-step, stereoselective synthesis of 2,4-dinitrophenyl  $\beta$ -D-glucopyranoside starting from glucose and 2,4-dinitrofluorobenzene (DNFB) in a 1:1 mixture of saturated  $\text{NaHCO}_3$  : EtOH at 20 °C in 20% yield.<sup>307</sup> Optimization of this reaction using 2-deoxy-2-fluoro-glucose as the starting material, led to the discovery that increasing the temperature to 37 °C led to an impressive >75% yield of the desired 2,4-dinitrophenyl 2-deoxy-2-fluoro- $\beta$ -D-glucopyranoside (**3.3**) in a 10 minute reaction time. The analogous reaction using 2-deoxy-2- $^{18}\text{F}$ -fluoro-glucose (**1.12**) as the starting material led to the formation of 2,4-dinitrophenyl 2-deoxy-2- $^{18}\text{F}$ -fluoro- $\beta$ -D-glucopyranoside (**4.19**) in excellent yield, as shown in Scheme 4.3.



**Scheme 4.3.** Radiosynthesis of 2,4-dinitrophenyl 2-deoxy-2- $^{18}\text{F}$ -fluoro- $\beta$ -D-glucopyranoside (**4.19**).  
i) DNFB, saturated  $\text{NaHCO}_3$ /EtOH, 37 °C, 80% radiochemical yield.

The starting material for the synthesis of **4.19** is FDG (**1.12**, Section 1.5.4.1), which is a widely available radiopharmaceutical used most often for diagnostic imaging in cancer treatment. The advantage of using **1.12** as the starting material in this radiosynthesis is that the radionuclide incorporation step is already very well understood, and **1.12** can be produced in large amounts and in high specific activity and radiochemical purity, which addressed the first criteria outlined above. Finally, **4.19** has the highest efficiency of inactivation for GCase of any of the three radioactive derivatives tested, as judged by the relative second order rate constants for inactivation:  $k_i/K_i = 0.012$ , 0.0017 and 0.0019  $\text{min}^{-1}\text{mM}^{-1}$  for **4.19**, **4.13** and **4.16** respectively, which may address the second criteria.

In the present case, we were grateful to the B.C. Cancer Agency for the generous gift of **1.12** (16.25 mCi) which was used as the starting material in the radiosynthesis following

quality assurance analysis to ensure no contaminating species, particularly  $^{18}\text{F}^-$ , were present. Treatment of **1.12** with DNFB in a 1:1 mixture of saturated  $\text{NaHCO}_3$  : EtOH at 37 °C gave a highly regio- and stereo-selective reaction with the anomeric hydroxyl group to yield **4.19**, along with a small amount of the starting material **1.12** (5%) and 2-deoxy-2- $^{18}\text{F}$ -fluoro-6-(2,4-dinitrophenyl)-D-glucose (15%). A radio-TLC of the crude reaction mixture is shown in Figure 4.7. In this technique, a TLC plate is developed and analyzed using a radiation detector to produce a two-dimensional plot of counts versus  $R_f$ , with the origin of the TLC plate on the left side of the plot and the solvent front on the right side, as indicated by the dashed red lines.

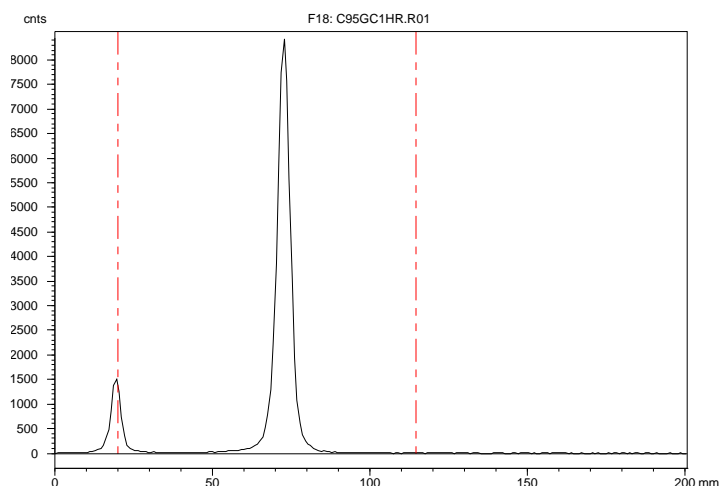


**Figure 4.7.** Radio-TLC analysis of the crude reaction mixture following treatment of **1.12** with DNFB, using a 4 : 1 EtOAc : MeOH eluent. The peak at the origin corresponds to unreacted **1.12**, and the peak at  $R_f = 0.6$  corresponds to the product **4.19**, as verified by co-spot TLC analysis with an authentic sample of **3.3**.

An advantage in this synthetic route was that the presence of a small amount of water does not generate a more efficient inactivator for the enzyme (as was the case in the synthesis of **4.13**), but instead harmlessly consumes some of the excess DNFB present, thus meeting the third criterion outlined above.

A  $\text{C}_{18}$  Sep-Pak was used for the initial purification of **4.19** from contaminating DNFB, and the radioactive fraction containing crude **4.19** was further purified by reverse-

phase HPLC using a Synergy (Phenomenex) column eluted using a gradient elution mobile phase of 60 : 40 MeOH : H<sub>2</sub>O → 100 % MeOH over 10 minutes. The desired compound **4.19** elutes after 14 minutes with a high percentage of methanol using this HPLC method. This was a beneficial feature of the purification procedure, as it meant that the solvent was evaporated relatively quickly, reducing the overall time of the radiosynthesis. Radio-TLC analysis of the purified **4.19** (3.25 mCi, 32% radiochemical yield decay corrected from **1.12**) shows the presence of only one radioactive peak, which corresponds to **4.19** (Figure 4.8).

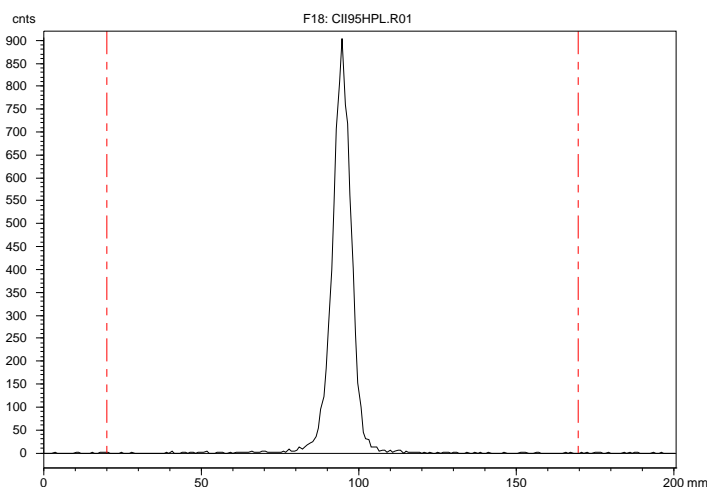


**Figure 4.8.** Radio-TLC analysis of **4.19** following HPLC purification using a 4:1 EtOAc : MeOH eluent. The peak at  $R_f = 0.6$  corresponds to the product **4.19**.

#### 4.2.3.2 Radiolabelling of Abg with **4.19**

Since Abg has proven to be such a useful model enzyme in many other applications, the ability of **4.19** to radiolabel Abg was tested prior to testing with GCase. Incubation of the purified **4.19** with Abg in a small volume (200  $\mu$ L) of the assay buffer used for the kinetic analysis of Abg activity (sodium phosphate buffer, pH = 6.8) led to an efficient radiolabelling reaction over the course of 10 minutes, as shown by radio-TLC (Figure 4.9). In this radio-TLC experiment, the radioactive peak at the origin corresponds to Abg labelled by **4.19**, since the protein is very polar. This efficient labelling reaction is the expected result since **3.3**, which is the [<sup>19</sup>F]-analogue of **4.19**, is an extremely efficient inactivator of Abg ( $k_i/K_i = 500 \text{ min}^{-1} \text{ mM}^{-1}$ ).<sup>58</sup>

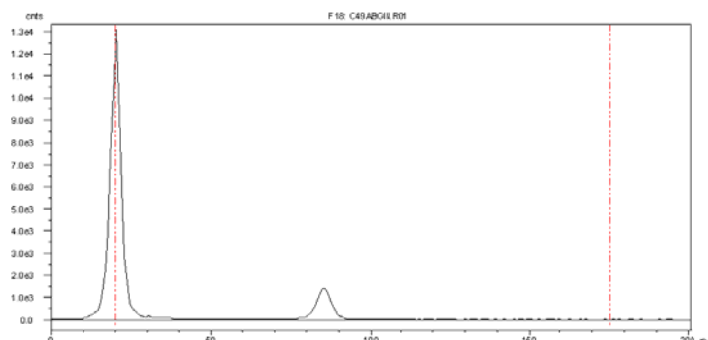


**Figure 4.9.** Radio-TLC analysis of **4.19** treated with Abg for 10 minutes using a 4:1 EtOAc : MeOH eluent. The peak at the origin corresponds to the radiolabelled covalent glycosyl-enzyme intermediate.

To demonstrate that **4.19** was reacting with the enzyme in an active site-specific manner, a Glu359Ala Abg variant protein, in which the catalytic nucleophile has been mutated to a non-nucleophilic alanine residue was incubated with **4.19**. No radiolabelling of the enzyme was observed by radio-TLC analysis (data not shown), confirming that labelling of wild-type Abg is an active site-specific process. Additionally, treatment of wild-type Abg with **4.19**, followed by incubation with 20 mM thiophenyl  $\beta$ -D-glucopyranoside led to loss of radioactivity on Abg, as measured by the time-dependent decrease in the radio-TLC peak at the origin corresponding to the radiolabelled Abg. This was accompanied by a time-dependent increase in a new peak with an  $R_f$  consistent with a neutral small molecule as seen in Figure 4.10. Scheme 4.4 shows the mechanism that is proposed to explain this observation, involving transglycosylation of the radiolabelled sugar from the enzyme onto the thiophenyl  $\beta$ -D-glucopyranoside, which produces a new radiolabelled disaccharide and regenerates free Abg. Both of these experiments are consistent with the generation of a radioactive covalent glycosyl-enzyme intermediate in the enzyme active site. In this instance, it was actually found that HPLC purification of **4.19** was not necessary, as radiolabelling of the protein could be achieved using either the **4.19** purified following Sep-Pak and HPLC purification, or by Sep-Pak purification alone.

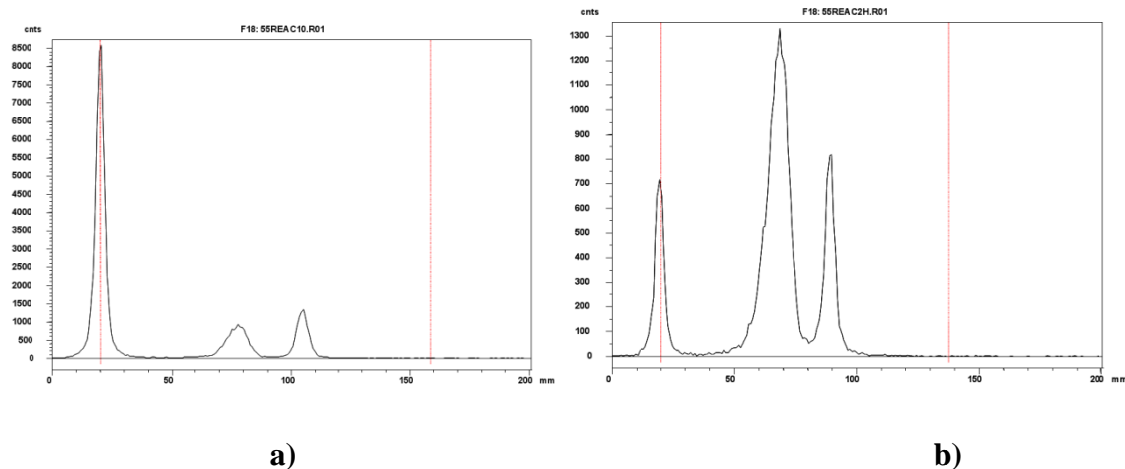
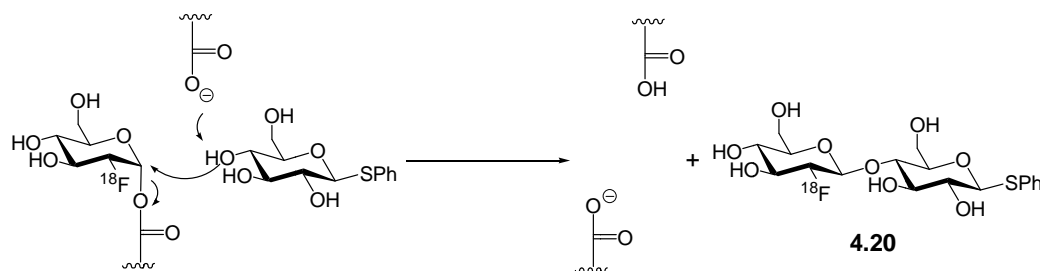


**Figure 4.10.** Radio-TLC analysis of **4.19** treated with Abg, followed by incubation with 20 mM thiophenyl  $\beta$ -D-glucopyranoside using a 4:1 EtOAc : MeOH eluent, sampled at a) 10 minutes, and b) 2 hours. The peak at the baseline corresponds to the radiolabelled covalent glycosyl-enzyme intermediate, the peak at  $R_f = 0.5$  is the newly formed peak, proposed to be **4.20**, and the peak at  $R_f = 0.6$  is residual **4.19**.



**Scheme 4.4.** Proposed mechanism for recovery of Abg activity following incubation with 20 mM thiophenyl  $\beta$ -D-glucopyranoside through transglycosylation of the radiolabelled glycosyl-enzyme intermediate.

#### 4.2.3.3 Radiolabelling of GCase with **4.19**

Following HPLC purification, **4.19** (2.81 mCi) was also reacted with GCase in a small amount of assay buffer (300  $\mu$ L,  $\sim$ 5 mg/mL GCase) in order to radiolabel GCase. Radio-TLC analysis after 45 minutes incubation revealed the presence of a major new radioactive peak at the baseline of the TLC plate (Figure 4.11), which is consistent with radiolabelled GCase. To verify this assignment, a separate experiment in which **4.19** was

incubated in the presence of both GCase and the known<sup>289</sup> competitive inhibitor 6-nonyl-isofagomine (1 mM,  $IC_{50} = 0.6$  nM), no baseline peak was observed (data not shown), consistent with the radiolabel being active site-directed.

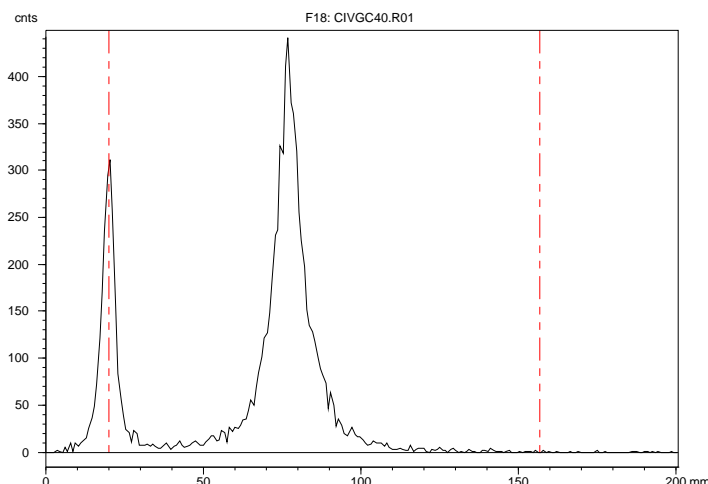


**Figure 4.11.** Radio-TLC analysis of the reaction of **4.19** with GCase using a 4:1 EtOAc : MeOH eluent. The peak at the origin corresponds to the radiolabelled covalent glycosyl-enzyme intermediate.

For the labelling reaction to be successful, it was important to keep the reaction mixture volume as low as possible to increase the concentration of **4.19** relative to the protein and therefore increase the efficiency of the labelling reaction. The solubility of the GCase protein limited the lowest achievable volumes; at concentrations  $> \sim 5$  mg/mL the protein aggregated and precipitated out of solution, making the labelling reaction ineffective. Unlike the case with Abg, the HPLC purification step was essential to avoid protein precipitation. This presumably arises from the reaction of GCase with small amounts of residual contaminating DNFB to modify amino acid residues on the surface of the enzyme. DNFB could have been carried through during the Sep-Pak purification but no longer be present in the samples of **4.19** purified by HPLC.

Following the labelling reaction, the final step involved purification of the radiolabelled protein from the remaining **4.19**. This was accomplished first by concentrating the protein by centrifugation using a 50 kDa molecular weight cut-off filter, followed by gel filtration using Pierce desalting columns. The filtrate was collected and analyzed by radio-

TLC analysis, showing the radiolabelled protein present in >98% radiochemical purity (Figure 4.12). The final activity was 0.147 mCi (7 % radiochemical yield, decay corrected from the HPLC-purification of **4.19**). The major reason for the low radiochemical yield in this step was sample loss during the handling of GCase. Following the radiolabelling reaction, significant amounts of radioactivity could be detected in both the molecular weight cut-off filters and the protein desalt columns during the protein purification steps. These handling losses likely occur because GCase is known to be prone to aggregation and adhering to the plastic laboratory equipment.<sup>212</sup>

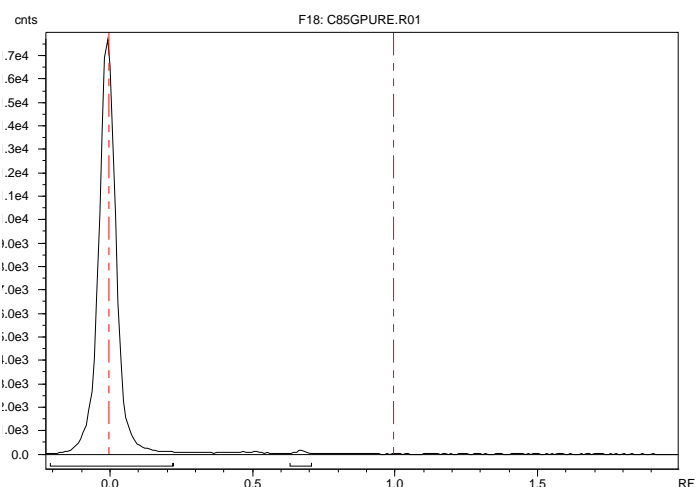


**Figure 4.12.** Radio-TLC analysis of purified radiolabelled GCase using a 4:1 EtOAc : MeOH eluent. The peak at the origin corresponds to the radiolabelled covalent glycosyl-enzyme intermediate.

The reaction between **4.19** and GCase is the first demonstration of the radiolabelling of that enzyme using an  $^{18}\text{F}$ -labelled covalent inactivator. The synthetic route used to generate **4.19** met the three criteria outlined at the beginning of Section 4.2.3.1, as described above, and furnished sufficient purified, radiolabelled GCase to facilitate preliminary MicroPET imaging experiments to be attempted, as described below.

#### 4.2.3.4 PET imaging experiments using GCase radiolabelled by 4.19

Note: PET imaging experiments were performed by Ms. Siobhan McCormick and Ms. Karin Yip using the MicroPET facilities and scanner at the UBC Hospital.

To assess the *in vivo* distribution of recombinant GCase, the purified, radiolabelled GCase (25-50  $\mu$ Ci) was injected into the tail vein of a Balb/c mouse in a volume less than 125  $\mu$ L. Following this, the mouse was anaesthetized and scanned using PET for two hours. A sample image generated from these experiments is shown in Figure 4.13. The PET scan shows uptake in the liver, gall bladder, bone marrow, spleen and bladder among other organs. No uptake was observed in the brain, as would be expected since ERT is known to be ineffective for patients suffering from neuronopathic forms of Gauchers disease.<sup>64</sup>

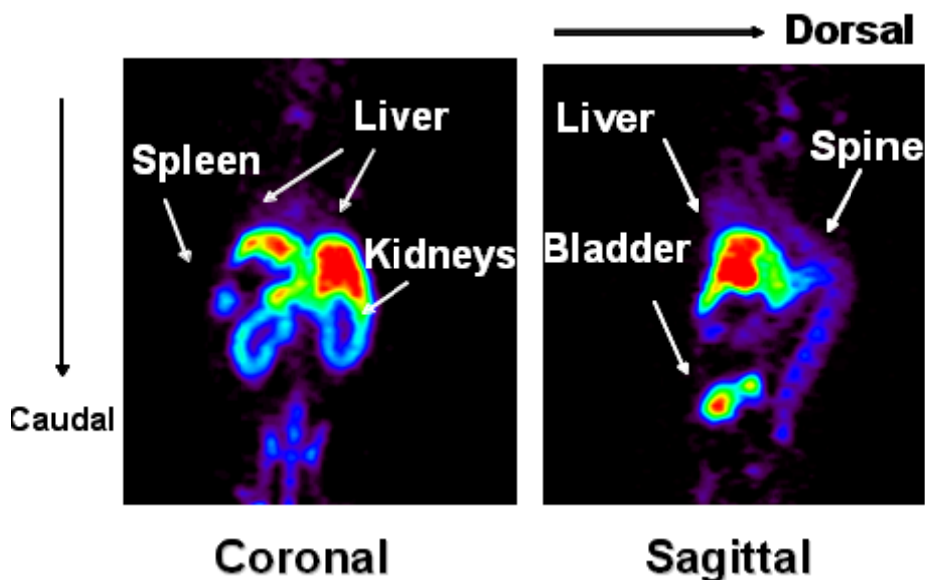


**Figure 4.13.** Micro-PET images generated by injection of radiolabelled GCase into a mouse. Regions showing high activity are coloured red and regions showing low activity are coloured blue.

To demonstrate that the PET image is visualizing intact radiolabelled GCase injected into the mouse, a receptor blocking experiment was undertaken. Since it is known that the recombinant form of GCase is taken up by cells and trafficked into the lysosome by the mannose receptors on the cell surface,<sup>67,71,73,267,303,308</sup> a competitive inhibitor of the mannose



receptor should reduce the uptake of the radiolabelled GCase if the process is receptor mediated. To test this, a mouse was first injected with yeast mannan (15 mg/kg), a known inhibitor of GCase uptake,<sup>266</sup> prior to injection with the radiolabelled enzyme. The rate of uptake in all organs was significantly lower in mice pre-treated with mannan than in those that were untreated, as can be seen in the PET images in Figure 4.14.

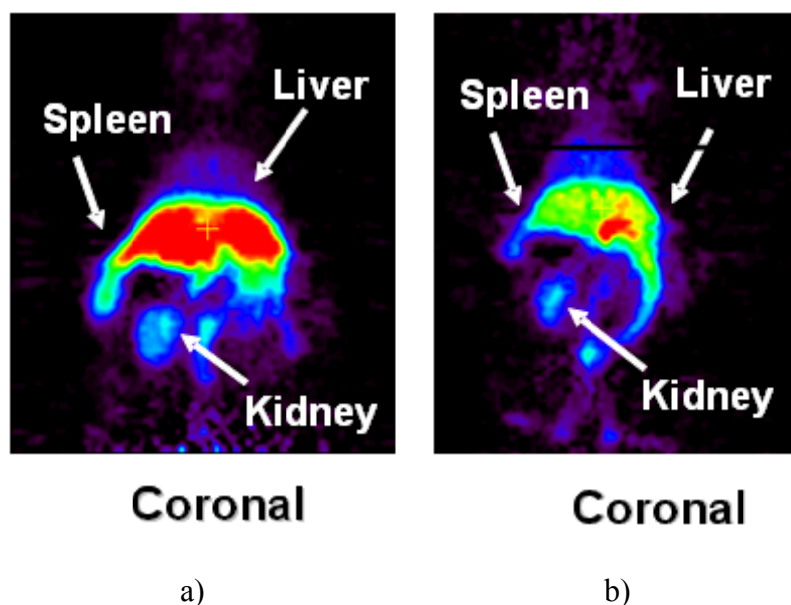


**Figure 4.14.** Comparison of PET images obtained for mice a) untreated and b) treated with mannan prior to injection by GCase radiolabelled by **4.19**. Regions showing high activity are coloured red and regions showing low activity are coloured blue.

Other experiments investigating the biodistribution of GCase that support the validity of the data interpreted from the above images have been performed, including post-mortem tissue  $\gamma$ -counting, detailed rates of tracer uptake expressed as a %-injected dose/mL/min and calculations of the specific activity of labelled enzyme. However, these experiments are not primarily the work of the author, and hence further detail is not included in this work. However, these details are the focus of a forthcoming publication under the primary authorship of Dr. Chris Phenix, Dr. Lorne Clarke, and Dr. Stephen Withers. Furthermore, some of the future experiments that are planned include metabolism studies, and imaging studies using a genetically engineered mouse model of Gauchers disease.<sup>240</sup>

#### 4.2.4 Conclusions and future directions

The objective for this section was to develop a radiosynthetic route to an activated fluorosugar containing  $^{18}\text{F}$  that would be suitable for radiolabelling GCase through the formation of a covalent glycosyl-enzyme intermediate. Such a species would be usable as a PET imaging agent for monitoring ERT for the treatment of Gauchers disease. The advantage of this approach is that since the radiolabel is on the interior of the protein, it is unlikely to have an effect on the biodistribution of the injected enzyme. There have been two previous attempts in the Withers group to use [ $^{18}\text{F}$ ]-labelled activated fluorosugars to radiolabel GCase using **4.13** or **4.16**. In the case of **4.13**, the radiolabelling of GCase was unsuccessful, likely because of contamination by **2.1** arising from hydrolysis of the triflate in the starting material **4.14**. Attempted radiolabelling of GCase using **4.16** also failed, probably because of the poor kinetic parameters of inactivation for **4.16** and because of the low specific activity. To address these challenges, a radiosynthetic route for **4.19** was developed that avoided generation of a more reactive contaminant and still maintained high specific activity by using **1.12** as a convenient starting material. Samples of **4.19** were shown to be active-site directed inactivators of both Abg, used as a model retaining  $\beta$ -glucosidase, and GCase. The GCase thus radiolabelled was purified and injected into healthy mice to study its biodistribution using PET imaging.

There remain many future avenues of research that can be explored using this new technology. In the short term, one goal will be to study whether the biodistribution of GCase is different in a genetically engineered mouse model of Gauchers disease compared to a healthy mouse. Additionally, while it seems unlikely, it remains to be proven that incorporation of the fluorosugar radiolabel does not alter the biodistribution of injected GCase. This could be accomplished by experiments in which GCase is non-specifically radiolabelled (with, for example, tritium), and reacted with an activated fluorosugar such as **2.1** or **3.3**, then injected into mice. At various time points the animals can be sacrificed and the radioactivity in various organs measured. Comparisons with experiments in which GCase has not been inactivated can then be used to determine if the fluorosugar inactivation process alters the biodistribution of the injected enzyme. As well, it will be desirable to study the

metabolic fate of the radiolabelled enzyme by studying the products of metabolism of the radiolabelled enzyme. In the longer term, this technology may be useful for testing different enzyme formulations or delivery systems to investigate more efficient delivery of the enzyme to affected tissues, or to investigate possible treatments for the neurological symptoms in Types II and III Gauchers disease using ERT. As well, PET scanning can be used to monitor the effects of a longer dosing regime on the possible development of an immunological response to the recombinant enzyme by repeatedly monitoring the same test subject without needing to sacrifice it. Finally, if the radiolabelling reaction can be successfully scaled up, then this technology may be used to monitor ERT in human patients.

From a radiochemical perspective, one improvement on this technology may be to devise a radiosynthetic route to generate a radiolabelled fluorosugar containing a phosphorus-based aglycone. A synthetic route analogous to the one used to generate **4.19**, using **1.12** as the starting material treated with an activated electrophilic phosphorus species such as a dibenzyl phosphoryl chloride, for example, appears to be a particularly promising future direction as well.

## **Chapter 5: Materials and Methods**

## 5.1 Synthetic chemistry

### 5.1.1 General procedures for chemical synthesis

All buffer chemicals and other reagents were obtained from Sigma-Aldrich Chemical Company, unless otherwise noted. Solvents and reagents used were either reagent or spectral grade. Anhydrous solvents were prepared as follows under a nitrogen atmosphere: methanol was distilled over magnesium turnings; carbon tetrachloride, acetonitrile, pyridine, toluene and dichloromethane were individually distilled over calcium hydride; diethyl ether was distilled over sodium in the presence of benzophenone. All solvents were used immediately after cooling to room temperature following distillation.

Synthetic reactions were monitored by TLC using Merck Kieselgel 60 F<sub>254</sub> aluminum-backed sheet (thickness 0.2 mm). Compounds were detected by illumination using ultraviolet light ( $\lambda=254$  nm) followed by charring with 10% ammonium molybdate in 2 M H<sub>2</sub>SO<sub>4</sub> and heating. Flash chromatography was performed under positive pressure using the in-house air system on Silicycle SilicaFlash F60 (230-400 mesh) silica gel using the specified eluants. <sup>1</sup>H NMR spectra were recorded on a Bruker AV300 spectrometer at 300 MHz or a Bruker AV400 spectrometer at 400 MHz, equipped with either indirect or direct proton detection. Proton chemical shifts are reported in  $\delta$  units (ppm), and are referenced to CDCl<sub>3</sub> at 7.27 ppm. <sup>19</sup>F NMR spectra were recorded on a Bruker AV300 spectrometer at 282 MHz. Fluorine chemical shifts are reported in  $\delta$  units (ppm), and are referenced to CFCl<sub>3</sub> at 0 ppm. <sup>31</sup>P NMR spectra were recorded on a Bruker AV300 spectrometer at 121 MHz. Phosphorus chemical shifts are reported in  $\delta$  units (ppm), and are referenced to 85% H<sub>3</sub>PO<sub>4</sub> at 0 ppm. <sup>13</sup>C NMR spectra were recorded on a Bruker AV300 spectrometer at 75 MHz or a Bruker AV400 spectrometer at 100 MHz, equipped with either indirect or direct carbon detection. Carbon chemical shifts are reported in  $\delta$  units (ppm), and are referenced to CDCl<sub>3</sub> at 77.23 ppm. Low resolution ESI mass spectrometry was performed on a Waters LC-MS equipped with an autosampler. High resolution ESI mass spectrometry was performed by the University of British Columbia Department of Chemistry Mass Spectrometry Laboratory using a Waters/Micromass LCT mass spectrometer. All compounds are drawn in <sup>4</sup>C<sub>1</sub> conformations for clarity.

#### 5.1.1.1 General procedure A for bromination

The compound of interest was dissolved in an appropriate volume of 33% (by weight) HBr in acetic acid (in a ratio of 500 mg of starting material to 1 mL of HBr solution) in an open flask equipped with a drying tube on top, and allowed to stir until the reaction was complete as determined by TLC. The solution was diluted in an appropriate volume of ethyl acetate, then washed successively with ice-cold H<sub>2</sub>O (2x), sat. NaHCO<sub>3</sub> (1x) and sat. NaCl. The organic layer was then dried over MgSO<sub>4</sub> for 10 minutes, filtered, and concentrated under reduced pressure.

#### 5.1.1.2 General procedure B for deprotection of esters

The compound of interest was dissolved in an appropriate volume of dry methanol (in a ratio of 50 mg starting material to 1 mL of methanol), and a small chunk of sodium was added. The reaction was stirred under N<sub>2(g)</sub> for 30 minutes. The solution was neutralized by addition of a small scoop of silica gel, and evaporated under reduced pressure to leave the crude product adsorbed onto silica gel.

#### 5.1.1.3 General procedure C for free radical bromination

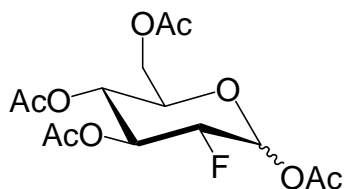
The compound of interest was dissolved in an appropriate volume of carbon tetrachloride (in a ratio of 50 mg starting material to 1 mL of carbon tetrachloride) and poured into the bottom of an Ace water jacket-cooled immersion-well photoreactor equipped with an N<sub>2(g)</sub> inlet. Solid *N*-bromosuccinimide (NBS, recrystallized from water) was added in one portion, and the reaction mixture stirred under illumination by a 600 W lamp under N<sub>2(g)</sub> until the reaction was deemed complete by TLC analysis. The resulting brown solution was filtered to remove the solid succinimide. The filtrate was collected and the solvent evaporated under reduced pressure to yield the crude product.

#### 5.1.1.4 General procedure D for deprotection of esters

The compound of interest was dissolved in an appropriate volume of dry methanol (in a ratio of 100 mg starting material to 1 mL of methanol), and cooled to 0 °C. Ammonia was then bubbled through the solution for 5 minutes, at which point the reaction was stirred at 0 °C until the reaction was deemed complete by TLC. A small portion of Celite was added, and the solvent was evaporated under reduced pressure to leave the crude product adsorbed onto Celite.

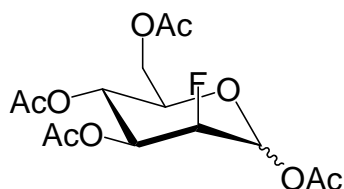
#### 5.1.2 Synthesis and compound characterization

1,3,4,6-Tetra-O-acetyl -2-deoxy-2-fluoro-D-glucopyranose (**2.11**)<sup>309</sup>



and

1,3,4,6-Tetra-O-acetyl-2-deoxy-2-fluoro-D-mannopyranose (**2.10**)<sup>309</sup>

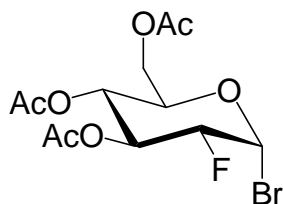


3,4,6-Tri-O-acetyl D-glucal (29.4 g, 108 mmol, 1.0 eq) was dissolved in acetonitrile (400 mL) and glacial acetic acid (150 mL). The reaction mixture was heated to 70 °C under N<sub>2(g)</sub>. To this was added Selectfluor<sup>TM</sup> (49.3 g, 0.139 mmol, 1.3 eq) and the solution allowed to stir for 2.5 hours before being cooled to room temperature. Following solvent evaporation under reduced pressure, the residue was dissolved in ethyl acetate and washed with 2 x H<sub>2</sub>O, 1 x saturated NaHCO<sub>3</sub>, 1 x brine and dried over MgSO<sub>4</sub>. After 10 minutes, the MgSO<sub>4</sub> was filtered off, and the solvent evaporated under reduced pressure. The products were purified by flash chromatography (3:1 hexane : ethyl acetate) to yield **2.11** (7.34 g, 21.0 mmol, 19%)

and **2.10** (7.47 g, 21.3 mmol, 20%) both as colourless oils. **2.11**: **<sup>1</sup>H NMR**: (300 MHz, CDCl<sub>3</sub>) δ 6.38 (1 H, d, J<sub>H1α-H2α</sub> 4.0 Hz, H1α), 5.75 (1 H, dd, J<sub>H1β-H2β</sub> 8.3 Hz, H1β-F2 3.0 Hz, H1β), 5.52 (1 H, dt, J<sub>H3α-F2</sub> 12.1 Hz, J<sub>H3α-H2α</sub> = J<sub>H3α-H4α</sub> 9.6 Hz, H3α), 5.35 (1 H, dt, J<sub>H3β-F2</sub> 14.4 Hz, J<sub>H3β-H2β</sub> = J<sub>H3β-H4β</sub> 8.3 Hz, H3β), 5.09 – 5.00 (2 H, m, H4α, H4β), 4.63 (1 H, ddd, J<sub>H2α-F2</sub> 48.5 Hz, J<sub>H2α-H3α</sub> 9.6 Hz, J<sub>H2α-H1α</sub> 4.0 Hz, H2α), 4.44 (1 H, dt, J<sub>H2β-F2</sub> 51.0 Hz, J<sub>H2β-H3β</sub> = J<sub>H2β-H1β</sub> 8.3 Hz, H2β), 4.22-4.08 (2 H, m, H6α, H6β), 4.08-4.00 (3 H, m, H5β, H6'α, H6'β), 3.69 (1 H, ddd, J 9.5 Hz, J 4.0 Hz, J 1.2 Hz, H5β), 2.17 (3 H, s, Ac), 2.15 (3 H, s, Ac), 2.05 (3 H, s, Ac), 2.04 (3 H, s, Ac), 2.03 (3 H, s, Ac), 2.01 (3 H, s, Ac), 2.00 (3 H, s, Ac), 1.99 (3 H, s, Ac); **<sup>19</sup>F NMR**: (282 MHz, CDCl<sub>3</sub>): δ -201.29 (1 F, ddd, J<sub>F2-H2β</sub> 51.0 Hz, J<sub>F2-H3β</sub> 14.4 Hz, J<sub>F2-H1β</sub> 3.0 Hz, F2β), -202.63 (1 F, dd, J<sub>F2-H1α</sub> 48.5 Hz, J<sub>F2-H3α</sub> 12.1 Hz, F2α); **ESI-MS (low res)**: m/z calc.: 373.1; **Found**: 373.3 [M + Na]<sup>+</sup>. **2.10**: **<sup>1</sup>H NMR**: (300 MHz, CDCl<sub>3</sub>) δ 6.13 (1 H, dd, J<sub>H1α-F2</sub> 6.5 Hz, J<sub>H1α-H2α</sub> 2.1 Hz, H1α), 5.76 (1 H, d, J<sub>H1β-F2</sub> 19.0 Hz, H1β), 5.37 (1 H, t, J<sub>H4α-H5α</sub> = J<sub>H4α-H3α</sub> 10.1 Hz, H4α), 5.32 (1 H, t, J<sub>H4β-H5β</sub> = J<sub>H4β-H3β</sub> 10.3 Hz, H4β), 5.23 (1 H, ddd, J<sub>H3α-F2</sub> 27.9 Hz, J<sub>H3α-H4α</sub> 10.1 Hz, J<sub>H3α-H2α</sub> 2.1 Hz, H3α), 5.05 (1 H, ddd, J<sub>H3β-F2</sub> 27.0 Hz, J<sub>H3β-H4β</sub> 10.1 Hz, J<sub>H3β-H2β</sub> 2.4 Hz, H3β), 4.83 (1 H, dd, J<sub>H2β-F2</sub> 51.2 Hz, J<sub>H2β-H3β</sub> 2.4 Hz, H2β), 4.71 (1 H, dt, J<sub>H2α-F2</sub> 46.6 Hz, J<sub>H2α-H1α</sub> = J<sub>H2α-H3α</sub> 2.1 Hz, H2α), 4.23-4.21 (2 H, m, H6α, H6β), 4.13-3.99 (3 H, m, H6'α, H6'β, H5α), 3.87 (1 H, ddd, J<sub>F2-H1β</sub> 10.1 Hz, J 4.7 Hz, J 2.2 Hz, H5β), 2.14 (6 H, s, 2 x Ac), 2.12 (3 H, s, Ac), 2.07 (3 H, s, Ac), 2.04 (3 H, s, Ac), 2.01 (3 H, s, Ac), 2.01 (3 H, s, Ac), 2.00 (3 H, s, Ac); **<sup>19</sup>F NMR**: (282 MHz, CDCl<sub>3</sub>): δ -201.34 (1 F, ddd, J<sub>F2-H2α</sub> 46.6 Hz, J<sub>F2-H3α</sub> 27.9 Hz, J<sub>F2-H1α</sub> 6.5 Hz, F2α), -220.21 (1 F, dd, J<sub>F2-H2β</sub> 51.2 Hz, J<sub>F2-H3β</sub> 27.0 Hz, F2β); **ESI-MS (low res)**: m/z calc.: 350.1; **Found**: 373.3 [M + Na]<sup>+</sup>.

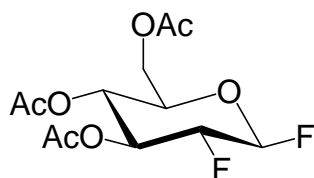


3,4,6-Tri-O-acetyl-2-deoxy-2-fluoro- $\alpha$ -D-glucopyranosyl bromide (**2.12**)<sup>184</sup>



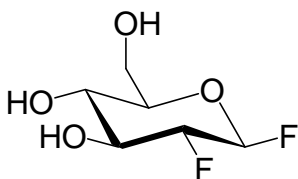
**2.11** (5.07 g, 14.5 mmol) was brominated according to General Procedure A overnight. The crude product (4.99 g, 13.4 mmol, 92%) was used without further purification or characterization.

3,4,6-Tri-O-acetyl-2-deoxy-2-fluoro- $\beta$ -D-glucopyranosyl fluoride (**2.13**)<sup>184</sup>



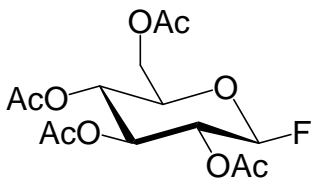
**2.12** (2.14 g, 5.77 mmol, 1.0 eq) was dissolved in 50 mL dry acetonitrile. Silver fluoride (1.27 g, 6.74 mmol, 1.2 eq) was added, and the resulting slurry stirred overnight under N<sub>2(g)</sub>, in the dark. The solution was filtered through a short plug of silica using ethyl acetate as the eluent to remove the silver salts. The filtrate was collected and the solvent evaporated under reduced pressure to yield the crude solid. The product was recrystallized from ethyl acetate/hexane to yield **2.13** as a white solid (1.61 g, 5.19 mmol, 90%). **<sup>1</sup>H NMR:** (300 MHz, CDCl<sub>3</sub>)  $\delta$  5.42 (1 H, ddd, J<sub>H1-F1</sub> 52.2 Hz, J<sub>H1-H2</sub> 6.2 Hz, J<sub>H1-F2</sub> 3.8 Hz, H1), 5.32 (1 H, ddd, J<sub>H3-F2</sub> 15.4 Hz, J<sub>H3-H2</sub> 8.0 Hz, J<sub>H3-H4</sub> 9.5 Hz, H3), 5.11 (1 H, t, J<sub>H4-H3</sub> = J<sub>H4-H5</sub> 9.5 Hz, H4), 4.47 (1 H, dddd, J<sub>H2-F2</sub> 50.0 Hz, J<sub>H2-F1</sub> 14.2 Hz, J<sub>H2-H3</sub> 8.0 Hz, J<sub>H2-H1</sub> 6.2 Hz, H2), 4.26 (1 H, dd, J<sub>H6-H6'</sub> 12.5 Hz, J<sub>H6-H5</sub> 4.8 Hz, H6), 4.18 (1 H, dd, J<sub>H6'-H6</sub> 12.5 Hz, J<sub>H6'-H5</sub> 2.8 Hz, H6'), 3.88 (1 H, ddd, J<sub>H5-H4</sub> 9.5 Hz, J<sub>H5-H6</sub> 4.8 Hz, J<sub>H5-H6'</sub> 2.8 Hz, H5), 2.08 (3 H, s, Ac), 2.04 (3 H, s, Ac), 2.03 (3 H, s, Ac); **<sup>19</sup>F NMR:** (282 MHz, CDCl<sub>3</sub>):  $\delta$  -140.01 (1 F, ddd, J<sub>F1-H1</sub> 52.2 Hz, J<sub>F1-F2</sub> 15.4 Hz, J<sub>F1-H2</sub> 14.2 Hz, F1), -200.48 (1 F, dtd, J<sub>F2-H2</sub> 50.0 Hz, J<sub>F2-F1</sub> = J<sub>F2-H3</sub> 15.4 Hz, J<sub>F2-H1</sub> 3.8 Hz, F2); **ESI-MS (low res):** m/z calc.: 310.25; **Found:** 333.3 [M + Na]<sup>+</sup>.

2-Deoxy-2-fluoro- $\beta$ -D-glucopyranosyl fluoride (**2.1**)<sup>184</sup>



**2.13** (0.594 g, 1.91 mmol) was dissolved in 15 mL of dry methanol and deacetylated according to General Procedure B for 30 minutes. The product was purified by flash chromatography (9:1 ethyl acetate : methanol) to yield a colourless oil that could be triturated with diethyl ether to yield **2.1** as a white powder (0.344 g, 1.87 mmol, 98%). **<sup>1</sup>H NMR:** (300 MHz, CD<sub>3</sub>OD)  $\delta$  5.33 (1 H, ddd,  $J_{H1-F1}$  53.5 Hz,  $J_{H1-H2}$  7.0 Hz,  $J_{H1-F2}$  3.3 Hz, H1), 4.10 (1 H, dddd,  $J_{H2-F2}$  51.8 Hz,  $J_{H2-F1}$  15.9 Hz,  $J_{H2-H3}$  8.8 Hz,  $J_{H2-H1}$  7.0 Hz, H2), 3.86 (1 H, d,  $J_{H6-H6'}$  12.0 Hz, H6), 3.69 (1 H, dd,  $J_{H6'-H6}$  12.0 Hz,  $J_{H6'-H5}$  4.9 Hz, H6'), 3.62 (1 H, dt,  $J_{H3-F2}$  16.3 Hz,  $J_{H3-H2}$  8.6 Hz =  $J_{H3-H4}$  8.6 Hz, H3), 3.45-3.35 (2 H, m, H4, H5). **<sup>19</sup>F NMR:** (282 MHz, CDCl<sub>3</sub>):  $\delta$  -145.60 (1 F, dt,  $J_{F1-H1}$  53.5 Hz,  $J_{F1-F2} = J_{F1-H2}$  15.9 Hz, F1), -204.07 (1 F, ddd,  $J_{F2-H2}$  51.8 Hz,  $J_{F2-H3}$  16.3 Hz,  $J_{F2-F1}$  15.9 Hz,  $J_{F2-H1}$  3.3 Hz, F2); **ESI-MS (high res):**  $m/z$  calc.: 204.0447; **Found:** 207.0445 [M + Na]<sup>+</sup>; **Anal. calc. for** C<sub>6</sub>H<sub>10</sub>F<sub>2</sub>O<sub>4</sub>: C, 39.14, H, 5.47; **Found:** C, 39.85, H, 5.56.

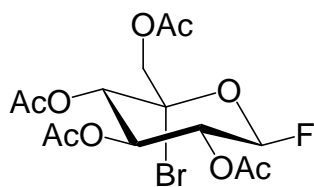
2,3,4,6-Tetra-O-acetyl- $\beta$ -D-glucopyranosyl fluoride (**2.15**)<sup>129</sup>



2,3,4,6-Tetra-O-acetyl- $\alpha$ -D-glucopyranosyl bromide<sup>310</sup> (2.51 g, 6.10 mmol) was dissolved in 50 mL dry acetonitrile. Silver fluoride (1.03 g, 8.12 mmol, 1.3 eq) was added, and the resulting slurry stirred overnight under N<sub>2(g)</sub>, in the dark. The solution was filtered through a short plug of silica using ethyl acetate as the eluent to remove the silver salts. The filtrate was

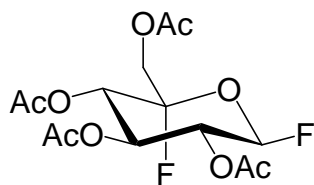
collected and the solvent evaporated under reduced pressure to yield the crude product, which was purified by flash chromatography (2:1 petroleum ether : ethyl acetate) to yield **2.15** as a white solid (1.46 g, 4.17 mmol, 68%). **<sup>1</sup>H NMR:** (300 MHz, CDCl<sub>3</sub>) δ 5.32 (1 H, dd, J<sub>H1-F1</sub> 52.0 Hz, J<sub>H1-H2</sub> 6.0 Hz, H1), 5.18-5.15 (2 H, m, H3, H4), 5.09-5.01 (1 H, m, H2), 4.23 (1 H, dd, J<sub>H6-H6'</sub> 12.4 Hz, J<sub>H6-H5</sub> 4.4 Hz, H6), 4.16 (1 H, dd, J<sub>H6'-H6</sub> 12.4 Hz, J<sub>H6'-H5</sub> 2.8 Hz, H6'), 3.86 (1 H, ddd, J<sub>H5-H4</sub> 9.8 Hz, J<sub>H5-H6</sub> 4.4 Hz, J<sub>H5-H6'</sub> 2.8 Hz, H5), 2.06 (3 H, s, Ac), 2.05 (3 H, s, Ac), 2.00 (3 H, s, Ac), 1.99 (3 H, s, Ac); **<sup>19</sup>F NMR:** (282 MHz, CDCl<sub>3</sub>): δ -137.75 (1 F, dd, J<sub>F1-H1</sub> 52.0 Hz, J<sub>F1-H2</sub> 9.9 Hz, F1); **<sup>13</sup>C NMR:** (75 MHz, CDCl<sub>3</sub>): δ 170.69, 170.14, 169.42, 169.25 (4 x C=O), 106.31 (d, J<sub>C1-F1</sub> 220 Hz, C1), 72.11 (d, J<sub>C5-F1</sub> 4 Hz, C5), 71.86 (d, J<sub>C3-F1</sub> 8 Hz, C3), 71.25 (d, J<sub>C2-F1</sub> 29 Hz, C2), 67.51 (C4), 61.83 (C6), 20.80 (2C), 20.67 (2C) (4 x Ac); **ESI-MS (low res):** m/z calc.: 373.1; **Found:** 373.2 [M + Na]<sup>+</sup>.

2,3,4,6-Tetra-O-acetyl-5-bromo-β-D-glucopyranosyl fluoride (**2.16**)<sup>129</sup>



**2.15** (0.749 g, 2.14 mmol) was photobrominated in 50 mL dry carbon tetrachloride using NBS (0.569 g, 3.20 mmol, 1.5 eq) according to General Procedure C. The product was used without further purification or characterization.

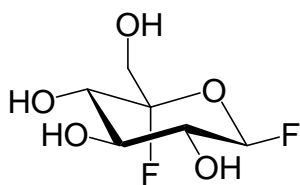
2,3,4,6-Tetra-O-acetyl-5-fluoro-β-D-glucopyranosyl fluoride (**2.17**)<sup>129</sup>



Crude **2.16** was dissolved in 35 mL dry diethyl ether. Silver tetrafluoroborate (0.525 g, 2.69 mmol) was added to this solution, and the resulting slurry was allowed to stir overnight in the

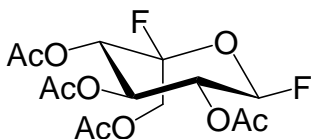
dark under N<sub>2(g)</sub>. The slurry was filtered through a plug of silica using ethyl acetate as the eluent to remove the silver salts, then the product was purified by flash chromatography (3:1 petroleum ether : ethyl acetate) to yield **2.18** (0.0256 g, 0.0695 mmol, 3% from **2.15**) and **2.17** as colourless oils (0.0231 g, 0.0627 mmol, 3% from **2.15**). **2.18**: Characterization described below. **2.17**: <sup>1</sup>H NMR: (300 MHz, CDCl<sub>3</sub>) δ 5.63 (1 H, dd, J<sub>H1-F1</sub> 52.3 Hz, J<sub>H1-H2</sub> 5.9 Hz, H1), 5.48-5.36 (2 H, m, H3, H4), 5.23-5.15 (1 H, m, H2), 4.35 (1 H, dd, J<sub>H6-H6'</sub> 12.0 Hz, J<sub>H6-F5</sub> 6.7 Hz, H6), 4.08 (1 H, dd, J<sub>H6'-H6</sub> 12.0 Hz, J<sub>H6'-F5</sub> 4.5 Hz, H6') 2.09 (3 H, s, Ac), 2.07 (3 H, s, Ac), 2.01 (3 H, s, Ac); <sup>19</sup>F NMR: (282 MHz, CDCl<sub>3</sub>): δ -128.59 (1 F, ddd, J<sub>F5-H4</sub> 22.0 Hz, J<sub>F5-H6</sub> 6.7 Hz, J<sub>F5-H6'</sub> 4.5 Hz, F5), -143.42 (1 F, dt, J<sub>F1-H1</sub> 52.3 Hz, J<sub>F1-F5</sub> = J<sub>F1-H2</sub> 9.0 Hz, F1).

5-Fluoro-β-D-glucopyranosyl fluoride (**2.2**)<sup>129</sup>



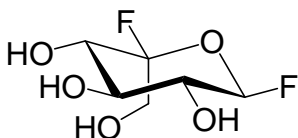
**2.17** (23.1 mg, 0.0627 mmol) was dissolved in 2 mL dry methanol and deacetylated according to General Procedure D. The crude product was purified by flash chromatography (19:1 ethyl acetate : methanol) to yield **2.2** as a colourless gum (9.6 mg, 0.0480 mmol, 76%). <sup>1</sup>H NMR: (300 MHz, CD<sub>3</sub>OD) δ 5.32 (1 H, dd, J<sub>H1-F1</sub> 54.4 Hz, J<sub>H1-H2</sub> 7.4 Hz, H1), 3.78 (1 H, dd, J<sub>H4-F5</sub> 21.8 Hz, J<sub>H1-H2</sub> 9.0 Hz, H4), 3.71-3.59 (3 H, m, H3, H6, H6'), 3.41 (1 H, ddd, J<sub>H2-F1</sub> 15.5 Hz, J<sub>H2-H3</sub> 8.6 Hz, J<sub>H2-H1</sub> 7.4 Hz, H2); <sup>19</sup>F NMR: (282 MHz, CD<sub>3</sub>OD): δ -138.85 (1 F, dt, J<sub>F5-H4</sub> 21.8 Hz, J<sub>F5-H6</sub> = J<sub>F5-H6'</sub> 6.0 Hz, F5), -152.80 (1 F, dd, J<sub>F1-H1</sub> 54.4 Hz, J<sub>F1-H2</sub> 21.8 Hz, F1).

2,3,4,6-Tetra-O-acetyl-5-fluoro- $\alpha$ -L-idopyranosyl fluoride (**2.18**)<sup>129</sup>



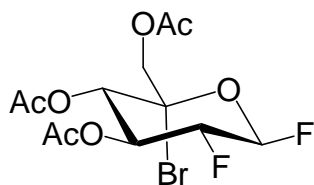
Crude **2.16** was dissolved in 35 mL dry acetonitrile. Silver fluoride (0.349 g, 2.75 mmol) was added to this solution, and the resulting slurry was allowed to stir overnight in the dark under  $N_2(g)$ . The slurry was filtered through a plug of silica using ethyl acetate as the eluent to remove the silver salts, then the product was purified by flash chromatography (3:1 petroleum ether : ethyl acetate) to yield **2.18** as a colourless oil (0.177 g, 0.480 mmol, 23% from **2.15**).  **$^1H$  NMR:** (300 MHz,  $CDCl_3$ )  $\delta$  5.59 (1 H, ddd,  $J_{H1-F1}$  52.5 Hz,  $J_{H1-H2}$  3.0 Hz,  $J_{H1-F5}$  1.1 Hz, H1), 5.39 (1 H, dd,  $J_{H4-F5}$  8.7 Hz,  $J_{H4-H3}$  6.3 Hz, H4), 5.30 (1 H, m, H2), 5.12 (1 H, t,  $J_{H3-H2} = J_{H3-H4}$  6.2 Hz, H3), 4.38-4.12 (2 H, m, H6, H6'), 2.07 (3 H, s, Ac), 2.06 (3 H, s, Ac), 2.05 (3 H, s, Ac), 2.04 (3 H, s, Ac);  **$^{19}F$  NMR:** (282 MHz,  $CDCl_3$ ):  $\delta$  -107.37 (1 F, m, F5), -123.65 (1 F, ddd,  $J_{F1-H1}$  52.5 Hz,  $J_{F1-H2}$  12.1 Hz,  $J_{F1-F5}$  1.4 Hz, F1).

5-Fluoro- $\alpha$ -L-idopyranosyl fluoride (**2.3**)<sup>129</sup>



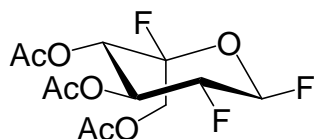
**2.18** (63.7 mg, 0.172 mmol) was dissolved in 5 mL dry methanol and deacetylated according to General Procedure D. The crude product was purified by flash chromatography (19:1 ethyl acetate : methanol) to yield **2.3** as a colourless gum (20.4 mg, 0.102 mmol, 59%).  **$^1H$  NMR:** (300 MHz,  $CD_3OD$ )  $\delta$  5.44 (1 H, ddd,  $J_{H1-F1}$  56.9 Hz,  $J_{H1-H2}$  4.4 Hz,  $J_{H1-F5}$  2.1 Hz, H1), 3.90-3.72 (4 H, m, H2, H3, H6, H6'), 3.58 (1 H, dd,  $J_{H4-F5}$  8.0 Hz,  $J_{H4-H3}$  6.6 Hz, H4);  **$^{19}F$  NMR:** (282 MHz,  $CD_3OD$ ):  $\delta$  -110.18 (1 F, m, F5), -125.30 (1 F, dt,  $J_{F1-H1}$  56.9 Hz,  $J_{F1-H2} = J_{F1-F5}$  14.1 Hz, F1).

3,4,6-Tri-O-acetyl-5-bromo-2-deoxy-2-fluoro- $\beta$ -D-glucopyranosyl fluoride (**2.19**)



**2.13** (0.230 g, 0.742 mmol, 1.0 eq) was dissolved in 25 mL dry carbon tetrachloride, and reacted with NBS (0.205 g, 1.15 mmol, 1.5 eq) for 24 hrs according to General Procedure C. The crude product was partially purified by flash chromatography (19:1 toluene : ethyl acetate) to give impure **2.19** (0.134 g), which was used without any further purification.  $^1\text{H}$  NMR: (300 MHz,  $\text{CDCl}_3$ )  $\delta$  5.74 (1 H, ddd,  $J_{\text{H1-F1}}$  46.7 Hz,  $J_{\text{H1-F2}}$  7.1 Hz,  $J_{\text{H1-H2}}$  5.0 Hz, H1), 5.61 (1 H, dd,  $J_{\text{H3-F2}}$  15.3 Hz,  $J_{\text{H3-H2}} = J_{\text{H3-H4}}$  9.8 Hz, H3), 5.16 (1 H, d,  $J_{\text{H4-H3}}$  9.8 Hz, H4), 4.69-4.42 (2 H, m, H2, H6), 4.42 (1 H, d,  $J_{\text{H6'-H6}}$  12.4 Hz H6'), 2.07 (3 H, s, Ac), 2.06 (3 H, s, Ac), 2.05 (3 H, s, Ac);  $^{19}\text{F}$  NMR: (282 MHz,  $\text{CDCl}_3$ ):  $\delta$  -150.66 (1 F, dt,  $J_{\text{F1-H1}}$  46.7 Hz,  $J_{\text{F1-F2}}$  15.3 Hz,  $J_{\text{F1-H2}}$  7.1 Hz, F1), -202.45 (1 F, dtd,  $J_{\text{F2-H2}}$  48.0 Hz,  $J_{\text{F2-F1}} = J_{\text{F2-H3}}$  15.3 Hz,  $J_{\text{F2-H1}}$  7.1 Hz, F2).

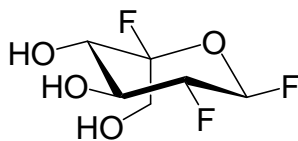
3,4,6-Tri-O-acetyl-2-deoxy-2,5-difluoro- $\alpha$ -L-idopyranosyl fluoride (**2.20**)



Impure **2.19** (0.134 g) was dissolved in 10 mL dry acetonitrile. Silver fluoride (0.175 g, 1.38 mmol) was added, and the resulting slurry stirred overnight. The solution was filtered through a short plug of silica using ethyl acetate as the eluent to remove the silver salts. The filtrate was collected and the solvent evaporated under reduced pressure to yield the crude product, which was further purified by flash chromatography (7:1  $\rightarrow$  5:1 petroleum ether : ethyl acetate) to give impure **2.20**. This was repurified by flash chromatography (40:10:1 dichloromethane : chloroform : diethyl ether) to yield pure **2.20** as a colourless oil (0.0691 g, 0.210 mmol, 28% from **2.13**).  $^1\text{H}$  NMR: (300 MHz,  $\text{CDCl}_3$ )  $\delta$  5.76 (1 H, dddd,  $J_{\text{H1-F1}}$  53.7 Hz,  $J_{\text{H1-F2}}$  11.3 Hz,  $J_{\text{H1-H2}}$  3.1 Hz,  $J_{\text{H1-F5}}$  0.7 Hz, H1), 5.35 (1 H, ddd,  $J_{\text{H4-F5}}$  8.1 Hz,  $J_{\text{H4-H3}}$  5.2

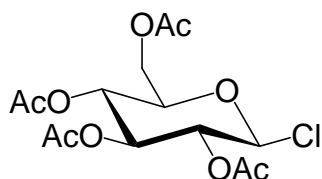
Hz,  $J_{H4-H2}$  2.0 Hz, H4), 5.24 (1 H, ddd,  $J_{H3-F2}$  16.8 Hz,  $J_{H3-H2}$  6.3 Hz,  $J_{H3-H4}$  5.2 Hz, H3), 4.88 (1 H, dddddd,  $J_{H2-F2}$  57.9 Hz,  $J_{H2-F1}$  9.5 Hz,  $J_{H2-H3}$  6.3 Hz,  $J_{H2-H1}$  3.2 Hz,  $J_{H2-H4}$  2.0 Hz, H2), 4.37 (1 H, dd,  $J_{H6-F5}$  19.8 Hz,  $J_{H6-H6'}$  12.1 Hz, H6), 4.26 (1 H, dd,  $J_{H6'-H6}$  12.1 Hz,  $J_{H6'-F5}$  11.1 Hz, H6') 2.1 (3 H, s, Ac), 2.07 (6 H, s, 2 x Ac);  **$^{19}\text{F}$  NMR**: (282 MHz,  $\text{CDCl}_3$ ):  $\delta$  -108.89 (1 F, m, F5), -126.60 (1 F, dddd,  $J_{F1-H1}$  53.6 Hz,  $J_{F1-F5}$  16.9 Hz,  $J_{F1-F2}$  11.3 Hz,  $J_{F1-H2}$  9.5 Hz, F1), -196.22 (1 F, ddd,  $J_{F2-H2}$  57.9 Hz,  $J_{F2-H3}$  16.8 Hz,  $J_{F2-F1}$  11.3 Hz, F2);  **$^{13}\text{C}$  NMR** (75 MHz,  $\text{CDCl}_3$ ):  $\delta$  170.4, 169.8, 169.2 (3 C, 3 x C=O), 109.84 (d,  $J_{C5-F5}$  218 Hz, C5), 106.85 (dd,  $J_{C1-F1}$  202 Hz,  $J_{C1-F2}$  32 Hz, C1), 92.44 (dd,  $J_{C2-F2}$  186 Hz,  $J_{C2-F1}$  24 Hz, C2), 72.40 (d,  $J_{C3-F2}$  12 Hz, C3), 70.21 (d,  $J_{C4-F5}$  18 Hz, C4), 62.45 (d,  $J_{C6-F5}$  28 Hz, C6), 20.49, 20.46, 20.12 (3 x Me); **ESI-MS (high res)**:  $m/z$  calc.: 351.0662; **Found**: 351.0658  $[\text{M} + \text{Na}]^+$ .

#### 2-Deoxy-2,5-difluoro- $\alpha$ -L-idopyranosyl fluoride (**2.4**)



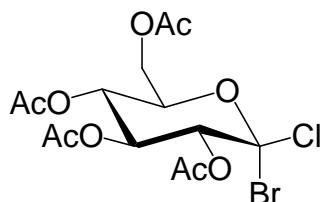
**2.20** (17.0 mg, 0.0518 mmol) was dissolved in 5 mL dry methanol, and deacetylated according to General Procedure D. The crude product was purified by flash chromatography (9:1 dichloromethane : methanol) to yield **2.4** as a colourless oil (10.0 mg, 0.0494 mmol, 95%).  **$^1\text{H}$  NMR**: (400 MHz,  $\text{CD}_3\text{OD}$ )  $\delta$  5.74 (1 H, ddd,  $J_{H1-F1}$  54.8 Hz,  $J_{H1-F2}$  12.6 Hz,  $J_{H1-H2}$  2.2 Hz, H1), 4.74-4.58 (1 H, m, H2), 3.95-3.85 (2 H, m, H3, H4), 3.81 (1 H, dd,  $J_{H6-H6'}$  =  $J_{H6-F5}$  12.4 Hz, H6), 3.73 (1 H, dd,  $J_{H6'-H6}$  =  $J_{H6'-F5}$  12.4 Hz, H6');  **$^{19}\text{F}$  NMR**: (282 MHz,  $\text{CDCl}_3$ ):  $\delta$  -110.67 (1 F, m, F5), -126.5 (1 F, m, F1), -196.81 (1 F, m, F2);  **$^{13}\text{C}$  NMR** (75 MHz,  $\text{CDCl}_3$ ):  $\delta$  109.62 (d,  $J_{C5-F5}$  216 Hz, C5), 105.44 (dd,  $J_{C1-F1}$  208 Hz,  $J_{C1-F2}$  30 Hz, C1), 91.68 (dd,  $J_{C2-F2}$  178 Hz,  $J_{C2-F1}$  21 Hz, C2), 73.33 (d,  $J_{C3-F2}$  24 Hz, C3), 72.21 (d,  $J_{C4-F5}$  22 Hz, C4), 62.22 (d,  $J_{C6-F5}$  24 Hz, C6); **ESI-MS (high res)**:  $m/z$  calc.: 225.0345; **Found**: 225.0315;  $[\text{M} + \text{Na}]^+$ ; **Anal. calc. for**  $\text{C}_6\text{H}_9\text{F}_3\text{O}_4$ : C, 35.65, H, 4.49; **Found**: C, 35.98, H, 4.68.

2,3,4,6-Tetra-O-acetyl- $\beta$ -D-glucopyranosyl chloride (**2.21**)<sup>178</sup>



**2.14** (10.21 g, 26.16 mmol, 1.0 eq) was dissolved in 50 mL dry chloroform, and aluminum trichloride (4.213 g, 31.60 mmol, 1.2 eq) was added. The reaction mixture was stirred under  $N_{2(g)}$  for 4 hours, after which time it was diluted in ice-cold chloroform and the organic layer was washed successively with 2 x ice-cold  $H_2O$ , 1 x sat.  $NaHCO_3$ , and 1 x sat.  $NaCl$ . The organic layer was then dried over  $MgSO_4$  for 10 minutes, filtered, and concentrated under reduced pressure. The product was dissolved in a small volume of diethyl ether and a large volume of petroleum ether was added. The product precipitated from this solution after standing overnight at 4 °C to give a **2.21** as a fine white powder (7.632 g, 20.81 mmol, 80%) which was used without characterization.

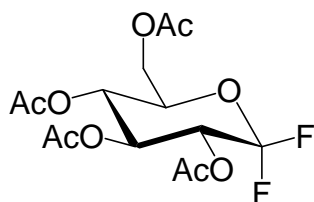
2,3,4,6-Tetra-O-acetyl-1-bromo- $\beta$ -D-glucopyranosyl chloride (**2.22**)<sup>178</sup>



**2.14** (7.632 g, 20.81 mmol, 1.0 eq) was photobrominated in 50 mL dry carbon tetrachloride using *N*-bromosuccinimide (5.23 g, 29.4 mmol, 1.4 eq) according to General Procedure C. The product was purified by flash chromatography (3:1  $\rightarrow$  2:1 petroleum ether : diethyl ether) to yield **2.22** (3.07 g, 6.91 mmol, 33%) as a colourless oil.  **$^1H$  NMR**: (300 MHz,  $CDCl_3$ )  $\delta$  5.32 (1 H, d,  $J_{H3-H2} = J_{H3-H4}$  9.7 Hz, H3), 5.25 (1 H, d,  $J_{H4-H3} = J_{H3-H2}$  9.7 Hz, H4), 5.15 (1 H, d,  $J_{H2-H3}$  9.7 Hz, H2), 4.33-4.23 (2 H, m, H5, H6), 4.16 (1 H, d,  $J_{H6'-H6}$  12.4 Hz, H6'), 2.15 (3 H, s, Ac), 2.10 (3 H, s, Ac), 2.01 (3 H, s, Ac), 1.98 (3 H, s, Ac);  **$^{13}C$  NMR** (75 MHz,  $CDCl_3$ ):  $\delta$  170.56, 169.76, 169.23, 168.93 (4 x C=O), 101.40 (C1), 76.46, 76.33 (C2, C5), 71.86 (C3), 66.53 (C4), 60.68 (C6), 20.78 (2 C), 20.70, 20.58 (4 x Me).

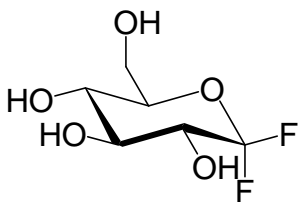


2,3,4,6-Tetra-O-acetyl-1-fluoro-D-glucopyranosyl fluoride (**2.23**)<sup>178</sup>



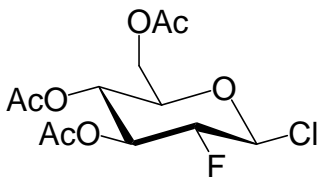
**2.22** (3.02 g, 6.78 mmol, 1.0 eq) was dissolved in 50 mL dry acetonitrile. Silver fluoride (2.48 g, 19.5 mmol, 2.9 eq) was added to this solution, and the resulting slurry was allowed to stir overnight in the dark under N<sub>2(g)</sub>. The slurry was filtered through a plug of silica using ethyl acetate as the eluent to remove the silver salts, then the product was partially purified by flash chromatography (5:1 → 4:1 petroleum ether : ethyl acetate) to yield **2.23** as an impure solid. The product was further purified by recrystallization from ethyl acetate/heptanes, to yield **2.23** as a white solid (2.09 g, 5.68 mmol, 84%). **<sup>1</sup>H NMR:** (300 MHz, CDCl<sub>3</sub>) δ 5.35-5.17 (3 H, m, H2, H3, H4), 4.26 (1 H, dd, J<sub>H6-H6'</sub> 13.4 Hz, J<sub>H6-H5</sub> 4.5 Hz, H6), 4.14-4.11 (2 H, m, H5, H6'), 2.07 (3 H, s, Ac), 2.05 (3 H, s, Ac), 1.98 (3 H, s, Ac), 1.96 (3 H, s, Ac); **<sup>19</sup>F NMR:** (282 MHz, CDCl<sub>3</sub>): δ -83.14 (1 F, d, J<sub>F1eq-F1ax</sub> 148 Hz, F1<sub>(eq)</sub>), -86.15 (1 F, dd, J<sub>F1ax-F1eq</sub> 148 Hz, J<sub>F1ax-H2</sub> 16.1 Hz, F1<sub>(ax)</sub>); **<sup>13</sup>C NMR** (75 MHz, CDCl<sub>3</sub>): δ 170.50, 169.81, 169.25, 169.09 (4 x C=O), 122.17 (dd, J<sub>C1-F1</sub> 272 Hz, J<sub>C1-F1</sub> 256 Hz, C1), 72.60 (C5), 70.82 (d, J<sub>C3-F1</sub> 9.8 Hz, C3), 68.82 (t, J<sub>C2-F1eq</sub> = J<sub>C2-F1ax</sub> 30.6 Hz, C2), 66.89 (C4), 60.65 (C6), 20.68 (2 C), 20.51, 20.40 (4 x Ac); **ESI-MS (high res):** m/z calc.: 391.0811; **Found:** 391.0817 [M + Na]<sup>+</sup>.

1-Fluoro-D-glucopyranosyl fluoride (**2.5**)<sup>178</sup>



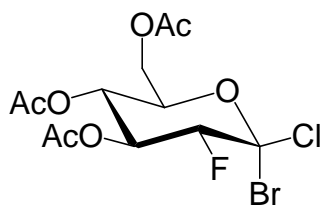
**2.23** (0.238 g, 0.646 mmol) was dissolved in 5 mL dry methanol and deacetylated according to General Procedure B. The product was purified by flash chromatography (9:1 ethyl acetate : petroleum ether → 9:1 ethyl acetate : methanol) to yield **2.5** as a colourless oil (0.0983 g, 0.491 mmol, 76%). **<sup>1</sup>H NMR:** (300 MHz, CD<sub>3</sub>OD) δ 3.85 (1 H,  $J_{H6-H6'}$  12.0 Hz, H6), 3.76-3.66 (2 H, m, H2, H6), 3.55-3.45 (3 H, m, H3, H4, H5); **<sup>19</sup>F NMR:** (282 MHz, CDCl<sub>3</sub>): δ -83.14 (1 F, d,  $J_{F1eq-F1ax}$  150.8 Hz, F1<sub>(eq)</sub>), -91.40 (1 F, dd,  $J_{F1ax-F1eq}$  150.8 Hz,  $J_{F1ax-H2}$  19.5 Hz, F1<sub>(ax)</sub>); **Anal. calc. for** C<sub>6</sub>H<sub>10</sub>F<sub>2</sub>O<sub>5</sub>: C, 36.01, H, 5.04; **Found:** C, 35.72, H, 5.34.

3,4,6-Tri-O-acetyl-2-deoxy-2-fluoro-β-D-glucopyranosyl chloride (**2.27**)



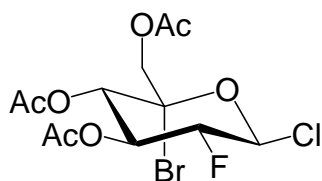
**2.12** (0.851 g, 2.29 mmol, 1.0 eq) was dissolved in 15 mL dry acetonitrile. Silver chloride (0.561 g, 3.91 mmol, 1.6 eq) was added, and the resulting slurry stirred 4 days under N<sub>2(g)</sub>, in the dark. The solution was filtered through a short plug of silica using ethyl acetate as the eluent to remove the silver salts. The filtrate was collected and the solvent evaporated under reduced pressure to yield the crude solid. The product was recrystallized from ethyl acetate/hexane to yield **2.27** as a white solid (0.577 g, 1.77 mmol, 77%). **<sup>1</sup>H NMR:** (300 MHz, CDCl<sub>3</sub>) δ 5.35-5.24 (2 H, m, H1, H3), 5.10 (1 H, t,  $J_{H4-H3} = J_{H4-H5}$  9.9 Hz, H4), 4.43 (1 H, dt,  $J_{H2-F2}$  49.2 Hz,  $J_{H2-H1} = J_{H2-H3}$  8.6 Hz, H2), 4.25 (1 H, dd,  $J_{H6-H6'}$  12.6 Hz,  $J_{H6-H5}$  4.9 Hz, H6), 4.14 (1 H, dd,  $J_{H6'-H6}$  12.6 Hz,  $J_{H6'-H5}$  2.3 Hz, H6'), 3.80 (1 H, ddd,  $J_{H5-H4}$  9.9 Hz,  $J_{H5-H6}$  4.9 Hz,  $J_{H5-H6'}$  2.3 Hz, H5), 2.08 (6 H, s, 2 x Ac), 2.02 (3 H, s, Ac); **<sup>19</sup>F NMR:** (282 MHz, CDCl<sub>3</sub>): δ -193.40 (1 F, dd,  $J_{F2-H2}$  49.2 Hz,  $J_{F2-H}$  14.1 Hz, F2).

3,4,6-Tri-O-acetyl-1-bromo-2-deoxy-2-fluoro- $\beta$ -D-glucopyranosyl chloride (**2.28**)



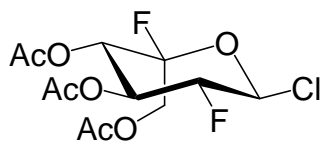
and

3,4,6-Tri-O-acetyl-5-bromo-2-deoxy-2-fluoro- $\beta$ -D-glucopyranosyl chloride (**2.29**)



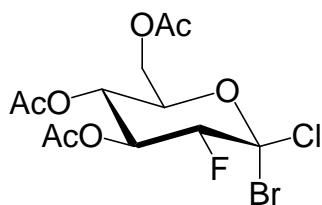
**2.27** (0.695 g, 2.13 mmol, 1.0 eq) was dissolved in 20 mL dry carbon tetrachloride and treated with NBS (0.516 g, 2.90 mmol, 1.3 eq) according to General Procedure C to yield an inseparable mixture of crude **2.28** and **2.29**, which were used in subsequent steps without further characterization or purification.

3,4,6-Tri-O-acetyl -2-deoxy-2,5-difluoro- $\alpha$ -L-idopyranosyl chloride (**2.30**)



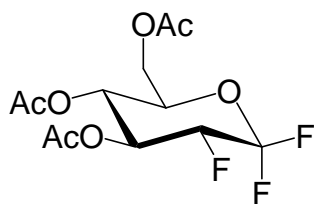
and

3,4,6-Tri-O-acetyl-1-bromo-2-deoxy-2-fluoro- $\beta$ -D-glucopyranosyl chloride (**2.28**)



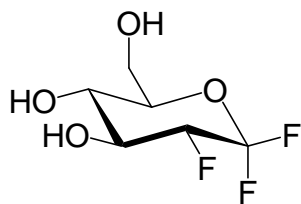
The crude mixture of **2.28** and **2.29** was dissolved in 20 mL dry acetonitrile. Silver fluoride (0.325 g, 2.56 mmol) was added, and the resulting slurry stirred overnight under  $N_{2(g)}$ , in the dark. The solution was filtered through a short plug of silica using ethyl acetate as the eluent to remove the silver salts. The crude product was purified using flash chromatography (9:1 petroleum ether : ethyl acetate) to yield **2.30** (0.0502 g, 0.146 mmol, 7% from **2.27**) and impure, unreacted **2.28** (0.208 g). **2.30**:  $^1H$  NMR: (300 MHz,  $CDCl_3$ )  $\delta$  5.96 (1 H, dd,  $J_{H1-F2}$  13.0 Hz,  $J_{H1-F2}$  4.2 Hz, H1), 5.44 (1 H, dd,  $J_{H4-F5}$  7.8 Hz,  $J_{H4-H3}$  4.9 Hz, H4), 5.23 (1 H, ddd,  $J_{H3-F2}$  17.3 Hz,  $J_{H3-H2}$  6.2 Hz,  $J_{H3-H4}$  4.9 Hz, H3), 4.99 (1 H, ddd,  $J_{H2-F2}$  47.9 Hz,  $J_{H2-H3}$  6.2 Hz,  $J_{H2-H1}$  4.2 Hz, H2), 4.34 (1 H, dd,  $J_{H6-F5}$  19.6 Hz,  $J_{H6-H6'}$  12.1 Hz, H6), 4.23 (1 H, dd,  $J_{H6'-F5}$  19.6 Hz,  $J_{H6'-H6}$  12.1 Hz, H6'), 2.12 (3 H, s, Ac), 2.08 (3 H, s, Ac), 2.07 (3 H, s, Ac);  $^{19}F$  NMR: (282 MHz,  $CDCl_3$ ):  $\delta$  -111.27 (1 F, dt,  $J_{F5-H6} = J_{F5-H6'}$  19.6 Hz,  $J_{F5-H4}$  7.8 Hz, F5), -182.36 (1 F, ddd,  $J_{F2-H2}$  47.9 Hz,  $J_{F2-H3}$  17.3 Hz,  $J_{F5-H1}$  13.0 Hz, F2);  $^{13}C$  NMR (75 MHz,  $CDCl_3$ ):  $\delta$  170.2, 169.6, 169.5 (3 C, 3 x C=O), 109.26 (d,  $J_{C5-F5}$  222 Hz, C5), 108.85 (d,  $J_{C1-F2}$  32 Hz, C1), 92.44 (d,  $J_{C2-F2}$  194 Hz, C2), 73.90 (d,  $J_{C3-F2}$  12 Hz, C3), 69.98 (d,  $J_{C4-F5}$  25 Hz, C4), 62.34 (d,  $J_{C6-F5}$  29 Hz, C6), 20.43, 20.41, 20.18 (3 x Me); **ESI-MS (high res)**:  $m/z$  calc.: 367.0367; **Found**: 367.0348  $[M + Na]^+$ .

3,4,6-Tri-O-acetyl -2-deoxy-1,2-difluoro-D-glucopyranosyl fluoride (**2.31**)



The impure, unreacted **2.28** (0.208 g, 0.513 mmol) was dissolved in 10 mL dry acetonitrile. Silver fluoride (0.468 g, 3.69 mmol, 7.2 eq) was added, and the resulting slurry stirred 10 days under  $N_{2(g)}$ , in the dark. The solution was filtered through a short plug of silica using ethyl acetate as the eluent to remove the silver salts. The filtrate was collected and the solvent evaporated under reduced pressure to yield the crude product, which was purified by flash chromatography (4:1 petroleum ether : ethyl acetate) to yield impure **2.31** as a colourless oil (0.152 g).  **$^1H$  NMR:** (300 MHz,  $CDCl_3$ )  $\delta$  5.45 (1 H, dt,  $J_{H3-F2}$  16.3 Hz,  $J_{H3-H2} = J_{H3-H4}$  9.5 Hz, H3), 5.14 (1 H, t,  $J_{H4-H3} = J_{H4-H5}$  9.5 Hz, H4), 4.60 (1 H, dddd,  $J_{H2-F2}$  49.2 Hz,  $J_{H2-F1(ax)}$  16.3 Hz,  $J_{H2-H3}$  9.4 Hz,  $J_{H2-F1(eq)}$  4.0 Hz, H2), 4.27 (1 H, dd,  $J_{H6-H6'}$  12.6 Hz,  $J_{H6-H5}$  4.1 Hz, H6), 4.18-4.10 (1 H, m, H5, H6'), 2.06 (3 H, s, Ac), 2.05 (3 H, s, Ac), 2.01 (3 H, s, Ac);  **$^{19}F$  NMR:** (282 MHz,  $CDCl_3$ ):  $\delta$  -84.27 (1 F, ddd,  $J_{F1(eq)-F1(ax)}$  146.8 Hz,  $J_{F1eq-F2}$  16.5 Hz,  $J_{F1eq-H2}$  4.0 Hz, F1(eq)), -89.59 (1 F, dt,  $J_{F1(ax)-F1(eq)}$  146.8 Hz,  $J_{F1(ax)-F2} = J_{F1(ax)-H2}$  16.3 Hz, F1(ax)), -206.52 (1 F, dq,  $J_{F2-H2}$  49.2 Hz,  $J_{F2-F1(eq)} = J_{F2-F1(ax)} = J_{F2-H3}$  16.3 Hz, F2).

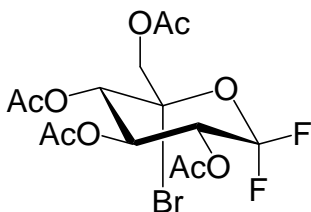
2-Deoxy-1,2-difluoro-D-glucopyranosyl fluoride (**2.6**)



The impure **2.31** (0.152 g) was dissolved in 10 mL dry methanol, and deacetylated according to General Procedure B. The product was purified by flash chromatography (19:1  $\rightarrow$  14:1 chloroform : methanol) to yield **2.6** as a colourless oil (45.1 mg, 0.223 mmol, 10% based on **2.27**).  **$^1H$  NMR:** (300 MHz,  $CD_3OD$ )  $\delta$  4.39 (1 H, dddd,  $J_{H2-F2}$  49.8 Hz,  $J_{H2-F1(ax)}$  16.6 Hz,  $J_{H2-}$

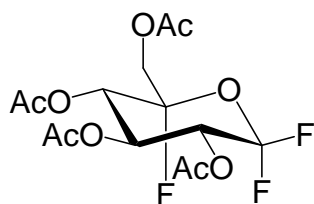
$_{\text{H3}}$  9.3 Hz,  $J_{\text{H2-F1(eq)}}$  4.3 Hz, H2), 3.88-3.52 (5 H, m, H3, H4, H5, H6, H6');  **$^{19}\text{F}$  NMR:** (282 MHz,  $\text{CD}_3\text{OD}$ ):  $\delta$  -84.35 (1 F, ddd,  $J_{\text{F1(eq)-F1(ax)}}$  146.5 Hz,  $J_{\text{F1eq-F2}}$  16.6 Hz,  $J_{\text{F1eq-H2}}$  4.3 Hz, F1<sub>(eq)</sub>), -89.59 (1 F, ddd,  $J_{\text{F1(ax)-F1(eq)}}$  146.5 Hz,  $J_{\text{F1(ax)-F2}}$  16.6 Hz,  $J_{\text{F1(ax)-H2}}$  16.6 Hz, F1<sub>(ax)</sub>), -208.69 (1 F, ddt,  $J_{\text{F2-H2}}$  49.8 Hz,  $J_{\text{F2-F1(eq)}}$  17.8 Hz,  $J_{\text{F2-F1(ax)}} = J_{\text{F2-H3}}$  16.6 Hz, F2);  **$^{13}\text{C}$  NMR** (75 MHz,  $\text{CD}_3\text{OD}$ ):  $\delta$  123.45 (dd,  $J_{\text{C1-F1}}$  268 Hz,  $J_{\text{C1-F1}}$  254 Hz, C1), 89.61 (dt,  $J_{\text{C2-F2}}$  196 Hz,  $J_{\text{C2-F1(ax)}} = J_{\text{C2-F1(eq)}}$  33 Hz, C2), 78.11 (C5), 72.79 (dd,  $J_{\text{C3-F2}}$  17 Hz,  $J_{\text{C3-F1}}$  9 Hz, C3), 68.18 (d,  $J_{\text{C4-F2}}$  7 Hz, C4), 59.91 (C6); **ESI-MS (high res):**  $m/z$  calc.: 225.0345; **Found:** 225.0355 [ $\text{M} + \text{Na}$ ] $^+$ ; **Anal. calc. for  $\text{C}_6\text{H}_9\text{F}_3\text{O}_4$ :** C, 35.65, H, 4.49; **Found:** C, 35.09, H, 4.79.

2,3,4,6-Tetra-O-acetyl-5-bromo-1-fluoro-D-glucopyranosyl fluoride (**2.24**)



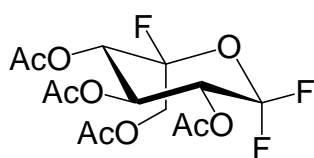
**2.23** (2.09 g, 5.68 mmol, 1.0 eq) was dissolved in 50 mL dry carbon tetrachloride, and reacted with *N*-bromosuccinimide (2.08 g, 11.7 mmol, 2.1 eq) for 48 hours according to General Procedure C. The crude product was partially purified by flash chromatography (19:1 toluene : ethyl acetate) to yield impure **2.24** (0.426 g) as a yellowish oil which was used without further purification.  **$^1\text{H}$  NMR:** (300 MHz,  $\text{CDCl}_3$ )  $\delta$  5.71 (1 H, t,  $J_{\text{H3-H2}} = J_{\text{H3-H4}}$  10.0 Hz, H3), 5.43 (1 H, ddd,  $J_{\text{H2-F1ax}}$  15.4 Hz,  $J_{\text{H2-H3}}$  10.0 Hz,  $J_{\text{H2-F1eq}}$  5.2 Hz, H2), 5.33 (1 H, d,  $J_{\text{H4-H3}}$  10.0 Hz, H4), 4.40 (1 H, d,  $J_{\text{H6-H6'}}$  12.6 Hz, H6 ) 4.35 (1 H, d,  $J_{\text{H6'-H6}}$  12.6 Hz, H6') 2.13 (3 H, s, Ac), 2.11 (3 H, s, Ac), 2.08 (3 H, s, Ac), 2.01 (3 H, s, Ac);  **$^{19}\text{F}$  NMR:** (282 MHz,  $\text{CDCl}_3$ ):  $\delta$  -74.79 (1 F, dd,  $J_{\text{F1eq-F1ax}}$  153 Hz,  $J_{\text{F1eq-H2}}$  5.2 Hz, F1<sub>(eq)</sub>), -80.16 (1 F, dd,  $J_{\text{F1ax-F1eq}}$  153 Hz,  $J_{\text{F1ax-H2}}$  15.4 Hz, F1<sub>(ax)</sub>).

2,3,4,6-Tetra-O-acetyl -1,5-difluoro-D-glucopyranosyl fluoride (**2.25**)



and

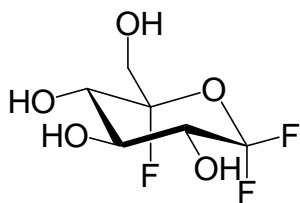
2,3,4,6-Tetra-O-acetyl-1,5-difluoro-L-idopyranosyl fluoride (**2.26**)



Crude **2.24** (0.426 g), was dissolved in 25 mL of dry diethyl ether. Silver tetrafluoroborate (0.379 g, 1.95 mmol) was added, and the resulting solution stirred overnight in the dark under N<sub>2</sub>(g). The slurry was filtered through a plug of silica using ethyl acetate as the eluent to remove the silver salts, then the products were purified by flash chromatography (19:1 toluene : ethyl acetate) to yield **2.25** (0.1046 g, 0.270 mmol, 5% from **2.23**) and **2.26** (0.0713 g, 0.185 mmol, 3% from **2.23**) both as colourless oils. **2.25**: <sup>1</sup>H NMR: (300 MHz, CDCl<sub>3</sub>) δ 5.57 (1 H, m, H2), 5.48-5.36 (2 H, m, H3, H4), 4.33 (1 H, dd, J<sub>H6-H6'</sub> 12.2 Hz, J<sub>H6-F5</sub> 6.2 Hz, H6), 4.06 (1 H, dd, J<sub>H6'-H6</sub> 12.2 Hz, J<sub>H6'-F5</sub> 3.9 Hz, H6') 2.12 (3 H, s, Ac), 2.10 (3 H, s, Ac), 2.07 (3 H, s, Ac), 2.00 (3 H, s, Ac); <sup>19</sup>F NMR: (282 MHz, CDCl<sub>3</sub>): δ -75.79 (1 F, dt, J<sub>F1ax-F1eq</sub> 155 Hz, J<sub>F1ax-F5</sub> = J<sub>F1ax-H2</sub> 16.1 Hz, F1<sub>(ax)</sub>), -78.20 (1 F, dd, J<sub>F1eq-F1ax</sub> 155 Hz, J<sub>F1eq-H2</sub> 14.1 Hz, F1<sub>(eq)</sub>), -127.43 (1F, m, F5); <sup>13</sup>C NMR (100 MHz, CDCl<sub>3</sub>): δ 170.93, 170.63, 170.50, 170.31 (4 x C=O), 121.52 (dd, J<sub>C1-F1</sub> 277 Hz, J<sub>C1-F1</sub> 256 Hz, C1), 109.56 (dd, J<sub>C5-F5</sub> 239 Hz, J<sub>C5-F1</sub> 7.0 Hz, C5), 70.12 (dd, J<sub>C2-F1</sub> 30 Hz, J<sub>C2-F1</sub> 28 Hz, C2), 68.61 (d, J<sub>C4-F5</sub> 8 Hz, C4), 68.45 (d, J<sub>C6</sub> 6 Hz, C3), 62.55 (d, J<sub>C6-F5</sub> 39 Hz, C6), 21.89, 21.75 (2 C), 21.68, (4 x Ac); **ESI-MS (high res)**: m/z calc.:409.0717; **Found**: 409.0722; [M + Na]<sup>+</sup>. **2.26**: <sup>1</sup>H NMR: (300 MHz, CDCl<sub>3</sub>) δ 5.65 (1 H, dddd, J<sub>H2-F1ax</sub> 14.8 Hz, J<sub>H2-H3</sub> 7.6 Hz, J<sub>H2-F1eq</sub> 3.0 Hz, J<sub>H2-H4</sub> 1.5 Hz, H2), 5.24 (1 H, m, H4), 5.14 (1 H, d, J<sub>H3-H2</sub> 7.6 Hz, H3), 4.44 (1 H, dd, J<sub>H6-F5</sub> 24.5 Hz, J<sub>H6-H6'</sub> 12.4 Hz, H6) 4.18 (1 H, t, J<sub>H6'-F5</sub> = J<sub>H6'-H6</sub> 12.4 Hz, (H6')), 2.12 (3 H, s, Ac), 2.10 (3 H, s, Ac), 2.09 (3 H, s,

Ac), 2.07 (3 H, s, Ac); **<sup>19</sup>F NMR**: (282 MHz, CDCl<sub>3</sub>): δ -73.00 (1 F, d, J<sub>F1eq-F1ax</sub> 155 Hz, F1<sub>(eq)</sub>), -76.61 (1 F, dt, J<sub>F1ax-F1eq</sub> 155 Hz, J<sub>F1ax-F5</sub> = J<sub>F1ax-H2</sub> 14.8 Hz, F1<sub>(ax)</sub>), -108.74 (1 F, m, F5); **<sup>13</sup>C NMR** (75 MHz, CDCl<sub>3</sub>): δ 169.65, 169.36, 168.97, 168.45 (4 x C=O), 115.08 (dd, J<sub>C1-F1</sub> 238 Hz, J<sub>C1-F1</sub> 226 Hz, C1), 109.56 ((d, J<sub>C5-F5</sub> 232 Hz, C5), 70.56 (d, J<sub>C2-F1ax</sub> 5 Hz, C2 ), 69.03 (C4), 68.44 (C3), 61.88 (d, J<sub>C6-F5</sub> 25 Hz, C6), 20.64, 20.55 (2 C), 20.46, (4 x Ac); **ESI-MS (high res)**: m/z calc.: 409.0717; **Found**: 409.0722; [M + Na]<sup>+</sup>.

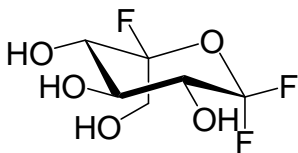
#### 1,5-Difluoro-D-glucopyranosyl fluoride (**2.7**)



**2.25** (71.3 mg, 0.185 mmol) was dissolved in 5 mL dry methanol and deacetylated according to General Procedure B. The crude product was purified by flash chromatography (9:1 ethyl acetate : petroleum ether) to yield **2.7** as a colourless gum (36.0 mg, 0.165 mmol, 89%). **<sup>1</sup>H NMR**: (400 MHz, CD<sub>3</sub>OD) δ 3.83-3.72 (3 H, m), 3.69-3.59 (2 H, m); **<sup>19</sup>F NMR**: (282 MHz, CD<sub>3</sub>OD): δ -80.34 (1 F, dd, J<sub>F1eq-F1ax</sub> 155 Hz, J<sub>F1eq-H2</sub> 5.9 Hz, F1<sub>(eq)</sub>), -81.38 (1 F, dt, J<sub>F1ax-F1eq</sub> 155 Hz, J<sub>F1ax-H2</sub> = J<sub>F1ax-F5</sub> 12.2 Hz, F1<sub>(ax)</sub>), -134.70 (1 F, m, F5); **<sup>13</sup>C NMR** (100 MHz, CD<sub>3</sub>OD): δ 119.45 (dd, J<sub>C1-F1</sub> 265 Hz, J<sub>C1-F1</sub> 254 Hz, C1), 112.44 (d, J<sub>C5-F5</sub> 224 Hz, C5), 73.55 (t, J<sub>C2-F1(ax)</sub> = J<sub>C2-F1(eq)</sub> 29 Hz, C2) 71.12 (d, J<sub>C3-F</sub> 8 Hz, C3) 70.57 (d, J<sub>C4-F5</sub> 24 Hz, C4), 62.38 (d, J<sub>C6-F5</sub> 36 Hz, C6); **ESI-MS (high res)**: m/z calc.: 241.0294; **Found**: 241.0300; [M + Na]<sup>+</sup>; **Anal. calc. for** C<sub>6</sub>H<sub>9</sub>F<sub>3</sub>O<sub>5</sub>: C, 33.04, H, 4.16; **Found**: C, 33.12, H, 4.12.

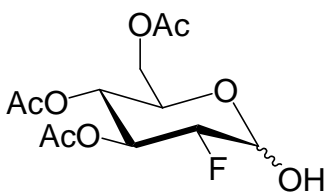


1,5-Difluoro-L-idopyranosyl fluoride (**2.8**)



**2.26** (0.105 g, 0.271 mmol) was dissolved in 5 mL dry methanol and deacetylated according to General Procedure B. The crude product was purified by flash chromatography (9:1 ethyl acetate : petroleum ether) to yield **2.8** as a colourless gum (0.0531 g, 0.244 mmol, 90%). **<sup>1</sup>H NMR:** (300 MHz, CD<sub>3</sub>OD) δ 4.01-3.80 (3 H, m), 3.75-3.62 (2 H, m); **<sup>19</sup>F NMR:** (282 MHz, CD<sub>3</sub>OD): δ -73.84(1 F, d,  $J_{F1eq-F1ax}$  158 Hz, F1<sub>(eq)</sub>), -82.10 (1 F, dt,  $J_{F1ax-F1eq}$  158 Hz,  $J_{F1ax-H2} = J_{F1ax-F5}$  13.8 Hz, F1<sub>(ax)</sub>), -114.9 (1 F, m, F5); **<sup>13</sup>C NMR** (75 MHz, CD<sub>3</sub>OD): δ 114.09 (dd,  $J_{C1-F1}$  234 Hz,  $J_{C1-F1}$  224 Hz, C1), 103.67 (d,  $J_{C5-F5}$  238 Hz, C5), 73.47 (d,  $J_{C3-F}$  8 Hz, C3) 72.73 (d,  $J_{C4-F5}$  35 Hz, C4) 70.74 (t,  $J_{C2-F1ax} = J_{C2-F1eq}$  28 Hz, C2), 61.74 (d,  $J_{C6-F5}$  26 Hz, C6) □ **ESI-MS (high res):** m/z calc.: 241.0294; **Found:** 241.0300; [M + Na]<sup>+</sup>; **Anal. calc. for** C<sub>6</sub>H<sub>9</sub>F<sub>3</sub>O<sub>5</sub>: C, 33.04, H, 4.16; **Found:** C, 33.08, H, 4.24.

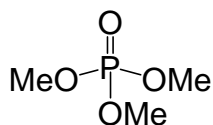
3,4,6-Tri-O-acetyl-2-deoxy-2-fluoro-D-glucopyranose (**2.41**)



**2.12** (0.695 g, 1.87 mmol) was dissolved in 20 mL 1:1 acetone : water. Silver carbonate (0.569 g, 2.06 mmol, 1.1 eq) was added, and the resulting slurry was stirred for 4 hours in the dark. The solution was filtered through a short plug of silica using ethyl acetate as the eluent to remove the silver salts. The filtrate was collected and the solvent evaporated under reduced pressure. The product was purified by flash chromatography (2:1 petroleum ether : ethyl acetate) to yield **2.41** (1:0.4 α : β) as a colourless oil (0.385 g, 1.25 mmol, 67%). **<sup>1</sup>H NMR:** (300 MHz, CDCl<sub>3</sub>) δ 5.53 (1 H, dt,  $J_{H3\alpha-F2\alpha}$  12.0 Hz,  $J_{H3\alpha-H2\alpha} = J_{H3\alpha-H2\beta}$  9.5 Hz, H3α), 5.41 (1 H, t,  $J_{H1\alpha-F2\alpha} = J_{H1\alpha-H2\alpha}$  3.5 Hz, H1α), 5.27 (1 H, dt,  $J_{H4\beta-F2\beta}$  14.1 Hz,  $J_{H4\beta-H3\beta}$

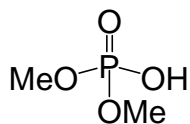
=  $J_{H4\beta-H5\beta}$  9.3 Hz, H4 $\beta$ ), 5.00-4.84 (3 H, m, H1 $\beta$ , H4 $\alpha$ , H4 $\beta$ ), 4.55-4.34 (2 H, m, H2 $\alpha$ , H2 $\beta$ ), 4.24-4.02 (5 H, m, H6 $\alpha$ , H6 $\beta$ , H6' $\alpha$ , H6' $\beta$ , H5 $\alpha$ ), 3.72 (1 H, ddd,  $J_{H5\beta-H4\beta}$  10.0 Hz,  $J_{H5\beta-H6\beta}$  4.7 Hz,  $J_{H5\beta-H6'\beta}$  2.7 Hz, H5 $\beta$ ), 2.03 (3 H, s, Ac), 2.02 (6 H, s, 2 x Ac), 2.01 (3 H, s, Ac), 1.99 (6 H, s, 2 x Ac), 1.98 (3 H, s, Ac);  **$^{19}\text{F}$  NMR:** (282 MHz,  $\text{CDCl}_3$ ):  $\delta$  -199.75 (1 F, ddd,  $J_{F2\beta-H2\beta}$  50.4 Hz,  $J_{F2\beta-H3\beta}$  14.1 Hz,  $J_{F2\beta-H1\beta}$  3.2 Hz, F2 $\beta$ ), -200.41 (1 F, ddd,  $J_{F2\alpha-H2\alpha}$  51.4 Hz,  $J_{F2\alpha-H3\alpha}$  12.0 Hz,  $J_{F2\alpha-H1\alpha}$  3.5 Hz, F2 $\alpha$ ).

#### Phosphoric acid trimethyl ester (**2.47**)



Phosphorus oxychloride (2.0 mL, 22 mmol, 1.0 eq) was dissolved in 20 mL dichloromethane and added dropwise to a stirred solution of methanol (20 mL) and triethylamine (4 mL) at 0 °C under  $\text{N}_{2(g)}$ . The reaction mixture was allowed to warm to RT over two hours, after which the solvent was evaporated under reduced pressure. The crude **2.47** was used without further purification or characterization.

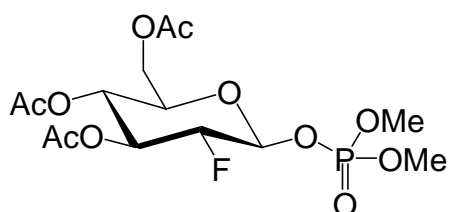
#### Phosphoric acid dimethyl ester (**2.48**)



The crude **2.47** was dissolved in 70 mL dry acetonitrile. Lithium bromide (2.10 g, 25.7 mmol, 1.2 eq) was added, and the solution refluxed under  $\text{N}_{2(g)}$  overnight. The solution was filtered to yield the lithium salt as a white powder. The powder was dissolved in methanol and stirred with Amberlite IR-120 ( $\text{H}^+$ ) resin for 10 minutes. The resin was filtered off, and the solvent evaporated under reduced pressure to yield pure **2.48** (2.11 g, 16.7 mmol, 77%) as a colourless oil. **2.48:**  **$^1\text{H}$  NMR:** (300 MHz,  $\text{CD}_3\text{OD}$ )  $\delta$  3.71 (6 H, d,  $J_{H-P}$  12.2 Hz,  $\text{CH}_3$ );

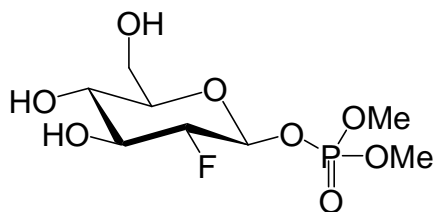
**<sup>31</sup>P NMR:** (121 MHz, CD<sub>3</sub>OD) δ 2.10 (1 p, s, J<sub>P-H</sub> 12.2 Hz); **ESI-MS (low res):** m/z calc.: 125.01; **Found:** 125.03 [M - H]<sup>-</sup>.

Dimethyl (3,4,6-tri-O-acetyl-2-deoxy-2-fluoro-β-D-glucopyranosyl) phosphate (**2.49**)



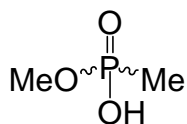
**2.12** (63.4 mg, 0.171 mmol) was dissolved in 5 mL dry acetonitrile. **2.48** (0.113 g, 0.896 mmol, 5.2 eq) was dissolved in 5 mL dry acetonitrile and added, along with silver carbonate (0.237 g, 0.866 mmol, 5.1 eq), to the acetonitrile solution. The resulting slurry was stirred overnight under N<sub>2(g)</sub>, in the dark. The solution was filtered through a short plug of silica using ethyl acetate as the eluent to remove the silver salts. The filtrate was collected and the solvent evaporated under reduced pressure. The product was purified by flash chromatography (2:1 → 1:1 → 1:2 petroleum ether : ethyl acetate) to yield **2.49** as a colourless oil (62.2 mg, 0.149 mmol, 87%). **<sup>1</sup>H NMR:** (300 MHz, CDCl<sub>3</sub>) δ 5.37-5.26 (2 H, m, H1, H3), 5.03 (1 H, t, J<sub>H4-H3</sub> = J<sub>H4-H5</sub> 9.8 Hz, H4), 4.38 (1 H, ddd, J<sub>H2-F2</sub> 50.6 Hz, J<sub>H2-H3</sub> 8.8 Hz, J<sub>H2-H1</sub> 8.0 Hz, H2), 4.24 (1 H, dd, J<sub>H6-H6'</sub> 12.8 Hz, J<sub>H6-H5</sub> 4.9 Hz, H6), 4.13 (1 H, dd, J<sub>H6'-H6</sub> 12.8 Hz, J<sub>H6'-H5</sub> 2.3 Hz, H6'), 3.82 (1 H, ddd, J<sub>H5-H4</sub> 9.8 Hz, J<sub>H5-H6</sub> 4.9 Hz, J<sub>H5-H6'</sub> 2.3 Hz, H5), 3.79 (3H, br s, OCH<sub>3</sub>), 3.75 (3H, br s, OCH<sub>3</sub>), 2.05 (3 H, s, Ac), 2.04 (3 H, s, Ac), 2.01 (3 H, s, Ac); **<sup>19</sup>F NMR:** (282 MHz, CDCl<sub>3</sub>): δ -200.59 (1 F, ddd, J<sub>F2-H2</sub> 50.6 Hz, J<sub>F2-H3</sub> 13.4 Hz, J<sub>F2-H1</sub> 3.0 Hz, F2); **<sup>31</sup>P (<sup>1</sup>H decoupled) NMR:** (121 MHz, CDCl<sub>3</sub>): δ 0.11; **<sup>13</sup>C NMR:** (75 MHz, CDCl<sub>3</sub>) δ 170.54, 169.91, 169.60 (3 x C=O), 95.87 (dd, J<sub>C1-F2</sub> 24 Hz, J<sub>C1-P</sub> 5 Hz, C1), 89.37 (dd, J<sub>C2-F2</sub> 193 Hz, J<sub>C2-P</sub> 9 Hz, C2), 72.81 (C5), 72.40 (d, J<sub>C3-F2</sub> 20 Hz, C3), 67.74 (d, J<sub>C4-F2</sub> 7 Hz, C4), 61.49 (C6), 54.75 (2C, 2 x OCH<sub>3</sub>), 20.75, 20.70, 20.64 (3 x Me); **ESI-MS (high res):** m/z calc.: 439.0776; **Found:** 439.0688 [M + Na]<sup>+</sup>.

Dimethyl (2-deoxy-2-fluoro-β-D-glucopyranosyl) phosphate (**2.37**)



**2.49** (42.0 mg, 0.101 mmol) was dissolved in 5 mL dry methanol, and deacetylated according to General Procedure B. The crude product was purified by flash chromatography (9:1 ethyl acetate : methanol) to yield pure **2.37** as a colourless oil (20.7 mg, 0.0713 mmol, 71%). **<sup>1</sup>H NMR:** (300 MHz, CD<sub>3</sub>OD) δ 5.23 (1 H, td,  $J_{H1-H2} = J_{H1-P}$  7.5 Hz,  $J_{H1-F2}$  2.9 Hz, H1), 4.12 (1 H, ddd,  $J_{H2-F2}$  51.4 Hz,  $J_{H2-H3}$  8.9 Hz,  $J_{H2-H1}$  7.5 Hz, H2), 3.88-3.80 (7 H, m, H3, 2 x OCH<sub>3</sub>), 3.73-3.60 (2 H, m, H4, H5), 3.45-3.37 (2 H, m, H6, H6'); **<sup>19</sup>F NMR:** (282 MHz, CD<sub>3</sub>OD): δ -201.87 (1 F, ddd,  $J_{F2-H2}$  51.4 Hz,  $J_{F2-H3}$  14.3 Hz,  $J_{F2-H1}$  2.9 Hz, F2); **<sup>31</sup>P (<sup>1</sup>H decoupled) NMR:** (121 MHz, CD<sub>3</sub>OD): δ -0.12; **<sup>13</sup>C NMR:** (100 MHz, CD<sub>3</sub>OD) δ 96.43 (dd,  $J_{C1-F2}$  24 Hz,  $J_{C1-P}$  7 Hz, C1), 88.98 (dd,  $J_{C2-F2}$  197 Hz,  $J_{C2-P}$  8 Hz, C2), 77.23 (d,  $J_{C3-F2}$  18 Hz, C3), 74.34 (d,  $J_{C4-F2}$  7 Hz, C4), 72.43 (C5), 60.70 (C6), 54.27, 54.22 (2 x OCH<sub>3</sub>); **ESI-MS (high res):** m/z calc.: 313.0459; **Found:** 313.0414 [M + Na]<sup>+</sup>; **Anal. calc. for** C<sub>8</sub>H<sub>16</sub>FO<sub>8</sub>P: C, 33.11, H, 5.56; **Found:** C, 32.99, H, 5.76.

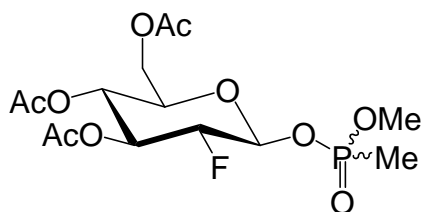
Methyl methylphosphonic acid (**2.50**)



Dimethyl methylphosphonate (1 mL, 9.36 mmol, 1 eq) and lithium bromide (1.10 g, 12.7 mmol, 1.4 eq) were dissolved in 40 mL dry acetonitrile and refluxed overnight under N<sub>2(g)</sub>. The resulting white powder was filtered and washed with a small amount of acetonitrile. The powder was dissolved in 30 mL methanol, and acidified by stirring with Amberlite IR-120 (H<sup>+</sup>) resin for 10 minutes. The resin was filtered off and the filtrate collected. The solvent

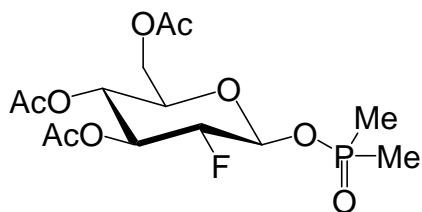
was evaporated under reduced pressure to yield **2.50** as a colourless liquid (0.762 g, 6.93 mmol, 74%). The compound was used without further characterization or purification.

Methyl methyl-(3,4,6-tri-O-acetyl-2-deoxy-2-fluoro- $\beta$ -D-glucopyranosyl) phosphonate  
(**2.51**)



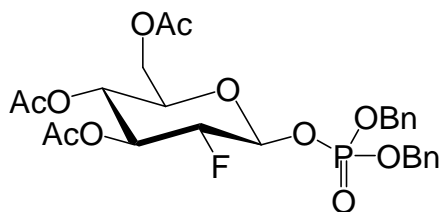
**2.12** (72.7 mg, 0.196 mmol, 1 eq) was dissolved in 10 mL dry acetonitrile. The crude **2.50** (0.436 g, 3.96 mmol, 20 eq) was added, along with silver carbonate (0.439 g, 1.59 mmol, 8.1 eq), to the solution. The resulting slurry was stirred overnight under  $N_{2(g)}$ , in the dark. The solution was filtered through a short plug of silica using ethyl acetate as the eluent to remove the silver salts. The filtrate was collected and the solvent evaporated under reduced pressure. The product was purified by flash chromatography (1:9 petroleum ether : ethyl acetate) to yield **2.51** as a colourless oil (64.1 mg, 0.160 mmol, 82% from **2.12**).  **$^1H$  NMR:** (300 MHz,  $CDCl_3$ )  $\delta$  5.44-5.26 (4 H, m,  $H_{1a}$ ,  $H_{1b}$ ,  $H_{3a}$ ,  $H_{3b}$ ), 5.05-4.99 (2 H, m,  $H_{4a}$ ,  $H_{4b}$ ), 4.48-4.08 (6 H, m,  $H_{2a}$ ,  $H_{2b}$ ,  $H_{6a}$ ,  $H_{6b}$ ,  $H_{6'a}$ ,  $H_{6'b}$ ), 3.87-3.78 (2 H, m,  $H_{5a}$ ,  $H_{5b}$ ), 3.74-3.70 (6 H, m,  $OCH_{3a}$ ,  $OCH_{3b}$ ), 2.06 (6 H, s, 2 x Ac), 2.05 (3 H, s, Ac), 2.03 (3 H, s, Ac), 2.02 (6 H, s, 2 x Ac), 1.57 (3 H, d,  $J_{H-P}$  18.3 Hz,  $PCH_{3a}$ ), 1.56 (3 H, d,  $J_{H-P}$  18.2 Hz,  $PCH_{3b}$ );  **$^{19}F$  NMR:** (282 MHz,  $CDCl_3$ ):  $\delta$  -200.42-200.83 (2 F, m,  $F_{2a}$ ,  $F_{2b}$ );  **$^{31}P$  ( $^1H$  decoupled) NMR:** (121 MHz,  $CDCl_3$ ):  $\delta$  33.57; **ESI-MS (high res):**  $m/z$  calc.: 423.0827; **Found:** 423.0832  $[M + Na]^+$ .

Dimethyl-(3,4,6-tri-O-acetyl-2-deoxy-2-fluoro-β-D-glucopyranosyl) phosphinate (**2.53**)



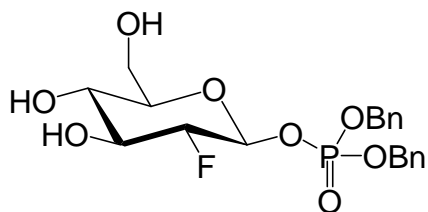
**2.12** (58.8 mg, 0.158 mmol) was dissolved in 5 mL dry acetonitrile. Dimethyl phosphinic acid (58.3 mg, 0.620 mmol, 3.9 eq) and silver carbonate (0.326 g, 1.18 mmol, 7.5 eq) were added, and the resulting slurry was stirred overnight under  $N_{2(g)}$ , in the dark. The solution was filtered through a short plug of silica using ethyl acetate as the eluent to remove the silver salts. The filtrate was collected and the solvent evaporated under reduced pressure. The product was purified by flash chromatography (9:1 ethyl acetate : methanol) to yield **2.53** as a colourless oil (50.3 mg, 0.131 mmol, 83%).  **$^1H$  NMR:** (300 MHz,  $CDCl_3$ )  $\delta$  5.43 (1 H, ddd,  $J_{H1-P}$  10.4 Hz,  $J_{H1-H2}$  8.5 Hz,  $J_{H1-F2}$  2.6 Hz, H1), 5.30 (1 H, ddd,  $J_{H3-F2}$  14.1 Hz,  $J_{H3-H4}$  9.8 Hz,  $J_{H3-H2}$  9.3 Hz, H3), 5.00 (1 H, t,  $J_{H4-H3} = J_{H4-H5}$  9.8 Hz, H4), 4.33 (1 H, ddd,  $J_{H2-F2}$  50.7 Hz,  $J_{H2-H3}$  9.3 Hz,  $J_{H2-H1}$  8.5 Hz, H2) 4.22 (1 H, dd,  $J_{H6-H6'}$  12.4 Hz,  $J_{H6-H5}$  5.0 Hz, H6), 4.11 (1 H, dd,  $J_{H6'-H6}$  12.4 Hz,  $J_{H6'-H5}$  2.9 Hz, H6'), 3.82 (1 H, ddd,  $J_{H5-H4}$  9.8 Hz,  $J_{H5-H6}$  5.0 Hz,  $J_{H5-H6'}$  2.9 Hz, H5), 2.04 (3 H, s, Ac), 2.03 (3 H, s, Ac), 2.00 (3 H, s, Ac), 1.61 (3H, d,  $J_{H-P}$  13.5 Hz,  $PCH_3$ ), 1.56 (3H, d,  $J_{H-P}$  13.4 Hz,  $PCH_3$ );  **$^{19}F$  NMR:** (282 MHz,  $CDCl_3$ ):  $\delta$  -200.42 (1 F, ddd,  $J_{F2-H2}$  50.7 Hz,  $J_{F2-H3}$  14.1 Hz,  $J_{F2-H1}$  2.6 Hz, F2);  **$^{31}P$  ( $^1H$  decoupled) NMR:** (121 MHz,  $CDCl_3$ ):  $\delta$  59.06;  **$^{13}C$  NMR:** (75 MHz,  $CDCl_3$ )  $\delta$  170.59, 169.91, 169.69 (3 x C=O), 93.44 (dd,  $J_{C1-F2}$  24 Hz,  $J_{C1-P}$  6 Hz, C1), 89.38 (dd,  $J_{C2-F2}$  201 Hz,  $J_{C2-P}$  8 Hz, C2), 72.60 (C5), 72.59 (d,  $J_{C3-F2}$  19 Hz, C3), 67.90 (d,  $J_{C4-F2}$  7 Hz, C4), 61.58 (C6), 20.87, 20.80, 20.73 (3 x Me), 17.68 (d,  $J_{C-P}$  93 Hz,  $PCH_3$ ), 16.75 (d,  $J_{C-P}$  96 Hz,  $PCH_3$ ); **ESI-MS (high res):** m/z calc.: 407.0878; **Found:** 407.0883  $[M + Na]^+$ .

Dibenzyl (3,4,6-tri-O-acetyl-2-deoxy-2-fluoro- $\beta$ -D-glucopyranosyl) phosphate (**2.61**)



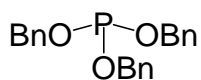
**2.12** (0.249 g, 0.671 mmol) was dissolved in 15 mL dry acetonitrile. Dibenzyl phosphoric acid (0.456 g, 1.64 mmol, 2.4 eq) and silver carbonate (0.688 g, 2.50 mmol, 3.7 eq) were added to the acetonitrile solution. The resulting slurry was stirred overnight under  $N_{2(g)}$ , in the dark. The solution was filtered through a short plug of silica using ethyl acetate as the eluent to remove the silver salts. The filtrate was collected and the solvent evaporated under reduced pressure. The product was purified by flash chromatography (2:1  $\rightarrow$  3:2 hexane : ethyl acetate) to yield **2.61** as a colourless oil (0.198 g, 0.358 mmol, 53%).  **$^1H$  NMR:** (300 MHz,  $CDCl_3$ )  $\delta$  7.35-7.30 (10 H, m, Ar-H), 5.42 (1 H, td,  $J_{H1-H2} = J_{H1-P}$  7.8 Hz,  $J_{H1-F}$  3.0 Hz, H1), 5.35 (1 H, ddd,  $J_{H3-F2}$  14.1 Hz,  $J_{H3-H4}$  9.6 Hz,  $J_{H3-H2}$  8.9 Hz, H3), 5.14-5.02 (5 H, m, H4, 2 x  $OCH_2Ph$ ), 4.41 (1 H, ddd,  $J_{H2-F2}$  50.6 Hz,  $J_{H2-H3}$  8.9 Hz,  $J_{H2-H1}$  7.8 Hz, H2), 4.23 (1 H, dd,  $J_{H6-H6'}$  12.5 Hz,  $J_{H6-H5}$  4.9 Hz, H6), 4.09 (1 H, dd,  $J_{H6'-H6}$  12.5 Hz,  $J_{H6'-H5}$  2.1 Hz, H6'), 3.82 (1 H, ddd,  $J_{H5-H4}$  10.1 Hz,  $J_{H5-H6}$  4.9 Hz,  $J_{H5-H6'}$  2.1 Hz, H5), 2.07 (3 H, s, Ac), 2.02 (3 H, s, Ac), 1.98 (3 H, s, Ac);  **$^{19}F$  NMR:** (282 MHz,  $CDCl_3$ ):  $\delta$  -200.27 (1 F, ddd,  $J_{F2-H2}$  50.6 Hz,  $J_{F2-H3}$  14.1 Hz,  $J_{F2-H1}$  3.0 Hz, F2);  **$^{31}P$  ( $^1H$  decoupled) NMR:** (121 MHz,  $CDCl_3$ ):  $\delta$  -2.33;  **$^{13}C$  NMR:** (75 MHz,  $CDCl_3$ )  $\delta$  170.54, 169.92, 169.61 (3 x C=O), 135.47 (d,  $J_{C-P}$  8 Hz), 135.36 (d,  $J_{C-P}$  9 Hz), 128.81, 128.78, 128.73 (2C), 128.69 (2C), 128.08 (4C) (12 x Ar), 95.98 (dd,  $J_{C1-F2}$  24 Hz,  $J_{C1-P}$  5 Hz, C1), 89.38 (dd,  $J_{C2-F2}$  193 Hz,  $J_{C2-P}$  9 Hz, C2), 72.78 (C5), 72.42 (d,  $J_{C3-F2}$  19 Hz, C3), 69.89 (d,  $J_{C-P}$  6 Hz,  $OCH_2Ph$ ), 69.80 (d,  $J_{C-P}$  6 Hz,  $OCH_2Ph$ ), 67.72 (d,  $J_{C4-F2}$  7 Hz, C4), 61.50 (C6), 20.71 (2C), 20.64 (3 x Ac); **ESI-MS (high res):** m/z calc.: 591.4712; **Found:** 591.4708  $[M + Na]^+$ .

Dibenzyl (2-deoxy-2-fluoro- $\beta$ -D-glucopyranosyl) phosphate (**2.62**)



**2.61** (40.3 mg, 0.0709 mmol) was dissolved in 5 mL dry methanol, and deacetylated according to General Procedure B. The crude product was purified by flash chromatography (24:1 ethyl acetate : methanol) to yield pure **2.62** as a colourless oil (21.1 mg, 0.0477 mmol, 65%). **<sup>1</sup>H NMR:** (300 MHz, CD<sub>3</sub>OD)  $\delta$  7.35-7.33 (10 H, m, Ar-H), 5.28 (1 H, td,  $J_{H1-H2} = J_{H1-P}$  7.4 Hz,  $J_{H1-F2}$  2.9 Hz, H1), 5.11 (2 H, d,  $J_{H-P}$  8.0 Hz, OCH<sub>2</sub>Ph), 5.10 (2 H, d,  $J_{H-P}$  8.2 Hz, OCH<sub>2</sub>Ph), 4.13 (1 H, ddd,  $J_{H2-F2}$  51.4 Hz,  $J_{H2-H3}$  8.2 Hz,  $J_{H2-H1}$  7.4 Hz, H2), 3.84 (1 H, ddd,  $J_{H3-F2}$  13.8 Hz,  $J_{H3-H4}$  9.6 Hz,  $J_{H3-H2}$  8.2 Hz, H3), 3.72-3.60 (2 H, m, H4, H5), 3.45-3.40 (2 H, m, H6, H6'); **<sup>19</sup>F NMR:** (282 MHz, CD<sub>3</sub>OD):  $\delta$  -201.53 (1 F, ddd,  $J_{F2-H2}$  51.4 Hz,  $J_{F2-H3}$  13.8 Hz,  $J_{F2-H1}$  2.9 Hz, F2); **<sup>31</sup>P (<sup>1</sup>H decoupled) NMR:** (121 MHz, CD<sub>3</sub>OD):  $\delta$  -2.68; **<sup>13</sup>C NMR:** (100 MHz, CD<sub>3</sub>OD)  $\delta$  134.68 (2 C, d,  $J_{C-P}$  8 Hz), 128.83, 128.78, 128.71 (2 C), 128.67 (2 C), 128.11 (4 C) (12 x Ar), 96.41 (dd,  $J_{C1-F2}$  23 Hz,  $J_{C1-P}$  7 Hz, C1), 88.96 (dd,  $J_{C2-F2}$  197 Hz,  $J_{C2-P}$  8 Hz, C2), 77.12 (d,  $J_{C3-F2}$  18 Hz, C3), 74.65 (d,  $J_{C4-F2}$  7 Hz, C4), 72.48 (C5), 70.29 (d,  $J_{C-P}$  10 Hz, OCH<sub>2</sub>Ph), 70.26 (d,  $J_{C-P}$  8 Hz, OCH<sub>2</sub>Ph), 60.73 (C6); **ESI-MS (high res):** m/z calc.: 465.1085; **Found:** 465.1080 [M + Na]<sup>+</sup>; **Anal. calc. for** C<sub>20</sub>H<sub>24</sub>FO<sub>8</sub>P: C, 54.30, H, 5.47; **Found:** C, 54.01, H, 5.79.

Tribenzyl phosphite (**2.63**)<sup>208</sup>

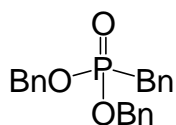


Phosphorus trichloride (0.85 mL, 9.7 mmol, 1.0 eq) was dissolved in 200 mL dichloromethane and stirred at 0 °C under N<sub>2</sub>(g). Dry pyridine (2.6 mL, 32 mmol, 3.3 eq) was dissolved in 10 mL dry dichloromethane, and added dropwise. Dry benzyl alcohol (3.4 mL, 33 mmol, 3.3 eq) was then dissolved in 10 mL dry dichloromethane, and added dropwise to



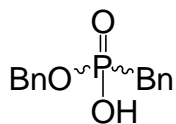
the solution. The reaction was allowed to warm to RT over two hours, after which the white precipitate was removed by filtration and the filtrate collected. The solvent was removed under reduced pressure, and the crude product was purified by flash chromatography (19:1 petroleum ether : ethyl acetate, 1% triethylamine) to yield **2.63** as a colourless liquid (2.60 g, 7.38 mmol, 76%). **<sup>1</sup>H NMR:** (300 MHz, CDCl<sub>3</sub>) δ 7.35-7.30 (15 H, m, Ar-H) 5.00 (6 H, d, J<sub>H-P</sub> 35.1 Hz, OCH<sub>2</sub>Ph); **<sup>31</sup>P (<sup>1</sup>H decoupled) NMR:** (121 MHz, CDCl<sub>3</sub>) δ -0.15.

Benzyl dibenzylphosphonate (**2.64**)<sup>208</sup>



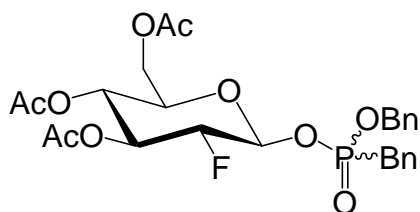
**2.63** (1.91 g, 5.42 mmol, 1 eq) and benzyl chloride (0.5 mL) were stirred, neat, overnight under N<sub>2(g)</sub> at 140 °C. The crude liquid was purified by flash chromatography (2:1 petroleum ether : ethyl acetate) to yield **2.64** as a colourless liquid (1.39 g, 3.94 mmol, 73%) along with recovered **2.63** (0.256 g, 0.727 mmol, 13%). **ESI-MS (low res):** m/z calc.: 375.1; **Found:** 375.3 [M + Na]<sup>+</sup>.

Benzyl benzylphosphonic acid (**2.65**)



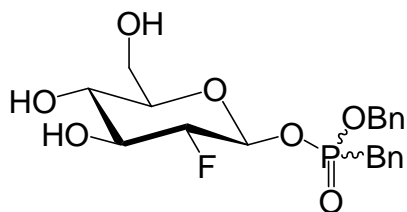
**2.64** (0.765 g, 2.17 mmol, 1 eq) and lithium bromide (0.377 g, 4.34 mmol, 2 eq) were dissolved in 40 mL dry acetonitrile, and refluxed overnight under N<sub>2(g)</sub>. The resulting white powder was filtered and washed with a small amount of acetonitrile. The powder was dissolved in 15 mL methanol, and acidified by stirring with Amberlite IR-120 (H<sup>+</sup>) resin for 10 minutes. The resin was filtered off and the filtrate collected. The solvent was evaporated under reduced pressure to yield **2.65** as a colourless oil (0.541 g, 2.06 mmol, 95%). The compound was used without further characterization or purification.

Benzyl benzyl-(3,4,6-tri-O-acetyl-2-deoxy-2-fluoro-β-D-glucopyranosyl) phosphonate  
(**2.66**)



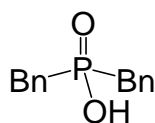
**2.12** (0.310 g, 0.835 mmol 1.2 eq) was dissolved in 10 mL dry acetonitrile. The crude **2.65** (0.180 g, 0.686 mmol, 1 eq) was dissolved in 5 mL dry acetonitrile and added, along with silver carbonate (0.563 g, 2.04 mmol, 2.4 eq) to the solution of **2.12**. The resulting slurry was stirred overnight under N<sub>2(g)</sub>, in the dark. The solution was filtered through a short plug of silica using ethyl acetate as the eluent to remove the silver salts. The filtrate was collected and the solvent evaporated under reduced pressure. The product was purified by flash chromatography (1:1 petroleum ether : ethyl acetate) to yield **2.66**, as a mixture of diastereomers, as a colourless oil (0.292 g, 0.523 mmol, 63% from **2.65**). **<sup>1</sup>H NMR:** (300 MHz, CDCl<sub>3</sub>) δ 7.32-7.25 (20 H, m, Ar-H) 5.46-5.25 (4 H, m, H1<sub>a</sub>, H1<sub>b</sub>, H3<sub>a</sub>, H3<sub>b</sub>), 5.09-4.94 (6 H, m, H4<sub>a</sub>, H4<sub>b</sub>, OCH<sub>2</sub>Ph<sub>a</sub>, OCH<sub>2</sub>Ph<sub>b</sub>), 4.48-4.06 (6 H, m, H2<sub>a</sub>, H2<sub>b</sub>, H6<sub>a</sub>, H6<sub>b</sub>, H6'<sub>a</sub>, H6'<sub>b</sub>), 3.86-3.74 (2 H, m, H5<sub>a</sub>, H5<sub>b</sub>), 3.35-3.22 (4 H, m, PCH<sub>2</sub>Ph<sub>a</sub>, PCH<sub>2</sub>Ph<sub>b</sub>), 2.08 (9 H, s, 3 x Ac), 2.07 (6 H, s, 2 x Ac), 1.97 (3 H, s, Ac); **<sup>19</sup>F NMR:** (282 MHz, CDCl<sub>3</sub>): δ -(199.97- 200.29) (2 F, m, F2<sub>a</sub>, F2<sub>b</sub>); **<sup>31</sup>P (<sup>1</sup>H decoupled) NMR:** (121 MHz, CDCl<sub>3</sub>): δ 28.08, 27.96; **ESI-MS (high res):** m/z calc.: 575.1453; **Found:** 575.1453 [M + Na]<sup>+</sup>.

Benzyl benzyl-(2-deoxy-2-fluoro- $\beta$ -D-glucopyranosyl) phosphonate (**2.67**)



**2.66** (56.5 mg, 0.133 mmol) was dissolved in 5 mL dry methanol, and deacetylated according to General Procedure B. The crude product was purified by flash chromatography (9:1 ethyl acetate : methanol) to yield pure **2.67**, as a mixture of diastereomers, as a colourless oil (36.2 mg, 0.851 mmol, 83%). **<sup>1</sup>H NMR:** (300 MHz, CD<sub>3</sub>OD)  $\delta$  7.30-7.25 (20 H, m, Ar-H), 5.31-5.21 (2 H, m, H1<sub>a</sub>, H1<sub>b</sub>), 5.07 (2 H, d,  $J_{H-P}$  7.7 Hz, OCH<sub>2</sub>Ph<sub>a</sub>), 5.03 (2 H, d,  $J_{H-P}$  8.0 Hz, OCH<sub>2</sub>Ph<sub>b</sub>) 4.23-3.99 (2 H, m, H2<sub>a</sub>, H2<sub>b</sub>), 3.88-3.84 (2 H, m, H3<sub>a</sub>, H3<sub>b</sub>), 3.72-3.58 (4 H, m, H4<sub>a</sub>, H4<sub>b</sub>, H5<sub>a</sub>, H5<sub>b</sub>) 3.43- 3.32 (8 H, m, H6<sub>a</sub>, H6<sub>b</sub>, H6'<sub>a</sub>, H6'<sub>b</sub>, PCH<sub>2</sub>Ph<sub>a</sub>, PCH<sub>2</sub>Ph<sub>b</sub>); **<sup>19</sup>F NMR:** (282 MHz, CD<sub>3</sub>OD):  $\delta$  - (201.10-201.34) (2 F, m, F<sub>2a</sub>, F<sub>2b</sub>); **<sup>31</sup>P (<sup>1</sup>H decoupled) NMR:** (121 MHz, CD<sub>3</sub>OD):  $\delta$  28.59, 28.51; **ESI-MS (high res):**  $m/z$  calc.: 449.1136; **Found:** 449.1126 [M + Na]<sup>+</sup>; **Anal. calc. for** C<sub>20</sub>H<sub>24</sub>FO<sub>7</sub>P: C, 56.34, H, 5.67; **Found:** C, 56.22, H, 5.89.

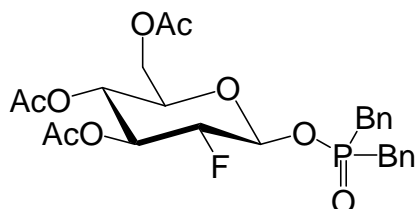
Dibenzyl phosphinic acid (**2.68**)<sup>207</sup>



Ammonium phosphinate (0.519 g, 6.25 mmol) was suspended in 15 mL dry dichloromethane at 0 °C under N<sub>2(g)</sub>. Diisopropyl ethyl amine (4.4 mL, 25.3 mmol, 4 eq) and trimethylsilyl chloride (3.2 mL, 25.3 mmol, 4 eq) were added, and the solution allowed to warm to room temperature over 2 hours. Following this, benzyl bromide (1.9 mL, 16.0 mmol, 2.5 eq) was added and stirred overnight. The solid was removed by filtration, the filtrate washed with 1 M HCl, and the organic layer was then dried over MgSO<sub>4</sub> for 10 minutes, filtered, and concentrated under reduced pressure. **2.68** was isolated as a white powder (1.08 g, 5.26

mmol, 84%). **<sup>1</sup>H NMR:** (300 MHz, CDCl<sub>3</sub>) δ 7.33-7.22 (10 H, m, Ar-H) 3.10 (4 H, d, J<sub>H-P</sub> 16.4 Hz, PCH<sub>2</sub>Ph); **<sup>31</sup>P (<sup>1</sup>H decoupled) NMR:** (121 MHz, CDCl<sub>3</sub>) δ 47.57; **ESI-MS (low res):** m/z calc.: 245.3; **Found:** 245.4 [M - H]<sup>-</sup>.

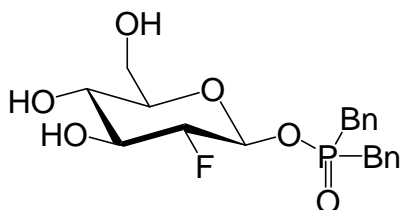
Dibenzyl-(3,4,6-tri-O-acetyl-2-deoxy-2-fluoro-β-D-glucopyranosyl) phosphinate (**2.69**)



**2.12** (0.130 g, 0.349 mmol) was dissolved in 10 mL dry acetonitrile. **2.68** (0.210 g, 0.853 mmol, 2 eq) and silver carbonate (0.365 g, 1.32 mmol, 3.5 eq) were added, and the resulting slurry was stirred overnight under N<sub>2(g)</sub>, in the dark. The solution was filtered through a short plug of silica using ethyl acetate as the eluent to remove the silver salts. The filtrate was collected and the solvent evaporated under reduced pressure. The product was purified by flash chromatography (1:1 → 1:3 petroleum ether : ethyl acetate) to yield **2.69** as a colourless oil (74.8 mg, 0.140 mmol, 36%) along with recovered **2.12** (84.2 mg, 0.227 mmol, 49%). **<sup>1</sup>H NMR:** (300 MHz, CDCl<sub>3</sub>) δ 7.30-7.17 (10 H, m, Ar-H), 5.38 (1 H, ddd, J<sub>H1-P</sub> 10.4 Hz, J<sub>H1-H2</sub> 7.8 Hz, J<sub>H1-F2</sub> 2.6 Hz, H1), 5.28 (1 H, ddd, J<sub>H3-F2</sub> 14.1 Hz, J<sub>H3-H4</sub> 9.8 Hz, J<sub>H3-H2</sub> 9.3 Hz, H3), 5.06 (1 H, t, J<sub>H4-H3</sub> = J<sub>H4-H5</sub> 9.8 Hz, H4), 4.33 (1 H, ddd, J<sub>H2-F2</sub> 50.7 Hz, J<sub>H2-H3</sub> 9.3 Hz, J<sub>H2-H1</sub> 7.8 Hz, H2) 4.22 (1H, dd, J<sub>H6-H6'</sub> 12.5 Hz, J<sub>H6-H5</sub> 4.6 Hz, H6), 4.07 (1 H, dd, J<sub>H6'-H6</sub> 12.5 Hz, J<sub>H6'-H5</sub> 2.2 Hz, H6'), 3.82 (1 H, ddd, J<sub>H5-H4</sub> 9.8 Hz, J<sub>H5-H6</sub> 4.6 Hz, J<sub>H5-H6'</sub> 2.2 Hz, H5), 3.18 (2 H, d, J<sub>H-P</sub> 39.8 Hz, PCH<sub>2</sub>Ph), 3.12 (2 H, d, J<sub>H-P</sub> 38.4 Hz, PCH<sub>2</sub>Ph), 2.06 (3 H, s, Ac), 2.03 (3 H, s, Ac), 2.02 (3 H, s, Ac); **<sup>19</sup>F NMR:** (282 MHz, CDCl<sub>3</sub>): δ -199.96 (1 F, ddd, J<sub>F2-H2</sub> 50.7 Hz, J<sub>F2-H3</sub> 14.1 Hz, J<sub>F2-H1</sub> 2.6 Hz, F2); **<sup>31</sup>P (<sup>1</sup>H decoupled) NMR:** (121 MHz, CDCl<sub>3</sub>): δ 53.08; **<sup>13</sup>C NMR:** (75 MHz, CDCl<sub>3</sub>) δ 170.55, 169.87, 169.70 (3 x C=O), 130.97 (2C, d, J<sub>C-P</sub> 99 Hz, PCH<sub>2</sub>Ph) 130.23 (2C), 130.15 (2C), 128.80 (2C), 127.30 (2C), 93.44 (dd, J<sub>C1-F2</sub> 26 Hz, J<sub>C1-P</sub> 6 Hz, C1), 89.38 (dd, J<sub>C2-F2</sub> 199 Hz, J<sub>C2-P</sub> 8 Hz, C2), 72.58 (C5), 72.56 (d, J<sub>C3-F2</sub> 19

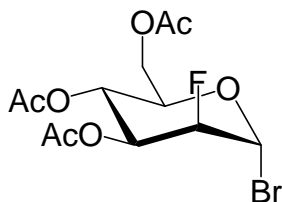
Hz, C3), 67.77 (d,  $J_{C4-F2}$  7 Hz, C4), 61.43 (C6), 20.80, 20.74, 20.67 (3 x Me); **ESI-MS (high res)**:  $m/z$  calc.: 559.1504; **Found**: 559.1520  $[M + Na]^+$ .

Dibenzyl-(2-deoxy-2-fluoro- $\beta$ -D-glucopyranosyl) phosphinate (**2.70**)



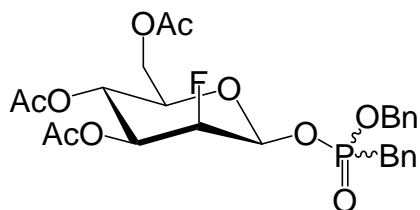
**2.69** (25.8 mg, 0.0481 mmol) was dissolved in 3 mL dry methanol, and deacetylated according to General Procedure B. The crude product was purified by flash chromatography (19:1  $\rightarrow$  9:1 ethyl acetate : methanol) to yield impure **2.70** as a colourless oil (5.32 mg).  **$^1H$  NMR**: (300 MHz,  $CD_3OD$ )  $\delta$  7.32-7.24 (10 H, m, Ar-H) 5.18 (1 H, ddd,  $J_{H1-P}$  10.2 Hz,  $J_{H1-H2}$  7.5 Hz,  $J_{H1-F2}$  2.6 Hz, H1), 4.10 (1 H, ddd,  $J_{H2-F2}$  51.2 Hz,  $J_{H2-H3}$  8.9 Hz,  $J_{H2-H1}$  7.5 Hz, H2), 3.92-3.54 (5 H, m, H3, H4, H5, H6, H6'), 3.40-3.24 (4 H, m,  $PC\bar{H}_2Ph$ );  **$^{19}F$  NMR**: (282 MHz,  $CD_3OD$ ):  $\delta$  -200.97 (1 F, ddd,  $J_{F2-H2}$  51.2 Hz,  $J_{F2-H3}$  14.3 Hz,  $J_{F2-H1}$  2.6 Hz, F2);  **$^{31}P$  ( $^1H$  decoupled) NMR**: (121 MHz,  $CD_3OD$ ):  $\delta$  54.16; **ESI-MS (high res)**:  $m/z$  calc.: 433.1192; **Found**: 433.1194  $[M + Na]^+$ ; **Anal. calc. for  $C_{20}H_{24}FO_6P$** : C, 58.54, H, 5.89; **Found**: C, 58.45, H, 5.95.

3,4,6-Tri-O-acetyl-2-deoxy-2-fluoro- $\alpha$ -D-mannopyranosyl bromide (**2.76**)



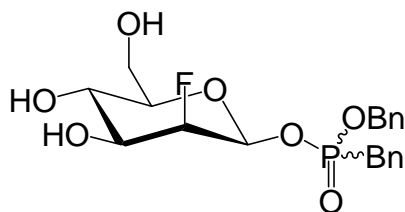
**2.10** (0.518 g, 1.48 mmol) was brominated according to General Procedure A overnight. The crude product (0.494 g, 1.33 mmol, 90%) was used without further purification or characterization.

Benzyl benzyl-(3,4,6-tri-O-acetyl-2-deoxy-2-fluoro- $\beta$ -D-mannopyranosyl) phosphonate  
(**2.77**)



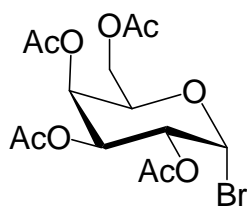
**2.76** (0.125 g, 0.337 mmol) was dissolved in 5 mL dry acetonitrile. The crude **2.65** (0.139 g, 0.518 mmol, 1.5 eq) was dissolved in 1 mL dry acetonitrile and added, along with silver carbonate (0.325 g, 1.18 mmol, 3.5 eq) to the solution of **2.76**. The resulting slurry was stirred for three days under  $N_{2(g)}$ , in the dark. The solution was filtered through a short plug of silica using ethyl acetate as the eluent to remove the silver salts. The filtrate was collected and the solvent evaporated under reduced pressure. The product was purified by flash chromatography (1:1 petroleum ether : ethyl acetate) to yield **2.77** as a colourless oil (0.118 g, 0.214 mmol, 63%).  **$^1H$  NMR:** (300 MHz,  $CDCl_3$ )  $\delta$  7.33-7.22 (20 H, m, Ar-H) 5.45-5.25 (4 H, m, H1<sub>a</sub>, H1<sub>b</sub>, H3<sub>a</sub>, H3<sub>b</sub>), 5.10-4.94 (6 H, m, H4<sub>a</sub>, H4<sub>b</sub>, OCH<sub>2</sub>Ph<sub>a</sub>, OCH<sub>2</sub>Ph<sub>b</sub>), 4.50-4.05 (6 H, m, H2<sub>a</sub>, H2<sub>b</sub>, H6<sub>a</sub>, H6<sub>b</sub>, H6'<sub>a</sub>, H6'<sub>b</sub>), 3.86-3.74 (2 H, m, H5<sub>a</sub>, H5<sub>b</sub>), 3.35-3.21 (4 H, m, PCH<sub>2</sub>Ph<sub>a</sub>, PCH<sub>2</sub>Ph<sub>b</sub>), 2.08 (3 H, s, Ac), 2.07 (6 H, s, 2 x Ac), 2.03 (3 H, s, Ac), 2.02 (3 H, s, Ac), 1.97 (3 H, s, Ac);  **$^{19}F$  NMR:** (282 MHz,  $CDCl_3$ ):  $\delta$  -199.97-200.30 (2 F, m, F2<sub>a</sub>, F2<sub>b</sub>);  **$^{31}P$  ( $^1H$  decoupled) NMR:** (121 MHz,  $CDCl_3$ ):  $\delta$  28.10, 27.98; **ESI-MS (high res):** m/z calc.: 575.1453; **Found:** 575.1456  $[M + Na]^+$ .

Benzyl benzyl-(2-deoxy-2-fluoro- $\beta$ -D-mannopyranosyl) phosphonate (**2.71**)



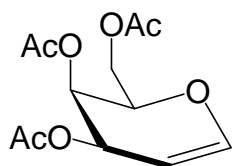
**2.77** (35.1 mg, 0.0635 mmol) was dissolved in 5 mL dry methanol, and deacetylated according to General Procedure B. The crude product was purified by flash chromatography (19:1 ethyl acetate : methanol) to yield pure **2.71** as a colourless oil (20.9 mg, 0.0490 mmol, 77%).  **$^1\text{H}$  NMR:** (300 MHz,  $\text{CD}_3\text{OD}$ )  $\delta$  7.30-7.27 (20 H, m, Ar-H), 5.31-5.21 (2 H, m, H1<sub>a</sub>, H1<sub>b</sub>), 5.07 (2 H, d,  $J_{\text{H-P}}$  7.7 Hz,  $\text{OCH}_2\text{Ph}_a$ ), 5.03 (2 H, d,  $J_{\text{H-P}}$  8.0 Hz,  $\text{OCH}_2\text{Ph}_b$ ) 4.23-3.99 (2 H, m, H2<sub>a</sub>, H2<sub>b</sub>), 3.88-3.84 (2 H, m, H3<sub>a</sub>, H3<sub>b</sub>), 3.72-3.58 (4 H, m, H4<sub>a</sub>, H4<sub>b</sub>, H5<sub>a</sub>, H5<sub>b</sub>) 3.43-3.30 (8 H, m, H6<sub>a</sub>, H6<sub>b</sub>, H6'<sub>a</sub>, H6'<sub>b</sub>,  $\text{PCH}_2\text{Ph}_a$ ,  $\text{PCH}_2\text{Ph}_b$ );  **$^{19}\text{F}$  NMR:** (282 MHz,  $\text{CD}_3\text{OD}$ ):  $\delta$  - (201.00-201.34) (2F, m, F2<sub>a</sub>, F2<sub>b</sub>);  **$^{31}\text{P}$  ( $^1\text{H}$  decoupled) NMR:** (121 MHz,  $\text{CD}_3\text{OD}$ ):  $\delta$  28.93, 28.52; **ESI-MS (high res):**  $m/z$  calc.: 449.1136; **Found:** 449.1134  $[\text{M} + \text{Na}]^+$ ; **Anal. calc. for  $\text{C}_{20}\text{H}_{24}\text{FO}_7\text{P}$ :** C, 56.34, H, 5.67; **Found:** C, 56.12, H, 5.78.

2,3,4,6-Tetra-O-acetyl- $\alpha$ -D-galactopyranosyl bromide (**2.78**)



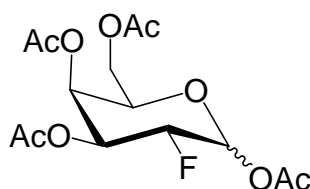
1,2,3,4,6-Penta-O-acetyl-D-galactopyranoside (7.68 g, 19.7 mmol) was treated according to General Procedure A (15 mL, 2 hours) to yield, after work-up, crude **2.78** as a colourless gum. The product was used without further characterization or purification.

3,4,6-Tri-O-acetyl-D-galactal (**2.79**)



**2.78** was dissolved in 300 mL of 1:1 acetic acid : water. Zinc (14.5 g, 0.222 mmol, 11 eq) was added, and the resulting slurry mechanically stirred at 0 °C overnight. The solution was filtered through Celite to remove the solid zinc and its salts, and the solvent removed under reduced pressure. The product was purified by flash chromatography (4:1 petroleum ether : ethyl acetate) to yield **2.79** as a white solid (2.54 g, 9.33 mmol, 48% from marjoram). <sup>1</sup>H NMR: (400 MHz, CDCl<sub>3</sub>) δ 6.39 (1 H, d, J<sub>H1-H2</sub> 6.6 Hz, H1), 5.48 (1 H, m, H3), 5.35 (1 H, m, H4), 4.66 (1 H, ddd, J<sub>H5-H4</sub> 6.3 Hz, J<sub>H5-H6</sub> 2.6 Hz, J<sub>H5-H6'</sub> 1.5 Hz, H5), 4.26 (1 H, t, J<sub>H2-H1</sub> = J<sub>H2-H3</sub> 6.6 Hz, H2), 4.22-4.12 (2 H, m, H6, H6'), 2.05 (3 H, s, Ac), 2.01 (3 H, s, Ac), 1.95 (3 H, s, Ac).

3,4,6-Tri-O-acetyl -2-deoxy-2-fluoro-D-galactopyranose (**2.80**)

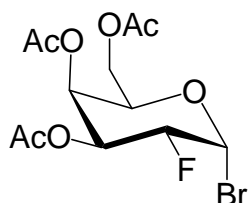


**2.79** (0.845 g, 3.10 mmol) was dissolved in 60 mL of 2:1 acetonitrile : acetic acid and stirred at 70 °C under N<sub>2(g)</sub>. To this solution was added Selectfluor (1.39 g, 3.93 mmol, 1.25 eq) and the mixture allowed to stir for 2.5 hours before being cooled to room temperature. Following solvent evaporation under reduced pressure, the residue was dissolved in ethyl acetate and washed with 2 x H<sub>2</sub>O, 1 x saturated NaHCO<sub>3</sub>, 1 x brine and dried over MgSO<sub>4</sub>. After 10 minutes, the MgSO<sub>4</sub> was filtered off, and the solvent evaporated under reduced pressure. The product was purified by column chromatography (4:1 hexane : ethyl acetate) to yield **2.80** (3:2 β:α) as a colourless oil (0.224 g, 0.639 mmol, 21%). <sup>1</sup>H NMR: (300 MHz, CDCl<sub>3</sub>) δ 6.39 (1 H, d, J<sub>H1α-F2α</sub> 3.9 Hz, H1α), 5.74 (1 H, dd, J<sub>H1β-F2β</sub> 8.0 Hz, J<sub>H1β-H2β</sub> 4.1 Hz, H2β),



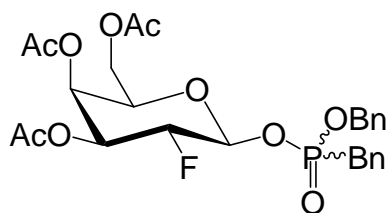
5.45-5.09 (4 H, m, H3 $\alpha$ , H3 $\beta$ , H4 $\alpha$ , H4 $\beta$ ), 4.85 (1 H, ddd,  $J_{H2\alpha-F2\alpha}$  49.1 Hz,  $J_{H2\alpha-H3\alpha}$  10.2 Hz,  $J_{H2\alpha-H1\alpha}$  4.0 Hz, H2 $\alpha$ ), 4.57 (1 H, ddd,  $J_{H2\beta-F2\beta}$  51.6 Hz,  $J_{H2\beta-H3\beta}$  9.6 Hz,  $J_{H2\beta-H1\beta}$  8.1 Hz, H2 $\beta$ ), 4.27-4.00 (6 H, m, H5 $\alpha$ , H5 $\beta$ , H6 $\alpha$ , H6 $\beta$ , H6' $\alpha$ , H6' $\beta$ ), 2.12 (3 H, s, Ac), 2.11 (3 H, s, Ac), 2.08 (3 H, s, Ac), 1.99 (3 H, s, Ac), 1.97 (3 H, s, Ac), 1.96 (3 H, s, Ac)  **$^{19}\text{F}$  NMR:** (282 MHz,  $\text{CDCl}_3$ ):  $\delta$  -208.5 (1 F, ddd,  $J_{F2\beta-H2\beta}$  51.6 Hz,  $J_{F2\beta-H3\beta}$  14.4 Hz,  $J_{F2\beta-H1\beta}$  8.0 Hz, F2 $\beta$ ), -202.63 (1 F, ddd,  $J_{F2\alpha-H1\alpha}$  48.5 Hz,  $J_{F2\alpha-H3\alpha}$  49.1 Hz,  $J_{F2\alpha-H3\alpha}$  12.4 Hz,  $J_{F2\alpha-H1\alpha}$  3.9 Hz, F2 $\alpha$ ).

3,4,6-Tri-O-acetyl-2-deoxy-2-fluoro- $\alpha$ -D-galactopyranosyl bromide (**2.81**)



**2.80** (0.104 g, 0.297 mmol) was treated according to General Procedure A (3 mL, 4 hours) to yield, after work-up, crude **2.81** a colourless gum. The product was used without further characterization or purification.

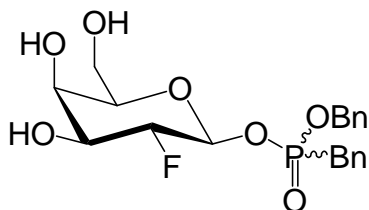
Benzyl benzyl-(3,4,6-tri-O-acetyl-2-deoxy-2-fluoro- $\beta$ -D-galactopyranosyl) phosphonate (**2.82**)



**2.81** was dissolved in 5 mL dry acetonitrile. The crude **2.65** (0.180 g, 0.686 mmol, 2.3 eq) was dissolved in 2 mL dry acetonitrile and added, along with silver carbonate (0.351 g, 1.27 mmol, 4.3 eq) to the solution of **2.81**. The resulting slurry was stirred overnight under  $\text{N}_2(\text{g})$ , in the dark. The solution was filtered through a short plug of silica using ethyl acetate as the eluent to remove the silver salts. The filtrate was collected and the solvent evaporated under

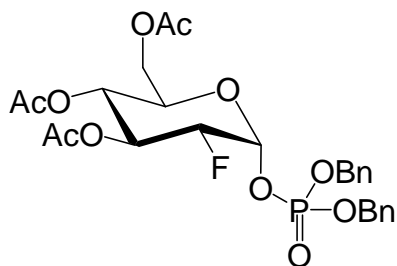
reduced pressure. The product was purified by flash chromatography (1:1 → 1:2 petroleum ether : ethyl acetate) to yield **2.66**, as a mixture of diastereomers, as a colourless oil (0.130 g, 0.235 mmol, 80% from **2.80**). **<sup>1</sup>H NMR:** (300 MHz, CDCl<sub>3</sub>) δ 5.45-5.25 (4 H, m, H1<sub>a</sub>, H1<sub>b</sub>, H3<sub>a</sub>, H3<sub>b</sub>), 5.09-4.94 (6 H, m, H4<sub>a</sub>, H4<sub>b</sub>, OCH<sub>2</sub>Ph<sub>a</sub>, OCH<sub>2</sub>Ph<sub>b</sub>), 4.48-4.05 (6 H, m, H2<sub>a</sub>, H2<sub>b</sub>, H6<sub>a</sub>, H6<sub>b</sub>, H6'<sub>a</sub>, H6'<sub>b</sub>), 3.84-3.75 (2 H, m, H5<sub>a</sub>, H5<sub>b</sub>), 3.32-3.22 (4 H, m, PCH<sub>2</sub>Ph<sub>a</sub>, PCH<sub>2</sub>Ph<sub>b</sub>), 2.08 (9 H, s, 3 x Ac), 2.07 (6 H, s, 2 x Ac), 2.03 (3 H, s, Ac); **<sup>19</sup>F NMR:** (282 MHz, CDCl<sub>3</sub>): δ -199.98-200.30 (2 F, m, F2<sub>a</sub>, F2<sub>b</sub>); **<sup>31</sup>P (<sup>1</sup>H decoupled) NMR:** (121 MHz, CDCl<sub>3</sub>): δ 28.08, 27.96; **ESI-MS (high res):** m/z calc.: 575.1458; **Found:** 575.1453 [M + Na]<sup>+</sup>.

Benzyl benzyl-(2-deoxy-2-fluoro-β-D-galactopyranosyl) phosphonate (**2.72**)



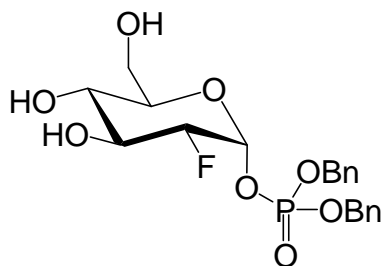
**2.82** (21.9 mg, 0.0396 mmol) was dissolved in 5 mL dry methanol, and deacetylated according to General Procedure B. The crude product was purified by flash chromatography (9:1 ethyl acetate : methanol) to yield pure **2.72**, as a mixture of diastereomers, as a colourless oil (16.6 mg, 0.0389 mmol, 98%). **<sup>1</sup>H NMR:** (300 MHz, CD<sub>3</sub>OD) δ 7.30-7.25 (20 H, m, Ar-H), 5.30-5.21 (2 H, m, H1<sub>a</sub>, H1<sub>b</sub>), 5.08 (2 H, d, J<sub>H-P</sub> 7.7 Hz, OCH<sub>2</sub>Ph<sub>a</sub>), 5.04 (2 H, d, J<sub>H-P</sub> 8.0 Hz, OCH<sub>2</sub>Ph<sub>b</sub>) 4.23-3.99 (2 H, m, H2<sub>a</sub>, H2<sub>b</sub>), 3.88-3.84 (2 H, m, H3<sub>a</sub>, H3<sub>b</sub>), 3.70-3.54 (4 H, m, H4<sub>a</sub>, H4<sub>b</sub>, H5<sub>a</sub>, H5<sub>b</sub>) 3.43- 3.32 (8 H, m, H6<sub>a</sub>, H6<sub>b</sub>, H6'<sub>a</sub>, H6'<sub>b</sub>, PCH<sub>2</sub>Ph<sub>a</sub>, PCH<sub>2</sub>Ph<sub>b</sub>), 2.08 (9 H, s, 3 x Ac), 2.07 (6 H, s, 2 x Ac), 1.97 (3 H, s, Ac);, **<sup>19</sup>F NMR:** (282 MHz, CD<sub>3</sub>OD): δ -(209.60-209.95) (2 F, m, F2<sub>a</sub>, F2<sub>b</sub>); **<sup>31</sup>P (<sup>1</sup>H decoupled) NMR:** (121 MHz, CD<sub>3</sub>OD): δ 28.87, 28.45; **ESI-MS (high res):** m/z calc.: 449.1136; **Found:** 465.1133 [M + Na]<sup>+</sup>; **Anal. calc. for** C<sub>20</sub>H<sub>24</sub>FO<sub>7</sub>P: C, 56.34, H, 5.67; **Found:** C, 56.26, H, 5.72.

Dibenzyl (3,4,6-tri-O-acetyl-2-deoxy-2-fluoro- $\alpha$ -D-glucopyranosyl) phosphate (**2.83**)



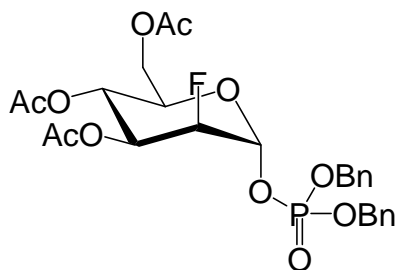
**2.61** (0.463 g, 0.814 mmol) was dissolved in 10 mL dry toluene. Dibenzyl phosphoric acid (0.450 g, 1.62 mmol, 2.0 eq) was added and the solution stirred under  $N_{2(g)}$  at 110 °C for 2 days. The solvent was then evaporated under reduced pressure, and the product was partially purified by flash chromatography (3:1  $\rightarrow$  2:1  $\rightarrow$  1:1 hexane : ethyl acetate) to yield an inseparable mixture of 1:4 **2.61** to **2.83** as a colourless oil (0.149 g, 0.262 mmol, 22%). **2.61**: Characterization previously described. **2.83**:  $^1H$  NMR: (300 MHz,  $CDCl_3$ )  $\delta$  7.34-7.32 (10 H, m, Ar-H), 5.95 (1 H, dd,  $J_{H1-P}$  6.7 Hz,  $J_{H1-H2}$  3.6 Hz, H1), 5.51 (1 H, dt,  $J_{H3-F2}$  11.9 Hz,  $J_{H3-H2} = J_{H3-H4}$  9.6 Hz, H3), 5.09-4.99 (5 H, m, H4, 2 x  $OCH_2Ph$ ), 4.56 (1 H, ddt,  $J_{H2-F2}$  48.6 Hz,  $J_{H2-H3}$  9.6 Hz,  $J_{H2-H1} = J_{H2-P}$  3.6 Hz, H2), 4.14 (1 H, dd,  $J_{H6-H6'}$  12.6 Hz,  $J_{H6-H5}$  4.0 Hz, H6), 4.01 (1 H, ddd,  $J_{H5-H4}$  9.4 Hz,  $J_{H5-H6}$  4.0 Hz,  $J_{H5-H6'}$  2.0 Hz, H5), 3.85 (1 H, dd,  $J_{H6'-H6}$  12.6 Hz,  $J_{H6'-H5}$  2.0 Hz, H6'), 2.06 (3 H, s, Ac), 2.01 (3 H, s, Ac), 1.97 (3 H, s, Ac);  $^{19}F$  NMR: (282 MHz,  $CDCl_3$ ):  $\delta$  -200.81 (1 F, dd,  $J_{F2-H2}$  48.6 Hz,  $J_{F2-H3}$  11.9 Hz, F2);  $^{31}P$  ( $^1H$  decoupled) NMR: (121 MHz,  $CDCl_3$ ):  $\delta$  -2.10;  $^{13}C$  NMR: (75 MHz,  $CDCl_3$ )  $\delta$  170.54, 169.92, 169.60 (3 x C=O), 135.53-135.30 (2 C, m), 128.78 (2 C), 128.73 (2 C), 128.70 (2 C), 128.69 (2 C), 128.07 (2 C) (12 x Ar), 95.99 (dd,  $J_{C1-F2}$  24 Hz,  $J_{C1-P}$  5 Hz, C1), 89.37 (dd,  $J_{C2-F2}$  192 Hz,  $J_{C2-P}$  9 Hz, C2), 72.78 (C5), 72.42 (d,  $J_{C3-F2}$  19 Hz, C3), 69.87 (d,  $J_{C-P}$  8 Hz,  $OCH_2Ph$ ), 69.80 (d,  $J_{C-P}$  8 Hz,  $OCH_2Ph$ ), 67.71 (d,  $J_{C4-F2}$  7 Hz, C4), 61.50 (C6), 20.72, 20.65, 20.31 (3 x Ac); **ESI-MS (high res)**: m/z calc.: 591.4712; **Found**: 591.4718  $[M + Na]^+$ .

Dibenzyl (2-deoxy-2-fluoro- $\alpha$ -D-glucopyranosyl) phosphate (**2.73**)



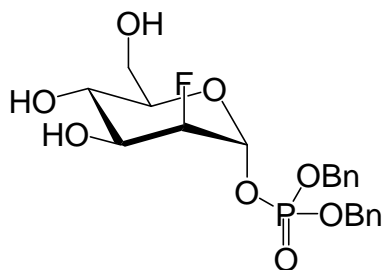
The impure **2.83** (51.9 mg, 0.0913 mmol) was dissolved in 10 mL dry methanol, and deacetylated according to General Procedure B. The crude product was purified by flash chromatography (50:1 ethyl acetate : methanol) to yield a 1:19 mixture of **2.62** to **2.73** as a colourless oil (31.0 mg, 0.0701 mmol, 77%). **2.62**: Characterization previously described. **<sup>1</sup>H NMR**: (300 MHz, CD<sub>3</sub>OD)  $\delta$  7.36-7.33 (10 H, m, Ar-H), 5.92 (1 H, dd,  $J_{H1-P}$  6.1 Hz,  $J_{H1-H2}$  3.7 Hz, H1), 5.11-5.08 (2 H, m, 2 x OCH<sub>2</sub>Ph), 4.38 (1 H, ddd,  $J_{H2-F2}$  48.5 Hz,  $J_{H2-H3}$  9.5 Hz,  $J_{H2-H1}$  3.7 Hz, H2), 3.85 (1 H, dt,  $J_{H3-F2}$  12.9 Hz,  $J_{H3-H2} = J_{H3-H4}$  9.5 Hz, H3), 3.73-3.63 (2 H, m, H4, H5), 3.53-3.41 (2 H, m, H6, H6'); **<sup>19</sup>F NMR**: (282 MHz, CD<sub>3</sub>OD):  $\delta$  -202.20 (1 F, dd,  $J_{F2-H2}$  48.5 Hz,  $J_{F2-H3}$  12.9 Hz, F2); **<sup>31</sup>P (<sup>1</sup>H decoupled) NMR**: (121 MHz, CD<sub>3</sub>OD):  $\delta$  -2.35; **<sup>13</sup>C NMR**: (100 MHz, CD<sub>3</sub>OD)  $\delta$  134.64 (2 C, d,  $J_{C-P}$  7 Hz), 128.82, 128.75, 128.71 (2 C), 128.61 (2 C), 128.11 (4 C) (12 x Ar), 96.41 (dd,  $J_{C1-F2}$  24 Hz,  $J_{C1-P}$  7 Hz, C1), 88.92 (dd,  $J_{C2-F2}$  194 Hz,  $J_{C2-P}$  8 Hz, C2), 77.54 (d,  $J_{C3-F2}$  18 Hz, C3), 74.62 (d,  $J_{C4-F2}$  7 Hz, C4), 72.58 (C5), 70.29 (d,  $J_{C-P}$  10 Hz, OCH<sub>2</sub>Ph), 70.26 (d,  $J_{C-P}$  8 Hz, OCH<sub>2</sub>Ph), 60.73 (C6); **ESI-MS (high res)**:  $m/z$  calc.: 465.1085; **Found**: 465.1078 [M + Na]<sup>+</sup>; **Anal. calc. for C<sub>20</sub>H<sub>24</sub>FO<sub>8</sub>P**: C, 54.30, H, 5.47; **Found**: C, 54.22, H, 5.56.

Dibenzyl (3,4,6-tri-O-acetyl-2-deoxy-2-fluoro- $\alpha$ -D-mannopyranosyl) phosphate (**2.84**)



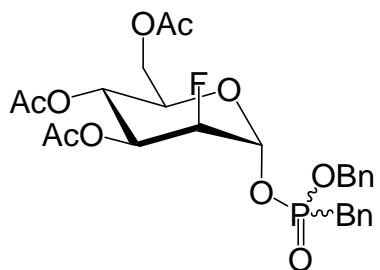
**2.76** (0.494 g, 1.33 mmol) was dissolved in 10 mL dry toluene. Dibenzyl phosphoric acid (0.617 g, 2.22 mmol, 1.7 eq) and silver carbonate (0.769 g, 2.79 mmol, 1.9 eq) were added to the toluene solution. The resulting slurry was stirred overnight under  $N_{2(g)}$ , in the dark. The solution was filtered through a short plug of silica using ethyl acetate as the eluent to remove the silver salts. The filtrate was collected and the solvent evaporated under reduced pressure. The product was purified by flash chromatography (9:1 toluene : acetone) to yield **2.84** as a colourless oil (0.0547 g, 0.0962 mmol, 7%).  **$^1H$  NMR:** (300 MHz,  $CDCl_3$ )  $\delta$  7.36-7.35 (10 H, m, Ar-H), 5.73 (1 H, br td,  $J_{H1-P}$  6.4 Hz,  $J_{H1-F2}$  5.5 Hz,  $J_{H1-H2}$  1.9 Hz, H1), 5.32 (1 H, t,  $J_{H4-H3} = J_{H4-H5}$  10.0 Hz, H4), 5.17 (1 H, ddd,  $J_{H3-F2}$  27.6 Hz,  $J_{H3-H4}$  10.0 Hz,  $J_{H3-H2}$  2.5 Hz, H3), 5.11-5.07 (4 H, m, 2 x  $OCH_2Ph$ ), 4.54 (1 H, br dt,  $J_{H2-F2}$  48.9 Hz,  $J_{H2-H3}$  2.5 Hz,  $J_{H2-H1}$  1.9 Hz, H2), 4.16 (1 H, dd,  $J_{H6-H6'}$  12.3 Hz,  $J_{H6-H5}$  4.1 Hz, H6), 3.99 (1 H, ddd,  $J_{H5-H4}$  10.0 Hz,  $J_{H5-H6}$  4.1 Hz,  $J_{H5-H6'}$  2.1 Hz, H5), 3.93 (1 H, dd,  $J_{H6'-H6}$  12.3 Hz,  $J_{H6'-H5}$  2.1 Hz, H6'), 2.09 (3 H, s, Ac), 2.03 (3 H, s, Ac), 2.00 (3 H, s, Ac);  **$^{19}F$  NMR:** (282 MHz,  $CDCl_3$ ):  $\delta$  -203.69 (1 F, ddd,  $J_{F2-H2}$  48.9 Hz,  $J_{F2-H3}$  27.6 Hz,  $J_{F2-H1}$  5.5 Hz, F2);  **$^{31}P$  ( $^1H$  decoupled) NMR:** (121 MHz,  $CDCl_3$ ):  $\delta$  -2.38;  **$^{13}C$  NMR:** (75 MHz,  $CDCl_3$ )  $\delta$  170.71, 170.02, 169.43 (3 x  $C=O$ ), 135.38, 135.31, 128.04 (3 C), 128.90 (3 C), 128.37 (2 C), 128.23 (2 C), (12 x Ar), 94.46 (dd,  $J_{C1-F2}$  32 Hz,  $J_{C1-P}$  5 Hz, C1), 88.78 (dd,  $J_{C2-F2}$  196 Hz,  $J_{C2-P}$  8 Hz, C2), 70.40 (C5), 70.19 (d,  $J_{C-P}$  10 Hz,  $OCH_2Ph$ ), 70.09 (d,  $J_{C-P}$  6 Hz,  $OCH_2Ph$ ), 69.00 (d,  $J_{C3-F2}$  17 Hz, C3), 65.08 (C4), 61.55 (C6), 20.71, 20.70 (2 C), (3 x Me); **ESI-MS (high res):**  $m/z$  calc.: 591.4712; **Found:** 591.4710 [ $M + Na$ ] $^+$ .

Dibenzyl (2-deoxy-2-fluoro- $\alpha$ -D-mannopyranosyl) phosphate (**2.74**)



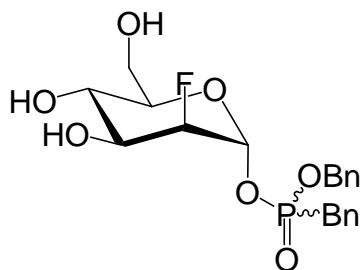
**2.84** (14.9 mg, 0.0262 mmol) was dissolved in 2 mL dry methanol, and deacetylated according to General Procedure B. The crude product was purified by flash chromatography (50:1 ethyl acetate : methanol) to yield pure **2.74** as a colourless oil (8.8 mg, 0.020 mmol, 76%). **<sup>1</sup>H NMR:** (300 MHz, CD<sub>3</sub>OD)  $\delta$  7.37 (10 H, m, Ar-H), 5.71 (1 H, td,  $J_{H1-F2} = J_{H1-P}$  6.2 Hz,  $J_{H1-H2}$  1.9 Hz, H1), 5.11 (2 H, d,  $J_{H-P}$  8.6 Hz, OCH<sub>2</sub>Ph), 5.10 (d,  $J_{H-P}$  9.6 Hz, OCH<sub>2</sub>Ph), 4.46 (1 H, dt,  $J_{H2-F2}$  48.9 Hz,  $J_{H2-H3} = J_{H2-H1}$  1.9 Hz, H2), 3.71-3.60 (5 H, m, H3, H4, H5, H6, H6'); **<sup>19</sup>F NMR:** (282 MHz, CD<sub>3</sub>OD):  $\delta$  -205.90 (1 F, ddd,  $J_{F2-H2}$  48.9 Hz,  $J_{F2-H3}$  22.6 Hz,  $J_{F2-H1}$  6.2 Hz, F2); **<sup>31</sup>P (<sup>1</sup>H decoupled) NMR:** (121 MHz, CD<sub>3</sub>OD):  $\delta$  -2.54; **<sup>13</sup>C NMR:** (75 MHz, CD<sub>3</sub>OD)  $\delta$  134.34 (2 C), 128.43 (2 C), 128.41 (2 C), 128.39 (2 C), 128.24 (2 C), 128.11 (2 C) (12 x Ar), 94.21 (dd,  $J_{C1-F2}$  30 Hz,  $J_{C1-P}$  6 Hz, C1), 88.94 (dd,  $J_{C2-F2}$  198 Hz,  $J_{C2-P}$  8 Hz, C2), 77.65 (d,  $J_{C3-F2}$  19 Hz, C3), 75.15 (d,  $J_{C4-F2}$  5 Hz, C4), 72.48 (C5), 70.43 (d,  $J_{C-P}$  9 Hz, OCH<sub>2</sub>Ph), 70.39 (d,  $J_{C-P}$  7 Hz, OCH<sub>2</sub>Ph), 60.73 (C6); **ESI-MS (high res):** m/z calc.: 465.1085; **Found:** 465.1082 [M + Na]<sup>+</sup>; **Anal. calc. for** C<sub>20</sub>H<sub>24</sub>FO<sub>8</sub>P: C, 54.30, H, 5.47; **Found:** C, 54.14, H, 5.59.

Benzyl benzyl-(3,4,6-tri-O-acetyl-2-deoxy-2-fluoro- $\alpha$ -D-mannopyranosyl) phosphonate  
(**2.85**)



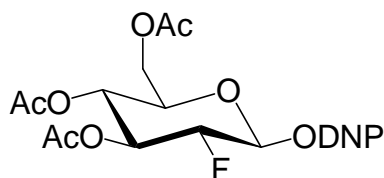
**2.76** (0.479 g, 1.29 mmol) was dissolved in 10 mL dry acetonitrile. The crude **2.65** (0.307 g, 1.83 mmol, 1.4 eq) was dissolved in 2 mL dry acetonitrile and added, along with silver carbonate (0.452 g, 1.64 mmol, 1.3 eq) to the solution of **2.76**. The resulting slurry was stirred overnight under  $N_{2(g)}$ , in the dark. The solution was filtered through a short plug of silica using ethyl acetate as the eluent to remove the silver salts. The filtrate was collected and the solvent evaporated under reduced pressure. The product was purified by flash chromatography (1:1 petroleum ether : ethyl acetate) to yield **2.85**, as a mixture of diastereomers, as a colourless oil (0.267 g, 0.483 mmol, 37%).  **$^1H$  NMR:** (300 MHz,  $CDCl_3$ )  $\delta$  7.31-7.26 (20 H, m, Ar-H) 5.79-5.63 (2 H, m, H1<sub>a</sub>, H1<sub>b</sub>), 5.31-4.97 (8 H, m, H3<sub>a</sub>, H3<sub>b</sub>, H4<sub>a</sub>, H4<sub>b</sub>, OCH<sub>2</sub>Ph<sub>a</sub>, OCH<sub>2</sub>Ph<sub>b</sub>), 4.52-3.83 (8 H, m, H2<sub>a</sub>, H2<sub>b</sub>, H5<sub>a</sub>, H5<sub>b</sub>, H6<sub>a</sub>, H6<sub>b</sub>, H6'<sub>a</sub>, H6'<sub>b</sub>), 3.31-3.13 (4 H, m, PCH<sub>2</sub>Ph<sub>a</sub>, PCH<sub>2</sub>Ph<sub>b</sub>), 2.08 (3 H, s, Ac), 2.07 (6 H, s, 2 x Ac), 2.01 (3 H, s, Ac), 1.97 (6 H, s, 2 x Ac);  **$^{19}F$  NMR:** (282 MHz,  $CDCl_3$ ):  $\delta$  -(203.25-203.92) (2 F, m, F2<sub>a</sub>, F2<sub>b</sub>);  **$^{31}P$  ( $^1H$  decoupled) NMR:** (121 MHz,  $CDCl_3$ ):  $\delta$  27.71, 27.25; **ESI-MS (high res):** m/z calc.: 575.1453; **Found:** 575.1448  $[M + Na]^+$ .

Benzyl benzyl-(2-deoxy-2-fluoro- $\alpha$ -D-mannopyranosyl) phosphonate (**2.75**)



**2.85** (56.5 mg, 0.133 mmol) was dissolved in 5 mL dry methanol, and deacetylated according to General Procedure B. The crude product was purified by flash chromatography (9:1 ethyl acetate : methanol) to yield pure **2.75**, as a mixture of diastereomers, as a colourless oil (36.2 mg, 0.851 mmol, 83%). **<sup>1</sup>H NMR:** (300 MHz, CDCl<sub>3</sub>)  $\delta$  7.33-7.29 (20 H, m, Ar-H) 5.70-5.67 (2 H, m, H1<sub>a</sub>, H1<sub>b</sub>), 5.10-5.04 (2 H, m, H4<sub>a</sub>, H4<sub>b</sub>), 4.86-4.81 (4 H, m, OCH<sub>2</sub>Ph<sub>a</sub>, OCH<sub>2</sub>Ph<sub>b</sub>) 4.48-4.25 (2 H, m, H2<sub>a</sub>, H2<sub>b</sub>), 3.81-3.30 (18 H, m, H3<sub>a</sub>, H3<sub>b</sub>, H4<sub>a</sub>, H4<sub>b</sub>, H5<sub>a</sub>, H5<sub>b</sub>, H6<sub>a</sub>, H6<sub>b</sub>, H6'<sub>a</sub>, H6'<sub>b</sub>, PCH<sub>2</sub>Ph<sub>a</sub>, PCH<sub>2</sub>Ph<sub>b</sub>); **<sup>19</sup>F NMR:** (282 MHz, CDCl<sub>3</sub>):  $\delta$  - (205.30-205.90) (2 F, m, F2<sub>a</sub>, F2<sub>b</sub>); **<sup>31</sup>P (<sup>1</sup>H decoupled) NMR:** (121 MHz, CDCl<sub>3</sub>):  $\delta$  28.55, 28.37; **ESI-MS (high res):**  $m/z$  calc.: 449.1136; **Found:** 449.1126 [M + Na]<sup>+</sup>; **Anal. calc. for C<sub>20</sub>H<sub>24</sub>FO<sub>7</sub>P:** C, 56.34, H, 5.67; **Found:** C, 56.23, H, 5.78.

2,4-Dinitrophenyl 3,4,6-tri-O-acetyl-2-deoxy-2-fluoro- $\beta$ -D-glucopyranoside (**3.9**)

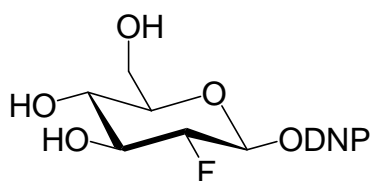


**2.41** (0.385 g, 1.25 mmol) was dissolved in 1 mL *N,N'*-dimethylformamide. 1,4-diazabicyclo[2.2.2]octane (0.523 g, 4.67 mmol, 3.8 eq) and dinitrofluorobenzene (0.348 g, 1.87 mmol, 1.5 eq) were added, and the mixture stirred for 2 hours under N<sub>2(g)</sub>. The solvent was then evaporated under reduced pressure, and the resulting syrup purified by flash chromatography (3:1 hexane : ethyl acetate) to yield **3.9** as a yellow solid (0.306 g, 0.645 mmol, 52%). **<sup>1</sup>H NMR:** (300 MHz, CDCl<sub>3</sub>)  $\delta$  8.73 (1 H, d, J<sub>H3Ar-H5Ar</sub> 2.7 Hz, H3<sub>Ar</sub>), 8.41 (1



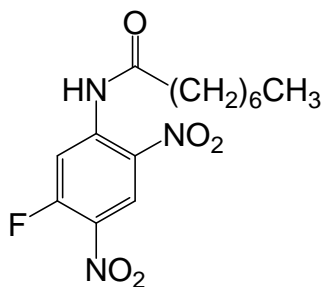
H, dd,  $J_{H5Ar-H6Ar}$  9.2 Hz,  $J_{H5Ar-H3Ar}$  2.7 Hz,  $H5_{Ar}$ ), 7.39 (1 H, d,  $J_{H6Ar-H5Ar}$  9.2 Hz,  $H6_{Ar}$ ) 5.47-5.36 (2 H, m,  $H1$ ,  $H3$ ), 5.11 (1 H, t,  $J_{H4-H3} = J_{H4-H5}$  9.5 Hz,  $H4$ ), 4.69 (1 H, ddd,  $J_{H2-F2}$  49.8 Hz,  $J_{H2-H3}$  8.4 Hz,  $J_{H2-H1}$  7.2 Hz,  $H2$ ) 4.24 (1 H, dd,  $J_{H6-H6'}$  12.5 Hz,  $J_{H6-H5}$  5.1 Hz,  $H6$ ), 4.17 (1 H, dd,  $J_{H6'-H6}$  12.5 Hz,  $J_{H6'-H5}$  2.7 Hz,  $H6'$ ), 3.97 (1 H, ddd,  $J_{H5-H4}$  9.5 Hz,  $J_{H5-H6}$  5.1 Hz,  $J_{H5-H6'}$  2.7 Hz,  $H5$ ), 2.10 (3 H, s, Ac), 2.04 (3 H, s, Ac), 2.03 (3 H, s, Ac);  **$^{19}F$  NMR:** (282 MHz,  $CDCl_3$ ):  $\delta$  -199.01 (1 F, ddd,  $J_{F2-H2}$  49.8 Hz,  $J_{F2-H3}$  14.1 Hz,  $J_{F2-H1}$  3.5 Hz,  $F2$ ).

### 2,4-Dinitrophenyl 2-deoxy-2-fluoro- $\beta$ -D-glucopyranoside (**3.3**)



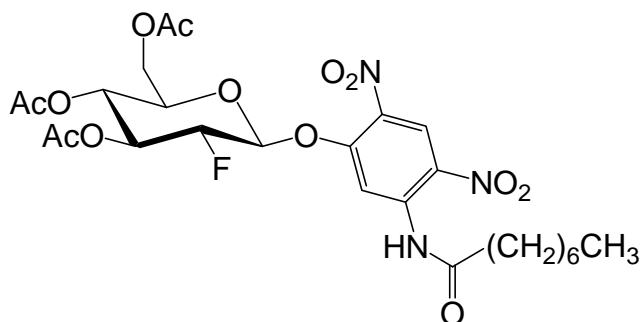
**3.9** (0.110 g, 0.232 mmol) was dissolved in 15 mL of dry methanol and stirred at 0 °C under  $N_2(g)$ . 0.1 mL acetyl chloride was then added, and the reaction mixture stirred overnight. The solvent was evaporated under reduced pressure, and the crude oil purified by flash chromatography (9:1 ethyl acetate : methanol) to yield **3.3** as a white solid (0.0594 g, 0.171mmol, 74%).  **$^1H$  NMR:** (300 MHz,  $CD_3OD$ )  $\delta$  8.67 (1 H, d,  $J_{H3Ar-H5Ar}$  2.5 Hz,  $H3_{Ar}$ ), 8.47 (1 H, dd,  $J_{H5Ar-H6Ar}$  9.2 Hz,  $J_{H5Ar-H3Ar}$  2.5 Hz,  $H5_{Ar}$ ), 7.64 (1 H, d,  $J_{H6Ar-H5Ar}$  9.2 Hz,  $H6_{Ar}$ ) 5.57 (1 H, dd,  $J_{H1-H2}$  7.6 Hz,  $J_{H1-F2}$  3.5 Hz,  $H1$ ), 4.31 (1 H, ddd,  $J_{H2-F2}$  51.5 Hz,  $J_{H2-H3}$  8.7 Hz,  $J_{H2-H1}$  7.6 Hz,  $H2$ ), 3.91 (1 H, dd,  $J_{H6-H6'}$  12.4 Hz,  $J_{H6-H5}$  1.8 Hz,  $H6$ ) 3.78-3.42 (4 H, m,  $H3$ ,  $H4$ ,  $H5$ ,  $H6'$ );  **$^{19}F$  NMR:** (282 MHz,  $CDCl_3$ ):  $\delta$  -203.35 (1 F, ddd,  $J_{F2-H2}$  51.5 Hz,  $J_{F2-H3}$  14.1 Hz,  $J_{F2-H1}$  3.5 Hz,  $F2$ ); **Anal. calc. for**  $C_{12}H_{13}FN_2O_9 \cdot H_2O$  : C, 39.35, H, 4.13, N, 7.65; **Found:** C, 39.21, H, 4.32, N, 7.59.

N-Octanoyl 5-fluoro-2,4-dinitroaniline (**3.11**)



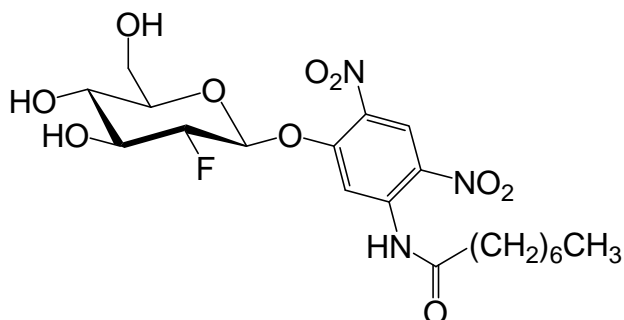
5-Fluoro-2,4-dinitroaniline (0.257 g, 1.28 mmol) was stirred in 5 mL dry toluene under  $N_{2(g)}$ . Octanoyl chloride (0.22 mL, 1.29 mmol, 1.01 eq) and dry pyridine (0.1 mL, 1.24 mmol, 0.97 eq) were added, and the solution refluxed for 6 days. The solution was allowed to cool, diluted with ethyl acetate and washed with 2 x  $H_2O$ , 1 x 1M HCl, 1 x saturated  $NaHCO_3$  and 1 x brine. The organic layer was then dried over  $MgSO_4$  for 10 minutes, filtered, and evaporated under reduced pressure. The product was purified by flash chromatography (40:1 toluene : ethyl acetate) to yield **3.11** as a yellow oil (0.381 g, 1.16 mmol, 91%).  **$^1H$  NMR:** (300 MHz,  $CDCl_3$ )  $\delta$  10.72 (1 H, br s, N-H) 9.08 (1 H, d,  $J_{H3-F}$  7.6 Hz, H3) 8.97 (1 H, d,  $J_{H6-F}$  13.7 Hz, H5) 2.53 (2 H, t,  $J$  = 7.5 Hz,  $COCH_2CH_2$ ), 1.74 (2 H, p,  $J$  = 7.5 Hz,  $COCH_2CH_2$ ), 1.41-1.26 (8 H, m,  $(CH_2)_n$ ), 0.876-0.842 (3 H, m,  $CH_3$ );  **$^{13}C$  NMR:** (100 MHz,  $CDCl_3$ )  $\delta$  173.59 (C=O), 160.32 (d,  $J_{C5-F}$  273 Hz, C5), 141.97 (d,  $J_{C4-F}$  14 Hz, C4), 138.94 (C2), 131.73 (C1), 126.53 (C3), 111.49 (C6), 39.75, 32.56, 29.95, 29.87, 25.93, 23.54, (6 x  $(CH_2)_n$ ), 15.00 ( $CH_3$ ).

5-Octanamido-2,4-dinitrophenyl 3,4,6-tri-O-acetyl-2-deoxy-2-fluoro- $\beta$ -D-glucopyranoside  
(**3.12**)



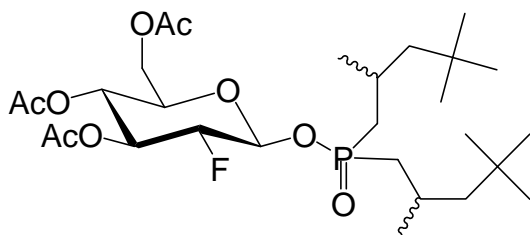
**2.41** (49.5 mg, 0.161 mmol) was dissolved in 0.5 mL dry *N-N'*-dimethylformamide. **3.11** (76.2 mg, 0.233 mmol, 1.45 eq) was dissolved in 1 mL dry dichloromethane and added along with 1,4-diazabicyclo[2.2.2]octane (39 mg, 0.348 mmol, 2.2 eq), and the resulting solution was stirred for 2 hours under  $N_{2(g)}$ . The solvent was then evaporated under reduced pressure, and the resulting syrup purified by flash chromatography (7:1  $\rightarrow$  5:1 toluene : ethyl acetate) to yield **3.12** as a yellow oil (42.3 mg, 0.0687 mmol, 43%) along with the corresponding  $\alpha$ -anomer (14.5 mg, 0.0236 mmol, 15%).  **$^1H$  NMR:** (300 MHz,  $CDCl_3$ )  $\delta$  10.79 (1 H, s, N-H), 9.08 (1 H, s, H3<sub>Ar</sub>), 8.97 (1 H, s, H5<sub>Ar</sub>), 5.49-5.40 (2 H, m, H1, H3), 5.17 (1 H, dd,  $J_{H4-H5}$  9.9 Hz,  $J_{H4-H3}$  9.5 Hz, H4), 4.73 (1 H, ddd,  $J_{H2-F2}$  50.4 Hz,  $J_{H2-H3}$  8.8 Hz,  $J_{H2-H1}$  7.5 Hz, H2) 4.35 (1 H, dd,  $J_{H6-H6'}$  12.7 Hz,  $J_{H6-H5}$  4.1 Hz, H6), 4.25 (1 H, dd,  $J_{H6'-H6}$  12.7 Hz,  $J_{H6'-H5}$  2.2 Hz, H6'), 4.06 (1 H, ddd,  $J_{H5-H4}$  9.9 Hz,  $J_{H5-H6}$  4.1 Hz,  $J_{H5-H6'}$  2.2 Hz, H5), 2.51 (2 H, t,  $J$  = 7.6 Hz,  $COCH_2CH_2$ ), 2.10 (3 H, s, Ac), 2.04 (3 H, s, Ac), 2.03 (3 H, s, Ac), 1.72 (2 H, p,  $J$  = 7.6 Hz,  $COCH_2CH_2$ ), 1.34-1.23 (8 H, m,  $(CH_2)_n$ ), 0.89-0.80 (3 H, m,  $CH_3$ );  **$^{13}C$  NMR:** (75 MHz,  $CDCl_3$ )  $\delta$  173.09, 170.62, 169.98, 169.52 (4 x C=O), 155.07 (C1<sub>Ar</sub>), 140.42 (C4<sub>Ar</sub>), 133.17 (C2<sub>Ar</sub>), 128.17 (C5<sub>Ar</sub>), 125.40 (C3<sub>Ar</sub>), 107.41 (C6<sub>Ar</sub>), 98.26 (d,  $J_{C1-F2}$  25 Hz, C1), 88.43 (d,  $J_{C2-F2}$  194 Hz, C2), 73.08 (C5), 72.39 (d,  $J_{C3-F2}$  20 Hz, C3), 67.25 (C4), 61.06 (C6), 39.14, 31.71, 29.02, 25.20, 22.70, 20.74, (6 x  $(CH_2)_n$ ), 14.17 ( $CH_3$ ); **ESI-MS (high res):**  $m/z$  calc.: 638.1968; **Found:** 638.1962  $[M + Na]^+$ .

5-Octanamido-2,4-dinitrophenyl 2-deoxy-2-fluoro- $\beta$ -D-glucopyranoside (**3.4**)



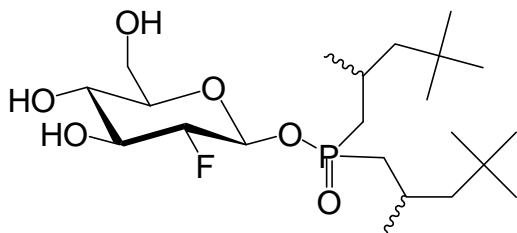
**3.12** (10.7 mg, 0.0174 mmol) was dissolved in 5 mL of dry methanol and stirred at 0 °C under N<sub>2(g)</sub>. Acetyl chloride (0.3 mL) was then added, and the reaction mixture allowed to stir overnight. The solvent was evaporated under reduced pressure, and the crude oil purified by flash chromatography (19:1 ethyl acetate : methanol) to yield **3.4** as a colourless oil (0.92 mg, 0.00188 mmol, 11%). **<sup>1</sup>H NMR:** (300 MHz, CD<sub>3</sub>OD)  $\delta$  8.84 (1 H, s, H3<sub>Ar</sub>), 8.75 (1 H, s, H5<sub>Ar</sub>), 5.49 (1 H, dd, J<sub>H1-H2</sub> 7.6 Hz, J<sub>H1-F2</sub> 3.5 Hz, H1), 4.34 (1 H, ddd, J<sub>H2-F2</sub> 51.5 Hz, J<sub>H2-H3</sub> 8.7 Hz, J<sub>H2-H1</sub> 7.6 Hz, H2), 3.96 (1 H, dd, J<sub>H6-H6'</sub> 12.4 Hz, J<sub>H6-H5</sub> 1.8 Hz, H6) 3.83-3.72 (2 H, m, H6', H3), 3.64-3.52 (2 H, m, H4, H5), 2.55 (2 H, t, J = 7.6 Hz, COCH<sub>2</sub>CH<sub>2</sub>), 1.73 (2 H, m, COCH<sub>2</sub>CH<sub>2</sub>), 1.39-1.28 (8 H, m, (CH<sub>2</sub>)<sub>n</sub>), 0.93-0.88 (3 H, m, CH<sub>3</sub>); **<sup>19</sup>F NMR:** (282 MHz, CD<sub>3</sub>OD):  $\delta$  -201.74 (1 F, ddd, J<sub>F2-H2</sub> 51.5 Hz, J<sub>F2-H3</sub> 14.1 Hz, J<sub>F2-H1</sub> 3.5 Hz, F2); **<sup>13</sup>C NMR:** (151 MHz, CD<sub>3</sub>OD)  $\delta$  174.93, (C=O), 155.90 (C1<sub>Ar</sub>), 140.4 (C4<sub>Ar</sub>), 133.24 (C2<sub>Ar</sub>), 125.58 (C5<sub>Ar</sub>), 125.40 (C3<sub>Ar</sub>), 110.61 (C6<sub>Ar</sub>), 100.03 (d, J<sub>C1-F2</sub> 24 Hz, C1), 92.90 (d, J<sub>C2-F2</sub> 187 Hz, C2), 78.98 (C5), 76.25 (d, J<sub>C3-F2</sub> 18 Hz, C3), 70.36 (C4), 61.79 (C6), 39.04, 33.01, 30.29 (2 C), 26.35, 23.83, (6 x (CH<sub>2</sub>)<sub>n</sub>), 14.57 (CH<sub>3</sub>); **ESI-MS (high res):** m/z calc.: 512.1651; **Found:** 512.1644 [M + Na]<sup>+</sup>.

Di-*iso*-octyl (3,4,6-tri-O-acetyl-2-deoxy-2-fluoro- $\beta$ -D-glucopyranosyl) phosphinate (**3.15**)



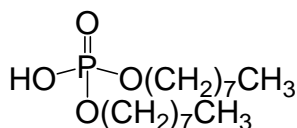
**2.12** (0.245 g, 0.657 mmol) was dissolved in 20 mL dry acetonitrile. A diastereomeric mixture of diisooctyl phosphinic acid (0.45 mL, 1.42 mmol, 2.2 eq, obtained from the Sigma-Aldrich Chemical Company) was added, along with silver carbonate (0.525 g, 1.90 mmol, 2.9 eq), to the acetonitrile solution. The resulting slurry was stirred overnight under  $N_{2(g)}$ , in the dark. The solution was filtered through a short plug of silica using 9:1 ethyl acetate : methanol as the eluent to remove the silver salts. The filtrate was collected and washed with 1 x saturated  $NaHCO_3$ , 1 x brine and dried over  $MgSO_4$ . After 10 minutes, the  $MgSO_4$  was filtered off, and the solvent evaporated under reduced pressure. The product was purified by flash chromatography (3:1  $\rightarrow$  2:1 petroleum ether : ethyl acetate) to yield **3.15**, as a mixture of four diastereomers, as a colourless oil (0.256 g, 0.441 mmol, 67%).  **$^1H$  NMR:** (300 MHz,  $CDCl_3$ )  $\delta$  5.42-5.34 (4 H, m,  $H1_a, H1_b, H1_c, H1_d$ ), 5.31-5.21 (4 H, m,  $H3_a, H3_b, H3_c, H3_d$ ), 5.03-4.95 (4 H, m,  $H4_a, H4_b, H4_c, H4_d$ ), 4.42-4.16 (8 H, m,  $H2_a, H2_b, H2_c, H2_d, H6_a, H6_b, H6_c, H6_d$ ), 4.08-4.04 (4 H, m,  $H6'_a, H6'_b, H6'_c, H6'_d$ ), 3.80-3.77 (4 H,  $H5_a, H5_b, H5_c, H5_d$ ), 2.03 (6 H, s, 2 x Ac), 2.02 (6 H, s, 2 x Ac), 2.01 (6 H, s, 2 x Ac), 1.98 (12 H, s, 6 x Ac), 1.07-1.02 (40 H, m,  $CH$ ), 0.86-0.84 (96 H, m,  $CH_3$ );  **$^{19}F$  NMR:** (282 MHz,  $CDCl_3$ ):  $\delta$  -199.50-199.84 (4 F, m,  $F2_a, F2_b, F2_c, F2_d$ );  **$^{31}P$  ( $^1H$  decoupled) NMR:** (121 MHz,  $CDCl_3$ ):  $\delta$  62.40, 62.19, 61.86, 61.79; **ESI-MS (high res):** m/z calc.: 603.3074; **Found:** 603.3064  $[M + Na]^+$ .

Di-*iso*-octyl (2-deoxy-2-fluoro- $\beta$ -D-glucopyranosyl) phosphinate (**3.5**)



**3.15** (0.164 g, 0.282 mmol) was dissolved in 10 mL dry methanol, and deacetylated according to General Procedure B. The crude product was purified by flash chromatography (50:1  $\rightarrow$  19:1 ethyl acetate : methanol) to yield **3.5**, as a mixture of four diastereomers, as a colourless gum (0.0997 g, 0.219 mmol, 78%).  **$^1\text{H}$  NMR:** (300 MHz,  $\text{CD}_3\text{OD}$ )  $\delta$  5.28-5.21 (4 H, m, H1<sub>a</sub>, H1<sub>b</sub>, H1<sub>c</sub>, H1<sub>d</sub>), 4.19-3.95 (4 H, m, H2<sub>a</sub>, H2<sub>b</sub>, H2<sub>c</sub>, H2<sub>d</sub>), 3.87-3.83 (4 H, m, H3<sub>a</sub>, H3<sub>b</sub>, H3<sub>c</sub>, H3<sub>d</sub>), 3.71-3.59 (8 H, m, H4<sub>a</sub>, H4<sub>b</sub>, H4<sub>c</sub>, H4<sub>d</sub>, H5<sub>a</sub>, H5<sub>b</sub>, H5<sub>c</sub>, H5<sub>d</sub>), 3.44-3.34 (8 H, m, H6<sub>a</sub>, H6<sub>b</sub>, H6<sub>c</sub>, H6<sub>d</sub>, H6'<sub>a</sub>, H6'<sub>b</sub>, H6'<sub>c</sub>, H6'<sub>d</sub>) 2.07-1.70 (24 H, m, 8 x  $\text{PCH}_2$ ), 1.48-0.93 (120 H, m,  $-\text{CH}_2$ ,  $\text{CH}_3$ );  **$^{19}\text{F}$  NMR:** (282 MHz,  $\text{CD}_3\text{OD}$ ):  $\delta$  -200.33-200.76 (4 F, m, F2<sub>a</sub>, F2<sub>b</sub>, F2<sub>c</sub>, F2<sub>d</sub>);  **$^{31}\text{P}$  ( $^1\text{H}$  decoupled) NMR:** (121 MHz,  $\text{CD}_3\text{OD}$ ):  $\delta$  63.48, 63.30, 63.05 (2 P); **ESI-MS (high res):**  $m/z$  calc.: 477.2757; **Found:** 477.2741  $[\text{M} + \text{Na}]^+$ ; **Anal. calc. for**  $\text{C}_{22}\text{H}_{44}\text{FO}_6\text{P}$ : C, 58.13, H, 9.76; **Found:** C, 58.03, H, 9.86.

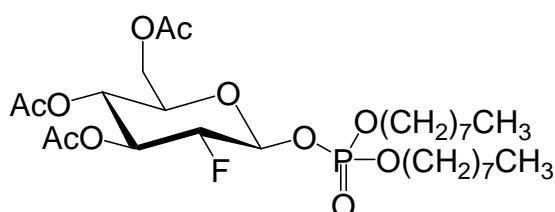
Phosphoric acid dioctyl ester (**3.13**)<sup>246</sup>



Phosphorus oxychloride (1.0 mL, 11 mmol, 1.0 eq) was dissolved in 15 mL dichloromethane and cooled to 0 °C under  $\text{N}_{2(\text{g})}$  with stirring. Octanol (3.5 mL, 22 mmol, 2 eq) and water (0.2 mL, 11 mmol, 1 eq) were both added slowly, and the reaction mixture allowed to warm to RT over 1 hour. The crude reaction mix was diluted with 35 mL dichloromethane and poured into a separatory funnel. The resulting two layers were washed with saturated sodium bicarbonate, and the top layer collected. The top layer was dissolved in 50 mL diethyl ether and washed with 1 x 1M HCl and saturated sodium chloride. The organic layer was then

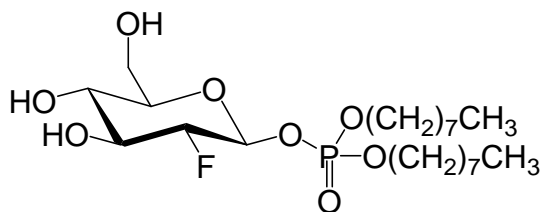
dried over  $\text{MgSO}_4$  for 10 minutes, filtered, and concentrated under reduced pressure to yield **3.13** as a crude oil that was used without further purification or characterization.

Dioctyl (3,4,6-tri-O-acetyl-2-deoxy-2-fluoro- $\beta$ -D-glucopyranosyl) phosphate (**3.14**)



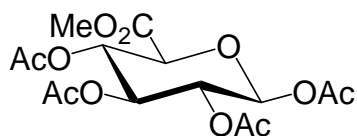
**2.12** (88.1 mg, 0.237 mmol) was dissolved in 5 mL dry acetonitrile. The crude **3.13** was dissolved in 4 mL dry dichloromethane and added, along with silver carbonate (0.456 g, 1.65 mmol, 7.0 eq), to the acetonitrile solution. The resulting slurry was stirred overnight under  $\text{N}_{2(g)}$ , in the dark. The solution was filtered through a short plug of silica using ethyl acetate as the eluent to remove the silver salts. The filtrate was collected and the solvent evaporated under reduced pressure. The product was purified by flash chromatography (3:1  $\rightarrow$  2:1  $\rightarrow$  3:2 petroleum ether : ethyl acetate) to yield **3.14** as a colourless oil (22.1 mg, 0.0361 mmol, 15% from **2.12**).  **$^1\text{H}$  NMR:** (300 MHz,  $\text{CDCl}_3$ )  $\delta$  5.36-5.26 (2 H, m, H1, H3), 5.03 (1 H, t,  $J_{\text{H4-H3}} = J_{\text{H4-H5}}$  9.8 Hz, H4), 4.37 (1 H, ddd,  $J_{\text{H2-F2}}$  50.5 Hz,  $J_{\text{H2-H3}}$  9.0 Hz,  $J_{\text{H2-H1}}$  7.9 Hz, H2), 4.25 (1 H, dd,  $J_{\text{H6-H6'}}$  12.5 Hz,  $J_{\text{H6-H5}}$  4.8 Hz, H6), 4.11 (1 H, dd,  $J_{\text{H6'-H6}}$  12.5 Hz,  $J_{\text{H6'-H5}}$  2.3 Hz, H6'), 4.08-3.99 (4 H, m, 2 x  $\text{OCH}_2\text{R}$ ) 3.81 (1 H, ddd,  $J_{\text{H5-H4}}$  9.8 Hz,  $J_{\text{H5-H6}}$  4.8 Hz,  $J_{\text{H5-H6'}}$  2.3 Hz, H5), 2.06 (3 H, s, Ac), 2.04 (3 H, s, Ac), 2.01 (3 H, s, Ac), 1.67-1.62 (4 H, m, 2 x  $\text{OCH}_2\text{CH}_2\text{R}$ ), 1.35-1.24 (20H, m, 10 x  $(\text{CH}_2)_n$ ), 0.873-0.829 (6H, m, 2 x  $\text{CH}_3$ );  **$^{19}\text{F}$  NMR:** (282 MHz,  $\text{CDCl}_3$ ):  $\delta$  -200.44 (1 F, ddd,  $J_{\text{F2-H2}}$  50.5 Hz,  $J_{\text{F2-H3}}$  13.4 Hz,  $J_{\text{F2-H1}}$  3.0 Hz, F2);  **$^{31}\text{P}$  ( $^1\text{H}$  decoupled) NMR:** (121 MHz,  $\text{CDCl}_3$ ):  $\delta$  -2.07;  **$^{13}\text{C}$  NMR:** (100 MHz,  $\text{CDCl}_3$ )  $\delta$  170.54, 169.94, 169.65 (3 x C=O), 96.12 (dd,  $J_{\text{C1-F2}}$  25 Hz,  $J_{\text{C1-P}}$  7 Hz, C1), 89.42 (dd,  $J_{\text{C2-F2}}$  193 Hz,  $J_{\text{C2-P}}$  6 Hz, C2), 72.73 (d,  $J_{\text{C3-F2}}$  20 Hz, C3), 72.71 (C5), 68.67-68.52 (3 C, m, C4, 2 x  $\text{OCH}_2$ ), 61.56 (C6), 31.88, 29.26, 29.21, 29.16, 25.45, 22.75 (6 x  $(\text{CH}_2)_n$ ), 20.86 (2 C), 20.48, 14.20 (4 x Me); **ESI-MS (high res):**  $m/z$  calc.: 635.2967; **Found:** 635.3005  $[\text{M} + \text{Na}]^+$ .

Dioctyl (2-deoxy-2-fluoro-β-D-glucopyranosyl) phosphate (**3.6**)



**3.14** (12.0 mg, 0.0197 mmol) was dissolved in 2 mL dry methanol, and deacetylated according to General Procedure B. The crude product was purified by flash chromatography (9:1 ethyl acetate : petroleum ether → 9:1 ethyl acetate : methanol) to yield pure **3.6** as a colourless gum (8.2 mg, 0.0169 mmol, 86%). **<sup>1</sup>H NMR:** (300 MHz, CD<sub>3</sub>OD) δ 5.22 (1 H, td,  $J_{H1-H2} = J_{H1-P}$  7.5 Hz,  $J_{H1-F2}$  3.8 Hz, H1), 4.13 (2 H, dd,  $J_{H-H'}$  6.4 Hz,  $J_{H-P}$  2.4 Hz, 2 x OCH<sub>2</sub>R), 4.09 (2 H, dd,  $J_{H'-H}$  6.4 Hz,  $J_{H'-P}$  2.4 Hz, 2 x OCH<sub>2</sub>), 4.09 (1 H, ddd,  $J_{H2-F2}$  51.6 Hz,  $J_{H2-H3}$  8.5 Hz,  $J_{H2-H1}$  7.5 Hz, H2), 3.85 (1 H, ddd,  $J_{H3-F2}$  14.3 Hz,  $J_{H3-H4}$  9.5 Hz,  $J_{H3-H2}$  8.5 Hz, H3) 3.73-3.60 (2H, m, H4, H5), 3.45-3.37 (2H, m, H6, H6') 1.71-1.67 (4 H, m, 2 x OCH<sub>2</sub>CH<sub>2</sub>R), 1.39-1.31 (20H, m, 10 x (CH<sub>2</sub>)<sub>n</sub>), 0.92-0.88 (6H, m, 2 x CH<sub>3</sub>); **<sup>19</sup>F NMR:** (282 MHz, CD<sub>3</sub>OD): δ -201.68 (1 F, ddd,  $J_{F2-H2}$  51.6 Hz,  $J_{F2-H3}$  14.3 Hz,  $J_{F2-H1}$  3.8 Hz, F2); **<sup>31</sup>P (<sup>1</sup>H decoupled) NMR:** (121 MHz, CD<sub>3</sub>OD): δ -2.37; **<sup>13</sup>C NMR:** (100 MHz, CD<sub>3</sub>OD) δ 96.02 (dd,  $J_{C1-F2}$  24 Hz,  $J_{C1-P}$  6 Hz, C1), 89.55 (dd,  $J_{C2-F2}$  195 Hz,  $J_{C2-P}$  4 Hz, C2), 77.16 (d,  $J_{C3-F2}$  19 Hz, C3), 74.35 (d,  $J_{C4-F2}$  7 Hz, C4), 72.68 (C5), 68.14, 67.75 (2 x OCH<sub>2</sub>), 61.56 (C6), 31.82, 29.22, 29.01, 28.44, 24.88, 23.64 (6 x (CH<sub>2</sub>)<sub>n</sub>), 14.14 (Me); **ESI-MS (high res):** m/z calc.: 509.2650; **Found:** 509.2612 [M + Na]<sup>+</sup>; **Anal. calc. for C<sub>22</sub>H<sub>44</sub>FO<sub>8</sub>P:** C, 54.31, H, 9.12; **Found:** C, 54.07, H, 9.55.

Methyl (1,2,3,4-tetra-O-acetyl-β-D-glucopyranosyl) uronate (**3.20**)<sup>260</sup>

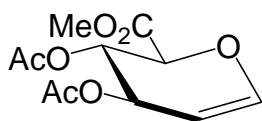


3,6-Glucuronolactone (49.1 g, 279 mmol) was dissolved in 350 mL dry methanol. Sodium hydroxide (0.125 g, 3.13 mmol, 0.01 eq) was added, and the resulting yellow solution stirred



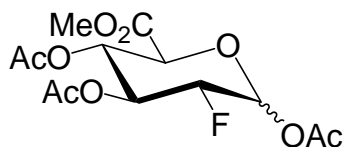
for one hour. Acetic acid (3 mL) was added to neutralize the solution, and the solvent carefully evaporated under reduced pressure. The resulting gum was dissolved in 115 mL pyridine, and 170 mL acetic anhydride added dropwise at 0 °C and allowed to stand in the refrigerator overnight. The resulting brown solution was filtered, and the solid washed with a small volume of methanol to remove residual colour. **3.20** was isolated as a white solid (40.4 g, 107 mmol, 39%). **<sup>1</sup>H NMR:** (300 MHz, CDCl<sub>3</sub>) δ 5.75 (1 H, d,  $J_{H1-H2}$  7.8 Hz, H1), 5.29 (1 H, dd,  $J_{H3-H4}$  9.3 Hz,  $H_{3-H2}$  7.8 Hz, H3), 5.22 (1 H, t,  $J_{H4-H3} = J_{H4-H5}$  9.3 Hz, H4) 5.13 (1 H, t,  $J_{H2-H1} = J_{H2-H3}$  7.8 Hz, H2), 4.16 (1 H, d,  $J_{H5-H4}$  9.3 Hz), 3.73 (3 H, s, CO<sub>2</sub>CH<sub>3</sub>), 2.10 (3 H, s, Ac), 2.02 (6 H, s, 2 x Ac), 2.01 (3 H, s, Ac); **ESI-MS (low res):** m/z calc.: 399.1; **Found:** 399.0 [M + Na]<sup>+</sup>.

Methyl (3,4-di-O-acetyl-D-glucal) uronate (**3.21**)



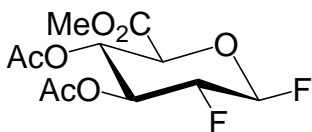
**3.20** (18.7 g, 49.7 mmol) was brominated according to General Procedure A for two hours. The crude product was used without further purification or characterization. The crude bromide was dissolved in 400 mL of 1:1 acetic acid : water. Zinc (80.3 g, 1.23 mol) was added, and the resulting slurry mechanically stirred at 0 °C overnight. The solution was filtered through Celite to remove the solid zinc and its salts, and the solvent evaporated under reduced pressure. The crude product was dissolved in ethyl acetate, and washed with 3 x saturated NaHCO<sub>3</sub>, 1 x brine and dried over MgSO<sub>4</sub>. After 10 minutes, the MgSO<sub>4</sub> was filtered off, and the solvent evaporated under reduced pressure. The crude solid was then recrystallized in isopropyl alcohol to yield **3.21** as a white solid (9.54 g, 36.9 mmol, 74% from **3.20**). **<sup>1</sup>H NMR:** (300 MHz, CDCl<sub>3</sub>) δ 6.67 (1 H, d,  $J_{H1-H2}$  5.7 Hz, H1), 5.41 (1 H,  $J_{H4-H3}$  4.3 Hz,  $J_{H4-H5}$  2.6 Hz, H4), 5.03-4.97 (2 H, m, H2, H3), 4.82 (1 H, dd,  $J_{H5-H4}$  2.6 Hz,  $J_{H5-H4}$  1.2 Hz, H5), 3.78 (3 H, s, CO<sub>2</sub>CH<sub>3</sub>), 2.11 (3 H, s, Ac), 1.98 (3 H, s, Ac); **ESI-MS (low res):** m/z calc.: 281.1; **Found:** 281.1 [M + Na]<sup>+</sup>.

Methyl (1,3,4-tri-O-acetyl-2-deoxy-2-fluoro-D-glucopyranosyl) uronate (**3.22**)



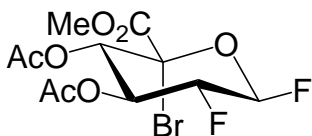
**3.21** (4.22 g, 16.3 mmol) was dissolved in 100 mL of acetonitrile and 50 mL water. The reaction mixture was heated to 70 °C under N<sub>2(g)</sub>. To this solution was added Selectfluor (8.77 g, 24.8 mmol, 1.5 eq) and the mixture allowed to stir overnight before being cooled to room temperature. Following solvent removal under reduced pressure, the residue was dissolved in ethyl acetate and washed with 2 x H<sub>2</sub>O, 1 x brine and dried over MgSO<sub>4</sub>. After 10 minutes, the MgSO<sub>4</sub> was filtered off, and the solvent removed under reduced pressure. The products were purified by flash chromatography (2:1 petroleum ether : ethyl acetate) to give the partially pure mixture of hemi-acetals. This mixture was dissolved in 25 mL acetic anhydride, iodine (0.416 g, 1.64 mmol) was added, and then stirred under N<sub>2(g)</sub> overnight. The brown solution was cooled to 0 °C, and the acetic anhydride quenched by the dropwise addition of methanol. The solvents were evaporated under reduced pressure, and the brown residue dissolved in ethyl acetate. The organic layer was washed with 1 x 1 M Na<sub>2</sub>SO<sub>4</sub>, 1 x saturated NaHCO<sub>3</sub>, 1 x brine and dried over MgSO<sub>4</sub>. After 10 minutes, the MgSO<sub>4</sub> was filtered off, and the solvent evaporated under reduced pressure. The colourless gum was then purified by flash chromatography (3:1 petroleum ether : ethyl acetate) to yield **3.22** (4:1 β:α) as a colourless gum (0.474 g, 1.41 mmol, 9%). **<sup>1</sup>H NMR:** (300 MHz, CDCl<sub>3</sub>) δ 6.45 (1 H, d, J<sub>H1α-H2α</sub> 3.9 Hz, H1α), 5.80 (1 H, dd, J<sub>H1β-H2β</sub> 7.9 Hz, H<sub>1β-F2</sub> 3.5 Hz, H1β), 5.57 (1 H, dt, J<sub>H3α-F2</sub> 12.0 Hz, J<sub>H3α-H2α</sub> = J<sub>H3α-H4α</sub> 9.8 Hz, H3α), 5.39 (1 H, dt, J<sub>H3β-F2</sub> 14.4 Hz, J<sub>H3β-H2β</sub> = J<sub>H3β-H4β</sub> 9.0 Hz, H3β), 5.18 – 5.11 (2 H, m, H4α, H4β), 4.65 (1 H, ddd, J<sub>H2α-F2</sub> 48.4 Hz, J<sub>H2α-H3α</sub> 9.8 Hz, J<sub>H2α-H1α</sub> 3.9 Hz, H2α), 4.45 (1 H, ddd, J<sub>H2β-F2</sub> 51.6 Hz, J<sub>H2β-H3β</sub> 8.9 Hz, J<sub>H2β-H1β</sub> 7.9 Hz, H2β), 4.34 (1 H, d, J<sub>H5α-H4α</sub> 10.2 Hz, H5α), 4.16 (1 H, d, J<sub>H5β-H4β</sub> 9.8 Hz, H5), 3.71 (6 H, br s, 2 x CO<sub>2</sub>CH<sub>3</sub>), 2.18 (3 H, s, Ac), 2.07 (6 H, s, 2 x Ac), 2.02 (3 H, s, Ac); **<sup>19</sup>F NMR:** (282 MHz, CDCl<sub>3</sub>): δ -201.05 (1 F, ddd, J<sub>F2-H2β</sub> 51.6 Hz, J<sub>F2-H3β</sub> 14.4 Hz, J<sub>F2-H1β</sub> 3.5 Hz, F2β), -202.98 (1 F, dd, J<sub>F2-H1α</sub> 48.4 Hz, J<sub>F2-H3α</sub> 12.0 Hz, F2α); **ESI-MS (low res):** m/z calc.: 359.1; **Found:** 359.1 [M + Na]<sup>+</sup>.

Methyl (3,4-di-O-acetyl-2-deoxy-2-fluoro- $\beta$ -D-glucopyranosyl fluoride) uronate (**3.23**)



**3.22** (0.488 g, 1.45 mmol) was brominated according to General Procedure A overnight. The crude product was used without further purification or characterization. The crude bromide was dissolved in 20 mL dry acetonitrile. Silver fluoride (0.232 g, 1.83 mmol) was added, and the resulting slurry stirred overnight under  $N_{2(g)}$ , in the dark. The solution was filtered through a short plug of silica using ethyl acetate as the eluent to remove the silver salts. The filtrate was collected and the solvent evaporated under reduced pressure to yield the crude solid. The product was purified by flash chromatography (4:1 petroleum ether : ethyl acetate) to yield **3.23** as a white solid (0.324 g, 1.09 mmol, 75%).  **$^1H$  NMR:** (300 MHz,  $CDCl_3$ )  $\delta$  5.50 (1 H, dt,  $J_{H1-F1}$  51.2 Hz,  $J_{H1-H2} = J_{H1-F2}$  5.2 Hz, H1), 5.37-5.28 (2 H, m, H3, H4), 4.53 (1 H, dddd,  $J_{H2-F2}$  49.1 Hz,  $J_{H2-F1}$  11.2 Hz,  $J_{H2-H3}$  10.4 Hz,  $J_{H2-H1}$  5.2 Hz, H2), 4.25 (1 H, d,  $J_{H5-H4}$  8.4 Hz, H5), 3.76 (3 H, s,  $CO_2CH_3$ ), 2.08 (3 H, s, Ac), 2.03 (3 H, s, Ac);  **$^{19}F$  NMR:** (282 MHz,  $CDCl_3$ ):  $\delta$  -138.45 (1 F, ddd,  $J_{F1-H1}$  51.2 Hz,  $J_{F1-F2}$  15.4 Hz,  $J_{F1-H2}$  11.2 Hz, F1), -199.83-200.13 (1 F, m, F2); **ESI-MS (high res):**  $m/z$  calc.: 319.0060; **Found:** 319.0054  $[M + Na]^+$ .

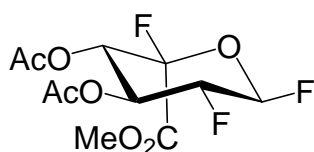
Methyl (3,4-di-O-acetyl-5-bromo-2-deoxy-2-fluoro- $\beta$ -D-glucopyranosyl fluoride) uronate (**3.24**)



**3.23** (0.190 g, 0.641 mmol) was dissolved in 15 mL dry carbon tetrachloride, and reacted with *N*-bromosuccinimide (2.08 g, 11.7 mmol, 2.1 eq) for 1 hour according to General Procedure C. The crude product was partially purified by flash chromatography (4:1

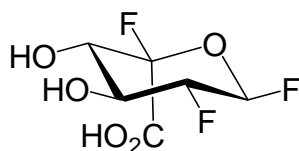
petroleum ether : ethyl acetate) to yield impure **3.24** as a yellowish oil which was used without further purification. **<sup>1</sup>H NMR:** (300 MHz, CDCl<sub>3</sub>) δ 5.78 (1 H, ddd, J<sub>H1-F1</sub> 51.4 Hz, J<sub>H1-H2</sub> 7.2 Hz, J<sub>H1-F2</sub> 4.6 Hz, H1), 5.61 (1 H, dt, J<sub>H3-F2</sub> 13.3 Hz, J<sub>H3-H2</sub> = J<sub>H3-H4</sub> 9.4 Hz, H3), 5.30 (1 H, d, J<sub>H4-H3</sub> 9.4 Hz, H4), 4.57 (1 H, dddd, J<sub>H2-F2</sub> 50.6 Hz, J<sub>H2-F1</sub> 13.7 Hz, J<sub>H2-H3</sub> 9.4 Hz, J<sub>H2-H1</sub> 7.2 Hz, H2), 3.78 (3 H, s, CO<sub>2</sub>CH<sub>3</sub>), 2.09 (6 H, s, 2 x Ac); **<sup>19</sup>F NMR:** (282 MHz, CDCl<sub>3</sub>): δ -151.45 (1 F, dt, J<sub>F1-H1</sub> 51.4 Hz, J<sub>F1-F2</sub> = J<sub>F1-H2</sub> 13.7 Hz, F1), -202.27 (1 F, ddd, J<sub>F2-H2</sub> 50.6 Hz, J<sub>F2-F1</sub> 13.7 Hz, J<sub>F2-H3</sub> 13.3 Hz, J<sub>F2-F1</sub> 4.6 Hz, F2).

Methyl (3,4-di-O-acetyl -2-deoxy-2,5-difluoro-α-L-idopyranosyl fluoride) uronate (**3.25**)



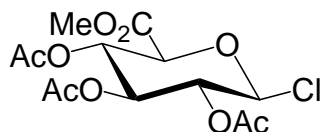
Crude **3.24** was dissolved in 15 mL dry acetonitrile. Silver fluoride (0.131 g, 1.03 mmol) was added, and the resulting slurry stirred overnight under N<sub>2(g)</sub>, in the dark. The solution was filtered through a short plug of silica using ethyl acetate as the eluent to remove the silver salts. The filtrate was collected and the solvent evaporated under reduced pressure to yield the crude solid. The product was purified by flash chromatography (9:1 toluene : ethyl acetate) to yield impure **3.25** as a colourless oil (18.6 mg). **<sup>1</sup>H NMR:** (300 MHz, CDCl<sub>3</sub>) δ 5.88 (1 H, ddd, J<sub>H1-F1</sub> 50.1 Hz, J<sub>H1-F2</sub> 10.8 Hz, J<sub>H1-H2</sub> 1.9 Hz, H1), 5.51 (1 H, ddd, J<sub>H4-F5</sub> 9.5 Hz, J<sub>H4-H3</sub> 7.0 Hz, J<sub>H4-H2</sub> 1.2 Hz, H4), 5.42 (1 H, ddd, J<sub>H3-F2</sub> 11.4 Hz, J<sub>H3-H4</sub> 7.0 Hz, J<sub>H3-H2</sub> 5.4 Hz, H3), 4.83 (1 H, ddddd, J<sub>H2-F2</sub> 48.2 Hz, J<sub>H2-F1</sub> 8.0 Hz, J<sub>H2-H3</sub> 5.4 Hz, J<sub>H2-H1</sub> 1.9 Hz, J<sub>H2-H4</sub> 1.2 Hz, H2), 3.87 (3 H, s, CO<sub>2</sub>CH<sub>3</sub>), 2.11 (3 H, s, Ac), 2.05 (3 H, s, Ac); **<sup>19</sup>F NMR:** (282 MHz, CDCl<sub>3</sub>): δ -107.47 (1 F, dd, J<sub>F5-F1</sub> 11.3 Hz, J<sub>F5-H4</sub> 9.5 Hz, F5), -127.81 (1 F, dddd, J<sub>F1-H1</sub> 50.1 Hz, J<sub>F1-F2</sub> 19.8 Hz, J<sub>F1-F5</sub> 11.3 Hz, J<sub>F1-H2</sub> 8.0 Hz, F1), -194.23 (1 F, dddd, J<sub>F2-H2</sub> 48.2 Hz, J<sub>F2-F1</sub> 19.8 Hz, J<sub>F2-H3</sub> 11.4 Hz, J<sub>F2-H1</sub> 10.8 Hz, F2).

2-Deoxy-2,5-difluoro- $\alpha$ -L-idopyranosyl uronic acid fluoride (**3.18**)



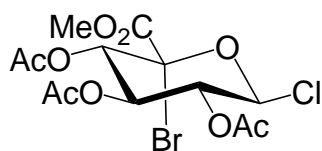
The impure **3.25** (18.6 mg) was dissolved in 5 mL of dry methanol and deacetylated according to General Procedure B for 30 minutes. The product was purified by flash chromatography (1:1 petroleum ether : ethyl acetate) to yield a colourless oil (12.7 mg, 0.0552 mmol) which was used immediately without further purification or characterization. The crude oil was dissolved in 5 mL methanol. Sodium hydroxide (10.0 mg, 0.25 mmol, 4.5 eq) was added, and the reaction mixture stirred for 15 minutes. The solution was neutralized with a few drops of acetic acid, and the solvent evaporated under reduced pressure. The product was purified by flash chromatography (7:2:1 ethyl acetate : methanol : water + 0.1% acetic acid) to yield **3.18** as a colourless gum (11.1 mg, 0.0513 mmol, 93%). **<sup>1</sup>H NMR:** (300 MHz, CD<sub>3</sub>OD)  $\delta$  5.81 (1 H, ddd,  $J_{H1-F1}$  55.5 Hz,  $J_{H1-F2}$  11.0 Hz,  $J_{H1-H2}$  3.6 Hz, H1), 4.54 (1 H, dddd,  $J_{H2-F2}$  50.2 Hz,  $J_{H2-F1}$  12.2 Hz,  $J_{H2-H3}$  7.4 Hz,  $J_{H2-H1}$  3.6 Hz, H2), 4.14 (1 H, ddd,  $J_{H3-F2}$  20.9 Hz,  $J_{H3-H4}$  8.2 Hz,  $J_{H3-H2}$  7.4 Hz, H3), 3.82 (1 H, dd,  $J_{H4-F5}$  13.2 Hz,  $J_{H4-H3}$  8.2 Hz, H4); **<sup>19</sup>F NMR:** (282 MHz, CD<sub>3</sub>OD):  $\delta$  -107.13-107.92 (1 F, m, F5), -130.98-131.21 (1 F, m, F1), -199.04-198.78 (1 F, m, F2); **<sup>13</sup>C NMR:** (100 MHz, CD<sub>3</sub>OD):  $\delta$  162.12 (d,  $J_{C-F5}$  10 Hz, C=O), 109.98 (d,  $J_{C5-F5}$  238 Hz, C5), 108.12 (dd,  $J_{C1-F1}$  230 Hz,  $J_{C1-F2}$  37 Hz, C1), 93.01 (dd,  $J_{C2-F2}$  188 Hz,  $J_{C2-F1}$  38 Hz, C2), 72.22 (ddd,  $J_{C3-F2}$  30 Hz,  $J_{C3-F1}$  9 Hz,  $J_{C3-F5}$  3 Hz, C3), 71.42 (dd,  $J_{C4-F5}$  26 Hz,  $J_{C4-F2}$  7 Hz, C4); **ESI-MS (high res):**  $m/z$  calc.: 215.0173; **Found:** 215.0169 [M - H]<sup>-</sup>; **Anal. calc. for** C<sub>6</sub>H<sub>7</sub>F<sub>3</sub>O<sub>5</sub> · 2 H<sub>2</sub>O: C, 28.58, H, 4.40; **Found:** C, 28.64, H, 4.35.

Methyl (2,3,4-tri-O-acetyl- $\beta$ -D-glucopyranosyl chloride) uronate (**3.26**)



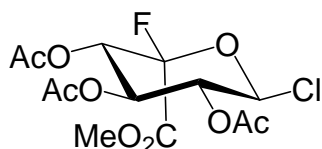
**3.20** (6.12 g, 16.3 mmol) was dissolved in 8 mL dichloromethyl-methylether and boron trifluoride-diethyl etherate (0.1 mL, 0.796 mmol, 0.05 eq) was added. The reaction mixture was stirred under  $N_{2(g)}$  overnight, after which time the reaction mixture was diluted in ice-cold chloroform and the organic layer was washed successively with 1 x ice-cold  $H_2O$ , 1 x sat.  $NaHCO_3$ , and 1 x sat.  $NaCl$ . The organic layer was then dried over  $MgSO_4$  for 10 minutes, filtered, and concentrated under reduced pressure. The product was then dissolved in a small volume of chloroform and a large volume of diethyl ether was added. The product precipitated from this solution after standing for 1 hour at room temperature, and was filtered to give **3.26** as a fine white powder (4.34 g, 12.3 mmol, 76%).  **$^1H$  NMR:** (300 MHz,  $CDCl_3$ )  $\delta$  5.34-5.16 (4 H, m, H1, H2, H3, H4), 4.11 (1 H, d,  $J_{H5-H4}$  9.6 Hz, H5), 3.76 (3 H, s,  $CO_2CH_3$ ), 2.06 (3 H, s, Ac), 2.01 (3 H, s, Ac), 2.00 (3 H, s, Ac); **ESI-MS (low res):** m/z calc.: 375.0; **Found:** 375.1  $[M + Na]^+$ .

Methyl (2,3,4-tri-O-acetyl-5-bromo- $\beta$ -D-glucopyranosyl chloride) uronate (**3.27**)



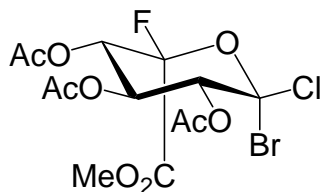
**3.26** (3.27 g, 9.27 mmol) was photobrominated in 50 mL dry carbon tetrachloride using *N*-bromosuccinimide (2.20 g, 12.4 mmol, 1.3 eq) according to General Procedure C. The product was used without further purification.  **$^1H$  NMR:** (300 MHz,  $CDCl_3$ )  $\delta$  5.73 (1 H, d,  $J_{H1-H2}$  9.1 Hz, H1), 5.47-5.22 (3 H, m, H2, H3, H4), 3.84 (3 H, s,  $CO_2CH_3$ ), 2.07 (3 H, s, Ac), 2.06 (3 H, s, Ac), 1.99 (3 H, s, Ac).

Methyl (2,3,4-tri-O-acetyl-5-fluoro- $\alpha$ -L-idopyranosyl chloride) uronate (**3.28**)



The crude **3.27** was dissolved in 40 mL dry acetonitrile. Silver fluoride (2.36 g, 18.6 mmol) was added to this solution, and the resulting slurry was allowed to stir overnight in the dark under N<sub>2(g)</sub>. The slurry was filtered through a plug of silica using ethyl acetate as the eluent to remove the silver salts, then the product purified by flash chromatography (200:1 → 100:1 dichloromethane : diethyl ether) to yield **3.28** as a colourless oil (0.969 g, 2.62 mmol, 29% from **3.26**). **<sup>1</sup>H NMR:** (300 MHz, CDCl<sub>3</sub>) δ 5.91 (1 H, dd, J<sub>H1-H2</sub> 4.3 Hz, J<sub>H1-F5</sub> 1.6 Hz, H1), 5.69 (1 H, dd, J<sub>H4-F5</sub> 10.9 Hz, J<sub>H4-H3</sub> 7.0 Hz, H4), 5.38 (1 H, dd, J<sub>H2-H1</sub> 4.3 Hz, J<sub>H2-H3</sub> 1.3 Hz, H2), 5.34 (1 H, dd, J<sub>H3-H4</sub> 7.0 Hz, J<sub>H3-H2</sub> 1.3 Hz, H3), 3.86 (3 H, s, CO<sub>2</sub>CH<sub>3</sub>), 2.09 (3 H, s, Ac), 2.04 (3 H, s, Ac), 2.03 (3 H, s, Ac); **<sup>19</sup>F NMR:** (282 MHz, CDCl<sub>3</sub>): δ -110.73 (1 F, dd, J<sub>F5-H4</sub> 10.9 Hz, J<sub>F5-H1</sub> 1.6 Hz, F5); **<sup>13</sup>C NMR** (75 MHz, CDCl<sub>3</sub>): δ 169.66, 169.28, 168.41, 163.68 (4 x C=O), 112.04 (d, J<sub>C5-F5</sub> 231 Hz, C5), 86.25 (C1), 73.93 (C3), 71.96 (C2), 69.53 (d, J<sub>C4-F5</sub> 36 Hz, C4), 53.83 (CO<sub>2</sub>CH<sub>3</sub>), 20.71 (2 C), 20.48 (3 x Ac); **ESI-MS (high res):** m/z calc.: 393.0365; **Found:** 393.0362 [M + Na]<sup>+</sup>.

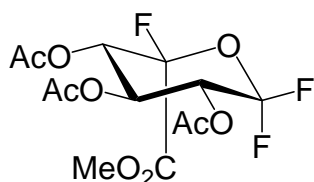
Methyl (2,3,4-tri-O-acetyl-1-bromo-5-fluoro- $\alpha$ -L-idopyranosyl chloride) uronate (**3.29**)



**3.28** (0.346 g, 0.935 mmol) was photobrominated in 40 mL dry carbon tetrachloride using *N*-bromosuccinimide (0.300 g, 1.69 mmol, 1.8 eq) according to General Procedure C. The product was used without further purification. **<sup>1</sup>H NMR:** (300 MHz, CDCl<sub>3</sub>) δ 5.75 (1 H, d, J<sub>H2-H3</sub> 7.8 Hz, H2), 5.51 (1 H, dd, J<sub>H4-F5</sub> 2.6 Hz, J<sub>H4-H3</sub> 1.0 Hz, H4), 5.29 (1 H, dd, J<sub>H3-H2</sub> 7.8

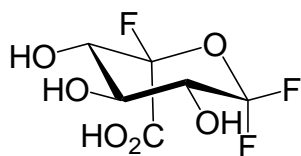
Hz,  $J_{H3-H4}$  1.0 Hz, H3), 3.88 (3 H, s,  $\text{CO}_2\text{CH}_3$ ), 2.19 (3 H, s, Ac), 2.13 (3 H, s, Ac), 2.10 (3 H, s, Ac);  $^{19}\text{F}$  NMR: (282 MHz,  $\text{CDCl}_3$ ):  $\delta$  -112.06 (1 F, d,  $J_{F5-H4}$  2.6 Hz, F5).

Methyl (2,3,4-tri-O-acetyl-1,5-difluoro-L-idopyranosyl fluoride) uronate (**3.30**)



The crude **3.29** was dissolved in 80 mL dry diethyl ether. Silver tetrafluoroborate (0.931 g, 4.78 mmol) was added, and the resulting slurry was allowed to stir for three days in the dark under  $\text{N}_2(\text{g})$ . The slurry was filtered through a plug of silica using ethyl acetate as the eluent to remove the silver salts, then the product was partially purified by flash chromatography (4:1  $\rightarrow$  3:1 hexane : ethyl acetate) to yield impure **3.30** as a colourless oil (43.6 mg).  $^{19}\text{F}$  NMR: (282 MHz,  $\text{CDCl}_3$ ):  $\delta$  -71.35 (1 F, d,  $J_{F1\text{eq}-F1\text{ax}}$  156.7 Hz,  $F1_{(\text{eq})}$ ), -77.57 (1 F, ddd,  $J_{F1\text{ax}-F1\text{eq}}$  156.7 Hz,  $J_{F1\text{ax}-H2}$  10.7 Hz,  $J_{F1\text{ax}-F5}$  5.6 Hz,  $F1_{(\text{ax})}$ ), -106.39 (1 F, t,  $J_{F5-H4} = J_{F5-F1(\text{ax})}$  5.6 Hz, F5).

1,5-Difluoro-L-idopyranosyl uronic acid fluoride (**3.19**)



The impure **3.30** (46.3 mg) was dissolved in 15 mL wet methanol. A small chunk of sodium was added, and the reaction mixture stirred for 25 minutes. The solution was then neutralized by the addition of a few drops of acetic acid, and the solvent evaporated under reduced pressure. The product was purified by flash chromatography (7:2:1 ethyl acetate : methanol : water + 0.1% acetic acid) to yield **3.19** as a colourless gum (25.6 mg, 0.110 mmol, 12% from **3.28**).  $^1\text{H}$  NMR: (300 MHz,  $\text{CD}_3\text{OD}$ )  $\delta$  3.95-3.83 (3 H, m, H2, H3, H4);  $^{19}\text{F}$  NMR: (282



MHz, CD<sub>3</sub>OD):  $\delta$  -72.08 (1 F, d,  $J_{F1eq-F1ax}$  157.0 Hz,  $F1_{(eq)}$ ), -82.63 (1 F, ddd,  $J_{F1ax-F1eq}$  157.0 Hz,  $J_{F1ax-H2}$  7.9 Hz,  $J_{F1ax-F5}$  5.6 Hz,  $F1_{(ax)}$ ), -107.94 (1 F, t,  $J_{F5-H4} = J_{F5-F1(ax)}$  5.6 Hz,  $F5$ ); **<sup>13</sup>C NMR** (75 MHz, CD<sub>3</sub>OD):  $\delta$  162.04 (d,  $J_{C6-F5}$  10 Hz, C6), 112.01 (dd,  $J_{C1-F1}$  238 Hz,  $J_{C1-F1}$  221 Hz, C1), 104.21 (d,  $J_{C5-F5}$  237 Hz, C5), 73.44 (d,  $J_{C3-F}$  8 Hz, C3) 72.67 (d,  $J_{C4-F5}$  32 Hz, C4) 70.72 (t,  $J_{C2-F1ax} = J_{C2-F1eq}$  27 Hz, C2); **ESI-MS (high res)**: m/z calc.: 231.0116; **Found**: 231.0123 [M - H]<sup>-</sup>; **Anal. calc. for** C<sub>6</sub>H<sub>7</sub>F<sub>3</sub>O<sub>6</sub> · H<sub>2</sub>O: C, 28.81, H, 3.63; **Found**: C, 28.68, H, 3.76.

## 5.2 Enzymology

### 5.2.1 Generous gifts

2,4-Dinitrophenyl  $\beta$ -D-glucopyranoside and 2,4-dinitrophenyl  $\alpha$ -D-mannopyranoside were kindly provided by Dr. Hongming Chen.  $\beta$ -Glucosidase from *Agrobacterium* sp (Abg) was cloned and expressed by Ms. Karen Rupitz.  $\alpha$ -L-iduronidase (Idua) and 4-methylumbelliferyl  $\alpha$ -L-idopyranosyl uronate (IdoA) were generous gifts from BioMarin. Glucocerebrosidase (GCase) was kindly provided by Dr. Lorne Clarke by collecting the leftovers from used patient vials. 2-deoxy-2-[<sup>18</sup>F]-fluoro-glucose (fluorodeoxyglucose, FDG) was kindly provided by Ms. Yulia Rozen and Mr. Milan Vuckovic of the BC Cancer Agency using the facilities at TRIUMF.  $\beta$ -Mannosidase from *Cellulomonas fimi* (Man2A) was expressed and purified by Dr. Dominik Stoll.

### 5.2.2 General enzymatic materials and methods

*E. coli*  $\beta$ -galactosidase (*E. coli*  $\beta$ -Gal), Jack Bean  $\alpha$ -mannosidase (JBAM) and Yeast  $\alpha$ -glucosidase (Yag) were all purchased from Sigma.

All enzymatic data analyses were performed using GraFit.<sup>311</sup> For all data analyses, the error bars have been omitted for clarity, although all calculated errors were  $\leq 10\%$  of the calculated value. All enzyme reactions were performed at 37 °C unless otherwise specified.

All enzymatic buffers were made up using water from a Millipore Direct-Q™ 5 Ultrapure Water System. The final concentration of each enzyme used in the assay cuvette was as follows: Abg (0.3 µg/mL), GCase (0.5 µg/mL), *E. coli* β-Gal (1.28 µg/mL), Man2A (0.4 µg/mL), JBAM (1.74 µg/mL), Yag (1.96 µg/mL), Idua (0.3 µg/mL). The following table shows the buffer conditions and substrates used in the course of this work:

Enzyme	Buffer	Substrate	K <sub>m</sub> (mM)
<i>Agrobacterium sp.</i> β-Glucosidase Abg	50 mM NaH <sub>2</sub> PO <sub>4</sub> /Na <sub>2</sub> HPO <sub>4</sub> pH = 6.8	pNP-β-D-Glc	0.087
Human Glucocerebrosidase GCCase	50 mM NaOAc, 0.2 % Triton X-100, 0.3% sodium taurocholate pH = 5.5	2,4-DNP-β-D-Glc	1.6
<i>E. coli</i> β-galactosidase <i>E. coli</i> β-Gal	50 mM NaH <sub>2</sub> PO <sub>4</sub> /Na <sub>2</sub> HPO <sub>4</sub> , 1 mM MgCl <sub>2</sub> pH = 7.0	pNP-β-D-Gal	0.03
<i>Cellulomonas fimi</i> β-Mannosidase Man2A	50 mM NaH <sub>2</sub> PO <sub>4</sub> /Na <sub>2</sub> HPO <sub>4</sub> pH = 6.8	pNP-β-D-Man	0.3
Jack Bean α-mannosidase JBAM	50 mM sodium citrate, pH = 4.5	2,4-DNP-α-D-Man	1.3
Yeast α-glucosidase Yag	50 mM NaH <sub>2</sub> PO <sub>4</sub> /Na <sub>2</sub> HPO <sub>4</sub> pH = 6.8	pNP-α-D-Glc	0.27
Human α-L-iduronidase Idua	100 mM sodium dimethyl glutarate, pH = 4.5	IdoA	0.051

### 5.2.3 Continuous enzymatic assays

The kinetic assays were performed using a Varian Cary 300-Bio UV-Visible Spectrophotometer equipped with an externally controlled continuously circulating water bath. Michaelis-Menten parameters were determined using GraFit version 5.0.13 by nonlinear fitting of the data to the Michaelis-Menten equation. The following enzymes were assayed by continuously monitoring ( $\lambda = 400$  nm) the release of *para*-nitrophenol from the substrate: Abg, *E. coli*  $\beta$ -Gal, Man2A and Yag. The following enzymes were assayed by continuously monitoring ( $\lambda = 400$  nm) the product release of 2,4-dinitrophenol from the substrate: GCase and JBAM. The slope of the resulting absorbance vs. time graph was used to determine the initial rate of enzyme catalyzed hydrolysis. The enzyme reaction was initiated by the addition of a small volume of enzyme solution to a pre-equilibrated assay cuvette containing an appropriate volume of buffer containing the chromogenic substrate.

### 5.2.4 Stopped enzymatic assays

The kinetic assay for Idua was performed using a Varian Cary Eclipse Fluorescence Spectrophotometer. Michaelis-Menten parameters were determined using GraFit version 5.0.13 by nonlinear fitting of the data to the Michaelis-Menten equation. Idua activity was determined in the following manner. Substrate/enzyme mixtures were incubated at 37°C in an eppendorf tube. At 3 minute intervals, 20  $\mu$ L aliquots were withdrawn and added to a large volume (1 mL) of quench buffer (100 mM glycine-carbonate, pH = 10.0) in a cuvette and vortexed thoroughly. The resulting fluorescence from the released methylumbelliferone was measured using the Spectrophotometer at three time points. The slope of the resulting fluorescence vs. time graph was used to determine the initial rate of enzyme catalyzed hydrolysis.

### 5.2.5 Enzyme inactivation assays

Compounds of interest were tested for time-dependent inactivation of their respective enzymes using the following general procedure. The enzyme was incubated in a small

eppendorf tube with an appropriate volume of buffer along with varying concentrations of the compound of interest, for a total volume of 180  $\mu\text{L}$ . The inactivation was initiated by the addition of 20  $\mu\text{L}$  of the enzyme solution. At appropriate time points, 20  $\mu\text{L}$  aliquots were withdrawn and added to a solution containing 2-10  $\times K_m$  of the appropriate substrate, along with a large volume (between 600-100  $\mu\text{L}$ ) of buffer. This halts the inactivation reaction both by dilution of the enzyme inactivator and by competition with a large excess of substrate. The residual enzyme activity was then assayed using either a continuous or stopped enzymatic assay, as appropriate. The rate of release of the chromophore is directly proportional to the concentration of catalytically active enzyme remaining in the solution. Pseudo-first order rate constants for the loss of enzymatic activity for each concentration of inactivator were determined by nonlinear fitting of the decay curve to a single exponential decay equation using GraFit. The individual  $k_{\text{obs}}$  values were then replotted as a function of inactivator concentration. Individual values for  $k_i$  and  $K_i$  were obtained by fitting to the equation:

$$k_{\text{obs}} = \frac{k_i [I]}{K_i + [I]}$$

For cases when inactivation was too rapid or the  $K_i$  value was too high, and saturation was not observed, then the  $k_i/K_i$  value was obtained by fitting the data to the equation:

$$k_{\text{obs}} = \frac{k_i [I]}{K_i}$$

where  $[I] \ll K_i$  and  $k_i/K_i$  is obtained from the initial slope of a plot of  $k_{\text{obs}}$  as a function of inactivator concentration.

### 5.2.6 Enzyme reactivation assays

A sample of the inactivated enzyme in a small volume of buffer was loaded onto the top of a protein desalting column and centrifuged at 2000 rpm for 2 minutes. The flow-through solution was collected and diluted in a large volume of the appropriate buffer, along with a suitable concentration of a small molecule transglycosylating ligand where

appropriate. Aliquots (20  $\mu\text{L}$ ) were removed at various time points and the enzyme solution assayed for activity using the appropriate assay. The rate constant for reactivation of enzyme activity was determined by fitting the rate vs. incubation time data to a first order equation using GraFit.

### **5.2.7 Test for a highly active contaminant**

The following method was employed to test a putative inactivator for the presence of a highly active but minor contaminant. The enzyme was incubated in a small volume of buffer along with the putative inactivator (10  $\mu\text{L}$  total volume). The relative concentrations of enzyme and inactivator were chosen such that  $[\text{Enzyme}] \sim 0.1 * [\text{Inactivator}]$ . Aliquots of this solution were removed at various time points and diluted into an assay cuvette containing a large volume of the appropriate buffer along with substrate to determine the amount of enzyme activity remaining. The data were analyzed in a manner similar to that described for the Enzyme Inactivation Assays in Section 5.2.5.

### **5.2.8 Determination of apparent $K_i'$ values**

The following method was used to determine  $K_i'$  values for compounds which were slow substrates for the enzyme of interest. An appropriate volume of buffer containing the known chromogenic substrate at a concentration  $\sim K_m$  and the compound of interest was pre-incubated at 37°C. A small volume of enzyme solution was added to this solution, and the release of the chromophore monitored using either a continuous or stopped assay, as appropriate.

### **5.2.9 Determination of $K_i$ values**

The testing of compounds as reversible competitive inhibitors was performed as follows. The enzyme of interest was incubated in the presence of buffer and an appropriate amount of inhibitor. The reaction was initiated by addition of the substrate, and the enzyme

activity assayed using the appropriate continuous or stopped assay. The residual enzyme activity was plotted as a Dixon plot (inverse of enzyme catalyzed rate of reaction vs. inverse of inhibitor concentration for a substrate concentration  $\sim K_m$ ) and an approximate  $K_i$  value obtained by multiplying by -1 the extrapolated intercept between the plotted line obtained by linear regression and a line corresponding to  $1/V_{max}$ .

### 5.3 Radiochemistry

Note: These experiments were performed jointly in collaboration with Dr. Chris Phenix, a postdoctoral fellow in the Withers lab.

#### 5.3.1 Radiosynthesis of 2,4-dinitrophenyl 2-deoxy-2-[ $^{18}F$ ]-fluoro- $\beta$ -D-glucopyranoside (4.19)

Pharmaceutical grade 2-deoxy-2-[ $^{18}F$ ]-fluoro-D-glucose (**1.12**, 16.25 mCi) in an isotonic saline solution was a generous gift of the B.C. Cancer Agency, following quality assurance to verify the absence of any radiochemical contaminants. The solution of **1.12** was placed in a 2 mL screw-cap vial with a rubber septum and containing a small stir bar. The water was evaporated at 100 °C under a stream of dry helium while simultaneously passing helium gas through the V-vial vented into a sodium lime trap. The vial was cooled to 37 °C, after which 150  $\mu$ L of saturated sodium bicarbonate and 150  $\mu$ L of ethanol containing 2.2 mg of dinitrofluorobenzene (DNFB) were added, and the resulting solution stirred for 10 minutes during which the solution turned yellow. 25  $\mu$ L glacial acetic acid was added to neutralize the reaction, following which the water was evaporated at 60 °C as described above. The yellow residue was dissolved in 300  $\mu$ L distilled water, and loaded onto a C<sub>18</sub> Sep-Pak (pre-equilibrated with 1 mL water). 1 mL of distilled water was used to elute the radioactivity into four fractions of approximately 0.33 mL. The second fraction (4.1 mCi, 53 minutes from beginning of radiosynthesis) was loaded onto a Synergy semi-prep reverse phase HPLC column and eluted using a gradient of 60% methanol 40% water to 100% methanol over 10 minutes, with the gradient maintained at 100% methanol for a further 10 minutes. The purified **4.19** (3.25 mCi, 72 minutes from beginning of radiosynthesis, 32% radiochemical

yield decay corrected from **1.12**) was collected at approximately 14 minutes in a high percentage of methanol, and evaporated at 60 °C as described above.

### **5.3.2 Radiochemical labelling of Abg with purified 4.19**

To the V-vial containing the freshly purified **4.19**, 200 µL of 60 mM phosphate, pH 6.5 buffer was added, containing Abg at a concentration of 6 mg/mL. The enzymatic reaction incubated for 10 minutes at 37 °C, following which it was studied by radio-TLC analysis.

To study the specificity of the enzymatic radiolabelling reaction, the above procedure was also carried out using the Glu359Ala mutant of Abg, following which the reaction mixture was studied by radio-TLC analysis.

Additionally, the radiolabelled enzyme produced by reaction of **4.19** and wild-type Abg was concentrated by centrifugation using a Microcon 50 kDa molecular weight cut-off filter at 14,000 rpm for 8 minutes to separate the radiolabelled Abg from the residual **4.19**. The enzyme was re-suspended in 200 µL of buffer containing 20 mM thiophenyl β-D-glucopyranoside and incubated at 37 °C. The reaction mixture was monitored by radio-TLC for up to 2 hours.

### **5.3.3 Radiochemical labelling of GCase with purified 4.19**

To the V-vial containing the freshly purified **4.19** (2.18 mCi), a concentrated solution of GCase (300 µL, ~5 mg/mL) in assay buffer was added and the mixture stirred for 45 minutes. Following radio-TLC analysis, the solution was diluted with 500 µL of MES buffer (50 mM MES, 100 mM NaCl, pH = 6.5) and loaded onto the top of a Microcon 50 kDa molecular weight cut-off filter and centrifuged at 14,000 rpm for 8 minutes. The enzyme solution was diluted with a second 500 µL portion of MES buffer and the enzyme centrifuged a second time. The final radiolabelled enzyme solution (generally approximately 100 µL volume) was loaded onto a Pierce Desalting Spin column pre-equilibrated with Cerezyme buffer (60 mM sodium citrate, 20 mM sodium phosphate, 0.1% Tween 80, pH



6.6) and subjected to two rounds of gel filtration. The final enzyme solution (0.147 mCi, 7% radiochemical yield) was loaded into a small screw-cap vial and shipped to the MicroPET facility at the UBC hospital for mouse experiments.

## **References**

- (1) Henrissat, B.; Bairoch, A. *Biochem. J* **1993**, 293, 781-788.
- (2) Henrissat, B. *Biochem. J* **1991**, 280, 309-316.
- (3) Cantarel, B. L.; Coutinho, P. M.; Rancurel, C.; Bernard, T.; Lombard, V.; Henrissat, B. *Nucleic Acids Res.* **2009**, 37, D233-D238.
- (4) Wolfenden, R.; Lu, X. D.; Young, G. *J. Am. Chem. Soc.* **1998**, 120, 6814-6815.
- (5) Zechel, D. L.; Withers, S. G. *Acc. Chem. Res.* **2000**, 33, 11-18.
- (6) Koshland, D. E. *Biol. Rev. Camb. Philos. Soc.* **1953**, 28, 416-436.
- (7) Heightman, T. D.; Vasella, A. T. *Angew. Chem. Int. Ed.* **1999**, 38, 750-770.
- (8) Phillips, D. C. *Proc. Natl. Acad. Sci. U. S. A.* **1967**, 57, 484-&.
- (9) Sinnott, M. L.; Souchard, I. J. *Biochem. J* **1973**, 133, 89-98.
- (10) Vocadlo, D. J.; Davies, G. J. *Curr. Opin. Chem. Biol.* **2008**, 12, 539-555.
- (11) Rempel, B. P.; Withers, S. G. *Glycobiology* **2008**, 18, 570-586.
- (12) Mosi, R. M.; Withers, S. G. In *Methods Enzymol.*; Academic Press Inc: San Diego, 2002; Vol. 354, p 64-84.
- (13) Wicki, J.; Rose, D. R.; Withers, S. G. In *Methods Enzymol.*; Academic Press Inc: San Diego, 2002; Vol. 354, p 84-105.
- (14) Kempton, J. B.; Withers, S. G. *Biochemistry* **1992**, 31, 9961-9969.
- (15) Knapp, S.; Vocadlo, D.; Gao, Z. N.; Kirk, B.; Lou, J. P.; Withers, S. G. *J. Am. Chem. Soc.* **1996**, 118, 6804-6805.
- (16) Mark, B. L.; Vocadlo, D. J.; Knapp, S.; Triggs-Raine, B. L.; Withers, S. G.; James, M. N. G. *J. Biol. Chem.* **2001**, 276, 10330-10337.
- (17) Vocadlo, D. J.; Withers, S. G. *Biochemistry* **2005**, 44, 12809-12818.
- (18) Macauley, M. S.; Whitworth, G. E.; Debowski, A. W.; Chin, D.; Vocadlo, D. *J. J. Biol. Chem.* **2005**, 280, 25313-25322.
- (19) Yip, V. L.; Withers, S. G. *Curr. Opin. Chem. Biol.* **2006**, 10, 147-155.
- (20) Watts, A. G.; Damager, I.; Amaya, M. L.; Buschiazzi, A.; Alzari, P.; Frasch, A. C.; Withers, S. G. *J. Am. Chem. Soc.* **2003**, 125, 7532-7533.
- (21) Asano, N. *Glycobiology* **2003**, 13, 93R-104R.
- (22) Butters, T. D.; Dwek, R. A.; Platt, F. M. *Glycobiology* **2005**, 15, R43-R52.
- (23) de Melo, E. B.; Gomes, A. D.; Carvalho, I. *Tetrahedron* **2006**, 62, 10277-10302.
- (24) Stick, R. V.; Williams, S. J. In *Carbohydrates The Essential Molecules of Life*; Elsevier: Amsterdam, 2009, p 265-272.
- (25) Asano, N.; Nash, R. J.; Molyneux, R. J.; Fleet, G. W. J. *Tetrahedron: Asymmetry* **2000**, 11, 1645-1680.
- (26) Gerber-Lemaire, S.; Juillerat-Jeanneret, L. *Mini-Rev. Med. Chem.* **2006**, 6, 1043-1052.
- (27) Kajimoto, T.; Node, M. *Curr. Top. Med. Chem.* **2009**, 9, 13-33.
- (28) Ogawa, S.; Kanto, M.; Suzuki, Y. *Mini-Rev. Med. Chem.* **2007**, 7, 679-691.
- (29) Lai, E. C. K.; Morris, S. A.; Street, I. P.; Withers, S. G. *Biorg. Med. Chem.* **1996**, 4, 1929-1937.
- (30) Stephens, M. C.; Bernatsky, A.; Burachinsky, V.; Legler, G.; Kanfer, J. N. *J. Neurochem.* **1978**, 30, 1023-1027.
- (31) Hurtado-Guerrero, R.; van Aalten, D. M. F. *Chem. Biol.* **2007**, 14, 589-599.

- (32) Tropak, M. B.; Blanchard, J. E.; Withers, S. G.; Brown, E. D.; Mahuran, D. *Chem. Biol.* **2007**, *14*, 153-164.
- (33) Tropak, M. B.; Kornhaber, G. J.; Rigat, B. A.; Maegawa, G. H.; Buttner, J. D.; Blanchard, J. E.; Murphy, C.; Tuske, S. J.; Coales, S. J.; Hamuro, Y.; Brown, E. D.; Mahuran, D. J. *ChemBioChem* **2008**, *9*, 2650-2662.
- (34) Gloster, T. M.; Meloncelli, P.; Stick, R. V.; Zechel, D.; Vasella, A.; Davies, G. J. *J. Am. Chem. Soc.* **2007**, *129*, 2345-2354.
- (35) Jespersen, T. M.; Dong, W. L.; Sierks, M. R.; Skrydstrup, T.; Lundt, I.; Bols, M. *Angew. Chem. Int. Ed.* **1994**, *33*, 1778-1779.
- (36) Davies, G. J.; Ducros, V. M. A.; Varrot, A.; Zechel, D. L. *Biochem. Soc. Trans.* **2003**, *31*, 523-527.
- (37) Davies, G. J.; Mackenzie, L.; Varrot, A.; Dauter, M.; Brzozowski, A. M.; Schulein, M.; Withers, S. G. *Biochemistry* **1998**, *37*, 11707-11713.
- (38) Ermert, P.; Vasella, A.; Weber, M.; Rupitz, K.; Withers, S. G. *Carbohydr. Res.* **1993**, *250*, 113-128.
- (39) Legler, G. *Adv. Carbohydr. Chem. Biochem.* **1990**, *48*, 319-384.
- (40) Withers, S. G.; Aebersold, R. *Protein Sci.* **1995**, *4*, 361-372.
- (41) Kitz, R. J.; Ginsburg, S.; Wilson, I. B. *Biochemical Pharmacology* **1965**, *14*, 1471-&.
- (42) Fersht, A. In *Structure and Mechanism in Protein Science*; W. H. Freeman and Company: New York, 1999, p 273-288.
- (43) Vodovozova, E. L. *Biochemistry-Moscow* **2007**, *72*, 1-20.
- (44) Kuhn, C. S.; Lehmann, J. *Carbohydr. Res.* **1987**, *160*, C6-C8.
- (45) Kuhn, C. S.; Lehmann, J.; Jung, G.; Stevanovic, S. *Carbohydr. Res.* **1992**, *232*, 227-233.
- (46) Marshall, P. J.; Sinnott, M. L.; Smith, P. J.; Widdows, D. J. *Chem. Soc., Perkin Trans. I* **1981**, 366-376.
- (47) Chir, J.; Withers, S.; Wan, C. F.; Li, Y. K. *Biochem. J* **2002**, *365*, 857-863.
- (48) Keresztessy, Z.; Kiss, L.; Hughes, M. A. *Arch. Biochem. Biophys.* **1994**, *315*, 323-330.
- (49) Tull, D.; Burgoyne, D. L.; Chow, D. T.; Withers, S. G.; Aebersold, R. *Anal. Biochem.* **1996**, *234*, 119-125.
- (50) Vocadlo, D. J.; Wicki, J.; Rupitz, K.; Withers, S. G. *Biochemistry* **2002**, *41*, 9736-9746.
- (51) Briggs, J. C.; Haines, A. H.; Taylor, R. J. K. *J. Chem. Soc., Chem. Commun.* **1992**, 1039-1041.
- (52) Driguez, P. A.; Barrere, B.; Chantegrel, B.; Deshayes, C.; Doutheau, A.; Quash, G. *Bioorg. Med. Chem. Lett.* **1992**, *2*, 1361-1366.
- (53) Hinou, H.; Kurogochi, M.; Shimizu, H.; Nishimura, S. I. *Biochemistry* **2005**, *44*, 11669-11675.
- (54) Ichikawa, M.; Ichikawa, Y. *Bioorg. Med. Chem. Lett.* **2001**, *11*, 1769-1773.
- (55) Kurogochi, M.; Nishimura, S. I.; Lee, Y. C. *J. Biol. Chem.* **2004**, *279*, 44704-44712.
- (56) Tsai, C. S.; Li, Y. K.; Lo, L. C. *Org. Lett.* **2002**, *4*, 3607-3610.
- (57) Withers, S. G.; Rupitz, K.; Street, I. P. *J. Biol. Chem.* **1988**, *263*, 7929-7932.

- (58) Withers, S. G.; Street, I. P.; Bird, P.; Dolphin, D. H. *J. Am. Chem. Soc.* **1987**, *109*, 7530-7531.
- (59) Winchester, B. *Glycobiology* **2005**, *15*, 1R-15R.
- (60) Gieselmann, V. *Biochim. Biophys. Acta-Mol. Bas. Dis.* **1995**, *1270*, 103-136.
- (61) Futerman, A. H.; van Meer, G. *Nat. Rev. Mol. Cell Biol.* **2004**, *5*, 554-565.
- (62) Childs, B.; Beaudet, A. L.; Valle, D.; Kinzler, K. W.; Vogelstein, B. *The Metabolic and Molecular Bases of Inherited Disease*; Eighth ed.; McGraw-Hill Professional: Columbus, USA, 2000.
- (63) Meikle, P. J.; Hopwood, J. J.; Clague, A. E.; Carey, W. F. *J. Am. Med. Assoc.* **1999**, *281*, 249-254.
- (64) Grabowski, G. A. *Lancet* **2008**, *372*, 1263-1271.
- (65) Butters, T. D.; Dwek, R. A.; Platt, F. M. *Chem. Rev.* **2000**, *100*, 4683-+.
- (66) Fan, J. Q. *Biol. Chem.* **2008**, *389*, 1-11.
- (67) Grabowski, G. A.; Hopkin, R. J. *Annu. Rev. Genom. Hum. Genet.* **2003**, *4*, 403-436.
- (68) Sands, M. S.; Davidson, B. L. *Mol. Ther.* **2006**, *13*, 839-849.
- (69) Desnick, R. J. *J. Inherit. Metab. Dis.* **2004**, *27*, 385-410.
- (70) Sawkar, A. R.; D'Haese, W.; Kelly, J. W. *Cell. Mol. Life Sci.* **2006**, *63*, 1179-1192.
- (71) Brady, R. O. *Annu. Rev. Med.* **2006**, *57*, 283-296.
- (72) Brunel-Guitton, C.; Rivard, G. E.; Galipeau, J.; Alos, N.; Miron, M. C.; Therrien, R.; Mitchell, G.; Lapierre, G.; Lambert, M. *Mol. Genet. Metab.* **2009**, *96*, 73-76.
- (73) Zirzow, G. C.; Sanchez, O. A.; Murray, G. J.; Brady, R. O.; Oldfield, E. H. *Neurochem. Res.* **1999**, *24*, 301-305.
- (74) Kakkis, E.; McEntee, M.; Vogler, C.; Le, S.; Levy, B.; Belichenko, P.; Mobley, W.; Dickson, P.; Hanson, S.; Passage, M. *Mol. Genet. Metab.* **2004**, *83*, 163-174.
- (75) Munoz-Rojas, M. V.; Vieira, T.; Costa, R.; Fagundes, S.; John, A.; Jardim, L. B.; Vedolin, L. M.; Raymundo, M.; Dickson, P. I.; Kakkis, E.; Giugliani, R. *Am. J. Med. Genet. A* **2008**, *146A*, 2538-2544.
- (76) Muenzer, J.; Wraith, J. E.; Clarke, L. A. *Pediatrics* **2009**, *123*, 19-29.
- (77) Baldellou, A.; Andria, G.; Campbell, P. E.; Charrow, J.; Cohen, I. J.; Grabowski, G. A.; Harris, C. M.; Kaplan, P.; McHugh, K.; Mengel, E.; Vellodi, A. *Eur. J. Pediatr.* **2004**, *163*, 67-75.
- (78) Butters, T. D. *Curr. Opin. Chem. Biol.* **2007**, *11*, 412-418.
- (79) Platt, F. M.; Jeyakumar, M.; Andersson, U.; Priestman, D. A.; Dwek, R. A.; Butters, T. D.; Cox, T. M.; Lachmann, R. H.; Hollak, C.; Aerts, J.; Van Weely, S.; Hrebicek, M.; Moyses, C.; Gow, I.; Elstein, D.; Zimran, A.; Kluwer Academic Publ: 2001, p 275-290.
- (80) Jmoudiak, M.; Futerman, A. H. *Br. J. Haematol.* **2005**, *129*, 178-188.
- (81) Kelly, J. W. *Curr. Opin. Struct. Biol.* **1998**, *8*, 101-106.
- (82) Lomas, D. A.; Carrell, R. W. *Nat. Rev. Genet.* **2002**, *3*, 759-768.
- (83) Stefani, M. *Biochim. Biophys. Acta-Mol. Bas. Dis.* **2004**, *1739*, 5-25.
- (84) Stefani, M.; Dobson, C. M. *J. Mol. Med.* **2003**, *81*, 678-699.
- (85) Herczenik, E.; Gebbink, M. *FASEB J.* **2008**, *22*, 2115-2133.
- (86) Vembar, S. S.; Brodsky, J. L. *Nat. Rev. Mol. Cell Biol.* **2008**, *9*, 944-U30.
- (87) Kaufman, R. J. *J. Clin. Invest.* **2002**, *110*, 1389-1398.
- (88) Westerheide, S. D.; Morimoto, R. I. *J. Biol. Chem.* **2005**, *280*, 33097-33100.

- (89) Sawkar, A. R.; Schmitz, M.; Zimmer, K. P.; Reczek, D.; Edmunds, T.; Balch, W. E.; Kelly, J. W. *ACS Chemical Biology* **2006**, *1*, 235-251.
- (90) Arakawa, T.; Ejima, D.; Kita, Y.; Tsumoto, K. *Biochim. Biophys. Acta-Proteins Proteomics* **2006**, *1764*, 1677-1687.
- (91) Leandro, P.; Gomes, C. M. *Mini-Rev. Med. Chem.* **2008**, *8*, 901-911.
- (92) Voet, D.; Voet, J. G.; Pratt, C. W. In *Fundamentals of Biochemistry*; John Wiley and Sons Inc: New York, 1999, p 894-901.
- (93) Sidransky, E.; Ginns, E. I. *Baillieres Clin. Haematol.* **1997**, *10*, 725-737.
- (94) Tybulewicz, V. L. J.; Tremblay, M. L.; Lamarca, M. E.; Willemsen, R.; Stubblefield, B. K.; Winfield, S.; Zabolocka, B.; Sidransky, E.; Martin, B. M.; Huang, S. P.; Mintzer, K. A.; Westphal, H.; Mulligan, R. C.; Ginns, E. I. *Nature* **1992**, *357*, 407-410.
- (95) Liu, Y. J.; Suzuki, K.; Reed, J. D.; Grinberg, A.; Westphal, H.; Hoffmann, A.; Doring, T.; Sandhoff, K.; Proia, R. L. *Proc. Natl. Acad. Sci. U. S. A.* **1998**, *95*, 2503-2508.
- (96) Xu, Y. H.; Quinn, B.; Witte, D.; Grabowski, G. A. *Am. J. Pathol.* **2003**, *163*, 2093-2101.
- (97) Schueler, U. H.; Kolter, T.; Kaneski, C. R.; Zirzow, G. C.; Sandhoff, K.; Brady, R. O. *J. Inherit. Metab. Dis.* **2004**, *27*, 649-658.
- (98) Zhao, H.; Grabowski, G. A. *Cell. Mol. Life Sci.* **2002**, *59*, 694-707.
- (99) McNaught, A. D. *Carbohydr. Res.* **1997**, *297*, 1-90.
- (100) Freeze, H. H. In *Essentials of Glycobiology*; Varki, A., Cummings, R., Esko, J., Freeze, H. H., Hart, G., Marth, J., Eds.; Cold Spring Harbor: New York, 1999, p 267-283.
- (101) Bunge, S.; Clements, P. R.; Byers, S.; Kleijer, W. J.; Brooks, D. A.; Hopwood, J. J. *Biochim. Biophys. Acta-Mol. Bas. Dis.* **1998**, *1407*, 249-256.
- (102) Terlato, N. J.; Cox, G. F. *Genet. Med.* **2003**, *5*, 286-294.
- (103) Aldenboven, M.; Boelens, F.; de Koning, T. F. *Biol. Blood Marrow Transplant.* **2008**, *14*, 485-498.
- (104) Burrow, T. A.; Hopkin, R. J.; Leslie, N. D.; Tinkle, B. T.; Grabowski, G. A. *Curr. Opin. Pediatr.* **2007**, *19*, 628-635.
- (105) Kakkis, E. D.; Muenzer, J.; Tiller, G. E.; Waber, L.; Belmont, J.; Passage, M.; Izykowski, B.; Phillips, J.; Doroshov, R.; Walot, I.; Hoft, R.; Yu, K. T.; Okazaki, S.; Lewis, D.; Lachman, R.; Thompson, J. N. *N. Engl. J. Med.* **2001**, *344*, 182-188.
- (106) Wraith, E. J.; Hopwood, J. J.; Fuller, M.; Meikle, P. J.; Brooks, D. A. *Biodrugs* **2005**, *19*, 1-7.
- (107) Wraith, J. E.; Clarke, L. A.; Beck, M.; Kolodny, E. H.; Pastores, G. M.; Muenzer, J.; Rapoport, D. M.; Berger, K. I.; Swiedler, S. J.; Kakkis, E. D.; Braakman, T.; Chadbourne, E.; Walton-Bowen, K.; Cox, G. F. *J. Pediatr.* **2004**, *144*, 581-588.
- (108) Bailey, D. L.; Townsend, D. W.; Valk, P. E.; Maisey, M. N. *Positron Emission Tomography*; Springer: London, 2005.
- (109) Adam, M. J.; Wilbur, D. S. *Chem. Soc. Rev.* **2005**, *34*, 153-163.
- (110) Fowler, J. S.; Wolf, A. P. *Acc. Chem. Res.* **1997**, *30*, 181-188.
- (111) Voet, D.; Voet, J. G.; Pratt, C. W. In *Fundamentals of Biochemistry*; John Wiley and Sons Inc: New York, 1999, p 382-423.
- (112) Ametamey, S. M.; Honer, M.; Schubiger, P. A. *Chem. Rev.* **2008**, *108*, 1501-1516.
- (113) Shih, J. C.; Chen, K.; Ridd, M. J. *Annu. Rev. Neurosci.* **1999**, *22*, 197-217.

- (114) Bugg, T. In *An Introduction to Enzyme and Coenzyme Chemistry*; Blackwell Science Ltd.: Oxford, 1997, p 118-120.
- (115) Bugg, T. In *An Introduction to Enzyme and Coenzyme Chemistry*; Blackwell Science Ltd.: Oxford, 1997, p 117-118.
- (116) Wakarchuk, W. W.; Greenberg, N. M.; Kilburn, D. G.; Miller, R. C.; Warren, R. A. J. *J. Bacteriol.* **1988**, *170*, 301-307.
- (117) Namchuk, M. N.; Withers, S. G. *Biochemistry* **1995**, *34*, 16194-16202.
- (118) Trimbur, D. E.; Warren, R. A. J.; Withers, S. G. *J. Biol. Chem.* **1992**, *267*, 10248-10251.
- (119) Gebler, J. C.; Trimbur, D. E.; Warren, A. J.; Aebersold, R.; Namchuk, M.; Withers, S. G. *Biochemistry* **1995**, *34*, 14547-14553.
- (120) Wang, Q.; Trimbur, D.; Graham, R.; Warren, R. A. J.; Withers, S. G. *Biochemistry* **1995**, *34*, 14554-14562.
- (121) Withers, S. G.; Rupitz, K.; Trimbur, D.; Warren, R. A. J. *Biochemistry* **1992**, *31*, 9979-9985.
- (122) Street, I. P.; Kempton, J. B.; Withers, S. G. *Biochemistry* **1992**, *31*, 9970-9978.
- (123) Withers, S. G.; Warren, R. A. J.; Street, I. P.; Rupitz, K.; Kempton, J. B.; Aebersold, R. *J. Am. Chem. Soc.* **1990**, *112*, 5887-5889.
- (124) Withers, S. G.; Street, I. P. *J. Am. Chem. Soc.* **1988**, *110*, 8551-8553.
- (125) Kim, Y. W.; Lee, S. S.; Warren, R. A. J.; Withers, S. G. *J. Biol. Chem.* **2004**, *279*, 42787-42793.
- (126) Mayer, C.; Zechel, D. L.; Reid, S. P.; Warren, R. A. J.; Withers, S. G. *FEBS Lett.* **2000**, *466*, 40-44.
- (127) Mackenzie, L. F.; Wang, Q. P.; Warren, R. A. J.; Withers, S. G. *J. Am. Chem. Soc.* **1998**, *120*, 5583-5584.
- (128) Hancock, S. M.; D Vaughan, M.; Withers, S. G. *Curr. Opin. Chem. Biol.* **2006**, *10*, 509-519.
- (129) McCarter, J. D.; Withers, S. G. *J. Am. Chem. Soc.* **1996**, *118*, 241-242.
- (130) McCarter, J. D.; Yeung, W.; Chow, J.; Dolphin, D.; Withers, S. G. *J. Am. Chem. Soc.* **1997**, *119*, 5792-5797.
- (131) Brayer, G. D.; Luo, Y. G.; Withers, S. G. *Protein Sci.* **1995**, *4*, 1730-1742.
- (132) Uitdehaag, J. C. M.; Mosi, R.; Kalk, K. H.; van der Veen, B. A.; Dijkhuizen, L.; Withers, S. G.; Dijkstra, B. W. *Nat. Struct. Biol.* **1999**, *6*, 432-436.
- (133) Sprogø, D.; van den Broek, L. A. M.; Mirza, O.; Kastrup, J. S.; Voragen, A. G. J.; Gajhede, M.; Skov, L. K. *Biochemistry* **2004**, *43*, 1156-1162.
- (134) McCarter, J. D.; Withers, S. G. *J. Biol. Chem.* **1996**, *271*, 6889-6894.
- (135) Stoll, D.; Stalbrand, H.; Warren, R. A. J. *Appl. Environ. Microbiol.* **1999**, *65*, 2598-2605.
- (136) Zechel, D. L.; Reid, S. P.; Stoll, D.; Nashiru, O.; Warren, R. A. J.; Withers, S. G. *Biochemistry* **2003**, *42*, 7195-7204.
- (137) Stoll, D.; He, S. M.; Withers, S. G.; Warren, R. A. J. *Biochem. J* **2000**, *351*, 833-838.
- (138) Juers, D. H.; Heightman, T. D.; Vasella, A.; McCarter, J. D.; Mackenzie, L.; Withers, S. G.; Matthews, B. W. *Biochemistry* **2001**, *40*, 14781-14794.

- (139) Jain, S.; Drendel, W. B.; Chen, Z. W.; Mathews, F. S.; Sly, W. S.; Grubb, J. H. *Nat. Struct. Biol.* **1996**, *3*, 375-381.
- (140) Tailford, L. E.; Money, V. A.; Smith, N. L.; Dumon, C.; Davies, G. J.; Gilbert, H. J. *J. Biol. Chem.* **2007**, *282*, 11291-11299.
- (141) Offen, W. A.; Zechel, D. L.; Withers, S. G.; Gilbert, H. J.; Davies, G. J. *Chem. Commun.* **2009**, 2484-2486.
- (142) Nashiru, O.; Zechel, D. L.; Stoll, D.; Mohammadzadeh, T.; Warren, R. A. J.; Withers, S. G. *Angew. Chem. Int. Ed.* **2001**, *40*, 417-420.
- (143) Zechel, D. L.; Reid, S. P.; Nashiru, O.; Mayer, C.; Stoll, D.; Jakeman, D. L.; Warren, P. A. J.; Withers, S. G. *J. Am. Chem. Soc.* **2001**, *123*, 4350-4351.
- (144) Howard, S.; Braun, C.; McCarter, J.; Moremen, K. W.; Liao, Y. F.; Withers, S. G. *Biochem. Biophys. Res. Commun.* **1997**, *238*, 896-898.
- (145) Ramana, C. V.; Vasella, A. *Helv. Chim. Acta* **2000**, *83*, 1599-1610.
- (146) Jordan, A. M.; Osborn, H. M. I.; Stafford, P. M.; Tzortzis, G.; Rastall, R. A. *J. Carbohydr. Chem.* **2003**, *22*, 705-717.
- (147) Li, Y. T. *J. Biol. Chem.* **1967**, *242*, 5474-&.
- (148) Howard, S.; He, S. M.; Withers, S. G. *J. Biol. Chem.* **1998**, *273*, 2067-2072.
- (149) Heikinhimo, P.; Helland, R.; Leiros, H. K. S.; Leiros, I.; Karlsen, S.; Evjen, G.; Ravelli, R.; Schoehn, G.; Ruigrok, R.; Tollersrud, O. K.; McSweeney, S.; Hough, E. *J. Mol. Biol.* **2003**, *327*, 631-644.
- (150) van den Elsen, J. M. H.; Kuntz, D. A.; Rose, D. R. *EMBO J.* **2001**, *20*, 3008-3017.
- (151) Herrchen, M.; Legler, G. *Eur. J. Biochem.* **1984**, *138*, 527-531.
- (152) Cupples, C. G.; Miller, J. H.; Huber, R. E. *J. Biol. Chem.* **1990**, *265*, 5512-5518.
- (153) Gebler, J. C.; Aebersold, R.; Withers, S. G. *J. Biol. Chem.* **1992**, *267*, 11126-11130.
- (154) McCarter, J. D.; Adam, M. J.; Withers, S. G. *Biochem. J* **1992**, *286*, 721-727.
- (155) Berkowitz, D. B.; Karukurichi, K. R.; de la Salud-Bea, R.; Nelson, D. L.; McCune, C. D. *J. Fluorine Chem.* **2008**, *129*, 731-742.
- (156) Plenio, H.; Diodone, R. *Chem. Ber. Recl.* **1997**, *130*, 633-640.
- (157) Dunitz, J. D.; Taylor, R. *Chem. Eur. J.* **1997**, *3*, 89-98.
- (158) Howard, J. A. K.; Hoy, V. J.; Ohagan, D.; Smith, G. T. *Tetrahedron* **1996**, *52*, 12613-12622.
- (159) Dunitz, J. D. *ChemBioChem* **2004**, *5*, 614-621.
- (160) Biffinger, J. C.; Kim, H. W.; DiMagno, S. G. *ChemBioChem* **2004**, *5*, 622-627.
- (161) Kim, H. W.; Rossi, P.; Shoemaker, R. K.; DiMagno, S. G. *J. Am. Chem. Soc.* **1998**, *120*, 9082-9083.
- (162) Numao, S.; He, S. M.; Evjen, G.; Howard, S.; Tollersrud, O. K.; Withers, S. G. *FEBS Lett.* **2000**, *484*, 175-178.
- (163) Braun, C.; Brayer, G. D.; Withers, S. G. *J. Biol. Chem.* **1995**, *270*, 26778-26781.
- (164) Hart, D. O.; He, S. M.; Chany, C. J.; Withers, S. G.; Sims, P. F. G.; Sinnott, M. L.; Brumer, H. *Biochemistry* **2000**, *39*, 9826-9836.



- (165) Zhang, R.; McCarter, J. D.; Braun, C.; Yeung, W.; Brayer, G. D.; Withers, S. G. *J. Org. Chem.* **2008**, *73*, 3070-3077.
- (166) Brumer, H.; Sims, P. F. G.; Sinnott, M. L. *Biochem. J* **1999**, *339*, 43-53.
- (167) Konstantinidis, A.; Sinnott, M. L. *Biochem. J* **1991**, *279*, 587-593.
- (168) Srinivasan, K.; Konstantinidis, A.; Sinnott, M. L.; Hall, B. G. *Biochem. J* **1993**, *291*, 15-17.
- (169) Wicki, J.; Schloegl, J.; Tarling, C. A.; Withers, S. G. *Biochemistry* **2007**, *46*, 6996-7005.
- (170) Skelton, B. W.; Stick, R. V.; Stubbs, K. A.; Watts, A. G.; White, A. H. *Aust. J. Chem.* **2004**, *57*, 345-353.
- (171) Vocadlo, D. J.; Mayer, C.; He, S. M.; Withers, S. G. *Biochemistry* **2000**, *39*, 117-126.
- (172) Stubbs, K. A.; Scaffidi, A.; Debowski, A. W.; Mark, B. L.; Stick, R. V.; Vocadlo, D. J. *J. Am. Chem. Soc.* **2008**, *130*, 327-335.
- (173) Nieman, C. E.; Wong, A. W.; He, S. M.; Clarke, L.; Hopwood, J. J.; Withers, S. G. *Biochemistry* **2003**, *42*, 8054-8065.
- (174) Wong, A. W.; He, S. M.; Withers, S. G. *Can. J. Chem.* **2001**, *79*, 510-518.
- (175) Ferrier, R. J.; Furneaux, R. H. *J. Chem. Soc., Perkin Trans. 1* **1977**, 1996-2000.
- (176) Blattner, R.; Ferrier, R. J. *J. Chem. Soc., Perkin Trans. 1* **1980**, 1523-1527.
- (177) Hartman, M. C. T.; Coward, J. K. *J. Am. Chem. Soc.* **2002**, *124*, 10036-10053.
- (178) Praly, J. P.; Brard, L.; Descotes, G.; Toupet, L. *Tetrahedron* **1989**, *45*, 4141-4152.
- (179) Kerr, J. A. *Chem. Rev.* **1966**, *66*, 465-&.
- (180) Praly, J. P.; Brendle, J. C.; Klett, J.; Pequery, F. *Comptes Rendus De L Academie Des Sciences Serie Ii Fascicule C-Chimie* **2001**, *4*, 611-617.
- (181) Lovering, A. L.; Lee, S. S.; Kim, Y. W.; Withers, S. G.; Strynadka, N. C. J. *J. Biol. Chem.* **2005**, *280*, 2105-2115.
- (182) Lee, S. S.; He, S. M.; Withers, S. G. *Biochem. J* **2001**, *359*, 381-386.
- (183) Numao, S.; Kuntz, D. A.; Withers, S. G.; Rose, D. R. *J. Biol. Chem.* **2003**, *278*, 48074-48083.
- (184) Adamson, J.; Foster, A. B.; Hall, L. D.; Johnson, R. N.; Hesse, R. H. *Carbohydr. Res.* **1970**, *15*, 351-&.
- (185) Kovac, P. *Carbohydr. Res.* **1986**, *153*, 168-170.
- (186) Nyffeler, P. T.; Duron, S. G.; Burkart, M. D.; Vincent, S. P.; Wong, C. H. *Angew. Chem. Int. Ed.* **2005**, *44*, 192-212.
- (187) Singh, R. P.; Shreeve, J. M. *Acc. Chem. Res.* **2004**, *37*, 31-44.
- (188) Vincent, S. P.; Burkart, M. D.; Tsai, C. Y.; Zhang, Z. Y.; Wong, C. H. *J. Org. Chem.* **1999**, *64*, 5264-5279.
- (189) Street, I. P.; Withers, S. G. *Can. J. Chem.* **1986**, *64*, 1400-1403.
- (190) Adam, M. J. *J. Labelled Compd. Radiopharm.* **2002**, *45*, 167-180.
- (191) Cai, L. S.; Lu, S. Y.; Pike, V. W. *Eur. J. Org. Chem.* **2008**, 2853-2873.
- (192) Barbieri, L.; Costantino, V.; Fattorusso, E.; Mangoni, A.; Basilico, N.; Mondani, M.; Taramelli, D. *Eur. J. Org. Chem.* **2005**, 3279-3285.
- (193) Dohi, H.; Perion, R.; Durka, M.; Bosco, M.; Roue, Y.; Moreau, F.; Grizot, S.; Ducruix, A.; Escaich, S.; Vincent, S. P. *Chem. Eur. J.* **2008**, *14*, 9530-9539.

- (194) Tarling, C. A.; He, S. M.; Sulzenbacher, G.; Bignon, C.; Bourne, Y.; Henrissat, B.; Withers, S. G. *J. Biol. Chem.* **2003**, 278, 47394-47399.
- (195) Ziser, L.; Setyawati, I.; Withers, S. G. *Carbohydr. Res.* **1995**, 274, 137-153.
- (196) Wong, A. W.; He, S. M.; Grubb, J. H.; Sly, W. S.; Withers, S. G. *J. Biol. Chem.* **1998**, 273, 34057-34062.
- (197) McCarter, J. D.; Adam, M. J.; Braun, C.; Namchuk, M.; Tull, D.; Withers, S. G. *Carbohydr. Res.* **1993**, 249, 77-90.
- (198) Hall, L. D.; Johnson, R. N.; Adamson, J.; Foster, A. B. *Can. J. Chem.* **1971**, 49, 118-&.
- (199) Koenigs, W.; Knorr, E. *Berichte Der Deutschen Chemischen Gesellschaft* **1901**, 34, 957-981.
- (200) McCarter, J. *Ph.D. Thesis*, University of British Columbia, 1995.
- (201) Lemieux, R. H. In *Methods in Carbohydrate Chemistry*; Whistler, R. L., Wolfrom, M. L., Eds.; Academic Press Inc.: New York and London, 1963; Vol. 2, p 224-225.
- (202) Carey, F. J.; Sundberg, R. J. In *Advanced Organic Chemistry. Part A: Structure and Mechanisms*; Kluwer Academic/Plenum Publishing: New York, 2000, p 295-298.
- (203) Cottaz, S.; Henrissat, B.; Driguez, H. *Biochemistry* **1996**, 35, 15256-15259.
- (204) Ortner, J.; Albert, M.; Weber, H.; Dax, K. *J. Carbohydr. Chem.* **1999**, 18, 297-316.
- (205) Klarner, F. G.; Kahlert, B.; Nellesen, A.; Zienau, J.; Ochsenfeld, C.; Schrader, T. *J. Am. Chem. Soc.* **2006**, 128, 4831-4841.
- (206) Berven, L. A.; Dolphin, D.; Withers, S. G. *Can. J. Chem.* **1990**, 68, 1859-1866.
- (207) Boyd, E. A.; Boyd, M. E. K.; Kerrigan, F. *Tetrahedron Lett.* **1996**, 37, 5425-5426.
- (208) Saady, M.; Lebeau, L.; Mioskowski, C. *Helv. Chim. Acta* **1995**, 78, 670-678.
- (209) Bhattacharya, A. K.; Thyagarajan, G. *Chem. Rev.* **1981**, 81, 415-430.
- (210) Wong, C. H.; Hayashi, T.; The Scripps Research Institute: USA, 1998.
- (211) Miao, S. C.; McCarter, J. D.; Grace, M. E.; Grabowski, G. A.; Aebersold, R.; Withers, S. G. *J. Biol. Chem.* **1994**, 269, 10975-10978.
- (212) Grabowski, G. A.; Gatt, S.; Horowitz, M. *Crit. Rev. Biochem. Mol. Biol.* **1990**, 25, 385-414.
- (213) Alattia, J. R.; Shaw, J. E.; Yip, C. M.; Prive, G. G. *Proc. Natl. Acad. Sci. U. S. A.* **2007**, 104, 17394-17399.
- (214) Abu-Baker, S.; Qi, X. Y.; Lorigan, G. A. *Biophys. J.* **2007**, 93, 3480-3490.
- (215) de Alba, E.; Weiler, S.; Tjandra, N. *Biochemistry* **2003**, 42, 14729-14740.
- (216) Hawkins, C. A.; de Alba, E.; Tjandra, N. *J. Mol. Biol.* **2005**, 346, 1381-1392.
- (217) Kacher, Y.; Brumshtein, B.; Boldin-Adamsky, S.; Toker, L.; Shainskaya, A.; Silman, I.; Sussman, J. L.; Futerman, A. H. *Biol. Chem.* **2008**, 389, 1361-1369.
- (218) Dvir, H.; Harel, M.; McCarthy, A. A.; Toker, L.; Silman, I.; Futerman, A. H.; Sussman, J. L. *EMBO Reports* **2003**, 4, 704-709.
- (219) Brumshtein, B.; Wormald, M. R.; Silman, I.; Futerman, A. H.; Sussman, J. L. *Acta Crystallogr., Sect D: Biol. Crystallogr.* **2006**, 62, 1458-1465.

- (220) Liou, B.; Kazimierczuk, A.; Zhang, M.; Scott, C. R.; Hegde, R. S.; Grabowski, G. A. *J. Biol. Chem.* **2006**, *281*, 4242-4253.
- (221) Shaaltiel, Y.; Bartfeld, D.; Hashmueli, S.; Baum, G.; Brill-Almon, E.; Galili, G.; Dym, O.; Boldin-Adamsky, S. A.; Silman, I.; Sussman, J. L.; Futerman, A. H.; Aviezer, D. *Plant Biotechnol. J.* **2007**, *5*, 579-590.
- (222) Premkumar, L.; Sawkar, A. R.; Boldin-Adamsky, S.; Toker, L.; Silman, I.; Kelly, J. W.; Futerman, A. H.; Sussman, J. L. *J. Biol. Chem.* **2005**, *280*, 23815-23819.
- (223) Brumshtein, B.; Greenblatt, H. M.; Butters, T. D.; Shaaltiel, Y.; Aviezer, D.; Silman, I.; Futerman, A. H.; Sussman, J. L. *J. Biol. Chem.* **2007**, *282*, 29052-29058.
- (224) Lieberman, R. L.; Wustman, B. A.; Huertas, P.; Powe, A. C.; Pine, C. W.; Khanna, R.; Schlossmacher, M. G.; Ringe, D.; Petsko, G. A. *Nat. Chem. Biol.* **2007**, *3*, 101-107.
- (225) Berent, S. L.; Radin, N. S. *Arch. Biochem. Biophys.* **1981**, *208*, 248-260.
- (226) Ho, M. W.; O'Brien, J. S. *Proc. Natl. Acad. Sci. U. S. A.* **1971**, *68*, 2810-&.
- (227) Daniels, L. B.; Glew, R. H.; Radin, N. S.; Vunnam, R. R. *Clin. Chim. Acta* **1980**, *106*, 155-163.
- (228) Boot, R. G.; Verhoek, M.; Donker-Koopman, W.; Strijland, A.; van Marle, J.; Overkleeft, H. S.; Wennekes, T.; Aerts, J. *J. Biol. Chem.* **2007**, *282*, 1305-1312.
- (229) Mikhaylova, M.; Wiederschain, G.; Mikhaylov, V.; Aerts, J. *Biochim. Biophys. Acta-Mol. Bas. Dis.* **1996**, *1317*, 71-79.
- (230) Hays, W. S.; Wheeler, D. E.; Eghtesad, B.; Glew, R. H.; Johnston, D. E. *Hepatology* **1998**, *28*, 156-163.
- (231) Morjani, H.; Aouali, N.; Belhoussine, R.; Veldman, R. J.; Levade, T.; Manfait, M. *Int. J. Cancer* **2001**, *94*, 157-165.
- (232) Deganuto, M.; Pittis, M. G.; Pines, A.; Dominissini, S.; Kelley, M. R.; Garcia, R.; Quadrifoglio, F.; Bembi, B.; Tell, G. *J. Cell. Physiol.* **2007**, *212*, 223-235.
- (233) Takagi, Y.; Kriehuber, E.; Imokawa, G.; Elias, P. M.; Holleran, W. M. *J. Lipid Res.* **1999**, *40*, 861-869.
- (234) Yatziv, S.; Newburg, D. S.; Livni, N.; Barfi, G.; Kolodny, E. H. *J. Lab. Clin. Med.* **1988**, *111*, 416-420.
- (235) Das, P. K.; Murray, G. J.; Gal, A. E.; Barranger, J. A. *Exp. Cell Res.* **1987**, *168*, 463-474.
- (236) Trajkovic-Bodenec, S.; Bodenec, J.; Futerman, A. H. *Blood Cells. Mol. Dis.* **2004**, *33*, 77-82.
- (237) Kanfer, J. N.; Legler, G.; Sullivan, J.; Raghavan, S. S.; Mumford, R. A. *Biochem. Biophys. Res. Commun.* **1975**, *67*, 85-90.
- (238) Beutler, E.; West, C.; Torbett, B. E.; Deguchi, H. *Mol. Med.* **2002**, *8*, 247-250.
- (239) Mizukami, H.; Mi, Y. D.; Wada, R.; Kono, M.; Yamashita, T.; Liu, Y. J.; Werth, N.; Sandhoff, R.; Sandhoff, K.; Proia, R. L. *J. Clin. Invest.* **2002**, *109*, 1215-1221.
- (240) Sinclair, G. B.; Jevon, G.; Colobong, K. E.; Randall, D. R.; Choy, F. Y. M.; Clarke, L. A. *Mol. Genet. Metab.* **2007**, *90*, 148-156.
- (241) Sun, Y.; Quinn, B.; Witte, D. P.; Grabowski, G. A. *J. Lipid Res.* **2005**, *46*, 2102-2113.
- (242) Marshall, J.; McEachern, K. A.; Kyros, J. A. C.; Nietupski, J. B.; Budzinski, T. L.; Ziegler, R. J.; Yew, N. S.; Sullivan, J.; Scaria, A.; van Rooijen, N.; Barranger, J. A.; Cheng, S. H. *Mol. Ther.* **2002**, *6*, 179-189.

- (243) Enquist, I. B.; Lo Bianco, C.; Ooka, A.; Nilsson, E.; Mansson, J. E.; Ehinger, M.; Richter, J.; Brady, R. O.; Kirik, D.; Karlsson, S. *Proc. Natl. Acad. Sci. U. S. A.* **2007**, *104*, 17483-17488.
- (244) Dinur, T.; Osiecki, K. M.; Legler, G.; Gatt, S.; Desnick, R. J.; Grabowski, G. A. *Proc. Natl. Acad. Sci. U. S. A.* **1986**, *83*, 1660-1664.
- (245) Reid, S. P. *M.Sc. Thesis*, University of British Columbia, 2004.
- (246) Samui, A. B.; Phadnis, S. M. *Prog. Org. Coat.* **2005**, *54*, 263-267.
- (247) McCarter, J. D.; Adam, M. J.; Withers, S. G. *J. Labelled Compd. Radiopharm.* **1992**, *31*, 1005-1009.
- (248) Wong, A. W.; Adam, M. J.; Withers, S. G. *J. Labelled Compd. Radiopharm.* **2001**, *44*, 385-394.
- (249) Hopwood, J. J. In *Heparin: Chemical and Biological Properties, Clinical Applications*; Lane, D., Lindahl, U., Eds.; Edward Arnold: London, 1989, p 191-227.
- (250) Freeman, C.; Hopwood, J. J. *Biochem. J* **1992**, *282*, 899-908.
- (251) Clements, P. R.; Brooks, D. A.; Saccone, G. T. P.; Hopwood, J. J. *Eur. J. Biochem.* **1985**, *152*, 21-28.
- (252) Clements, P. R.; Muller, V.; Hopwood, J. J. *Eur. J. Biochem.* **1985**, *152*, 29-34.
- (253) Hopwood, J. J.; Muller, V.; Smithson, A.; Baggett, N. *Clin. Chim. Acta* **1979**, *92*, 257-265.
- (254) Durand, P.; Lehn, P.; Callebaut, I.; Fabrega, S.; Henrissat, B.; Mornon, J. P. *Glycobiology* **1997**, *7*, 277-284.
- (255) Brooks, D. A.; Fabrega, S.; Hein, L. K.; Parkinson, E. J.; Durand, P.; Yogalingam, G.; Matte, U.; Guigliani, R.; Dasvarma, A.; Eslahpazire, J.; Henrissat, B.; Mornon, J. P.; Hopwood, J. J.; Lehn, P. *Glycobiology* **2001**, *11*, 741-750.
- (256) Ruth, L.; Eisenberg, D.; Neufeld, E. F. *Acta Crystallogr. Sect. D-Biol. Crystallogr.* **2000**, *56*, 524-528.
- (257) James, M. N. G., Personal Communication.
- (258) Rempel, B. P.; Clarke, L. A.; Withers, S. G. *Mol. Genet. Metab.* **2005**, *85*, 28-37.
- (259) Sugawara, K.; Saito, S.; Ohno, K.; Okuyama, T.; Sakuraba, H. *J. Hum. Genet.* **2008**, *53*, 467-474.
- (260) Root, Y. Y.; Wagner, T. R.; Norris, P. *Carbohydr. Res.* **2002**, *337*, 2343-2346.
- (261) Brady, R. O. *N. Engl. J. Med.* **1966**, *275*, 312-&.
- (262) Lonser, R. R.; Walbridge, S.; Murray, G. J.; Aizenberg, M. R.; Vortmeyer, A. O.; Aerts, J.; Brady, R. O.; Oldfield, E. H. *Ann. Neurol.* **2005**, *57*, 542-548.
- (263) Barton, N. W.; Brady, R. O.; Dambrosia, J. M.; Dibisceglie, A. M.; Doppelt, S. H.; Hill, S. C.; Mankin, H. J.; Murray, G. J.; Parker, R. I.; Argoff, C. E.; Grewal, R. P.; Yu, K. T. *N. Engl. J. Med.* **1991**, *324*, 1464-1470.
- (264) Grabowski, G. A.; Barton, N. W.; Pastores, G.; Dambrosia, J. M.; Banerjee, T. K.; McKee, M. A.; Parker, C.; Schiffmann, R.; Hill, S. C.; Brady, R. O. *Ann. Intern. Med.* **1995**, *122*, 33-39.
- (265) Furbish, F. S.; Blair, H. E.; Shiloach, J.; Pentchev, P. G.; Brady, R. O. *Proc. Natl. Acad. Sci. U. S. A.* **1977**, *74*, 3560-3563.
- (266) Bijsterbosch, M. K.; Donker, W.; VandeBilt, H.; VanWeely, S.; VanBerkel, T. J. C.; Aerts, J. *Eur. J. Biochem.* **1996**, *237*, 344-349.

- (267) Van Patten, S. M.; Hughes, H.; Huff, M. R.; Piepenhagen, P. A.; Waire, J.; Qiu, H. W.; Ganesa, C.; Reczek, D.; Ward, P. V.; Kutzko, J. P.; Edmunds, T. *Glycobiology* **2007**, *17*, 467-478.
- (268) Sato, Y.; Beutler, E. *J. Clin. Invest.* **1993**, *91*, 1909-1917.
- (269) Furbish, F. S.; Steer, C. J.; Krett, N. L.; Barranger, J. A. *Biochim. Biophys. Acta* **1981**, *673*, 425-434.
- (270) de Fost, M.; Hollak, C. E. M.; Greener, J. E. M.; Aerts, J.; Maas, M.; Poll, L. W.; Wiersma, M. G.; Haussinger, D.; Brett, S.; Brill, N.; vom Dahl, S. *Blood* **2006**, *108*, 830-835.
- (271) Weinreb, N. J.; Charrow, J.; Andersson, H. C.; Kaplan, P.; Kolodny, E. H.; Mistry, P.; Pastores, G.; Rosenbloom, B. E.; Scott, C. R.; Wappner, R. S.; Zimran, A. *Am. J. Med.* **2002**, *113*, 112-119.
- (272) Connock, M.; Burls, A.; Frew, E.; Fry-Smith, A.; Juarez-Garcia, A.; McCabe, C.; Wailoo, A.; Abrams, K.; Cooper, N.; Sutton, A.; O'Hagan, A.; Moore, D. *Health Technol. Assess.* **2006**, *10*, 1-152.
- (273) Charrow, J.; Andersson, H. C.; Kaplan, P.; Kolodny, E. H.; Mistry, P.; Pastores, G.; Prakash-Cheng, A.; Rosenbloom, B. E.; Scott, C. R.; Wappner, R. S.; Weinreb, N. J. *J. Pediatr.* **2004**, *144*, 112-120.
- (274) Lanpher, B.; Brunetti-Pierri, N.; Lee, B. *Nat. Rev. Genet.* **2006**, *7*, 449-460.
- (275) Andersson, U.; Butters, T. D.; Dwek, R. A.; Platt, F. M. *Biochem. Pharmacol.* **2000**, *59*, 821-829.
- (276) Platt, F. M.; Neises, G. R.; Reinkensmeier, G.; Townsend, M. J.; Perry, V. H.; Proia, R. L.; Winchester, B.; Dwek, R. A.; Butters, T. D. *Science* **1997**, *276*, 428-431.
- (277) Alfonso, P.; Pampin, S.; Estrada, J.; Rodriguez-Rey, J. C.; Giraldo, P.; Sancho, J.; Pocovi, M. *Blood Cells. Mol. Dis.* **2005**, *35*, 268-276.
- (278) Erikson, A.; Groth, C. G.; Mansson, J. E.; Percy, A.; Ringden, O.; Svennerholm, L. *Acta Paediatr. Scand.* **1990**, *79*, 680-685.
- (279) Ringden, O.; Groth, C. G.; Erikson, A.; Backman, L.; Granqvist, S.; Mansson, J. E.; Svennerholm, L. *Transplantation* **1988**, *46*, 66-70.
- (280) Enquist, I. B.; Nilsson, E.; Ooka, A.; Mansson, J. E.; Olsson, K.; Ehinger, M.; Brady, R. O.; Richter, J.; Karlsson, S. *Proc. Natl. Acad. Sci. U. S. A.* **2006**, *103*, 13819-13824.
- (281) McEachern, K. A.; Nietupski, J. B.; Chuang, W. L.; Armentano, D.; Johnson, J.; Hutto, E.; Grabowski, G. A.; Cheng, S. H.; Marshall, J. *J. Gene Med.* **2006**, *8*, 719-729.
- (282) Bonetta, L. *Nat. Med.* **2002**, *8*, 1189-1189.
- (283) Marshall, E. *Science* **2003**, *299*, 320-320.
- (284) Zheng, W.; Padia, J.; Urban, D. J.; Jadhav, A.; Goker-Alpan, O.; Simeonov, A.; Goldin, E.; Auld, D.; LaMarca, M. E.; Inglese, J.; Austin, C. P.; Sidransky, E. *Proc. Natl. Acad. Sci. U. S. A.* **2007**, *104*, 13192-13197.
- (285) Yu, Z. Q.; Sawkar, A. R.; Whalen, L. J.; Wong, C. H.; Kelly, J. W. *J. Med. Chem.* **2007**, *50*, 94-100.
- (286) Steet, R. A.; Chung, S.; Wustman, B.; Powe, A.; Do, H.; Kornfeld, S. A. *Proc. Natl. Acad. Sci. U. S. A.* **2006**, *103*, 13813-13818.
- (287) Yu, L.; Ikeda, K.; Kato, A.; Adachi, I.; Godin, G.; Compain, P.; Martin, O.; Asano, N. *Biorg. Med. Chem.* **2006**, *14*, 7736-7744.

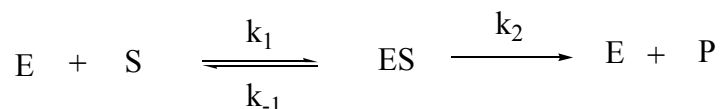
- (288) Egado-Gabas, M.; Canals, D.; Casas, J.; Llebaria, A.; Delgado, A. *Chemmedchem* **2007**, *2*, 992-994.
- (289) Zhu, X. X.; Sheth, K. A.; Li, S. H.; Chang, H. H.; Fan, J. Q. *Angew. Chem. Int. Ed.* **2005**, *44*, 7450-7453.
- (290) Kornhaber, G. J.; Tropak, M. B.; Maegawa, G. H.; Tuske, S. J.; Coales, S. J.; Mahuran, D. J.; Hamuro, Y. *ChemBioChem* **2008**, *9*, 2643-2649.
- (291) Shen, J. S.; Edwards, N. J.; Bin Hong, Y.; Murray, G. J. *Biochem. Biophys. Res. Commun.* **2008**, *369*, 1071-1075.
- (292) Chang, H. H.; Asano, N.; Ishii, S.; Ichikawa, Y.; Fan, J. Q. *FEBS J.* **2006**, *273*, 4082-4092.
- (293) Lieberman, R. L.; D'aquino, J. A.; Ringe, D.; Petsko, G. A. *Biochemistry* **2009**, *48*, 4816-4827.
- (294) <http://www.amicustherapeutics.com/clinicaltrials/at2101.asp> (April 24, 2009).
- (295) Stevenson, A. D. *M.Sc. Thesis*, University of British Columbia, 1994.
- (296) Schramm, V. L. *J. Biol. Chem.* **2007**, *282*, 28297-28300.
- (297) McCarter, J. D.; Adam, M. J.; Hartman, N. G.; Withers, S. G. *Biochem. J* **1994**, *301*, 343-348.
- (298) Buller, H. A.; Vanwassenaer, A. G.; Raghavan, S.; Montgomery, R. K.; Sybicki, M. A.; Grand, R. J. *Am. J. Physiol.* **1989**, *257*, G616-G623.
- (299) Yildiz, Y.; Matern, H.; Thompson, B.; Allegood, J. C.; Warren, R. L.; Ramirez, D. M. O.; Hammer, R. E.; Hamra, F. K.; Matern, S.; Russell, D. W. *J. Clin. Invest.* **2006**, *116*, 2985-2994.
- (300) Hayashi, Y.; Okino, N.; Kakuta, Y.; Shikanai, T.; Tani, M.; Narimatsu, H.; Ito, M. *J. Biol. Chem.* **2007**, *282*, 30889-30900.
- (301) Wester, H. J. *Clin. Cancer Res.* **2007**, *13*, 3470-3481.
- (302) Xu, Y. H.; Ponce, E.; Sun, Y.; Leonova, T.; Bove, K.; Witte, D.; Grabowski, G. A. *Pediatr. Res.* **1996**, *39*, 313-322.
- (303) Friedman, B. A.; Vaddi, K.; Preston, C.; Mahon, E.; Cataldo, J. R.; McPherson, J. M. *Blood* **1999**, *93*, 2807-2816.
- (304) Mistry, P. K.; Wraight, E. P.; Cox, T. M. *Lancet* **1996**, *348*, 1555-1559.
- (305) Wong, A. W. *Ph.D. Thesis*, University of British Columbia, 2001.
- (306) Lim, N., Personal Communication.
- (307) Sharma, S. K.; Corrales, G.; Penades, S. *Tetrahedron Lett.* **1995**, *36*, 5627-5630.
- (308) Lamghari, M.; Barrias, C. C.; Miranda, C. S.; Barbosa, M. A. *Blood Cells. Mol. Dis.* **2005**, *35*, 348-354.
- (309) Albert, M.; Dax, K.; Ortner, J. *Tetrahedron* **1998**, *54*, 4839-4848.
- (310) Lemieux, R. H. In *Methods in Carbohydrate Chemistry*; Whistler, R. L., Wolfrom, M. L., Eds.; Academic Press Inc.: New York and London, 1963; Vol. 2, p 221-222.
- (311) Leatherbarrow, R. J.; Grafit 5.0.13 ed.; Erithracus Software Limited: 2006.
- (312) Michaelis, L.; Menten, M. L. *Biochem. Z.* **1913**, *49*, 333-369.
- (313) Briggs, G. E.; Haldane, J. B. S. *Biochem. J* **1925**, *19*, 338-339.

## **Appendix I**

### **Equations Representing Enzyme Kinetics**

## Michaelis-Menten kinetics

A simple model to explain the observed kinetic behaviour of an enzyme was first proposed by Michaelis and Menten in 1913.<sup>312</sup> This model offered a rationale for the observed relationship between the rate of enzymatic reaction and the concentration of the enzyme's substrate. This model was expanded upon by Briggs and Haldane in 1925 to include the steady-state approximation.<sup>313</sup> A scheme representing a simple reaction catalyzed by an enzyme is shown below. Free enzyme, E, combines with free substrate, S, to form an enzyme-substrate complex, ES, that is turned over to produce the product, P.



Under steady-state conditions:

$$\frac{d[\text{ES}]}{dt} = k_1 [\text{E}][\text{S}] - k_{-1}[\text{ES}] - k_2[\text{ES}] = 0 \quad (1)$$

The total concentration of enzyme,  $[\text{E}]_o$ , is equal to the sum of the concentrations of free enzyme,  $[\text{E}]$ , and enzyme bound to substrate in the ES complex,  $[\text{ES}]$ .

$$[\text{E}]_o = [\text{E}] + [\text{ES}] \quad (2)$$

By combining equations (1) and (2) to solve for the  $[\text{ES}]$ , we obtain:

$$[\text{ES}] = \frac{[\text{E}]_o[\text{S}]}{[\text{S}] + \frac{k_{-1} + k_2}{k_2}} \quad (3)$$

If we make the assumption that the rate of product formation is rate-limiting, or that  $k_2 < k_1$  or  $k_{-1}$ , then the initial velocity of the reaction,  $v$ , will be equal to the rate of formation of product:

$$v = \frac{dP}{dt} = k_2[\text{ES}] \quad (4)$$

By substituting the expression for  $[\text{ES}]$  obtained in equation (3), we obtain an expression for the initial rate of reaction:

$$v = \frac{k_2[\text{E}]_o[\text{S}]}{[\text{S}] + \frac{k_{-1} + k_2}{k_2}} \quad (5)$$



The ratio of the rate constants in the denominator,  $(k_{-1}+k_2)/k_1$ , is defined as  $K_m$ , the Michaelis constant. Similarly, the rate constant  $k_2$  is defined as  $k_{cat}$ , which represents the catalytic constant or turnover number of the enzyme, since  $k_2$  is assumed to be the rate-limiting step of the catalytic reaction. Therefore, equation (5) can be expressed in the commonly used form of the Michaelis-Menten equation:

$$v = \frac{k_{cat}[E]_o[S]}{[S] + K_m} \quad (6)$$

When the initial reaction rate,  $v$ , is equal to half the maximum rate, ( $v = V_{max}/2$ ), then the substrate concentration is equal to  $K_m$ . The  $K_m$  value is an apparent binding constant which represents the binding affinity of the enzyme for a given substrate. However, the  $K_m$  value differs from a  $K_d$  value, which is equal to  $k_1/k_{-1}$ . The inclusion of  $k_2$  in the expression for  $K_m$  means that for very proficient enzymes (large  $k_2$  values) the  $K_m$  value will be much higher than the  $K_d$  value for the same substrate. Alternatively, as the rate of enzyme turnover approaches zero (in the extreme example of  $k_2 = 0$ , the “enzyme” has become a receptor) then the value of  $K_m$  approaches  $K_d$ .

When the concentration of substrate becomes very large relative to the  $K_m$  value,  $[S] \gg K_m$ , then  $v$  approaches its maximum value,  $V_{max}$ , and the rate becomes largely independent of  $[S]$ . In this situation, the Michaelis-Menten equation can be rewritten as:

$$V_{max} = k_{cat}[E]_o \quad (7)$$

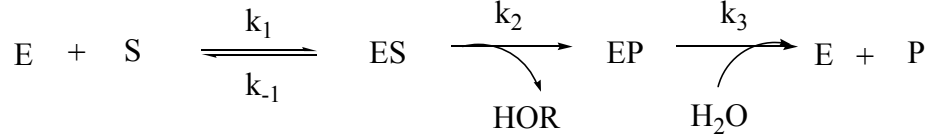
When the concentration of substrate is low with respect to  $K_m$  ( $[S] \ll K_m$ ), then the initial rate of the enzyme-catalyzed reaction is proportional to  $[S]$ :

$$v = \frac{k_{cat}[E]_o[S]}{K_m} \quad (8)$$

A graphical representation of these equations is shown below.

The Michaelis-Menten equation can also be adapted to represent more complex enzymatic reactions as well, such as the double-displacement mechanism of a retaining glycosidase. The reaction is represented schematically below. The enzyme (E) and substrate (S) combine to form the enzyme-substrate complex (ES) with the associated rate constants of

formation ( $k_1$ ) and dissociation ( $k_{-1}$ ). The first step, the glycosylation step, is represented by the formation of the enzyme-product complex (EP) with a rate constant  $k_2$  that represents that rate of glycosylation, and loss of the aglycone (HOR). The deglycosylation step involves attack of water on the EP complex and leads to breakdown of the EP complex to give free enzyme and product, with an associated rate constant ( $k_3$ ).



By making the steady-state assumption, then:

$$k_2[\text{ES}] = k_3[\text{EP}] \quad (9)$$

and therefore:

$$\frac{d[\text{ES}]}{dt} = k_2[\text{E}][\text{S}] - k_{-1}[\text{ES}] + k_2[\text{ES}] = 0 \quad (10)$$

The total concentration of enzyme,  $[\text{E}]_0$  is equal to all forms of the enzyme, and so:

$$[\text{E}]_0 = [\text{E}] + [\text{ES}] + [\text{EP}] \quad (11)$$

By substituting for  $[\text{EP}]$  in equation (11) using equation (9), we obtain:

$$[\text{E}]_0 = [\text{E}] + [\text{ES}] + \frac{k_2[\text{ES}]}{k_3} \quad (12)$$

By solving for  $[\text{E}]$  in equation (12) and substituting this expression into equation (10), we obtain, after rearrangement to isolate  $[\text{ES}]$ :

$$[\text{ES}] = \frac{k_1[\text{E}]_0[\text{S}]}{k_{-1} + k_2 + \frac{k_1(k_2+k_3)}{k_3}} \quad (13)$$

Once a steady state is achieved, then the rate of product formation is:

$$v = \frac{dP}{dt} = k_3[\text{EP}] = k_2[\text{ES}] \quad (14)$$

Finally, substitution of equation (13) into equation (14) yields an expression in the form of the Michaelis-Menten equation:

$$v = \frac{\frac{k_2 k_3}{k_2 + k_3} E_0 [S]}{\left( \frac{k_3}{k_2 + k_3} \right) \left( \frac{k_{-1} + k_2}{k_1} \right) + [S]} \quad (15)$$

Therefore in this kinetic scheme, the Michaelis-Menten parameters can be assigned the following values:

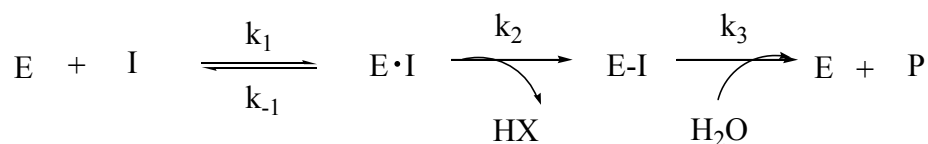
$$k_{\text{cat}} = \frac{k_2 k_3}{k_2 + k_3} \quad (16)$$

$$K_m = \left( \frac{k_3}{k_2 + k_3} \right) \left( \frac{k_{-1} + k_2}{k_1} \right) \quad (17)$$

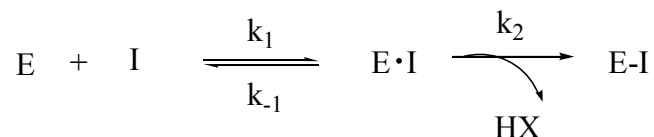
Therefore, the values obtained experimentally for both  $k_{\text{cat}}$  and  $K_m$  are composed of individual rate constants that are representative of the proposed chemical steps.

### Enzyme kinetics with a mechanism-based inactivator

The behaviour of an enzyme in the presence of a mechanism-based inactivator that is subsequently hydrolyzed is shown in the following scheme:



This kinetic scheme represents the behaviour of a retaining glycosidase in the presence of an activated fluorosugar. In the case of a retaining  $\beta$ -glycosidase in the presence of an activated 2-deoxy-2-fluoro- $\beta$ -glycoside, the rate of hydrolysis of the E-I intermediate is extremely low ( $k_3$  approaches zero) with respect to the other rate constants. Therefore, the kinetic scheme can be simplified to the following:



This model predicts a time-dependent inactivation of the enzyme in the presence of the mechanism-based inactivator. Assuming that  $[I] \gg [E]$ , then the  $[I]$  can be assumed to remain constant throughout the course of the reaction, and therefore pseudo first-order

kinetics with respect to [E] will be observed. The equation for this process is very similar to the Michaelis-Menten equation for substrate hydrolysis:

$$v = \frac{k_i[E][I]}{K_i + [I]} \quad (18)$$

where  $k_i$  is the rate constant for inactivation ( $k_i = k_2$ ) and  $K_i$  is an apparent dissociation constant for all forms of enzyme-bound ( $K_i = k_{-1}/k_1$ ), assuming that  $k_{-1} \gg k_2$ . Equation (18) can be rewritten as:

$$v = k_{\text{obs}}[E] \quad (19)$$

where

$$k_{\text{obs}} = \frac{k_i[I]}{K_i + [I]} \quad (20)$$

If  $K_i \gg [I]$ , then equation (20) can be simplified to give:

$$k_{\text{obs}} = \frac{k_i[I]}{K_i} \quad (21)$$

where  $k_{\text{obs}}$  is the observed rate constant for the time-dependent loss of enzyme activity, which is obtained by fitting the value for the residual enzyme activity to an exponential decay equation.

## **Appendix II: List of Publications**

Rempel, B.P.; Withers, S.G.. *Glycobiology*, **2008**, *18*, 570-586.

Rempel, B.P.; Withers, S.G. *Aus. J. Chem.*, **2009**, In Press.